Autophagy, senescence and nitrogen remobilization in barley

Liliana Astrid Avila Ospina

UNIVERSITÉ PARIS-SUD

ÉCOLE DOCTORALE 145: SCIENCES DU VÉGÉTAL

Laboratoire : *Institut Jean-Pierre Bourguin*

THÈSE DE DOCTORAT

BIOLOGIE

par

Liliana Astrid AVILA OSPINA

Autophagie, sénescence et remobilisation de l'azote chez l'orge

Date de soutenance : 08/09/2014

<u>Composition du jury</u> :

Directeur de thèse: Dr. Céline MASCLAUX-DAUBRESSE Directeur de Recherche INRA IJPB Versailles

Rapporteurs:	Pr. Christine FOYER	Professeur à l'Université de Leeds, UK
	Dr. Jacques LE GOUIS	Directeur de Recherche INRA GDEC Clermont-Ferrand
Examinateurs:	Pr. Jean-Christophe AVICE	Professeur à l'Université de Basse Normandie, Caen
	Dr. Michael HODGES	Directeur de Recherche CNRS IBP Orsay

ACKNOWLEDGEMENTS

I would like to thank to my supervisor Céline most sincerely for all her support and commitment to me from the very first moment and for give me the opportunity to spend three very pleasant years in her team where I had the chance to meet great people and at the same time to work in a very nice project. During this time, I have learned a lot from her and from the other guys from the institute, although not as much French as she or me wanted to but…. I just say thanks also for her patience during the many times when she understood only half of what I said.

I would like to thank to Fabienne and Marianne for being so helpful and funny all the time, and to Fabienne in particular for being such a good apprentice!! It was very nice to work with her. To Kohki for taking the time to discuss with me and help me when I needed to. To Michelle for helping me with her critical reviews in the writing of this manuscript and for always having a smile or a kind word for me. To the other people of the Bât 3 and the green house, Jöel, Akira, Giorgiana, Laure, Michael, Fabien, Anne M., Magali, Rozenn and the others for create a very amicable environment of work.

I would like to thank most specially to my friend Loreto for everything, to make it short, things would not have been as they were without her, she was a great support during my time here and she was always there during the good, the regular and the bad times. Also I would like to say GRACIAS to my mates from the Spanish/Latino-american lunch, those that are left and those that are still here, specially to Maria Jesus who has saved me more than once from burocratic tornados and who is also one of the nicest and friendly persons I have ever known.

I also would like to acknowledge people from the Croplife network, they made me have a good time during our very frequent meetings and secondments, and the consortium gave me the opportunity to travel and to know many people and places.

Last but not least, I would like to thank to my family, my mom, my dad, my siblings and my aunt for their support throught the distance. They always make feel loved no matter what. To my Colombian friends that make me feel some times like I have never left my hometown. To my previous supervisor Fernando Echeverri for always believe in me and because working with him made possible for me to be here today.
Finally I would like to thank with all my heart and soul to my best friend and love of my life Eduard. None of the things I have achieved could have been possible without you. You are my biggest support and I love you for that, always and forever.

Table of content

INTRODUCTION

PREAMBLE

This thesis is the first study on leaf senescence, remobilisation and autophagy in barley in the SATURN research team. Barley is not a common model of study at the IJPB-INRA, therefore the introduction chapter provides a detailed description of barley, and in the following chapter I describe senescence processes in plants, with emphasis on monocarpic cereal crops like barley. Also in this chapter, I summarize the relationships of autophagy with important agronomical traits such as yield and grain protein content.

The reader will also find a recent review published in a peer-reviewed journal, in which I am first author, about autophagy and nitrogen remobilisation in plants. Complementing this review, I have dedicates several pages to a more detailed description of the autophagy pathway, and function and regulation of the autophagy (ATG) core molecular machinery.

Finally, as this research project is within a consortium supported by the European Union, I will describe the structure of this scientific network and my role in achieving its aim of enhancing plant productivity through control of lifespan.

INTRODUCTION

I. BARLEY (*Hordeum Vulgare* L.), A MODEL PLANT AND A CROP

Barley (*Hordeum vulgare* L.) is one of the most important cereals in the world. It was one of the first domesticated crops and has been used for centuries for human and animal consumption (Badr et al., 2000). Nowadays, barley ranks fourth in world cereal crop production and is used for animal feed, brewing malts and human food (Akar et al., 2004). Barley is also a very adaptable crop, growing from 330 m below sea level near the Dead Sea up to 4200 m in the Bolivian Andes, and is mainly cultivated in unfavorable climate and soil conditions (FAO, 2009). Barley is also a very well known model crop used for plant breeding, genetics, cytogenetics, pathology, virology and biotechnology studies (Heneen, 2010).

I.1. Botany and taxonomy

Kingdom: Plantae - Plants
Subkingdom: Tracheobionta - Vascular plants
Superdivision: Spermatophyta - Seed plants
Division: Magnoliophyta - Flowering plants
Class: Liliopsida - Monocotyledons
Subclass: Commelinidae
Order: Cyperales
Family: Poaceae - Grass family
Genus: *Hordeum* – barley
Species: *H. vulgare*

Morphological and anatomical characters are the usual basis for distinguishing the various species in the genus *Hordeum* and may be associated with agricultural productivity in many ways. For instance, their straw length and strength (lodging resistance), response to diseases, photosynthesis, watering and agrochemical (fertilizer and pesticide) requirements and susceptibility to environmental stresses (drought, soil deficiencies, toxicities, among others) are all related to the plant anatomy and morphology and have an impact on productivity (Reid, 1985).

Barley anatomy is similar to other grasses. The stem (culm) is cylindrical with 5 to 7 internodes and the leaves borne alternately at each node on opposite sides of the stem. The spike (head, ear) at the top of the stem consists of flowers arranged in single-flowered spikelets (each bearing two glumes and the floret). Three spikelets are attached at each node of a flat, zigzag rachis, all of which are fertile in the six rowed cultivars while in the two rowed cultivars, the two lateral spikelets are sterile. As in other cereals, the kernel is a caryopsis (Wiebe and Reid, 1961), (Figure 1).

I.2. Barley Development

I.2.1. Grown features

Cultivated barley is a grass that can be either a winter or spring cereal. The growth stages of barley comprise germination, seedling development, tillering, stem elongation, heading (ear emergence), flowering and ripening (Figure 2). The duration of the different developmental stages varies depending on the weather, water supply, soil fertility, the degree of competition with other plants, the presence of pest and pathogens and the time of planting. The total time to maturity depends on variety, location and planting date (Robertson and Stark, 1993).

After germination, the coleoptile, which is a leaf sheath enclosing the embryonic plant emerges as the first leaf. Subsequently, other leaves arise on the main stem and tillers until the emergence of the final (flag) leaf. The mature leaves progressively senesce and gradually the whole plant dries out until full maturity when the grain is ripe (Briggs, 1978). Flag leaf senescence is of major importance for grain filling and yield.

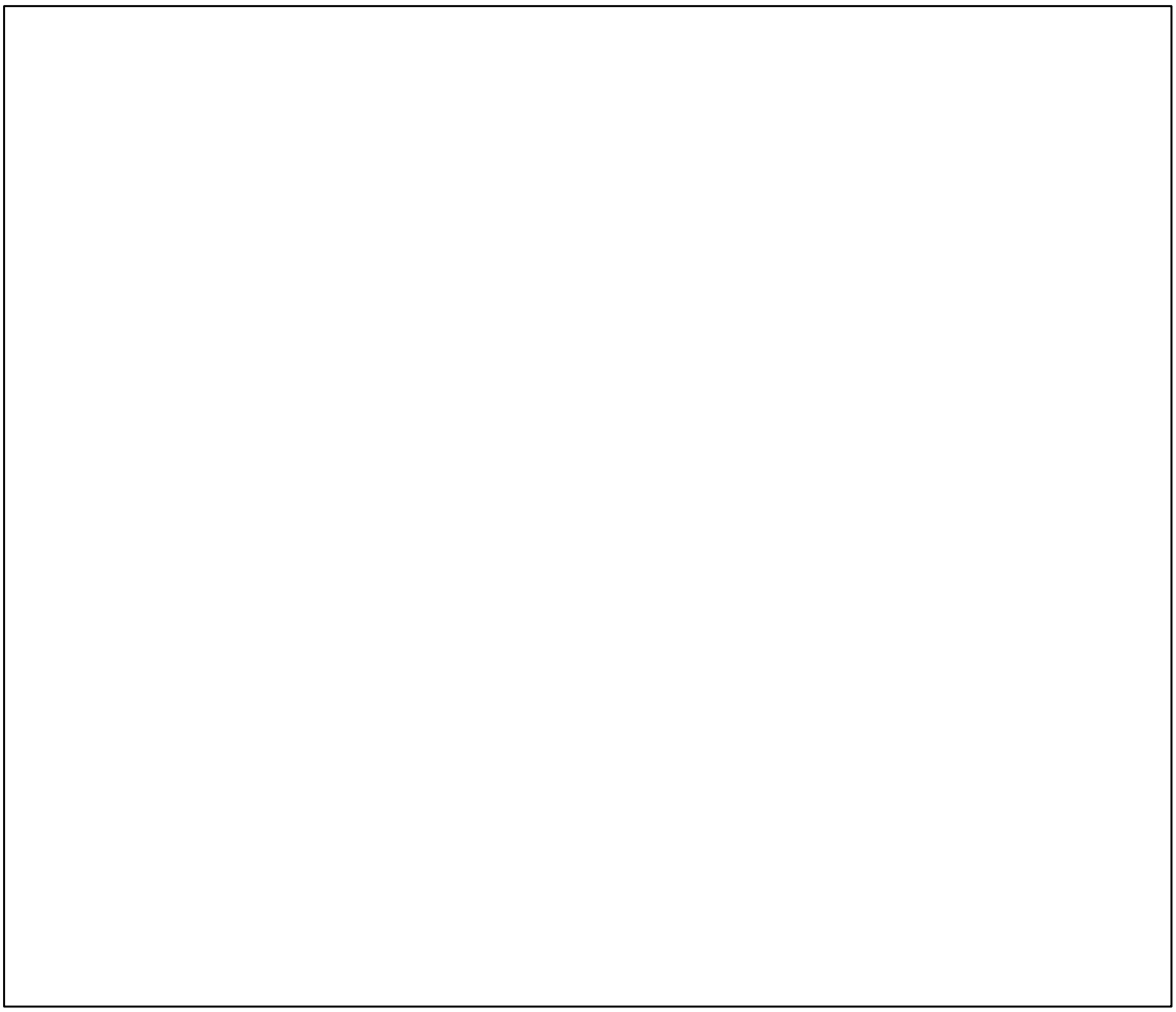

Figure 1. Parts of the barley plant (**A**); junction of blade and leaf sheath (**B**); mature floret (**C**); two rowed spike (**D**); six rowed spike (**E**); two rowed, sterile lateral spikelets (**F**); six rowed, fully fertile and awned lateral spikelets (**G**); kernel types, hulled (**H**) and naked (**I**). Figures A-C and H-I taken from (Wiebe & Reid, 1961). Figures D-G taken from (Komatsuda et al., 2007)

Barley plants usually consist of several tillers which start to develop around the 3-leaf stage (Figure 2). The number of tillers and their duration of tillering is dependent upon variety and growth conditions, e.g. two-rowed and winter varieties typically develop more tillers than six-rowed and spring varieties (Box, 2008; Briggs, 1978; Robertson & Stark, 1993). Although all tillers produce adventitious roots, not all tillers produce ears and the late tillers often remain unrooted and die prematurely (Hussien et al., 2014).

The whole plant development is coordinated, as the internode elongation begins when the vegetative meristem changes to reproductive status. During internode elongation, the spike differentiates in preparation for pollination and grain development (Briggs, 1978). Pollination usually takes place in barley just before or during head emergence from the boot (heading), beginning in the central portion of the head and proceeding toward the tip and the base

(Briggs, 1978). There is also a different development of the spikelets of the head. Central spikelets develop first, followed by those at the base and the tip of the spike. Therefore, spikelets in the central portion of the spike are the heaviest, while spikelets from the tip are the lightest. In six-rowed barley, the central kernels are heavier than the lateral ones (Robertson & Stark, 1993).

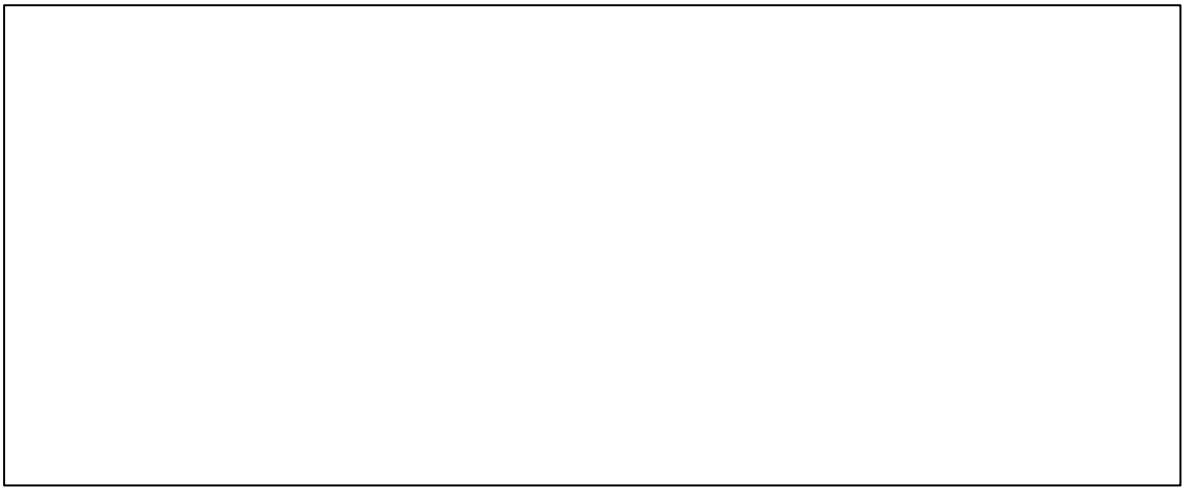

Figure 2. Schematic diagram of barley plants at successive stages of development. Taken from Box, 2008.

Once head emergence and pollination have occurred, kernels begin to develop first by lengthening then by swelling (Briggs, 1978). The first period of kernel development is designated the "watery ripe" and "milk" stages and lasts about 10 days. During this period, the watery substances contained in the kernels become milky (Figures 3A and B). This phase is extremely important because it determines the number of cells that will subsequently be used for storing starch. During the next period, which also lasts 10 days, kernels store starch and grow rapidly acquiring a white color and semi-solid consistency, this stage is known as "soft dough". As the kernel approaches maturity and begins losing water rapidly, its consistency becomes more solid, this stage is known as "hard dough" (Figure 3C). At this stage, the kernel loses its green color and reaches physiological maturity when its moisture decrease to about 30 to 40 percent (Anderson et al., 2013).

No further dry matter will accumulate and the final yield potential has been reached at this time (Anderson et al., 2013). An easily identifiable field indicator of physiological maturity is a 100 percent loss of green color in the glumes and peduncle. The barley kernel is ready for

combining and threshing when kernel moisture has decreased to 13 to 14 percent, (FAO, 2009). This stage is called harvest ripe (Figure 3D).

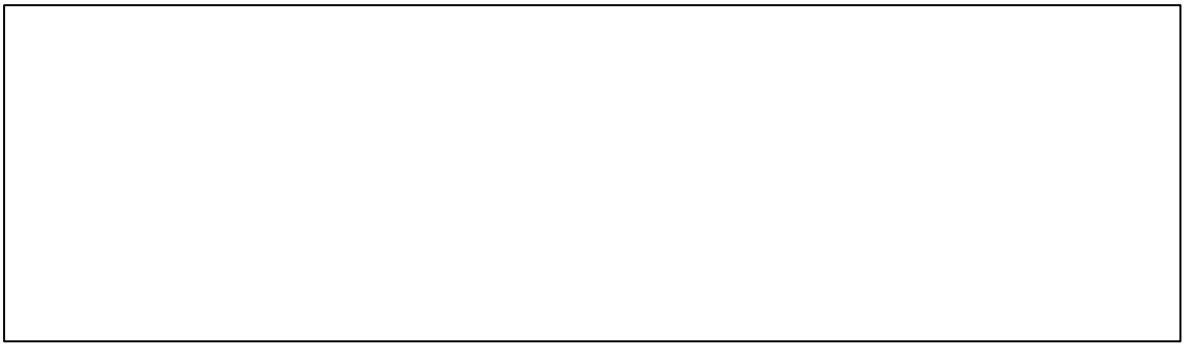

Figure 3. Kernel development: (**A**) watery ripe; (**B**) late milk; (**C**) hard dough; (**D**) harvest ripe with lemma and palea attached. Taken from (Anderson et al., 2013).

I.2.2. Reproduction

The production of rooted tillers has occasionally been described as a form of vegetative reproduction (Briggs, 1978), as tillers separated from the plant can grow supported by the adventitious roots only. Otherwise barley is not capable of vegetative spreading (Hussien et al., 2014).

For sexual reproduction, winter barley requires a period of cold stimulus (vernalization) to initiate floral development while spring barley does not. Flowering begins in the floret in the middle of the ear and spreads upwards and downwards taking one to four days to complete the whole process. Ears on different tillers may mature at varying times (Briggs, 1978).

The pollen and ovules in each floret mature together. Pollen viability is estimated from a few hours to at least 26 hours while the stigma is receptive and able to be fertilised for a period of six to eight days following the first flower opening (Riddle & Suneson, 1944). Cereals can be either closed-flowering (cleistogamous) or open-flowering depending on the variety, for example many winter barley varieties are open-flowering whereas spring barley is usually cleistogamous (Nair et al., 2010).

Barley pollen is small and relatively light (35 to 45 □m diameter) shape. Within 5 minutes of adhering to the stigma, pollen grains take up moisture and germinate. The rates of pollen tube growth, cell division and other aspects of the grain development are strongly temperature dependent, but generally the pollen tube takes about 45 minutes to grow (Briggs, 1978). Barley pollen is extremely sensitive to drying and remains

viable for only a few hours after dehiscence, time enough to allow cross fertilisation over a period of at least 26 hours at temperatures up to 40°C (Parzies, Schnaithmann, & Geiger, 2005).

Annual *Hordeum* species are mainly inbreeders (self-fertilization) although cross pollination can also occur. Cultivated barley and its wild progenitor reproduce entirely by self-fertilisation with a low gene flow (Bellucci et al., 2013; Ritala et al., 2002). Barley is not generally pollinated by insects (McGregor, 1976) so any outcrossing occurs by wind pollination and distance of pollen migration is the most important factor affecting outcrossing rates (Gatford et al., 2006).

As in all angiosperms, double fertilisation occurs in barley and results in a diploid embryo with equal nuclear contributions from the male and female gametes (2n = 2x =14). The triploid endosperm, where starch and proteins will be stored (Radchuk et al., 2009), is derived from a second fusion between one male gamete from the pollen and two polar nuclei from the embryo sac (Briggs, 1978). The total number of cells in the endosperm is higher than in wheat or rice, which explains why barley grains contain more cell wall material (such as -glucans) than these other cereals (Sabelli & Larkins, 2009).

H. vulgare has large and heavy seeds, but special bristles on the spikelets enable them to adhere to the fur of larger animals, feathers of birds and clothing of people, reaching a great dispersal range(Pourkheirandish & Komatsuda, 2007; Von Bothmer et al., 1992; Zohary, 1989). There is no evidence of barley seeds being dispersed by endozoochory although some percentage of the barley grain fed to cattle is excreted whole and undamaged.

Dormancy is defined as the inability of seeds to germinate under favourable conditions. During barley domestication, the non-dormancy of seeds was selected, so in cultivated barley more than 90% of seeds germinate at four days of imbibition, whereas in the wild form *H. spontaneum*, seed germination is highly irregular (Von Bothmer et al., 1992).

In addition to the influence of the genotype, dormancy varies with grain maturity and with the environmental conditions during grain ripening, harvest and storage. Freshly harvested grain is the most dormant and dormancy declines as grain ripens (Rodriguez et al., 2001).

1.2. Barley chromosomes and genome

Hordeum vulgare L., comprises the two sub-species, *vulgare* and *spontaneum* (C. Koch), which are diploid with seven chromosome pairs, like in other triticaceae species, (x = 7; 2n = 14).

The seven barley chromosomes are designated an arabic number from 1 to 7, according to the homologous relationship with the chromosomes of other members of the Triticeae (Laursen *et al.*, 1997), followed by the genomic symbol H and the symbols S (short) or L (long) according to the chromosome arm length (Ullrich, 2011).

The genome size in barley is 5.1 Gb (IBGSC, 2012) smaller than the hexaploid bread wheat (*Triticum aestivum*) (2n = 42) with a genome size of 17 Gb and bigger than other diploid genomes of grasses such as maize (*Zea mays*,2n = 20) and rice (*Oriza sativa*, 2n = 24) with genome sizes of 2.5 Gb and 0.4 Gb, respectively (Eckardt, 2008).

Recent genomic studies indicate that the gene-set of barley is of approximately 30.400 genes which were defined as high-confidence genes by gene-family-directed comparison with the genomes of *Sorghum*, rice, *Brachypodium* and Arabidopsis. However, another 53.220 transcript loci were considered as low-confidence genes due to the lack of homology and missing support from the gene family clustering (IBGSC, 2012).

The barley genome also contains an abundance of repetitive DNA. Approximately 84% of the genome comprises mobile elements or other repeated structures, most of them retrotransposons. There is evidence of the importance of post-transcriptional processing as a central regulatory system supported by extensive alternative splicing (IBGSC, 2012). The barley gene space represents a core for trait isolation, understanding and exploiting natural genetic diversity.

Characteristics such as diploidism, inbreeding and temperate growing make barley a good model for plant biotechnology and genetic research. Large germplasm collections containing geographically diverse elite varieties, land-races and wild accessions are readily available and undoubtedly contain alleles that can improve the quality of the grain or the response of the crop to stress (IBGSC, 2012; Saisho and Takeda, 2011). Barley mutant collections are available, containing a broad morphological and developmental variation, which have been characterized and meticulously maintained. These, along with barley's recently sequenced genome, makes barley a great model for fundamental research and breeding in monocot crops.

1.3. Evolution of the domesticated barley and natural diversity

Barley is one of the crops of the Old World agriculture. Archaeological remains of barley grains indicate that this plant was domesticated about 10.000 B.C. The wild relative of barley is *Hordeum spontaneum* C. Koch. (Badr et al., 2000). This species still colonizes southwest

Asia from the eastern Mediterranean coasts to the semi-deserts of Afganistan (Jakob et al., 2014). Characteristics such as non-brittle rachis, six rowed spike and naked caryopsis are associated with the transition of barley from wild to cultivated plant (Pourkheirandish and Komatsuda, 2007). Migration of barley to regions outside its place of origin was accelerated through mutations developing reduced vernalization and photoperiod insensitivity (Von Bothmer et al., 1992). The accumulation of diversity for all these traits allowed barley to spread to different geographic areas.

The most important trait for barley domestication is probably non-brittle rachis. This characteristic results in efficient harvest without loss of grains. Spikes of the non-brittle mutant remain on the plant for longer after maturation in the field, therefore spikes with this mutation were harvested with higher frequency by ancient farmers than spikes with brittle rachis (Pourkheirandish & Komatsuda, 2007). Seed dispersal systems are designed to enable wild plants to survive in nature, but the loss of natural dispersal mechanisms was essential for agriculture.

One of the most conspicuous selections for increased seeds was the appearance of a six-rowed spike during barley domestication in the Middle East. The appearance of six-rowed barley crops producing three times more seeds per spike than two-rowed barley, constituted a milestone in the history of agriculture. The two-rowed phenotype exhibited by wild barley suggests that this phenotype is the ancestral form, which was left aside when six-rowed spike mutants were selected during cultivated barley domestication (Komatsuda et al., 2007).

The hulled or naked caryopsis of barley is also an important agronomic trait due to its direct link to dietary use. Hulled barley has a caryopsis with the husk cemented to the grain, while naked barley grows with easily separable husks upon threshing (Pourkheirandish & Komatsuda, 2007).

Other traits such as seed dormancy, vernalization and photoperiod requirements have also been modified by human selection (Pourkheirandish & Komatsuda, 2007). These traits have major implications for adaptation to diverse geographic regions, survival against adverse conditions and wider seed dispersal. In summary, all the traits manipulated during barley domestication allowed for its worldwide spread.

I.4. Socio-economic impact of the crop

Barley is the fourth most important cereal crop in the world after wheat, maize and rice and it is among the top ten crop plants in the world (Akar et al., 2004). Globally, more than 132 million tons were produced in 2012 (FAOSTAT, 2013), and the biggest producers were Russia, (13.9 million tons), France (11.3 million tons), Germany (10.4 million tons), Australia (8.2 million tons), Canada (8 million tons), Turkey (7.1 million tons), Ukraine (6.9 million tons), Spain (5.9 million tons), Argentina (5.1 million tons), USA (4.8 million tons), Poland (4.1 million tons) and Denmark (4 million tons) (FAOSTAT, 2013). In 2012, the world's main exporter of barley was France (5 million tons) followed by Australia (4.5 million tons), Germany (2.2 million tons), Argentina (2.1 million tons), Ukraine (2.1 million tons), Russia (2 million tons) and Canada (1 million tons). Most of these countries mainly export malting barley obtaining a profit 20% to 30% higher than that obtained from feed barley (Akar et al., 2004).

In 2011 Saudi Arabia was the main importer of barley with 6.1 million tons, followed by China (1.8 million tons), Belgium (1.7 million tons), Netherlands (1.6 million tons), Japan (1.3 million tons), Germany (1.3 million tons) and Spain (1 million tons) (FAOSTAT, 2013). Generally, Asian countries and Saudi Arabia import barley for animal and human consumption (Akar et al., 2004).

I.5. Major Uses of barley

Barley is mainly used to feed animals in European countries such as Germany, France, UK, Denmark and Italy. The grain is also a very important source for malt and human food (FAO, 2009). In regions of the world where maize cannot be cultivated due to short growing period, low temperatures in the spring, rainfall deficiency and higher evaporation, barley is cultivated as the primary food source for animals (Akar et al., 2004).

Barley grains are normally ground when used as feed to improve nutrient intake. Barley is considered an excellent source of carbohydrates and protein for livestock, although protein content is strongly affected by environmental conditions and can fluctuate from 10% to 15% (Akar et al., 2004). Other uses of barley include seed, for which 5% of the world production is reserved, and animal bedding and feed with barley straw commonly used in rural areas of developing countries. Mix cropping with vetches is another practice for production of high quality forage, hay or silage (Akar et al., 2004).

The second largest use of barley grain is for malt, although only 13% of the worldwide barley production is processed into malt (FAO, 2009). Malt barley is one of the principal ingredients in the manufacture of beer. Brewers can either purchase barley to produce their own malt or purchase the malt directly from malting companies. In either case, barley must meet strict standards (Table 1), otherwise the product cannot be sold as premium for malting and brewing and must be used for livestock feed. The malting characteristics of barley also depend on growing, harvesting, and storage conditions (FAO, 2009).

Table 1. Required criteria for barley grain to be used in the brewing industry (FAO, 2009).

Criteria	*Requirements for brewing industry*
Germination capacity (High)	min. 97% after 3 days Germination index*: min. 6.0
Grain Humidity	Water content: 12.0%, max. 13.0%
Protein content (Low)	between 9 % and 11.5%
Graded grain	Grading: min. 90%, > 2.5 mm.
β-glucan content	max. 4%
Purity (in the variety)	min. 99%
Pesticide and toxin contents	Pesticide residues according to local national law Ochratoxin according to local national law Aflatoxin according to local national law
Microorganisms content	Micro-organisms below setting levels

*Germination index (GI) is measured according to the European Brewery Convention (EBC). Kernels are germinated in the dark at 20°C in petri dishes on filter papers wetted with water. The germinated grains are counted after 24, 48 and 72 h of imbibition and GI is calculated by the EBC method (Frančáková et al., 2012).

During the malting process, barley seeds germinate producing two enzymes of major importance: □-amylase and □-amylase. These enzymes hydrolyse starch to dextrins and fermentable sugars. Although other grains also produce these enzymes, barley is the preferred grain because: (1) the barley husk protects the germinating shoot (acrospire) during germination, (2) the texture of the steeped barley kernel is firm, and (3) its use is traditional in the brewing industry (Robertson and Stark, 1993).

Production of malting barley is favoured by a long and cool growing season with uniform but adequate moisture and nutrient supplies. Maltsters, which are firms that purchase malting barley, usually specify the variety to be grown and have strict acceptance specifications (Bamforth, 2003). In addition to brewing, barley malt is used in the manufacturing of whisky,

snacks, sauces, chocolate powders, soft drinks, sprouted bread, and other products.

As barley grains have a higher soluble dietary fiber and lower low density lipoprotein (LDL) content than wheat, food manufacturers promote barley as a healthier food (Ensminger et al., 1994). Considering these factors, several hull-less barley varieties have been registered for human consumption and its acreage has increased in the western countries. In developing countries, various recipes contain barley products, and it is used mostly in baking mixed with other flours due its lower price compared to wheat and its nutritional value (Akar et al., 2004).

II. Senescence and Nitrogen Remobilization in Barley

Senescence (from Latin: *senescere*) refers to the natural process of growing old and is the last developmental stage in the lifespan of an organism. Senescence can be triggered by exogenous and endogenous factors and comprises several events regulated by a complex molecular machinery, the ultimate purpose of which is to guarantee the fitness and/or survival of the individual itself or of its progeny (Breeze et al., 2011; Guiboileau, et al., 2010; Lim et al., 2007). Senescence is characterized by deterioration at cellular, tissue, organ or organismal level (in case of monocarpic plants such as barley, wheat, rice and maize) (Avila-Ospina et al., 2014; Davies and Gan, 2012; Thomas, 2012).

After the onset of senescence, extensive remobilization of nutrients from senescing tissues to sink organs occurs. During this process, high quantities of nitrogen-containing compounds such as proteins and nucleic acids are disassembled and transformed into amino acids, urea and allantoin. Interconversion of amino acids to glutamate and glutamine facilitates further nitrogen loading in the phloem and translocation to the developing sinks.

The whole senescence process (initiation and rate of progress) is known as senescence timing, and influences key agronomic traits such as yield, nutrient use efficiency and quality of the crop (Hoffmann et al., 2012; Mickelson, 2003; Schmalenbach and Pillen, 2009; Uauy et al., 2006). Therefore, the understanding of intrinsic (genetic and epigenetic) and environmental factors regulating senescence, as well as the system of nutrient remobilisation (especially nitrogen) is needed to undertake efficient crop improvement strategies (Distelfeld et al., 2014).

II.1. Senescence timing

Senescence in plants varies depending on reproduction strategies and lifespan. For example polycarpic plants can live longer and produce seeds over several years, while monocarpic plants usually live shorter, senesce and die after flowering. It is important to point out that during the vegetative growth of monocarpic or perennial plants, organ senescence also occurs (Guiboileau et al., 2010) and promotes the remobilisation of nutrients from senescing organs to younger tissues.

Leaf senescence is the most studied type of senescence due to its impact on grain quality and yield. It occurs mainly due to ageing even if the plant is kept under optimal growth conditions

(well watered and fertilized). However, when the plant is grown under stress conditions or nutrient deficiency, the onset of leaf senescence may happen earlier and at an accelerated rate. During the vegetative stage, all nutrients needed by developing organs come mostly from root uptake rather than by remobilisation from senescing parts. In the reproductive stage, all nutrients are translocated from the senescing plant, making it the major source of nutrients for grain filling with a small contribution from root uptake as described in wheat (Distelfeld et al., 2014; Kichey et al., 2007). In monocarpic plants, flag leaf and glumes senesce last and are the main intermediaries in nitrogen remobilisation to the developing grains, (Davies and Gan, 2012).

Environmental factors influence senescence timing in plants. Nitrogen deficiency induces a decline in photosynthesis associated with the disassembly of cellular organelles and the increase of proteases (Gregersen et al., 2008; Parrott et al., 2010). In contrast, high nitrogen levels delay senescence (Hollmann et al., 2014) and retard the degradation of the photosynthetic apparatus.

II.1.1. Chlorophyll breakdown and STAY GREEN phenotype

Yellowing is the most visible symptom of plant senescence and is caused by chlorophyll degradation. This process is a mark of the transition of chloroplasts to gerontoplasts (Matile et al., 1999) and indicates the onset of disassembly of cellular components and the initiation of the remobilisation process (Martínez et al., 2008). The maintenance of cell metabolism during the whole senescence process is required to facilitate efficient nutrient remobilisation. In that way, an efficient chlorophyll catabolic pathway is essential since the accumulation of phototoxic chlorophyll degradation products induces the production of reactive oxygen species (ROS) that cause cellular damages (Hörtensteiner, 2009). Impaired or delayed chlorophyll catabolism ileads to *STAY GREEN* (*SG*) phenotypes. *SG* phenotypes are divided in cosmetic *SG* (phenotype confined to pigment catabolism while all the other senescence-related factors are unaffected) and functional *SG* (in which the whole senescence process is delayed) (Thomas and Ougham, 2014). The *senescence-induced degradation* (*sid*) locus of *Festuca pratensis* shows an *SG* phenotype due to the retention of chlorophyll, light harvesting chlorophyll a/b protein (LHCP) complexes and thylakoid membranes during senescence (Thomas and Ougham, 1999). The discovery of the *sid* locus led to great advances in the study of leaf senescence and chlorophyll breakdown (Thomas et al., 2002) and created new

perspectives for the use of this trait in horticulture, fruit quality and ornamental grass improvement (Barry, 2009).

Genetic studies on quantitative trait loci (QTL) for drought response showed that this phenotype coincided with *SG* QTLs in Sorghum (Harris et al., 2007; Kassahun et al., 2009). Selection of drought resistant plants was then based on the *SG* phenotype. The mechanism of drought tolerance in *SG* Sorghum, although not fully understood, seems to be associated with QTLs for xylem pressure potential that results in the enhancement of nitrogen uptake during the grain filling period (Thomas and Ougham, 2014).

II.1.2. Senescence timing and yield

Productivity in barley is quantified by the total grain yield per area, which is determined by features such as the (i) number of spikes per plant, (ii) number of spikelets per spike, (iii) number of grains per spikelet and (iv) grain weight (Distelfeld et al., 2014). The three first characteristics are determined genetically before the onset of senescence (Koppolu et al., 2013; Sreenivasulu and Schnurbusch, 2012) while the last one is determined throughout the reproductive stage depending on both genetic and environmental factors. Therefore, a good synchronization between senescence and grain filling is required in order to have optimal grain yields.

In late senescing cultivars of sorghum, wheat and barley showing an *SG* phenotype, an increase in biomass and a slight increase in grain yield have been observed (Howard Thomas and Ougham, 2014). This phenotype is also associated with drought resistance and a better performance under low nitrogen conditions in sorghum (Borrell et al., 2014). However, the increase in grain yields is not always significant and is highly influenced by environmental conditions (Gregersen et al., 2013), indicating that sink capacity may be a limitation to reaching high yields when senescence is delayed (Bingham et al., 2007).

II.1.3. Grain Protein Content (GPC)

Plant senescence is an important factor determining GPC in barley and thus defining the fate of the barley. High GPC is prefered for animal feeding while low GPC is desired for malt production (FAO, 2009). Studies for improvement of GPC through traditional breeding have

shown that a selection for high GPC is often associated with reduced yield (Jukanti and Fischer, 2008). This phenomenon has been explained by the dilution of grain proteins due to the extended carbohydrate accumulation that leads to a higher grain yield in stay green plants. The prolonged grain filling due to a lengthy photosynthesis in late senescing crops might also be associated with low grain nutrient remobilisation and consequently low grain nutrient content. In contrast, early senescing cultivars would have a more efficient nutrient remobilisation, producing high GPC with lower yields. Such effects of leaf senescence on yield and GPC is referred to as « the dilemma of senescence » (Gregersen, 2011). Genes controlling GPC trait such as the NAMB1 transcription factor, have been found in wheat and barley (Jukanti and Fischer, 2008; Uauy et al., 2006; see below in transcription factor paragraph).

II.1.4. Nutrient Remobilisation

In monocarpic, perennial and annual plants, senescence is not restricted to the reproductive stage. Senescence in barley starts from the lowest leaves (oldest) to the upper leaves (youngest) (Figure 4). Within the leaf, senescence starts from the tip and progresses to the base. During vegetative growth, the oldest leaves senesce during the early stages and the nitrogen they contain is translocated to younger leaves *via* the phloem and possibly xylem in the form of amino acids (principally glutamine and glutamate) (Feller et al., 2008; Figure 4). After anthesis, nitrogen is remobilised mostly to the flag leaf and developing grains *via* the phloem (Gregersen et al., 2008; Figure 4). Recent publications show that other nitrogen forms such as nitrate can be mobilized *via* both the phloem and xylem during leaf senescence in Arabidopsis (Fan et al., 2009; Hsu and Tsay, 2013). The nitrogen sources used for remobilisation are certainly different depending on the developmental stage and nitrogen nutritient conditions.

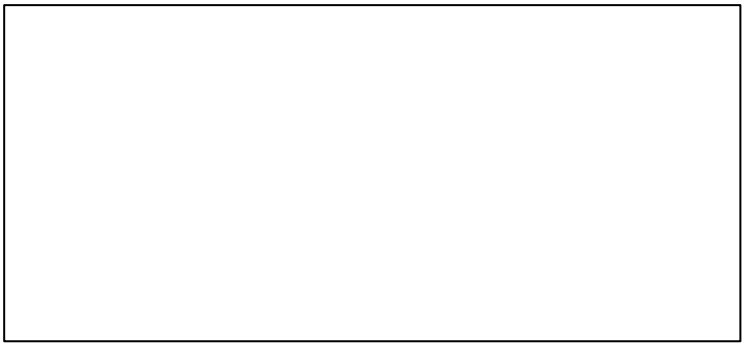

Figure 4. Representative scheme of nitrogen mobilisation into and out of plant organs during three developmental stages in the monocarpic cereal wheat. Positive signs indicate minor (+) and major (++++++) fluxes of nitrogen into each organ. Negative signs indicate minor (-) and major (--) nitrogen fluxes out of the plant organ in wheat plants before anthesis and after anthesis during early and late grain filling. Taken from Feller et al., 2008.

During leaf expansion, the nitrogen that is mainly used to synthetize Rubisco and other proteins is recycled after leaf maturation. During senescence these proteins become the major nitrogen sources for the other developing parts of the plant (Feller et al., 2008).

Nutrient recycling during leaf senescence is not only for nitrogen compounds. The catabolism of carbohydrates and lipids also occurs during senescence and requires a large ensemble of enzymes to perform it. Transcriptomic analyses have shown that transcripts coding for phosphoenolpyruvate carboxylase, citrate synthase, aconitase and isocitrate dehydrogenase are up-regulated during senescence in wheat (Gregersen and Holm, 2007). These enzymes participate in the formation of carbon skeletons and intermediate compounds for metabolic pathways involved in □-oxidation of fatty acids, glycolysis, neoglucogenesis and amino acid biosynthesis. Starch and fructan are considered to be the largest carbon storage compounds in grasses. During senescence, starch degradation into sucrose (the main form of carbon for transport in plants) facilitates carbon transport *via* the phloem to the sinks (Cerasoli et al., 2004; Reidel et al., 2009). Although transcriptomic data indicates that carbon is recycled and possibly exported to sinks during leaf senescence, fluxomic studies performed in maize for example, show that the rate of carbon remobilisation from senescing leaves to seeds is far lower than the nitrogen remobilisation rate (Cliquet et al., 1990). Carbon for grain filling mainly comes from CO_2 fixation in leaves, stems, glumes or silique envelopes.

II.2. Signaling and Regulation

Plant senescence has been studied for decades. Physiological, biochemical and molecular approaches have been used in order to unravel the mechanisms of nutrient remobilisation

during senescence and the regulatory machinery (endogenous and exogenous factors) controlling it. In recent years, systems biology approaches, with the use of the "omics", *i.e.* transcriptomics, proteomics and metabolomics (Breeze et al., 2011; Simons et al., 2014; Watanabe et al., 2013), have provided extensive lists of senescence related molecules and Senescence Associated Genes (*SAGs*). These genes are involved in a wide spectrum of functions that are up-regulated at different stages of the senescence process and include genes coding for proteases, autophagy, transmembrane transporters, metal ion binding proteins, catalases, DNA binding proteins, caspases, -oxidation pathway enzymes, pectinesterases, proteins related to reactive oxygen species (ROS) response, abscisic acid (ABA) and jasmonic acid (JA) response and transcription factors (Breeze et al., 2011; Christiansen et al., 2011; Hollmann et al., 2014; Parrott et al., 2007). An integrative picture of the senescence regulation pathways is starting to emerge from all the "omics" studies as well as from the QTL mapping studies performed on senescence related traits.

II.2.1. Transcription factors

During senescence, extensive changes in the transcriptome are observed. Studies of the transcriptomic profile performed in Arabidopsis showed 6323 differentially expressed genes during senescence (Breeze et al., 2011). In barley 750 genes showed at least a 2 fold change in their expression during senescence (Hollmann et al., 2014) and 6582 genes were differentially expressed in barley leaves when senescence was induced by steam-girdling (D. L. Parrott et al., 2007). A high proportion of these genes correspond to transcription factors that can themselves be either induced or repressed during senescence.

NAC and WRKY transcription factors are among the most studied genes involved in the regulation of senescence in Arabidopsis (Guo and Gan, 2006; Zentgraf et al., 2010). In barley, *NAC* genes have recently been characterized that are suggested to play a role in leaf senescence, root and seed development and hormone-regulated stress responses (Christiansen at al., 2011). It was shown that *NAC* genes are differentially expressed during senescence in barley, suggesting different roles of these genes throughout this process. Christiansen and Gregersen (2014) clustered *HvNAC* genes in three groups: group (1) formed by *HvNAC026, SaDH, XTH-like* and *nuclease I* represents genes highly up-regulated during senescence and with almost no expression in non-senescing leaves. Group (2) genes, *HvNAC005, HvNAC023, HvNAC027, HvNAC029* and *HvNAC030,* show an early up-regulation with a tendency to

stabilise at later stages of senescence. And group (3), formed by *HvNAC013, HvNAC022* and *HvNAC025*, contains genes which are highly expressed during the latest stage of senescence.

The role of NAC factors during leaf senescence has mainly been studied in Arabidopsis (Balazadeh et al., 2011; Hickman et al., 2013; Matallana-Ramirez et al., 2013; Yang et al., 2011). In wheat, the *NAC* gene *TaNAM* is highly up-regulated in flag leaves in the post-anthesis stages and controls timing of senescence, grain protein, Zn and Fe contents (Uauy et al., 2006). Transgenic plants with an RNAi construct reducing transcript levels of all copies of the *TaNAM* genes present on the three wheat genomes, showed a stay green phenotype and a reduction of 30% in grain protein content (GPC), 36% in Zn and 38% in Fe contents compared with non-transgenic plants. Grains did not show an increase in size despite the extended grain filling period, suggesting that the reduced grain protein, Zn and Fe contents resulted from impaired remobilisation from leaves rather than a dilution effect caused by a higher carbon filling of grains (Uauy et al., 2006).

WRKY genes and their role in the regulation of senescence have been studied in some detail in Arabidopsis as important regulators of senescence and plant-pathogen interaction (Zentgraf et al., 2010). *WRKY53* is the most studied gene in Arabidopsis (Miao et al., 2004; Miao et al., 2013). The over-expression and knock-out of *WRKY53* cause accelerated and delayed senescence phenotypes respectively (Miao et al., 2004). *WRKY53* induces the expression of *WRKY62* and catalase genes *CAT1*, *CAT2* and *CAT3* in response to treatment with hydrogen peroxide. This effect is strongly reduced in *WRKY53* RNAi plants (Miao et al., 2004).

WRKY70 is up-regulated during developmental senescence, and in response to dark stress and salicylic acid (Zentgraf et al., 2010). *WRKY70* knock-out Arabidopsis plants showed accelerated senescence and it is believed that this transcription factor is able to regulate other *SAGs* and senescence repressed genes (*SRGs*) since *WRKY70* deficient mutants showed an over-accumulation of *SEN1, SEN2* and *SRG1*. These genes contain several W box elements which are known as binding sites for WRKY transcription factors (Ulker et al., 2007). These W boxes can also be found in the promoters of several *WRKY* genes, indicating that the regulation of senescence processes by WRKY transcription factors is part of a complex network rather than a linear signalling pathway (Chi et al., 2013; A. M. Fischer, 2012).The transcriptomic analyses performed on Arabidopsis and barley have shown that members of other transcription factor families including C2H2-type Zinc finger, MYB, GRASS, bZIP and HIN are also up-regulated during senescence (Breeze et al., 2011; Hollmann et al., 2014; D. L. Parrott et al., 2007); however, their role in the regulation of senescence has not yet been established.

II.2.2. Sugar signaling and C:N Ratio

Plant senescence is strongly influenced by source-sink relationships, due to the importance of the distribution of nutrients and signalling compounds. Several studies in different species showed that senescence of mature leaves (source) can be induced by the accumulation or limitation of carbohydrates (Fischer and Feller, 1994; Parrott et al., 2005; Weaver and Amasino, 2001; Wingler et al., 2009). These conditions were coined by Koch (1996), as *carbon feast* and *carbon famine.*

A wide variety of studies using detached leaves, dark, different light intensities, sugar supply and steam girdling (influencing the accumulation or limitation of carbohydrates in plant organs), have shown accelerated senescence, induction of protease activities, accumulation of free amino acids and the degradation of chlorophyll, Rubisco and other photosynthetic proteins in barley and wheat (Fischer and Feller, 1994; Herrmann and Feller, 1998; Matile et al., 1988; Parrott et al., 2007; Parrott et al., 2005; van Doorn, 2008). *SAGs* such as protease genes were highly up-regulated in plants grown under high glucose and low nitrogen supplies but not in plants grown under high carbohydrate and high nitrogen conditions (Parrott et al., 2010; Pourtau et al., 2006; Schmid et al., 2005; Wingler et al., 2004), suggesting a strong influence of the ratio of carbohydrate to nitrogen concentrations (C:N ratio) on senescence.

A high accumulation of sugars was observed in mature leaves in tobacco and Arabidopsis at the transition checkpoint between sink and source leaves (Diaz et al., 2005; Céline Masclaux-Daubresse et al., 2010) which has been suggested as a trait characteristic of the sink-source transition. Further pharmacological studies indicated that sugar accumulation plays a role in early-*SAG* induction and in late-*SAG* repression (Masclaux-Daubresse et al., 2005).

Hexokinase has emerged as a sensor for the carbohydrate status. Transgenic plants over-expressing hexokinase showed early leaf senescence, while plants with down-regulated hexokinase showed delayed senescence (Dai et al., 1999; Moore et al., 2003). Such results indicated that sugar levels are one of the signals that can induce leaf senescence.

In addition, the finding that extracellular invertases are required for the cytokinin-mediated delay of senescence also suggested connections between sugar management, leaf senescence and sink-source relationships (Balibrea Lara et al., 2004).

II.2.3. Phytohormones and senescence signaling

The contribution of plant phytohormones to the regulation of senescence has been studied for years (Thomas and Stoddart, 1980). Cytokinins and ethylene are the best understood regulatory mechanisms related to senescence (Fischer, 2012).

Several studies have undoubtedly proved the senescence-delaying effect of cytokinins. Two studies have highlighted the importance of these plant hormones during leaf senescence; Zavaleta-Mancera et al. (1999) showed the *re-greening* of decapitated tobacco plants after cytokinins treatment while Gan and Amasino (1995) showed the delayed senescence of tobacco leaves in plants expressing an isopentenyl transferase gene (*IPT*) under the control of the *SAG12* promoter. Such findings gave rise to one of the most developed research strategies to manipulate leaf senescence in order to enhance plant yield and biomass called the P_{SAG12}-*IPT* autoregulatory senescence inhibition system (Guo and Gan, 2014). Many P_{SAG}-*IPT* transgenic crops with delayed leaf senescence phenotypes have been engineered (Liu, et al. 2010; Sykorová et al., 2008; Young et al., 2004) and these have enabled improved understanding of senescence-related processes that could be manipulated for agricultural improvement.

Gibberellins and auxins are also associated with senescence retardation, although their role in the regulation of senescence is much less well understood than that of cytokinins. Studies showed that mutations in the gene *ORE14* encoding the Auxin Response Factor 2 (ARF2), a repressor of auxin signalling, led to delayed senescence in Arabidopsis (Lim et al., 2010).

In contrast to the phytohormones discussed above, ethylene promotes leaf senescence. However ethylene can only induce senescence in leaves that have reached a defined age (L M Weaver et al., 1998). The effect of this compound in leaf senescence depends on age related changes. Ethylene treatment does not induce senescence in young Arabidopsis leaves, but it does induce senescence in older leaves, and its effect increases with ageing. Then, beyond a certain age, senescence is induced independently of ethylene (Jing et al., 2005). This finding produced the concept of *senescence window* that divides leaf lifespan in three phases: (I) never senescence, (II) ethylene dependent and (III) adaptative senescence (Figure 5). This model integrates other factors such as other hormones and signalling molecules with the regulation of leaf senescence (Jing et al., 2005).

In Arabidopsis and barley, genes related to the abscisic acid (ABA) pathway are up-regulated during leaf senescence (Buchanan-Wollaston et al., 2005; Jukanti et al., 2008). Drought induced leaf senescence increased the levels of ABA and decreased the levels of cytokinin in

wheat. In addition, ABA levels have been positively correlated with remobilisation of carbon and grain filling in this crop (Yang et al., 2003).

Application of brassinosteroids (BR) induces premature senescence which correlates with the study of mutants in the BR pathway, supporting a role for in the regulation of tsenescence (Schippers et al., 2007). The *det2* (*de-etiolated*) mutant, defective in the early stages of BR synthesis, shows a late senescence phenotype compared to WT plants (Chory et al., 1991).

Arabidopsis plants defective in the salicylic acid (SA) signalling pathway, *npr1* and *pad4* mutants and transgenic plants expressing the *NahG* gene (encoding a *Pseudomonas* salicylate hydroxylase) showed delayed yellowing (Morris et al., 2000). The role of SA in senescence is also supported by transcriptomic analyses made on *NahG* plants, which showed that induction of several genes (including putative disease resistance genes and hydrolases such as *SAG12*) during senescence actually depends on SA (Buchanan-Wollaston et al., 2005). Yoshimoto et al., (2009) also found that SA-deficient autophagy mutants (*atg*) do not show the early-senescence phenotype of *atg* mutants and that autophagy is induced by SA agonists.

In Arabidopsis, jasmonate (JA) levels and JA pathway related transcripts are increased in senescing leaves. JA treatment causes premature senescence in leaves of WT Arabidopsis but fails to induce early-senescence in *coi1* mutants (JA-insensitive), suggesting that the JA signalling pathway is also required to promote leaf senescence (He et al., 2002).

All these studies demonstrate the important role of phytohormones in leaf senescence and despite the fact that most of them have been carried out in Arabidopsis, it is believed that the senescence process in cereals crops is also regulated by these compounds.

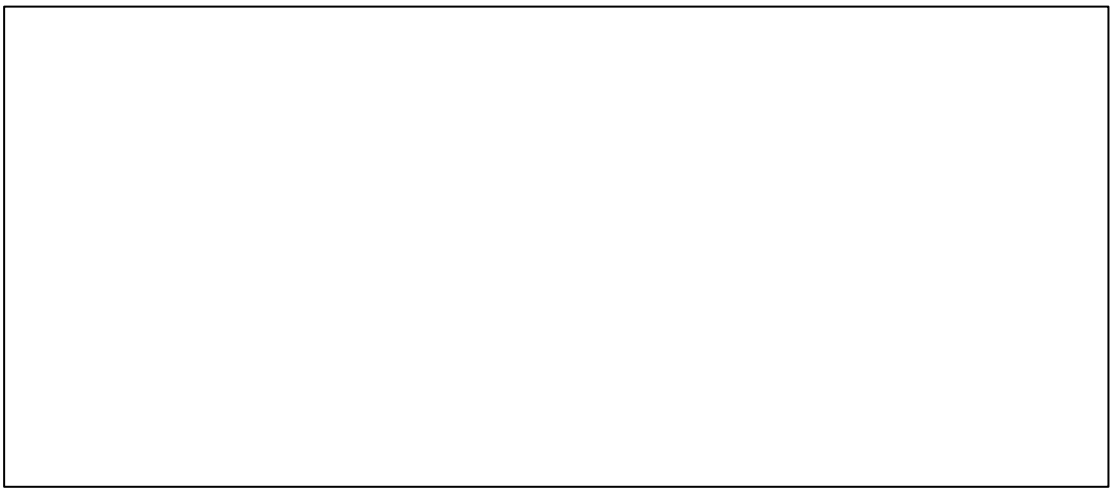

Figure 5. Concept of *senescence window* created by Jing et al., (2005) and Schippers et al., (2007) **for the regulation of leaf senescence by phytohormones.** The scheme shows the regulation of senescence by ethylene (and other phytohormones) and the three phases: Never senescence (phase I), green arrow; Ethylene dependent (phase II), yellow rhombus; and Ethylene independent or adaptative

senescence (phase III), yellow arrow. The effect of ethylene on leaf lifespan depends on each hormone. The action of senescence-repressing hormones is decreased with leaf age (blue triangle) while the action of senescence-promoting hormones is increased (orange triangle). Differences in size of black arrows for each hormone represent their importance in leaf senescence control. (GA) gibberellic acid; (JA) jasmonic acid; (ABA) abscisic acid; (SA) salicylic acid. Taken from Guiboileau et al. (2010).

II.2.4. Reactive oxygen species and senescence signalling

Reactive oxygen species (ROS) include both free radical (superoxide radicals, O_2^-; hydroxyl radical, OH^-; perhydroxy radical, HO_2 and alkoxy radicals, RO) and non-radical molecular forms (hydrogen peroxide, H_2O_2 and singlet oxygen, O_2*). These species have long been associated with senescence as signalling molecules in response to stress and through the oxidative modification of proteins during cellular degradation (Foyer & Noctor, 2005). For instance, the expression of the senescence related *WRKY53* is induced by hydrogen peroxide (Miao et al., 2004; Zentgraf et al., 2010). H_2O_2 also increases the expression of the NAC gene, *JUB1*, in Arabidopsis. The over-expression of *JUB1* delays senescence, confers resistance to abiotic stress and reduces levels of hydrogen peroxide while in *Jub1-1* knockout plants early senescence and hypersensitivity to stress is observed (Wu et al., 2012).

In wheat, the *stay green* and drought resistant mutant, *tasg1*, shows lower content of malondialdehyde and higher antioxidative activities compared to WT (Tian et al., 2012). When the spikelets (reproductive sink) are removed from the wheat plant during anthesis, flag leaves show a delayed senescence compared with plants where the spikelets have been left intact (control). Plants with removed spikelets also have a lower glutathione/oxidized glutathione ratio (GSH/GSSG) and antioxidant enzyme activity compared to control plants (Srivalli and Khanna-Chopra, 2009). These studies suggest that ROS-mediated signalling has a key role in senescence in wheat. However, the specific factors involved in this process (*e.g.* functional homologues of Arabidopsis WRKY53 and JUB1) remain to be determined.

II.3. Nitrogen Remobilisation

Leaf proteins and in particular photosynthetic proteins of plastids are degraded en-mass during senescence, providing an enormous source of nitrogen that plants can use to satisfy demands of sinks during the grain filling (Masclaux-Daubresse et al., 2010). Nitrogen remobilisation is a gradual process involving different plant organs and is highly regulated

during senescence. The efficiency of the mechanisms of degradation, assimilation and transport of nitrogen-containing compounds from source to sink organs guarantee an effective grain filling and in the case of crops it can also bring economic profit.

II.3.1. Disassembly of chloroplastic components

As mentioned above, chloroplast degradation is a significant event in senescence as Rubisco and the photosynthetic apparatus (major components of the chloroplast) represent the biggest source of nitrogen and carbon that is translocated to the grain (Gregersen et al., 2008).

Nitrogen comes mainly from proteolysis of proteins contained in the source organs (mostly senescing leaves and stems) (Masclaux-Daubresse et al., 2008). During senescence, high levels of protease transcripts and proteolytic activity are both induced (Hollmann et al., 2014; Parrott et al., 2005), including plastidial (aminopeptidases), cytosolic (proteasome) and vacuolar proteases (cysteine and serine proteases), the vacuolar cysteine endopeptidases being the most biochemically active ones (Distelfeld et al., 2014). This suggests that plastidial peptidases, though not as active as vacuolar endopeptidases, initiate and accelerate degradation through oxidative modification of proteins prior to their final degradation in the vacuole (Feller et al., 2008). In senescing wheat leaves, Rubisco, chloroplastic glutamine synthetase, other stromal proteins and their degradation products are localized into small spherical vesicles called Rubisco Containing Bodies (RCB) (Chiba et al., 2003) (Figure 6). These bodies are released from chloroplasts, and their cargo can be degraded before they reach the central vacuole by proteolytic vesicles such as Senescence-Associated Vesicles (SAVs) (Martínez et al., 2008) or by autophagy (Izumi et al., 2010) (Figure 6). This suggests that both plastidial and vacuolar degradation machineries work together to disassemble the chloroplast proteome.

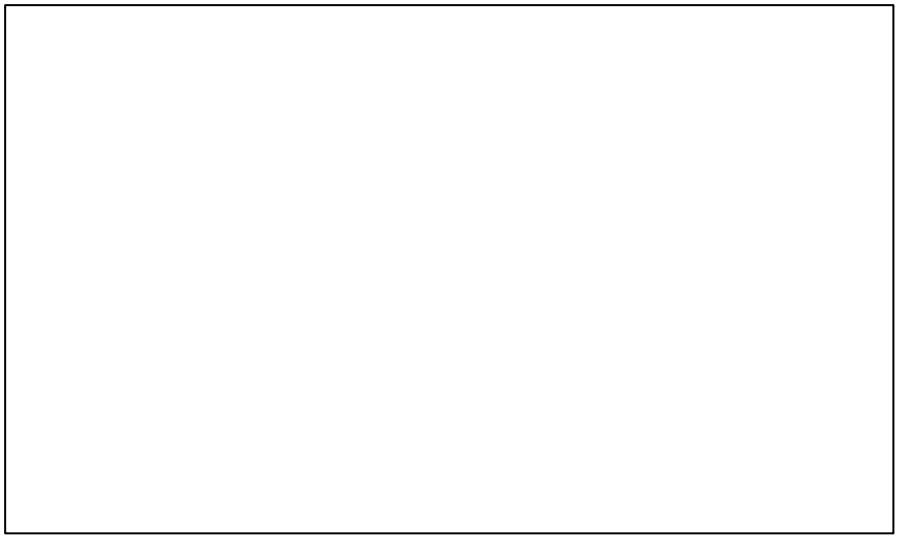

Figure 6. Scheme of chloroplast degradation and release of Rubisco Containing Bodies (RCB). RCB are released in the cytosol from the senescing chloroplast for their further degradation in the central vacuole. RCB can either be directly engulfed by the central vacuole (a), may fuse (b1) or be engulfed (b2) by Senescence Associated Vacuoles (SAVs) and the products may afterwards fuse with the tonoplast membrane (b1 and b2) or be engulfed by autophagosomes that later are released into the central vacuole (c). Taken from Gregersen et al. (2008).

II.3.2. Proteases involved in cell protein degradation

Organelles such as chloroplast have a dynamic protein environment and proteases are probably one of their major components. However, the identities of these proteases remain largely unknown. Several members of the proteolytic machinery of chloroplasts and other organelles such as mitochondria have been described in Arabidopsis, although their exact role has not been elucidated (Sinvany-villalobo et al., 2004). They include the ATP-dependent proteases (Clp, Lon and FtsH), the ATP-independent protease Deg and the Spp protease (Adam and Clarke, 2002; Ostersetzer et al., 2007; Schuhmann and Adamska, 2012).

Other proteases have been identified during senescence in Arabidopsis including the zinc protease of pea chloroplast EP1 which degrades Rubisco and the chloroplast Zn^{2+} dependent metaloprotease FtsH6 responsible for the degradation of the light harvesting complex of photosystem II (LHCII) (Zelisko et al., 2005).A contribution of vacuolar proteases to the degradation of Rubisco has been shown through the use of protease inhibitors. Thoenen et al. (2007) showed that degradation of the LSU subunit of Rubisco during senescence in wheat was delayed by the use of the (vacuolar) cysteine protease inhibitor, E-64. Similarly, Martínez et al. (2007) found four cysteine proteases of 36, 39, 42 and 46 kDa by gel-activity assays and the use of protease inhibitors in senescing flag leaves of wheat.

Transcriptomic analyses of senescing barley leaves (in experiments using a girdling system or different nitrogen treatments) showed an increase in the expression of several cysteine proteases and some other genes coding for proteins located in lytic vacuoles (Hollmann et al., 2014; Parrott et al., 2010, 2007). Parrott et al. (2007) showed that proteases were up-regulated at 4 and 8 days after girdling and also in senescent plants grown under standard and high nitrogen supply. High nitrogen treatment caused a delay in senescence and some proteases only showed up-regulation in plants from the standard nitrogen treatment (Table 2).

Prins et al. (2008) over-expressed the cysteine protease inhibitor of rice cystatin OC-1 in tobacco plants. They showed that the presence of antiproteases resulted in a delay in the senescence-associated decline of Rubisco and photosynthesis under both optimal and stress conditions. OC-1 transgenics showed an increase in the amount of remaining Rubisco after flowering, compared to WT plants. These results suggest that cysteine proteases are involved in the degradation of Rubisco during leaf senescence (Prins et al. 2008).

All these findings confirm that the degradation of organelle proteins during senescence is a process involving several types of proteases at different stages and in multiple cell compartments. They also indicate a selective degradation of some chloroplast proteins. For instance, Rubisco is pre-degraded inside the chloroplast and its degradation products are released through RCB to be translocated to the central vacuole (Figure 6). By contrast, there is no evidence of transfer of thylakoid proteins into vacuolar compartments (Distelfeld et al., 2014), suggesting that different catabolic pathways may be used for the degradation of stromal and thylakoid proteins. The ensemble of senescence-associated proteins are not completely characterized, therefore further studies are needed in order to fully understand this complex process.

Table 2. Cysteine protease genes up-regulated during barley senescence. (A) Genes reported by Parrott et al. (2007) in senescing barley plants induced by girdling (*carbon feast*). (B) Genes reported by Hollmann et al. (2014) from barley plants grown under standard and high nitrogen conditions.

A. Relative expression data for candidate genes in 8 days girdled barley (*Hordeum vulgare*) leaves (Parrott et al. (2007)		
		Fold change compared to control
Gene contig	**Tentative activity**	**Girdling 8g/8c***
Contig10941_at	SAG12 protein	1.962
Contig12029_s_at	Subtilase family protein	11.69
Contig6013_at	Cnd41-like chloroplast nucleoid DNA-binding prot.	2.296
Contig6202_at	Proline iminopeptidase	2.562
Contig4312_s_at	Neutral leucine aminopeptidase preprotein	4.028
Contig2779_at	Aspartic endopeptidase	3.258
Contig9006_at	Papain-like cysteine peptidase	3.701
Contig600_at	Serine carboxypeptidase III precursor (CP-MIII)	15.02

B. Relative expression of genes in both senescing flag leaves of plants from plots with standard and excess nitrogen supply (Hollmann et al. 2014)			
		Fold change compared to non senescing leaves	
		Nitrogen treatment	
Accession	**name**	**Standard**	**High**
AM941123	Cysteine protease	2,59	2,18
AM941124	Cysteine protease	5,26	2,92
BF256720	Cysteine protease	2,18	2,17
TA35023_4513	Ubiquitin protease	2,61	2,78
AM941127	Cysteine protease	4,27	1,69
AM941122	Cysteine protease	3,66	1,98
AM941116	Cysteine protease	2,37	1,01
TA45222_4513	Cysteine protease	2,36	0,97
EX594583	Cysteine protease	2,24	1,38
CD663018	Cysteine protease	2,17	1,32
AK251038	Serine protease	3,56	1,63
TA57593_4513	Serine protease	2,61	0,48
BY868089	Ubiquitin.E2	2,24	0,96
TA31497_4513	Ubiquitin.proteasome	2,03	1,31

*Analysis was performed after 8 days of girdling comparing gene expression in girdled plants (8g) with non-girdled plants (8c). Grey shade highlights genes overexpressed only in standard nitrogen conditions.

II.3.3. Nitrogen metabolism associated with remobilisation

Nitrogen remobilisation from senescing source leaves to developing sinks (younger leaves or seeds) during vegetative and reproductive stages in monocarpic plants has been studied in several plant species. In this process, proteolytic activities associated with senescence ensure that proteins are degraded into amino acids, amides and ammonium to be re-assimilated, interconverted and transported *via* the phloem (Gregersen et al., 2008). Glutamate is the major phloem-exported amino acid in barley and wheat, followed by aspartate, glutamine, threonine and serine (Caputo et al., 2001; Distelfeld et al., 2014; Winter et al., 1992). Glutamate is an important compound for senescence metabolism. It is involved in the tricarboxylic acid (TCA) cycle (as precursor of 2-oxoglutarate) (Forde and Lea, 2007) and its level is increased in the phloem of wheat during senescence (Simpson and Dalling, 1981).

Most of the amino acids produced by the degradation of proteins during senescence undergo modifications previous to their uploading into the phloem, and the glutamate synthase cycle (GS-GOGAT) appears to be of major importance in this context.

The pathway of biosynthesis of glutamine differs depending on the leaf age. This pathway has been divided in two: i) the synthesis of this amino acid in young tissues and ii) it's synthesis in senescing tissues (such as leaves) (Figure 6). In young leaves, glutamine synthesis is performed in the chloroplast using the chloroplastic form of glutamine synthetase (GS2) and a ferredoxin-dependent glutamate synthase (Fd-GOGAT) (Masclaux-Daubresse et al., 2008). Nitrate reduction, photorespiration and the TCA cycle supply the nitrogen and carbon needed for the glutamine biosynthesis. Then, with the onset of senescence and chloroplast disassembly, the chloroplastic enzymes and redox potential are modified and the activity of the GS2/GOGAT cycle decreases (Masclaux et al., 2000). In senescing leaves, glutamine is synthesised in the cytosol by the cytosolic glutamine synthetase isoforms (GS1) from the ammonia released by proteases, mitochondrial glutamate dehydrogenase GDH and other hydrolases (Figure 6). Utilizing the amino acids derived from proteolysis in the chloroplast, a series of transamination reactions results in an increase of glutamate that serves as a substrate for GDH. This process provides 2-oxoglutarate to support respiration and ammonia, which in turn is re-assimilated by GS1 to produce glutamine for phloem uploading (Masclaux-Daubresse et al., 2008).

GS2 is encoded by a single nuclear gene, while GS1 isoforms are encoded by several loci (Goodall et al., 2013; Orsel et al., 2014). The GS2 protein is the main form in young leaves and is degraded during leaf senescence (Mitsuhashi and Feller, 1992). The *GS2* gene is also highly expressed in young leaves but decreases throughout senescence. In contrast, *GS1* genes are induced during early senescence at late developmental stages. There is evidence that GS activity in flag leaves of wheat is a good candidate to improve efficient remobilisation of nitrogen to the grain (Kichey et al., 2007), and *GS1* loci have been associated with QTLs for nitrogen grain content and grain weight in wheat (Habash et al., 2007). In addition, the manipulation of GS1 activities through the over-expression of different *GS1* genes in leaves of maize led to an increased yield (kernel number and size were increased) (Martin et al., 2006).

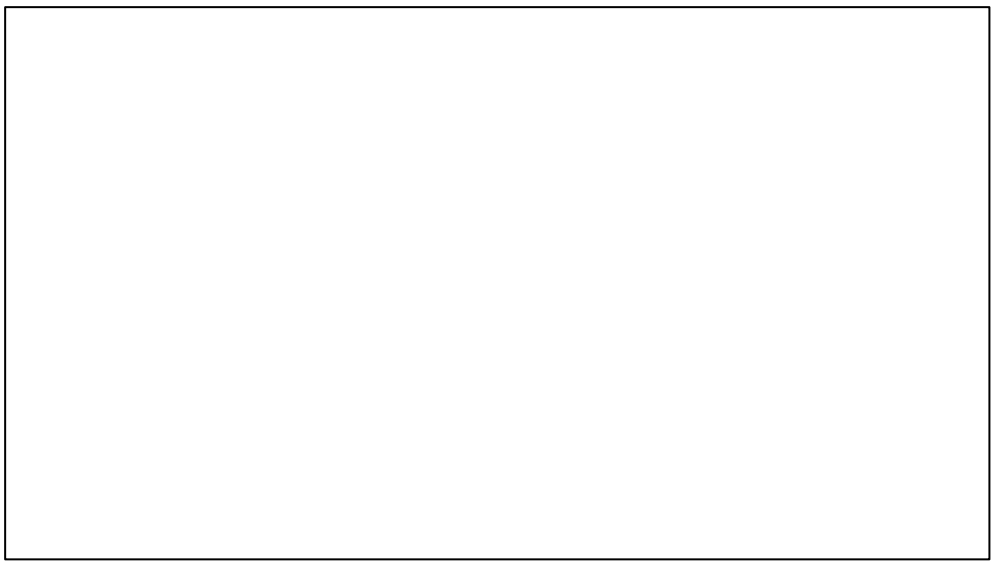

Figure 6. Biosynthesis of glutamine in young and old tissues and loading into the phloem for remobilisation. Two metabolic pathways for the synthesis of glutamine in mesophyll and companion cells of young (left, green) and senescing (right, yellow) leaves. Glutamate dehydrogenase (GDH); Glutamate decarboxylase (GAD); Cytosolic Glutamine Synthetase (GS1); Chloroplastic Glutamine Synthetase (GS2); Asparagine Synthetase (AS); Glutamine (GLN); Glutamate (GLU). Taken from Masclaux et al., 2008.

Glutamine and glutamate are not the only nitrogen forms for translocation. Other amino acids can be generated from them by enzymes such as asparagine synthetase (AS) and aminotransferases. In barley and Arabidopsis, AS isoforms are encoded by several *ASN* genes (Møller et al., 2003). Transcriptomic analyses of near isogenic early vs. late senescing germplasms showed an up-regulation of an *ASN* gene in flag leaves at 21 days after anthesis (Jukanti et al., 2008).

II.3.4. Nitrogen transport to the developing sink

In order to transfer the nitrogen derived from proteolysis in senescing source leaves to the protein bodies in the endosperm of developing grains (sink), several short and long distance transport steps are required. The release of amino acids or peptides from vacuoles or chloroplasts into the cytosol is mediated by unknown membrane transporters (Chen et al., 2001). In addition, amino acid remobilisation necessitates loading into sieve element companion cell (SE–CC) complexes of the minor veins (Tegeder and Rentsch, 2010). Although all protein amino acids are found in the phloem, their concentration is different from that found in the whole leaf, with glutamate, glutamine, asparagine, aspartate, alanine,

and serine being the most abundant (Zhang et al., 2010). This suggests a certain kind of selectivity in phloem loading.
Phloem loading of nitrogen may be done through an apoplasmic or symplasmic route depending on the plant species (Turgeon and Wolf, 2009). In the symplasmic pathway, amino acids diffuse down their respective concentration gradients towards the phloem. The apoplasmic phloem loading involves the release of amino acids into the cell wall space and is generally observed in crop plants including barley and wheat. In Arabidopsis, this transport is mediated by amino acid transporters and one of them, SIARS1, has recently been characterized (Ladwig et al., 2012).

It is speculated that amino acid translocation from senescing leaves to the grain could transit *via* the root system. The majority of root amino acids are transported to leaves through the xylem, and xylem-phloem exchange may occur in the major veins of leaves. Transfer of amino acids from the xylem to the phloem takes place in order to directly deliver nitrogen to the fast growing sinks, and is a strongly conserved mechanism in most species. This mechanism is important for the transport of root-generated amino acids to the sinks and also for indirect transport (*via* the root system) of leaf-synthesized amino acids to the grains (Distelfeld et al., 2014; Tegeder, 2014).

Amino acid transport is selective and depends on the charge and side chain of each compound. In cereals, transfer was shown to be more efficient for basic and bulky hydrophobic amino acids than for acidic amino acids (Fischer and Feller, 1994).
In Arabidopsis, the amino acid permease 2 (AAP2) was demonstrated to be essential for amino acid phloem loading (Zhang et al., 2010). In addition *aap6* deficient mutants (AAP6 is localized in xylem parenchyma cells) showed reduced phloem amino acid levels, indicating its function in the exchange of nitrogen between xylem and phloem (Hunt et al., 2010).

III. Autophagy and its role in nutrient remobilisation during senescence

This introduction chapter will be completed by the review presented in chapter IV.

During organelle disassembly, cytoplasmic components are partially degraded and transported to the central vacuole for further breakdown and remobilisation. Vesicles with or without high levels of protease activity seem to be associated with the degradation and transport of proteins during senescence and nutrient starvation (Masclaux-Daubresse et al., 2008). The *senescence-associated vacuoles* (SAVs) and *Rubisco-containing bodies* (RCBs) are such kinds of vesicles. They have been associated with the degradation of chloroplast stroma proteins during leaf senescence, although their exact role still remains unclear (Izumi et al., 2010; Martínez et al., 2008).

In addition to SAVs and RCBs, macro-autophagy vesicles have also been described in plants. Autophagy is considered as the predominant pathway for transporting proteins and organelles to the central vacuole for degradation (Bassham, 2009; Thompson and Vierstra, 2005). Autophagy describes portions of the cytoplasm, including entire organelles like peroxisomes or mitochondria, being engulfed into a double membrane vesicle (called autophagosome) and delivery of these autophagosomes to the central vacuole (Figure 7). When the vesicle is anchored to the vacuole, the outer membrane of the autophagosome fuses with the tonoplast to release the internal vesicle, composed of the inner membrane and its cargo (a structure called an autophagic body), which afterwards is degraded by vacuolar hydrolases (Li and Vierstra, 2012) (Figure 7).

Figure 7. Autophagy in plants. The autophagosome, a double membrane structure, is formed around a cytoplasmic cargo. The autophagosome then transports the cargo to the vacuole and fuses its outer membrane with the tonoplast releasing the inner vesicle (autophagic body) into the vacuole. The autophagic bodies are then degraded by vacuolar hydrolases and the degradation products are exported out of the vacuole for reuse. Taken from Liu and Bassham (2012).

Genetic screens of yeast (*Saccharomyces cerevisiae*) allowed the identification of a set of AuTophaGy related genes (*ATG*) required for carrying out this process. These genes are highly conserved between organism (yeast, animals and plants) and several studies using knockout mutants and fusion protein systems with autophagy markers (GFP-ATG8) have demonstrated their role in nutrient recycling during senescence and under stress conditions (Guiboileau et al., 2012; Izumi et al., 2010; Slavikova et al., 2008; Thompson et al., 2005; Yoshimoto et al., 2004).

III.1. Autophagy machinery and mechanisms in plants

As mentioned above, *ATG* genes were first discovered in yeast, and then homologues of these genes were also identified in animals and plants. Studies in Arabidopsis, followed up by recent studies in maize, rice, wheat, soybean and tobacco have suggested that a similar *ATG*-mediated system exists throughout the plant kingdom (Chung et al., 2009; Guiboileau et al., 2012; Kuzuoglu-Ozturk et al., 2012; Xia et al., 2012; Zientara-Rytter et al., 2011). More than 30 *ATG* genes have been identified in *S. cerevisiae*. These genes are related not only to autophagy (considered a non-selective process) in yeast but also with other morphologically and mechanistically similar processes that target specific cargos such as the cytoplasm to vacuole targeting (*Cvt* pathway), pexophagy (targeting peroxysomes) and mitophagy (targeting mitochondria) (Yang and Klionsky, 2010).

Although these four types of autophagy require different *ATG* genes in order to perform their function, around 17 *ATG* genes (depending on the species) are needed in all four events for the formation of the autophagosome and transport of the cargo to the vacuole. These genes are known as the core molecular machinery and their counterparts have been found in plants (Kim et al., 2012).

ATG genes belonging to the core molecular machinery have been divided into four functional groups: the ATG1-ATG13 kinase complex, *ATG9* and associated proteins, a phosphatidylinositol 3-kinase (PtdIns3K) complex, and two ubiquitin-like conjugation systems (ATG5-ATG12 and ATG8). The ATG1-ATG13 kinase and the PtdIns3K complexes are in charge of the initiation and formation of the autophagosome membrane, ATG9 and associated proteins are responsible for lipid recruitment and the ATG5-ATG12 and ATG8 ubiquitin-like conjugation systems elongate and close the autophagosome membrane (He and

Klionsky, 2009). Homologous genes belonging to these complexes have been found in Arabidopsis (Avin-Wittenberg et al., 2012).

III.1.1. ATG1-ATG13 kinase complex

In yeast this complex comprises ATG1, ATG11, ATG13, ATG17, ATG29 and ATG31. The protein kinase ATG1 is involved in the regulation of autophagy initiation in response to nutrient limitation. In optimal nutrient conditions, the target of rapamycin (TOR) protein hyperphosphorylates *ATG13* and *ATG1*, precluding their activation and mutual interaction (Figure 8). During starvation, TOR is inhibited and triggers the dephosphorylation of ATG1 and ATG13, allowing their interaction as well as interaction with several other factors such as ATG17 (Thompson and Vierstra, 2005) (Figure 8). Subsequently, the assembled and activated ATG1-ATG13 kinase complex is able to stimulate processes either directly or indirectly related to autophagic vesiculation (Li and Vierstra, 2012) (Figure 9). In Arabidopsis, *ATG13a* and *ATG13b* double knockout mutants are hypersensitive to nutrient limitations and show accelerated senescence. Synthesis of the ATG12-ATG5 and the ATG8-phosphatidylethanolamine (ATG8-PE) conjugation systems (essential for autophagy) still occurs in this knockout, but the plants are impaired in the construction of autophagic bodies, indicating that the ATG1-ATG13 kinase complex regulates downstream events related to the enclosure of the autophagosome and/or vacuolar delivery (Suttangkakul et al., 2011).

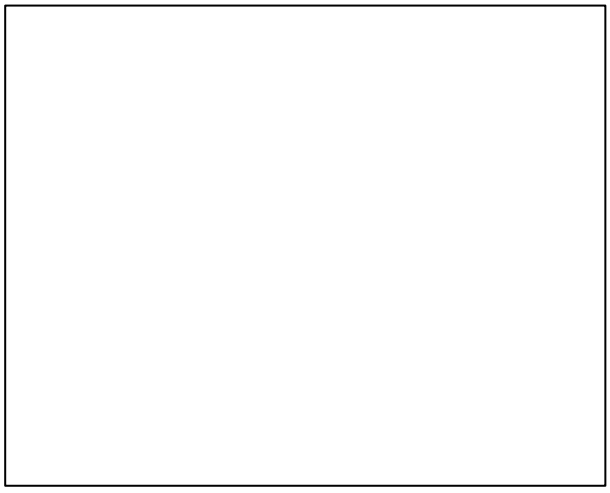

Figure 8. Regulation of the autophagy pathway by nutritional status in yeast. Under optimal nutritional conditions, TOR kinase phosphorylates ATG1 kinase and ATG13 and promotes dissociation from the complex that includes ATG11, ATG17 and VAC18. Under nutrient limiting conditions, ATG1 and ATG13 are dephosphorylated promoting the assembly of these components and activation of the kinase complex. The active ATG1–ATG13 kinase complex promotes nucleation of the pre-autophagic structures (PAS) to form the autophagosome in a process involving the PtdIns3K complex. Taken from Thompson and Vierstra, 2005.

III.1.2. Phosphatidylinositol 3-kinase (PtdIns3K) Complex

In yeast the PtdIns3K complex is known to participate in various membrane trafficking events and is in charge of the Phagophore Assembly Site (PAS) induction and nucleation (Figure 9). The complex includes Vps34 (a serine threonine kinase), Vps15 (a protein kinase), ATG6 and ATG14 (Xie and Klionsky, 2007). Vps15 is required for the association of Vps34 to the PAS and ATG14 is in charge of the association of Vps34 and ATG6. The role of ATG6 in the PtdIns3K complex is still not clear (Yang and Klionsky, 2009). It is believed that this complex recruits other PtdIns3K binding proteins to the PAS including ATG18 and the proteins from the ATG9 cycling system (Liu and Bassham, 2012). In Arabidopsis, Vps34, ATG6 and Vps15 have been shown to be essential for pollen germination and development (Fujiki et al., 2007; Lee et al., 2008; Wang et al., 2012; Xu et al., 2011). Plants deficient in the expression of *ATG6* showed a range of phenotypic abnormalities including short roots, small leaves, dwarfism, fewer flowers, early senescence and low fertility (Qin et al., 2007). In other studies, *ATG6* proved to be essential for restricting cell death to the infection site in plants undergoing programmed cell death (PCD) induced by pathogen infection in Tobacco (Liu et al., 2005). Homologous genes of yeast *ATG14* have not been described in Arabidopsis or other plants so far.

III.1.3. ATG9 Cycling system

ATG9 is an integral membrane protein that seems to work as a *membrane carrier* during the autophagosome assembly process (Yang and Klionsky, 2009). Unlike other ATG proteins, which are localized at the PAS, ATG9 localizes both to the PAS and to non-PAS punctuated structures, and it is believed that this protein cycles between these two structures (Liu and Bassham, 2012) (Figure 9).

In yeast, ATG9 has been observed to be localized at non-PAS punctuated structures close to the surface of the mitochondria (Reggiori et al., 2012), while in mammalian cells it localizes to the *trans*-Golgi network and late endosomes (Young et al., 2006), suggesting that these organelles may be membrane sources for the elongation of the autophagosome in these organisms. In plants, the origin of the membranes used in this process is still unknown. The traffic of ATG9 from non-PAS structures to PAS requires *ATG11*, *ATG13* and *ATG27*, while the retrieval of ATG9 from PAS involves the ATG1-ATG13 complex, ATG2, ATG18 and the PtdIns3K complex (Xie and Klionsky, 2007). Any malfunction of these components leads to

either the restriction of ATG9 localization at PAS or its accumulation at PAS (Reggiori et al., 2004; Yen et al., 2007). Homologous of *ATG1*, *ATG2*, *ATG9*, *ATG13* and *ATG18* have been found in Arabidopsis (Avin-Wittenberg et al., 2012). *ATG18* includes eight family members, each member with a different expression pattern according to senescence and nutritional conditions (Xiong et al., 2005). Plants with a deficient *ATG9* or *ATG18* gene expression displayed a typical autophagy-deficient phenotype (early senescence, hypersensitivity to stress) and also an impaired remobilisation of nitrogen from source to sink organs during senescence (Guiboileau et al., 2012).

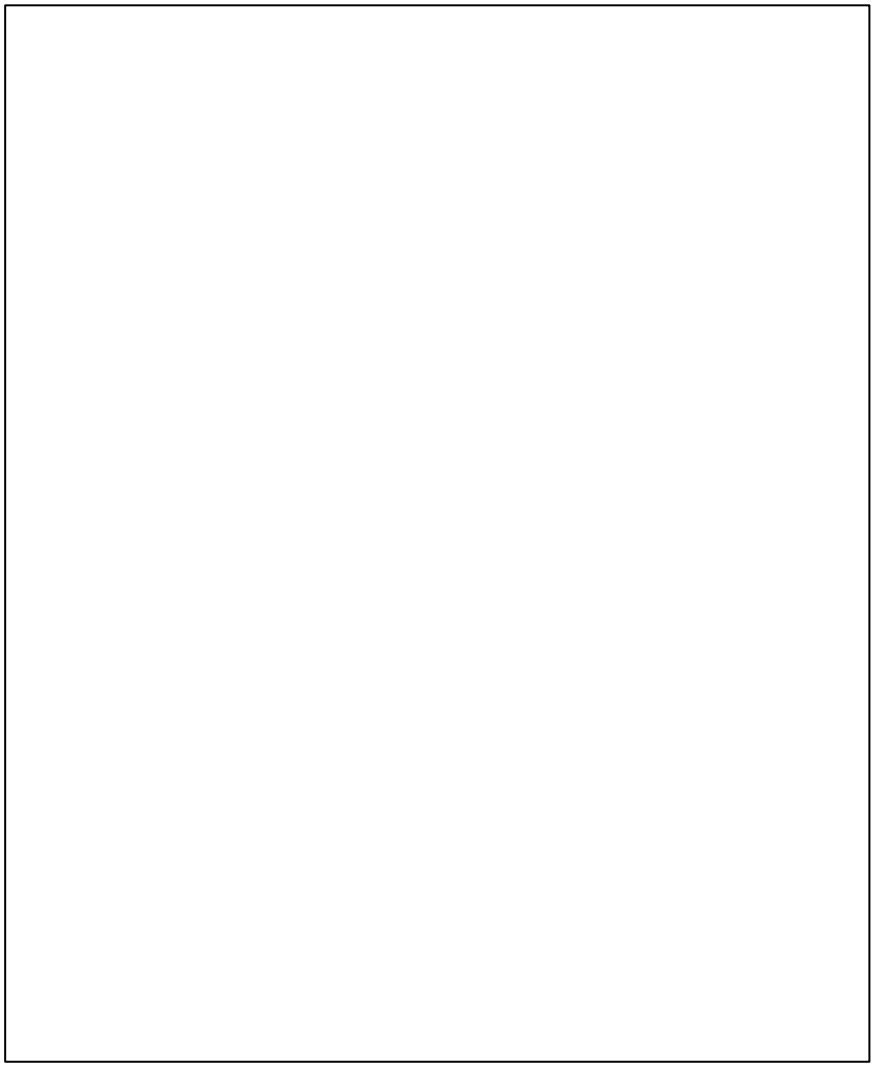

Figure 9. Autophagosome formation at the phagophore assembly site (PAS). Different protein complexes from the core machinery are involved in different stages of the formation process. The yellow shading indicates the site of action of the proteins mentioned. (**a**) ATG9 cycles between the PAS and non-PAS peripheral sites carrying membrane fragments required for autophagosome elongation. Delivery of membrane fragments to the PAS includes several transport factors (ATG11, ATG13 and ATG27) while ATG9 retrieval from PAS involves the ATG1-ATG13 complex, ATG2, ATG18 and the PtdIns3K complex (arrows indicate the factors needed for transport in the indicated direction). (**b**) The localization of ATG2 and ATG18 is regulated by ATG9, ATG1 and the PtdIns3K

complex. (**c**) The PtdIns3K complex includes Vps34, Vps15 and ATG6. During the membrane expansion ATG18 binds PtdIns3K. Other components include the ATG5-ATG12 and ATG8-PE ubiquitin-like conjugation systems. Their localization in the PAS depends on ATG9 and the PtdIns3K complex. The function of ATG5-ATG12 and ATG8-PE systems during the autophagosome formation is still not known but they are essential for this process. Taken from Xie and Klionsky, 2007.

III.1.4. ATG5-ATG12 and ATG8-PE Ubiquitin-like conjugation systems

Autophagosome formation requires two ubiquitin-like conjugation systems involving two ubiquitin-like proteins (Ohsumi, 2001). During this process ATG8 is cleaved at its C-terminus by the cysteine protease ATG4 exposing a glycine residue (Figure 10A). This glycine is then activated by the E1-like ATG7 and then transferred to the E2-like ATG3. Finally, ATG8 is conjugated to the membrane lipid phosphatidylethanolamine (PE) (Figure 10A). This conjugation is reversible since ATG4 is able to cleave ATG8 from PE and these two components can thus be recycled (Liu & Bassham, 2012).

In the case of ATG12 there is no protease priming since the amino acid sequence of this protein ends with a glycine residue. In this case ATG7 activates ATG12, which is then transferred to the E2-like ATG10 and eventually conjugated to the target protein ATG5 (Figure 10B). The ATG12-ATG5 system interacts further with the coiled-coil protein ATG16 to form a tetrameric ATG5-ATG12-ATG16 complex (Figure 10B). This process is essential for autophagy (Geng and Klionsky, 2008).

Both ATG8-PE and ATG5-ATG12-ATG16 complexes localize at the PAS. ATG8-PE localizes equally in both inner and outer membranes of the autophagosome while ATG5-ATG12-ATG16 is mainly found in the outer membrane (Yang and Klionsky, 2009).

In Arabidopsis, homologues of all the ubiquitin-like conjugation systems have been found. Some of them are single genes as in yeast (*ATG3*, *ATG5*, *ATG7* and *ATG10*) whereas other gene families contain several members, *ATG4* and *ATG12* include two members each and *ATG8* contains nine members (Avin-Wittenberg et al., 2012).

In Arabidopsis, despite their amino acid sequence similarities, *ATG12a* was shown to play an important role in basal autophagy while *ATG12b* is more important for induced autophagy (Chung et al., 2010).

ATG4 and *ATG8* genes are expressed ubiquitously and their expression is induced by nitrogen starvation. In addition, *ATG4a* and *ATG4b* mutants are unable to produce autophagosomes (Yoshimoto et al., 2004). The over-expression of *GFP:ATG8* in plants led to an increase in

the growth and altered responses to nutrient limitation, suggesting the role of this gene in response to abiotic stress (Slavikova et al., 2008). In mammals, the *ATG8* homologues (*LC3*, *GATE16*, *GABARAP* and *ATG8L*) undergo similar modifications by ATG4, ATG3 and ATG7 and form the complex ATG8-interacting motif (AIM), which seems to be involved in selective autophagy (Noda et al., 2010). In plants, two proteins have been identified that use the AIM to interact with ATG8: NBR1 (Neighbor of *BRAC1* gene) and TSPO (Tryptophan-rich sensory protein) (Svenning et al., 2011; Vanhee et al., 2011).

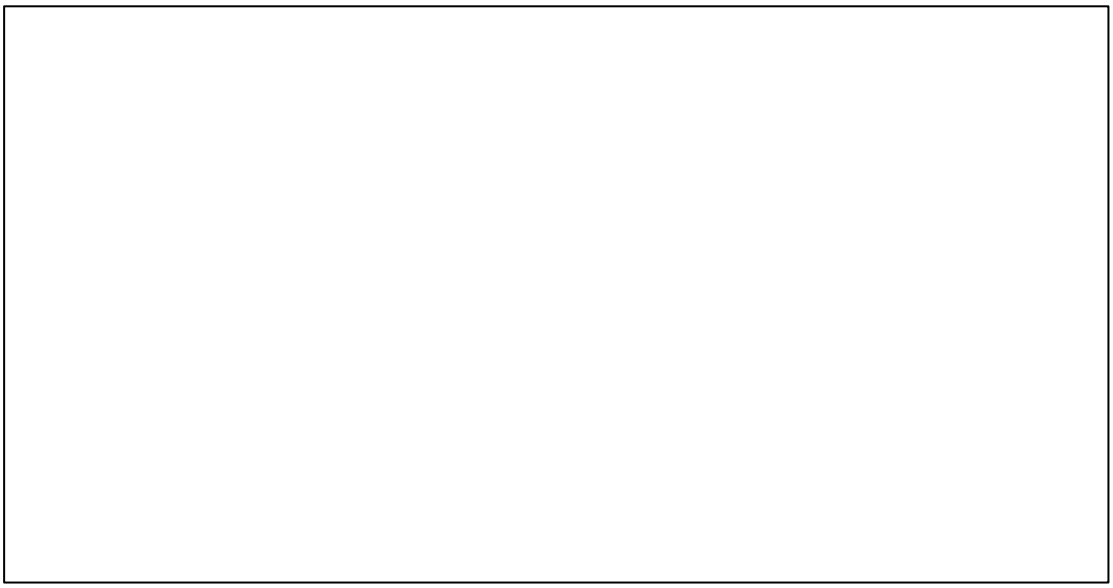

Figure 10. Ubiquitin-like conjugation processes in yeast. (**A**) ATG8-PE. ATG8 is cleaved in its C-terminus by ATG4 exposing a glycine residue (priming). This glycine is then activated by the E1-like ATG7 and transferred to ATG3. Finally, ATG8 is conjugated to the membrane lipid phosphatidylethanolamine (PE). (**B**) ATG5-ATG12. The ATG12 protein sequence ends with a glycine residue, which is activated by ATG7, then transferred to ATG10 and eventually conjugated to the target protein ATG5. The conjugated ATG12-ATG5 interacts further with ATG16 to form a tetrameric ATG5-ATG12-ATG16 complex. AMP, adenosyl monophosphate; PPi, pyrophosphate. Taken from Geng and Klionsky, 2008.

III.2. Selective autophagy

Autophagy has usually been described as a non-selective degradation process. However, evidence of degradation of specific cargo such as organelles and protein aggregates through autophagy suggests a degree of target specificity to degrade cellular components with a similar selectivity to the ubiquitin system. The target of specific substrates by the autophagosome (such as mitochondria, peroxisomes, ribosomes, signalling molecules) has been observed in yeast, mammals and more recently in plants (Kraft et al., 2008; Paul et al.,

2012; Reggiori et al., 2012; Shibata et al., 2013). In selective autophagy, adaptor proteins provide a linkage between the specific cargo and the proteins from the autophagy core machinery (Johansen and Lamark, 2011). Despite the specific mechanisms behind this process not being known in some cases, some evidence suggests an important role for ATG8 proteins and the ubiquitin system in selective autophagy in eukaryotes (Noda et al., 2010; Svenning et al., 2011).

As mentioned above, the ATG8 protein is able to form conjugates with other molecules besides PE. These include the protein NBR1 (Svenning *et al.*, 2011), which has been linked with the targeting of ubiquitin-tagged proteins and facilitation of their degradation through autophagy in animals (Shaid et al., 2013). Homologues of *NBR1* have been described in plants (Yoshimoto, 2012). Arabidopsis AtNBR1 is able to bind both to ATG8 and ubiquitin-tagged proteins and to be selectively targeted by the autophagy system (Floyd et al., 2012). In addition to NBR1, AtTSPO (Tryptophan-rich sensory protein) is also able to bind ATG8 and be selectively degraded by autophagy (Vanhee et al., 2011).

III.3. Phenotype of *ATG* deficient plants

Studies of plants with altered *ATG* components have demonstrated that autophagy, although not essential for survival, plays an important role in natural senescence and stress responses during nutrient limiting conditions and pathogen attack (Guiboileau et al., 2012; Hayward and Dinesh-Kumar, 2011; Hofius et al., 2011; Xiong et al., 2005). Consistent with these functions, the transcript levels of many plant *ATG* genes are substantially elevated in senescing leaves and during nutrient starvation (Chung et al., 2010; Gregersen and Holm, 2007; Hollmann et al., 2014; Lundgren Rose et al., 2006). A low expression of *ATG* genes causes impaired plant fitness in optimal and stress conditions most likely due to the arrest of the autophagy pathway. These plants show a typical autophagy-deficient phenotype, which includes early senescence, reduced size and sensitivity to biotic and abiotic stress (Kim *et al.*, 2012) (Table 2). In contrast, over-expression of *ATG* components leads to larger plants and higher resistance to abiotic stress conditions (Slavikova et al., 2008). Transgenic plants over-expressing *ATG* genes (GFP:ATG8:HA) or deficient in the expression of these genes (knockout mutants and RNAi-ATG) have been used as tools for the study of autophagy molecular mechanisms and their implications at the biochemical and physiological level (Kim et al., 2012; Liu and Bassham, 2012; Patel and Dinesh-Kumar, 2008; Sláviková et al., 2005; Yoshimoto et al., 2004).

Table 2. Phenotypes shown by autophagy mutants and transgenic plants in Arabidopsis. Altered genes belong to the autophagy core machinery. Modified from Kim *et al.*, 2012.

Genotype	Gene	Phenotype	Reference
Knockout mutant	*ATG2*	Spontaneous cell death, early senescence, defects in autophagosome formation, powdery mildew resistance, enhanced cell death by infection	Yoshimoto et al., 2009 Wang et al., 2011
Knockout double mutant	*ATG4a; ATG4b*	Early senescence, hypersensitivity to nitrogen and carbon limitation	Yoshimoto et al., 2004 Chung et al., 2010
Knockout mutant	*ATG5*	Early senescence, hypersensitivity to nitrogen and carbon limitation, delayed differentiation of tracheary elements, enhanced cell death by infection, impaired nitrogen remobilisation.	Thompson et al., 2005 Inoue et al., 2006 Phillips et al., 2008 Yoshimoto et al., 2009 Chung et al., 2010 Kwon et al., 2010 Lenz et al., 2011 Guiboileau et al., 2012
Knockout mutant	*ATG6*	Homozygotes not recovered due to male sterility	Fujiki et al., 2007 Qin et al., 2007
Antisense		Early senescence, hypersensitivity to nitrogen and carbon limitation, multiple developmental phenotypes including stunted growth, enhanced cell death by infection	Patel and Dinesh-Kumar, 2008
Knockout mutant	*ATG7*	Early senescence, hypersensitivity to nitrogen and carbon limitation, delayed cell death by infection	Doelling et al., 2002 Thompson et al., 2005 Hofius et al., 2009 Chung et al., 2010 Suttangkakul et al., 2011
Transgenic plant	*GFP:ATG8f:HA*	Accelerated flowering, altered root architecture in response to cytokinin, big-sized plants, survival under light limiting conditions, improved tolerance to salt stress	Slavikova et al., 2008
Knockout mutant	*ATG9*	Early senescence, hypersensitivity to nitrogen and carbon limitation, delayed cell death by infection	Hanaoka et al., 2002 Inoue et al., 2006 Hofius et al., 2009
Knockout mutant	*ATG10*	Early senescence, hypersensitivity to nitrogen and carbon limitation, enhanced cell death by infection	Phillips et al., 2008 Chung et al., 2010 Lenz et al., 2011 Wang et al., 2011
Knockout double mutant	*ATG13a; ATG13b*	Early senescence, hypersensitivity to nitrogen and carbon limitation	Suttankakul et al., 2011
RNAi	*ATG18a*	Early senescence, hypersensitivity to nitrogen and carbon limitation, hypersensitivity to drought stress, hypersensitivity to salt stress, enhanced cell death by infection	Xiong et al., 2005 Liu et al., 2009 Lenz et al., 2011

III.4. Techniques to the study of autophagy

Transmission electron microscopy (TEM) has been considered as the golden standard to the study of autophagy. It was the technique that allowed the first descriptions of autophagy in mammalian cells (Ashford and Porter, 1962). Nevertheless, over the years, several molecular

tools have been developed for the study of specific mechanisms related to autophagy processes and regulation in different biological models.

III.4.1. Transmission electron microscopy (TEM)

This technique has been used since the earliest studies of autophagy in the 60's, and it is still one of the most reliable methods to monitor autophagy in cells and tissues. TEM allows the detailed observation of autophagosomes and their cargos in cells, and combined with other techniques such as immunogold-labelling of autophagy specific markers (ATG8), it allows a precise approach according to the experimental needs. However, sample preparation and proper interpretation of TEM data requires expertise in both technical aspects and histology (Mitou et al., 2009).

III.4.2. Transgenic plants

The use of plants with altered expression of *ATG* genes has been useful for the understanding of the role of autophagy in several molecular and physiological processes in different organisms. These plants also allow determination of the function of specific proteins and their interaction with other molecular components.

III.4.3. ATG8 and ATG8-PE accumulation

As already mentioned, the ATG8 protein (more specifically its conjugated form ATG8-PE) is the only component of the autophagy core machinery that remains in the autophagosome until its degradation in the vacuole. The ATG8/ATG8-PE ratio has been considered as an indicator of autophagy activity (Chung *et al.,* 2009). Western blot analysis using specific antibodies against ATG8 allows the detection of both the ~15 kDa (free form) and the ~13 kDa (lipidated form) forms of ATG8 in Maize and Arabidopsis (Yoshimoto *et al.,* 2004; Chung *et al.,* 2009). In transgenic plants expressing the fusion protein GFP:ATG8, both free GFP and GFP:ATG8 have been detected by immunoblotting using antibodies against GFP (Yoshimoto *et al.,* 2004). The detection by western blot of proteins associated with ATG8 such as NBR1 (NBR1 is conjugated to ATG8 by the ubiquitin-like system), using specific antibodies, has been suggested to indicate selective autophagy activity (Svenning *et al.*, 2011).

In GFP:ATG8 plants, localization of the fluorescent protein fusion is commonly used to detect autophagosomes in cells. Fluorescent dots can be observed in cells using fluorescence

microscopy, and the number of dots observed in cells often estimates the autophagic activity (Merkulova et al., 2014).

Although these methods are accurate in most of the research cases, care must be taken since the quantity of fluorescent dots observed in the samples is not always correlated with the autophagy activity (Merkulova *et al.,* 2014). The ATG8/ATG8-PE ratio differs among tissues, depending on stimuli and the antibodies used, therefore reliable controls must be added and it is strongly advisable to monitor the ATG8 lipidation at several time points in order to avoid misinterpretations due to kinetics of autophagy (Mitou *et al.,* 2009).

III.4.4. Test of vacuolar activity

Basic amines can be accumulated in cellular compartments at low internal pH; this characteristic allows the detection of organelles by microscopy using specific pH sensitive probes. Lysotracker, Acridine Orange (AO) and Monodansylcadaverine (MDC) are fluorescent probes used for labelling vacuoles and lysosomes due to their protonation and retention in the membranes of these organelles (Mitou *et al.,* 2009). The quantification of the fluorescence observed in these organelles suggests the degree of acidity and the volume of the cellular acidic compartments. However, this technique is not considered as an autophagy-specific marker since it has been observed that lytic activities are also generated by other structures such as endosomes and lamellar bodies (Munafó and Colombo, 2001).

These probes must be used in combination with more specific markers of autophagy (such as GFP:ATG8) in order to discriminate autophagic activity from other events increasing vacuolar activity (Merkulova *et al.,* 2014). Also, proper sample manipulation is required so as not to alter the absorption properties of the probes (Freundt et al., 2007).

Other methods such as the determination of enzymatic activities of proteins from the autophagy core machinery, for example ATG1 (kinase) and ATG4 (protease), and the analyses of selective and non-selective protein degradation have also been used to monitor autophagy in plants (Mitou *et al.,* 2009). However, these methods require complementary studies to ensure specificity.

III.5. Non-autophagic roles of autophagy proteins

Autophagy is considered as an important mechanism associated with essential processes in eukaryotic cells, and the components of the autophagy core machinery are crucial for

homeostasis. However, these proteins seem to be involved in other cellular events non-related with autophagy, but equally important for cellular fitness and survival. Although these functions have been described mainly in animals, similar processes may occur in plants as well.

ATG8 facilitates vacuolar fusion in yeast. Non-lipidated ATG8 localizes to the vacuolar membranes and, due to its ability to interact with other proteins through the ATG8-interacting motif (AIM), is able to recruit SNAREs and other fusion components that facilitate vacuolar fusion (Nakatogawa et al., 2007; Tamura et al., 2010).

The ATG12-ATG5 complex acts as a suppressor of innate immune signalling in mammalian cells infected by viruses. The ATG12-ATG5 conjugate negatively regulates the interferon response generated by the virus-derived immunostimulatory RNA structures (isRNA) in infected cells, and leads to a increase in viral replication (Jounai et al., 2007).

ATG5, ATG7, ATG4 and the animal ATG8 homologues (LC3) participate in the secretion of cathepsin K and hydrochloric acid into the extracellular space (resorptive lacuna) in osteoclasts (Deselm et al., 2011) promoting bone reabsorption and the formation of bone cavities.

In animals, autophagy and apoptosis are induced by similar stresses (for example nutritional stress). However, the inactivation of the autophagy pathway causes cell death by apoptosis during stress conditions. ATG6 (also called Beclin-1) is able to interact with the anti-apoptotic protein Bcl2 producing the inhibition of autophagy. In this way autophagy and apoptosis are regulated in an antagonistic manner (Maiuri et al., 2007).

These new roles of the components of the autophagy core machinery suggest a complex interaction between autophagy and cell proliferation, development and death in animals that probably could be found in other organisms like plants as well.

IV. Autophagy, Senescence and N remobilisation. JXB review

BLANK PAGE

REVIEW Autophagy, plant senescence and nutrient recycling. Avila Ospina *et al*. 2014. Journal of experimental botany, Vol. 65, No. 14, pp. 3799–3811.

V. CropLife ITN consortium

CropLife is a research consortium created in 2010 under the 7th research framework program of the European Union. CropLife functions as an Initial Training Network (ITN) which provides opportunities to early stage researchers (ESR; PhD students) and experienced researchers (ER; post-docs within their first five years of career) for the advancement of their careers by integrating partners from the public and private sectors. The ITN includes local training activities in the host laboratory and network-wide courses, summer schools and workshops. ESRs and ERs are trained in a range of cutting edge research skills, as well as in complementary skills to enhance their career prospects.

Further benefits arise from secondments to partner laboratories and inter-sectoral visits to associated partners from the private sector.
In order to guarantee training at the highest level, outstanding scientists in the field are integrated as visiting researchers. Workshops and a final network conference provide a platform for dissemination of the network's achievements, which are expected to increase the competitiveness of European plant research and agriculture.

The CropLife program focuses on leaf lifespan as a major determinant of plant productivity and aims to develop new breeding strategies for prolonging leaf photosynthesis and delaying senescence processes in two model grasses, barley as a grain crop and perennial ryegrass as a biomass and forage crop.

Due to the interdisciplinary character of its members, CropLife's main objectives have been addressed in five work packages covering different aspects such as the identification of key factors initiating senescence and regulator proteins of lifespan (WP1 and 2), the elucidation of molecular mechanism of senescence-associated protein degradation and nitrogen remobilisation (WP3) and the analysis and exploitation of genetic variation of lifespan in order to breed new varieties with increased productivity (WP3). There are two additional work packages, one in charge of the dissemination and exploitation of the research results (WP5) and a second dedicated to the management and organization of the consortium activities (WP6).

V.1. Work packages and their scientific and technological objectives

WP1

The main objective is to determine the role of reactive oxygen species (ROS) in senescence and to identify changes in the redox state that may represent early senescence signals. The overall objective of this work package includes development of novel non-invasive methods for monitoring senescence processes in the field. This WP includes ESR5 (University of Zurich) and ESR7 (Jagiellonian University-Krakow) (Figure 11).

WP2

The overall objective is to establish the roles of senescence-associated transcription factors and histone modifications at the promoters of transcriptional master regulators in the control of lifespan for crop plants. This WP includes ESR1 (University of Kiel), ESR2 (Aarhus University), ESR3 (University of Halle), ESR11 (EuroGrass B.V) and ER1 (Aarhus University) (Figure 11).

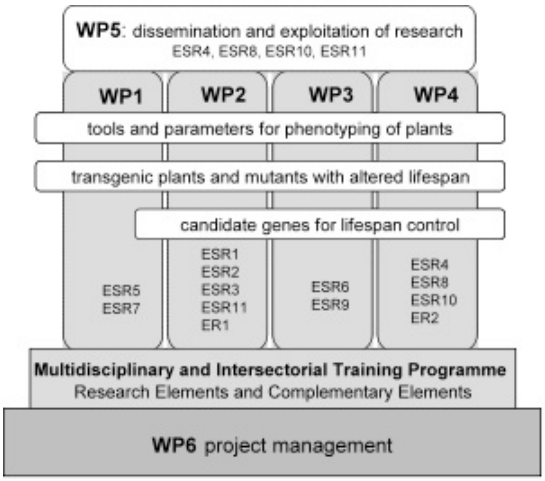

Figure 11. CropLife work packages and organizational structure. Work packages WP1-5 are based on the multidisciplinary and inter-sectoral training program of CropLife and are complemented by WP6. Knowledge and material exchange is depicted by horizontal bars. PhD students or Early Stage Researchers (ESR) and post-docs or Experienced Researchers (ER) are assigned to WP1-4 and partly to WP5.

WP3

As part of this WP, myself (ESR6, INRA-Versailles) together with ESR9 (University of Leeds) have the main objective to elucidate the molecular mechanisms underlying chloroplast

protein degradation and nitrogen remobilisation with special attention to the role of autophagy (Figure 11).

WP4

The aim of this WP is to discover and exploit genes involved in prolonging lifespan, and increasing productivity and efficiency in European barley and biofuel/forage ryegrass breeding programs. WP4 includes the ESR4 (Aberystwyth University), ESR8 (Carlsberg Research), ESR10 (NPZ-Lembke) and ER2 (Aberystwyth University) (Figure 11).

WP5

WP5 involves the evaluation and definition of the main interests and targets of the private project partners in the research fields of CropLife and support of transfer of research results to the private sector. It also comprises the practical implementation of protocols and results of new methods that may be helpful to improve and support existing processes. Superior germplasms have entered into the existing breeding programs (Figure 11). Croplife also has an newsletter for public dissemination by the website of the consortium in order to promote exchange of knowledge. This newsletter is compiled by WP6 every six months and is also disseminated in the SenNet webpage (http://www.sidthomas.net/Plant_senescence/sennet.htm).

WP6

The objective of this work package is to ensure a smooth implementation of the project in accordance with the Grant Agreement and with its annexes (Figure 11).

V.2. Partners and supervisory board

Members of CropLife include principal investigators (PI) at universities, research centers or company research departments around Europe. They are in charge of the supervision of the ESR and ER projects. The supervisory board is constituted by the scientists in charge of CropLife partners as well as by representatives of associated partners (AP) from industry and academia. Table 3 lists all CropLife partners, ESRs, ERs and supervisory partners.

Table 3. CropLife members. PIs, ESR, ER, associated partners and supervisory board members are included.

Researcher	Institution	Position	Country	WP
Karin Krupinska	Christian-Albrechts University of Kiel	PI	Germany	WP2 – Network coordinator
Weronika Kucharewicz		ESR1		WP2
Per Gegersen	University of Aarhus	PI	Denmark	WP2
Dagmara Podzimska		ESR2		
Colette Matthewman		ER1		
Klaus Humbeck	Martin-Luther-University of Halle	PI	Germany	WP2
Paula Paramon		ESR3		
Daniel Thorogood	Aberystwyth University	PI	UK	WP4
Meraluna Canunayon		ESR4	UK	
Julien Hollmann		ER2.1	Germany/UK	
Peter Muth		ER2.2	UK	
Stefan Hörtensteiner	University of Zürich	PI	Switzerland	WP1
Aditi Das		ESR5		
Céline Masclaux-Daubresse	Institut National de la Recherche Agronomique, INRA-Versailles,	PI	France	WP3
Liliana Avila-Ospina		ESR6		
Kazimierz Strzalka	Jagiellonian University (UNIJAG)	PI	Poland	WP1
Ivan Jajic		ESR7		
Christine Foyer	University of Leeds (UNIVLEEDS)	PI	UK	WP3
Gloria Comadira		ESR9		
Mats Hansson	Carlsberg Laboratory		Denmark	WP4
Isabella Matyszczak		ESR8		
Gunhild Leckband	Norddeutsche Pflanzenzucht Hans-Georg Lembke KG	Head of research department	Germany	WP4
Luca Boschian		ESR10		
Ulf Feuerstain	Euro Grass Breeding GmbH & Co. KG	Head of research and development department	Germany	WP2
Andrea Culetic		ESR11		
Associated partners				
Robbie Waugh	The James Hutton Institute	PI	Scotland	
Visiting Researchers				
Andreas Fischer	Montana State University	PI	USA	
Diter von Wettstein	Washington State University	Emeritus Professor	USA	
Steve Scofield	Purdue University	PI	USA	
Supervisory board				
Henrik Vibe Scheller	Bioenergy Institute of the Lawrence Berkeley National Laboratory	PI	USA	
Susheng Gan	Cornell University	PI	USA	
Vicky Buchanan-Wollaston	Warwick University	PI	UK	

RESULTS

RESULTS

Introduction to Paper 1 and Paper 2.

Senescence is the last developmental stage in the lifespan of an organism and is characterized by the decay of cells, organs and in some cases the whole individual. This is a complex and highly regulated process with the ultimate aim to ensure either the robustness or the survival of the plant progeny. Senescence may be triggered by different factors such as ageing, stress and development and, in the case of monocarpic crops (such as barley and wheat), it constitutes a very important process that influences key agronomic traits such as yield and quality of the grain. Therefore, understanding of the senescence related processes in plants, especially of those with high agronomical importance, is essential for their future improvement.

The aims of is the research presented here are to have a close look on the process of natural and stress induced leaf senescence in barley (*Hordeum vulgare*) with a special emphasis in the physiological, metabolic and molecular processes occurring from its onset to the latest stages. This work will identify processes related to cell ageing, cellular disassembly, stress response and nutrient remobilisation during two different developmental stages (vegetative and reproductive).

For this, I have first standardized growing conditions for barley (cv. Golden promise) plantlets in growth chambers which provide both optimal and limiting conditions for nitrate and light in order to study traits related to nutrient stress and senescence. For the study of senescence related processes during the vegetative stage, we analysed separately leaf ranks in our three week old plantlets (leaf 1, L1; leaf 2, L2; leaf 3, L3), these leaves represented old leaf L1, mature leaf L2 and young leaf L3. Sequential senescence of leaves during the pre-anthesis stage is a characteristic trait of monocarpic cereals and it is characterized by senescence of the oldest leaves and remobilisation of nutrients to the youngest (Feller *et al.*, 2007).

Afterwards, in collaboration with the CropLife ITN partners, we grew barley (cv. Carina) plants in the field until the reproductive stage (post-anthesis) to analyse features related to senescence and remobilisation of nutrients in the flag leaf. During the reproductive stage, all vegetative organs senesce and there is a massive remobilisation of nutrient to the developing

seeds. The flag leaf is the last leaf to senesce and links both the senescing plant and the ear during grain filling (Gregersen *et al.*, 2008).

Subsequently, I analysed physiological markers of leaf senescence such as chlorophyll, Rubisco and total soluble protein contents in both leaf ranks of plantlets grown under nitrate and carbon stress (dark) and flag leaf. Analyses of other traits that are markers of leaf senescence, cell component degradation or nutrient remobilisation related processes were performed such as photosynthetic efficiency, CO_2 assimilation, amino acid contents, GS1/GS2 ratio and protease and GS activities.

In order to obtain a more detailed view of the metabolic changes happening in our plants, together with Dr. Gilles Clément I performed a metabolome analysis of both leaf ranks of plants grown under nitrate stress and flag leaf, through HPLC/MS. In this study we observed changes in the abundance of primary and secondary metabolites including amino acids, carbohydrates and lipids, related to leaf age, nitrate stress and developmental stage. Our results were compared to similar analyses performed in other plant species such as Arabidopsis.

In a second part, I analysed the transcript levels of genes related to metabolic processes associated with senescence and nutrient remobilisation. For that, I decided to monitor the expression of genes belonging to the Glutamine Synthetase (*GS1* and *GS2*), Asparagine SyNthetase (*ASN*) and AuTophaGy (*ATG*) families. All these processes have been described as intimately related to senescence and nutrient stress responses in several plant species (Lam *et al.*, 1998; Chung *et al.*, 2009; Guiboileau *et al.*, 2013).

Only two isoforms of *ASN* (Moller *et al.*, 2003), three isoforms of *GS1* (Goodall *et al.*, 2013) and the *GS2* genes (Baima *et al.*, 1989) had been described for barley. Therefore, I started a search of other sequences that code for ASN and GS1 functions in barley as well as genes that code ATG functions. I used yeast, Arabidopsis and rice gene and protein sequences as queries. I also carried out several *in silico* analyses of predicted protein sequences in order to find amino acids essential for their corresponding function, and in this way validate the genes as potential *HvASN*, *HvGS* and *HvATG* genes. I then designed specific primers in order to measure the expression levels of these genes during natural senescence in both vegetative and

reproductive stages and also to monitor their responses to nitrate limitation and dark treatment.

In the case of *HvATG5*, I performed a complementation assay by cloning its CDS sequence and over-expressing it in Arabidopsis *atg5* mutants. I validated the complementation of the protein function by performing assays with concanamycin-A (Yoshimoto *et al.,* 2004) to observe a recovery of the autophagy activity and also by growing the transformed plants in different nitrate conditions to observe if their size, response to stress or lifespan resembled *atg5* mutants or wild type plants (Guiboileau *et al.,* 2013).

I used RT-qPCR to quantify the transcript levels of all the genes identified in this study. I evaluated several primers to ensure high efficiency and obtain reliable results (specially for gene families). The same experiments were performed to test housekeeping genes that allowed me to compare several stress conditions, different types of samples and the two different plant varieties. I determined two senescence related gene markers that represented a *SAG* (Senescence Associated Gene) and a *SRG* (Senescence Repressed Gene) in order to compare their expression trend with that of our samples. For this, I chose *HvNAC13* as *SAG* (Christiansen *et al.,* 2011) and *HvLSU* as *SRG* (Feller *et al.,* 2008). After the optimal qPCR conditions were stablished, the expression of *HvGS1*, *HvGS2*, *HvASN* and *HvATG* was measured in plantlet leaves (vegetative stage) grown under nitrate and dark stress conditions and in flag leaves (reproductive stage) grown in the field.

Based on the results obtained, we decided to divide our work into two different research papers.
The first one, entitled "**Studying leaf senescence in barley (*Hordeum vulgare* L.) seedlings and flag leaves reveals specific metabolic shifts in sugar, amino acid and lipid metabolisms"**, presents a picture of the metabolic and physiological events occurring in barley leaves during leaf senescence. The metabolic profiling of barley leaf senescence emphasises the differences and similarities with the model plant *Arabidopsis thaliana*. This paper also includes the response of remobilisation related genes such as *ASN* and *GS* to senescence and nitrate and dark stress in barley. This report will be helpful to standardize conditions in which the senescence of barley wild type and mutants/transformants can be compared.

The second paper, called "**The nineteen autophagy genes found in barley (*Hordeum vulgare* L.) are differentially regulated during leaf senescence, chronic nitrogen limitation and in response to dark treatment"**, describes barley autophagy genes. Since the genomic *HvATG5* sequence we found was incomplete, we performed the validation of the *HvATG5* cDNA through functional validation by over-expressing this gene in Arabidopsis *atg5* mutants. We also present the response of the different *HvATG* genes identified to nutritional stress and senescence in barley.

Although the results contained in these two reports can be considered as descriptive work, all the gene and metabolomic analysis and experimental evidence presented therein are essential for further study of autophagy in cereals, including plant engineering for functional analysis.

PAPER 1

Studying senescence in barley (*Hordeum vulgare* L.) primary leaves and flag leaves reveals specific metabolic shifts in sugar, amino acids and lipid metabolisms

Liliana Avila-Ospina[1,2], Gilles Clément[1,2], Anne Marmagne[1,2], Joël Talbotec[1,2], Karin Krupinska[3] and Céline Masclaux-Daubresse[1,2,*]

(1) INRA, UMR1318, Institut Jean-Pierre Bourgin, RD10, F-78000 Versailles, France
(2) AgroParisTech, Institut Jean-Pierre Bourgin, RD10, F-78000 Versailles, France
(3) Institute of Botany, Christian-Albrechts-University of Kiel, Olshausenstraße 40, 24098 Kiel, Germany

*Corresponding author:
Dr Céline Masclaux-Daubresse
Institut Jean-Pierre Bourgin (IJPB), UMR 1318, INRA 78026 Versailles Cedex, France
phone +33 (0)1 30 83 30 88
fax +33 (0)1 30 83 30 96
e-mail celine.masclaux@versailles.inra.fr

Financial supports:
This work was supported by the FP7 Marie Curie Actions – Networks for Initial Training Project FP7-MC-ITN N° 264394 acronyme CropLife for L.A-O.

Keywords: Dark treatment, nitrate, glutamine synthetase, asparagine synthetase, endoprotease, metabolite profiling
Number of words: 9917
Number of Figures: 12

Abstract

Metabolic and enzymatic changes occurring during leaf senescence in barley (*Hordeum vulgare* L.) were investigated on both developmental and stress-induced leaf senescence models. Developmental senescence was studied on different leaf ranks of plantlets grown under controlled conditions and on flag leaves of plants grown in the field. Leaf senescence under stress condition was studied on plantlets submitted to dark treatments and on plantlets grown under low nitrate conditions. The known senescence markers chlorophyll, Rubisco, nitrogen content and nitrogen remobilisation enzymes were monitored and showed the same typical leaf senescence modifications as described in other plant species like tobacco (*Nicotiana tabaccum* L.) and *Arabidopsis thaliana* L. New genes coding for the nitrogen related enzymes cytosolic glutamine synthetase (*HvGS1*) and asparagine synthetase (*HvASN*) were characterized. The *HvGS1* expression levels increased during developmental leaf senescence in plantlets and flag leaves, while opposite effects of senescence on the expression of *HvASN* genes were observed depending on nitrate conditions. Under low nitrate conditions *HvASN* transcript levels globally decreased with senescence while they increased under high nitrate conditions. A metabolic profiling performed using gas chromatography and mass spectrometry showed a decrease of amino acid and hexose concentrations with senescence and an increase of minor carbohydrates. Senescence related modifications were similar in flag leaves and leaf ranks of plantlets. Metabolite profiling revealed that the modifications of minor amino acid, hexose and lipid concentrations with senescence are different in Arabidopsis and in barley leaves.

Introduction

Barley (*Hordeum vulgare* L.) is a major grain cereal grown widely and used as animal fodder and for grain fermentation to make beer or whisky. Cereals are of primary importance to ensure food security and nitrogen use efficiency is a key target for improvement. Grain protein content (GPC) is influenced by leaf senescence. The characterization of the Gpc-1 (NAM-1) gene that controls both senescence and GPC in wheat and barley showed the interdependence of both traits (Uauy *et al.,* 2006; Avni *et al.,* 2014). Barley is cultivated on substantially less surface than maize, rice or wheat. Its smaller and simpler genome (2n =2x=14) compared to wheat and the fact that a whole-genome shotgun assembly and an integrated physical map are available (Mayer *et al.,* 2012), makes it a useful model system for the study of temperate cereal crops especially wheat, whose genome is much more complex.

Senescence is the last developmental stage before leaves die and a very important physiological process for the plant. The numerous molecular and biological processes that contribute to senescence syndrome are indeed essential for the recycling and remobilisation of mineral nutrients and nitrogen containing molecules from the leaves to the rest of the plant (Himelblau and Amasino, 2001; Diaz *et al.,* 2008). During leaf senescence, proteins and nucleic acids are used as nutrient source for the building of new organs and for grain filling in cereals (Kichey *et al.,* 2007; Distelfeld *et al.,* 2012). In the case of wheat and barley, the understanding of the molecular mechanisms controlling productivity and grain filling should be addressed at the reproductive stage and on flag leaves (Gregersen *et al.,* 2013; Fischer, 2012).

Molecular mechanisms involved in nitrogen remobilisation have been studied for a long time, in several plant species and using both reverse and forward genetics (see Masclaux-Daubresse *et al.,* 2010). Nitrogen

availability has a strong effect on leaf senescence and on nitrogen remobilisation efficiency (Lemaître *et al.,* 2008). The main source of nitrogen for remobilisation is chloroplasts. Enzymes suspected to manage nitrogen during leaf senescence have been identified (Buchanan-Wollaston, 1997). Endopeptidase activities working with acidic pH optima in the vacuole (Martinez *et al.,* 2008) and the autophagy pathway (Ishida *et al.,* 2008) are the most probable mechanisms involved in chloroplast protein degradation (Guiboileau *et al.,* 2013). Protein degradation releases a large variety of amino acids, however it seems that all of them cannot be mobilized and loaded in the phloem saps efficiently (Tegeder, 2014). Glutamine and asparagine are usually considered as the main amino acids involved in nitrogen translocation in the phloem saps (Masclaux-Daubresse *et al.,* 2008; Taylor *et al.,* 2012). Therefore their biosynthesis in source leaves is important for nitrogen remobilisation. Glutamine synthetases are in charge of the assimilation and re-assimilation of ammonium in young and old leaves respectively. While the chloroplastic glutamine synthetase GS2 decreases with leaf ageing, the cytosolic ones (GS1) are induced in the mesophyll of senescing leaves (Masclaux *et al.,* 2000; Brugière *et al.,* 2000; Martin *et al.,* 2006; Diaz *et al.,* 2008; Orsel *et al.,* 2014). The importance of GS1 isoforms in plant productivity has been shown for maize and rice (Martin *et al.,* 2006; Tabuchi *et al.,* 2005; Lothier *et al.,* 2011). Besides glutamine synthetase, asparagine synthetase is also able to assimilate ammonium in plants and might be involved in remobilisation (Masclaux-Daubresse *et al.,* 2006; Gaufichon *et al.,* 2010).

Many studies describe the metabolic changes occurring during leaf senescence and some reports propose that the induction, the timing and the progression of leaf senescence itself can be controlled by the accumulation of some specific metabolites (Wingler *et al.,* 2006). Although this is still under debate, several studies suggest a mechanistic interaction between metabolism and senescence process (Schippers *et al.,* 2008). Recently, Watanabe *et al.* (2013) have conducted a large profiling of metabolite changes during senescence in Arabidopsis. They observed an increase of the Gln/Glu and Asn/Asp ratios, which suggested a more active interconversion of Asp to Asn and of Glu to Gln during leaf senescence. While most of the studies dedicated to senescence-related metabolic changes have been performed on model plants (tobacco and Arabidopsis), it seems now important to verify whether their metabolic models are adapted to crops and in our case, to barley.

Our study aims at giving a picture of the metabolic changes occurring in barley leaves during senescence using classical approaches of molecular physiology as done previously on tobacco and Arabidopsis (Avila-Ospina *et al.,* 2014 for review). From such a picture, the physiological comparison of different senescence and plant models can be done. The comparison of natural and stress-induced leaf senescence and of plantlet and flag leaf senescence can allow us to determine whether leaf rank models in young plantlets could give a good approximation of what happens in flag leaves during grain filling. The picture of the metabolic changes occurring in barley leaves during senescence is a first step in the comparison of cereal leaf senescence and the Arabidopsis model previously published (Watanabe *et al.*, 2013).

Material and methods

Plant material and growth conditions

Hordeum Vulgare L. cultivar Golden Promise was grown in growth chamber (16h/8h photoperiod – 25/17°C). Seeds were sown on a seedbed and five-days plantlets were transferred into polyvinyl chloride (PVC) tubes (6 ø – 45 cm units) containing sand as a substrate. Plantlets were watered eight times per day with a high nitrate (5

mM NO_3^-; HN) or low nitrate (0.5 mM NO_3^-; LN) nutritive solutions (Annex 1 available online). 20 days after sowing (DAS) leaves were harvested individually (L1 to L4 in HN; L1 to L3 in LN; from bottom to top leaves). Four independent leaf rank samples (containing 18 leaves each) were harvested between 10:00 and 12:00 and stored at -80°C for further experiments. Before harvest, chlorophyll content in leaves was estimated using a SPAD (SPAD-502 Chlorophyll meter Konica Minolta, Japan). Three plantings were performed and analyses were carried out on at least two plant cultures.

Dark stress experiments were carried out in the same growth chamber on plantlets watered eight times per day with HN solution. 14 DAS, the whole plants were either covered (dark stress) or not (control) during 4 days. At the end of the dark stress (time point T1) half of the plants were harvested and leaf ranks collected. The remaining plants were left growing in the normal day/night conditions for 3 days (Recovery) and harvested just after at T2. Three independent leaf rank samples (containing 12 leaves each) were harvested at T1 and T2 between 10:00 and 12:00 and stored at -80°C until further experiments.

In field experiments, spring barley (*Hordeum Vulgare* L.) Cultivar Carina was sown using a drill on April 2 of 2013 at *Hohenschulen research farm at 15.5 km west of Kiel* during the 2013 growing season. The barley was managed organically (70 kg N ha^{-1}). Four replicate plots of 150 m^2 each with 300 plants/m^2 and 12.5 cm of row distance were done. 30 flag leaves from the main shoots were harvested from each plot between 10:00 and 12:00 and immediately stored at -80°C for further experiments. 3 whole plants were taken from each plot and dark adapted for 30 to 45 min for further photosynthesis and CO_2 assimilation measurements. Harvests were performed 91 DAS (T0), 96 DAS (T1) and from T1 every 2 days during 2 weeks. Senescence was monitored by measuring chlorophyll contents (SPAD), photosystem II efficiency using a photosynthesis yield analyzer (Mini-PAM, H. Walz Effeltrich, Germany) and CO_2 assimilation using a portable gas exchange fluorescence system GFS-3000 (H. Walz Effeltrich, Germany).

After harvesting, all plant material was immediately frozen using liquid nitrogen and ground to obtain a fine homogenous powder. This powder was stored at -80°C for further analysis.

Determination of total nitrogen and carbon contents

50 mg of grounded frozen plant material were weighed and freeze dried. 5 mg of dry material were weighed in tin capsules to determine total N and C contents using a FLASH 2000 Organic Elemental Analyzer (Thermo Fisher Scientific, Villebon, France).

Chlorophyll, ammonium, total amino acid, total soluble protein and anions determinations

Chlorophyll content was determined spectrophotometrically in crude leaf extracts according to Arnon (1949), (Annex 1). Total soluble protein was extracted in 50 mM Tris-HCl, pH 7.6 buffer and protein was determined using a commercially available kit (Bio-Rad, Hercules, CA). Amino acids and NH_4^+ contents were determined after extraction in a 2% (w/v) solution of 5-sulfosalicylic acid by the Rosen colorimetric method using glutamine as a reference (Rosen, 1957). Anion concentrations were determined using Dionex HPLC (HPLC Dionex DX 120; Thermo Fischer Scientific, Courtaboeuf, France) on the same extract as used for metabolite profiling.

Glutamine synthetase activity measurement

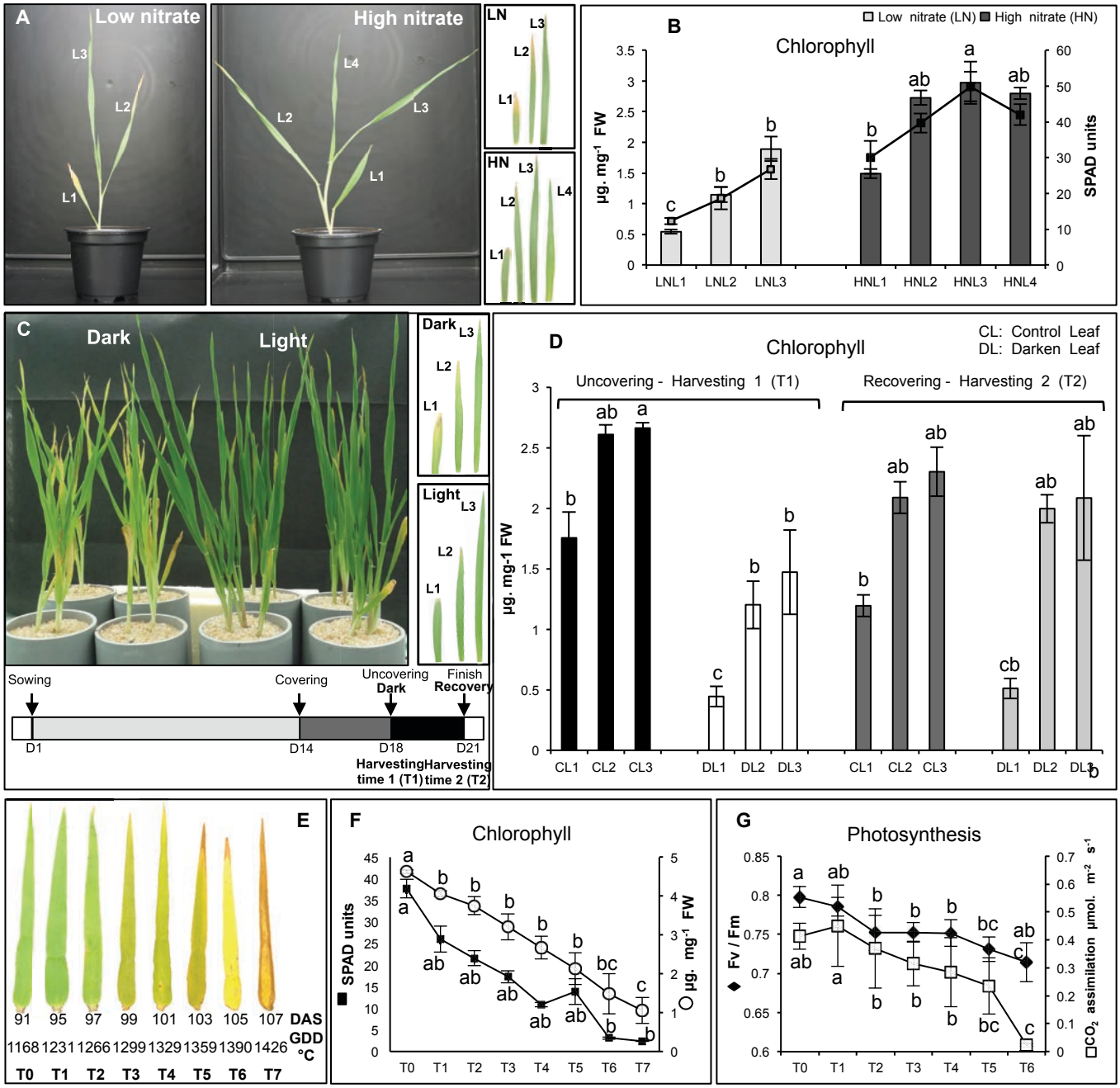

Figure 1. Changes in chlorophyll and photosynthesis during leaf senescence in barley. (A;B) Leaves of plantlets grown under low (LN) and high (HN) nitrate conditions. **(C;D)** Leaves of plantlets submitted or not to dark treatment. T1: 4 d of dark treatment. T2: 3 d of recovering under day/night conditions after T1. CL (control untreated leaves: black and dark grey bars), DL (darkened leaves: white and light grey bars). **(E-F)** Flag leaves harvested at different time points after heading (from T0 to T7). DAS (days after sowing); GDD °C (growing degree days in °C). **(F)** Chlorophyll contents in flag leaves measured by SPAD (●) and spectrophotometer (■). **(G)** Photosystem II efficiency (circles) and CO_2 assimilation (squares) in flag leaves. All data represent mean ± SD of 3-4 biological replicates. The different letters indicate values significantly different at $P < 0.05$ as determined using XLSTAT ANOVA Newman–Keuls (SNK) comparisons.

Enzymes were extracted from frozen ground leaf material stored at -80°C in 50 mM Tris HCl (pH 7.5), 1mM EDTA, 1mM $MgCl_2$, 0.5% polyvinyl pyrrolidone (w/v), 0.1% β-mercaptoethanol (v/v) and 2X protease inhibitor cocktail complete EDTA-free (Roche). GS activity was measured according to Masclaux *et al.* (2000), (Annex 1). The total soluble protein content was determined in the crude leaf extracts used for GS activity measurement using a commercially available kit (Coomassie Protein assay reagent, BioRad, Hercule, California, USA).

Protease activity assays

Analyses of endo- and exoproteolytic activities were performed according to Guiboileau *et al. (*2013).

Metabolite profiling using GC-MS and statistical analysis

Metabolite profiling by GC-MS was performed as previously described (Masclaux-Daubresse *et al.*, 2014; see Annexe 1). Statistical analysis was made with TMEV (http://www.tm4.org/mev.html); univariate analysis by permutation (1 way-anova and 2 way-anova) was firstly used to select the significant metabolites. Multivariate analysis (hierarchical clustering and principal component analysis; PCA) was then made in order to establish the metabolite clusters. Only metabolites showing repeatable and significant differences (based on t-test) according to leaf rank, nitrate treatment and senescence stage are reported.

RNA purification and RT-qPCR analysis

RNA isolation was performed with TRIzol reagent (Ambion) according to manufacture specifications. RNA suspended in nuclease free water was stored at -80°C. cDNA synthesis was performed using the first strand cDNA synthesis kit (Thermo Scientific). qPCR mix was composed of 10 µL of MESA FAST qPCR master mix plus for SYBR assay (Eurogentec), 3.8 µL water, 1.2 µL of 10 mM specific forward and reverse primers and 5 µL diluted cDNA 1:30 (v/v) in nuclease free water. Reactions were carried out in triplicate in 96 well plates in a Bio-Rad CFX connect thermocycler on the following program: 94°C for 5 min followed by 39 cycles of 94°C for 5 s and 72°C for 20 s sequences. Melt curve from 50°C to 95°C increasing by 0.5°C every 30 s was performed. Fluorescence readings were taken during the elongation step (72°C). Ct values were calculated by the CFX connect software. Genes and primers are listed in Supplemental Table 1. Several reference genes (including *GADPH*, *Actin*, *SAMd*, *CHS90*, *α-Tubulin*, *β-Tubulin*, *EF1a*, *ADPrf1*, *CDC48* and *Ubiquitin*) were validated across all samples and conditions in accordance with geNorm algorithm. The *GADPH* and *Actin* were used to calculate gene expression relative values of plantlets and flag leaf samples respectively since they showed the lowest variation across samples and conditions.

Protein separation, gel electrophoresis and western blot analysis

Proteins were extracted at 4°C in Tris HCl (25 mM; pH 7.5), EDTA (0.5 mM) and 2X protease inhibitor cocktail complete EDTA-free (Roche) and denatured at 70°C for 10 min after adding one volume of NuPAGE LDS sample buffer 4X 1:0.1 (v/v) of NuPAGE sample reducing agent 10X (Life Technologies) to three volumes of protein extract. Proteins were then separated by SDS-PAGE on 10% polyacrylamide gels; with an equal amount of protein in each lane. Denatured proteins were either transferred to PVDF membranes or stained directly in the gel with Coomassie blue for GS and Rubisco detection respectively. For GS blotting, polyclonal antibodies were

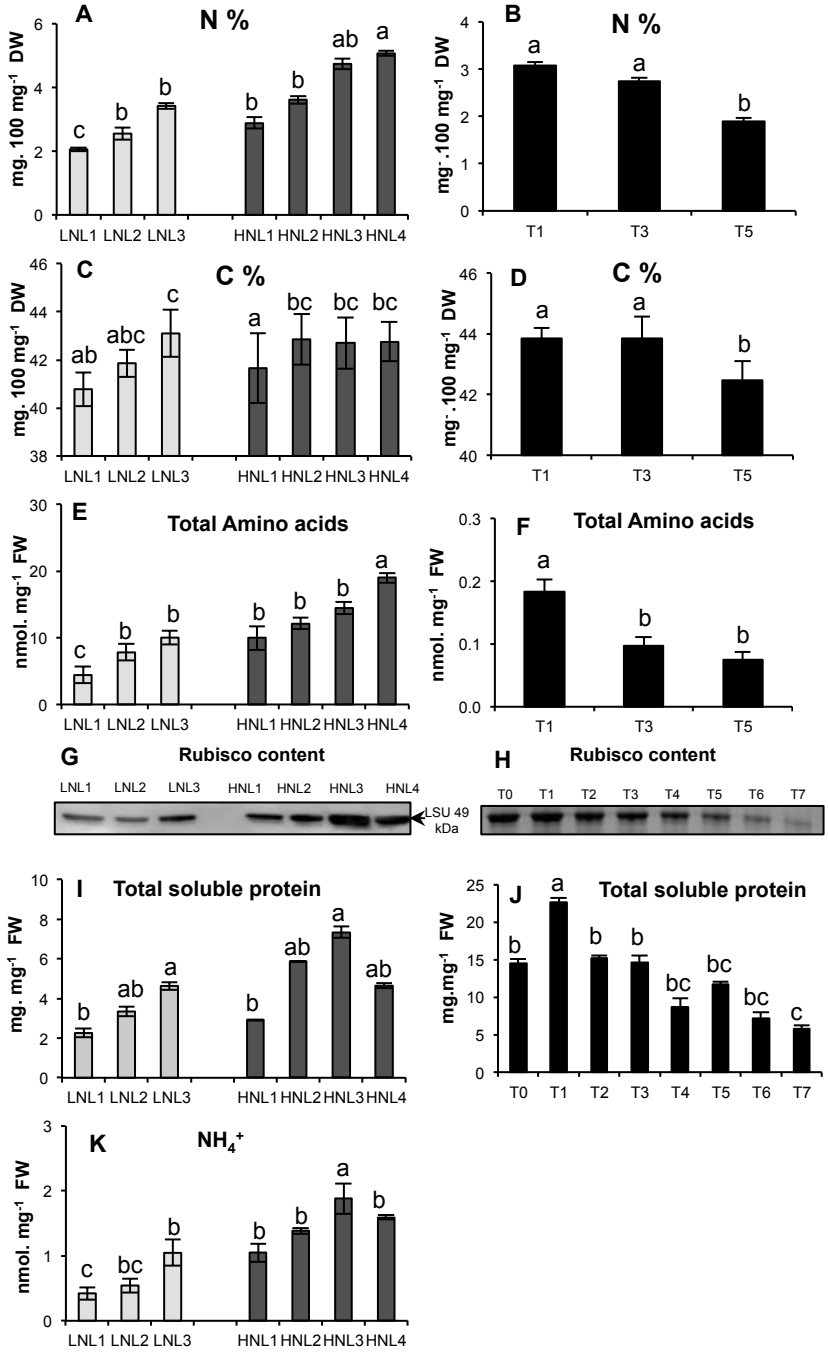

Figure 2. Changes in carbon, nitrogen and nitrogen-containing compounds during leaf senescence. Leaf ranks of plantlets grown under low (LN; light grey) and high (HN; dark grey) **(A, C, E, G, I, K)** and flag leaves **(B, D, F, H, J)** were analysed. In flag leaves, only total protein **(J)** and Rubisco contents **(H)** were measured in eight time points (T0 to T7). Rubisco content was determined using antibodies against the barley Rubisco C-terminal. For gels, equal protein amounts were loaded in each lane. Experiments have been repeated twice and gave similar results. Data represent mean ± SD of 3-4 biological replicates and the different letters indicate values significantly different at P <0.05 as determined using XLSTAT ANOVA Newman–Keuls (SNK) comparisons.

used for detection of both GS1 and GS2 isoenzymes (Lemaître *et al.*, 2008). Antibodies against barley N-terminal and C-terminal Rubisco were kindly provided by Dr. Urs Feller (University of Bern, Switzerland).

Analysis and description of barley *HvGS* and *HvASN* genes

HvGS2 and three isoforms of *HvGS1* (GS1_1, GS1_2 and GS1_3) were characterized by Baima *et al.* (1989) and Goodall *et al.* (2013) respectively. Two more sequences with similarities to prokaryotic *GS* genes were found through BLAST using *A. thaliana* [*AtGLN*1.1 (NM_123119, *At*5g37600), *AtGLN*1.2 (NM_105291, *At*1g66200), *AtGLN*1.3 (NM_112663, *At*3g17820), *AtGLN*1.4 (NM_121663, *At*5g16570), and *AtGLN*1.5 (NM_103743, *At*1g48470)] and *O. sativa* [*OsGLN*1_1 (NM_001054580.1, *Os*02g0735200), *OsGLN*1_2 (NM_001055959.2, *Os*03g0223400) and *OsGLN*1_3 (NP_001051067, *Os*03g0712800)] GLN1 predicted protein sequences as queries in Genbank (www.ncbi.nlm.nih.gov/nuccore) and EnsemblPlants (http://plants.ensembl.org/Multi/enasearch) databases (Supplemental Table 2). Primers for the *HvASN1* and *HvASN2* genes previously described by Moller *et al.*, (2003) were designed. Other *HvASN* genes were found through BLAST algorithm using Arabidopsis [*AtASN1* (*At*3g47340.1, NM_114602.3), *AtASN2* (*At*5g65010.2, NM_180941.2) and *AtASN3* (*At*5g10240.1, NM_121062.4)], rice [*OsASN1* (NM_001048300, *Os*12g38630), *OsASN2* (*Os*03g18130), *OsASN3* (*Os*06g15420), *OsASN4* (*Os*01g65260) and *OsASN5* (*Os*05g35580)] and maize [*ZmASN1* (GRMZM2G074589), *ZmASN2* (NM_001137541, GRMZM2G093175) *ZmASN3* (NM_001137542, GRMZM2G053669), *ZmASN4* (NM_001137543, GRMZM2G078472)]. Contigs for *HvGS* and *HvASN* genes were found through alignments of EST sequences with barley genome and gene structure was obtained through contigs and ESTs alignments, using ApE plasmid editor (http://biologylabs.utah.edu/jorgensen/wayned/ape/) and Exon-Intron graphic maker (http://wormweb.org/exonintron). Multiple protein sequence alignments and phylogenetic trees were generated using ClustalW algorithm (Supplemental Table 4, 5 and 6). EST accession numbers and contigs are listed in Supplemental Table 3.

Statistical analysis

For all data (except metabolite profiling) and comparisons, SNK tests from Student and Newman & Keuls were computed using XLSTAT software.

Results

Characterization of metabolic markers associated with leaf senescence in barley

Leaf senescence in barley was studied at vegetative stage using leaf ranks of plantlets and at reproductive stage on flag leaves. The induction of leaf senescence by nitrate limitation or dark treatment was investigated at vegetative stage.

In plantlets grown under low (LN) or high (HN) nitrate conditions, decreases in chlorophyll content were observed in old leaf ranks (Figure 1A-B). The leaf rank L4 of plants grown under HN did not exhibit higher chlorophyll concentration than HNL3. Chlorophyll concentrations in same leaf ranks were lower in LN than in HN showing that leaf senescence is enhanced under nitrate limitation (Figure 1A-B). Senescence-related decrease of the chlorophyll concentrations was also observed in the dark treated plantlets and in their controls (Figure 1C-D). The darkened leaves showed less chlorophyll than control leaves at T1. After 3 days of recovery

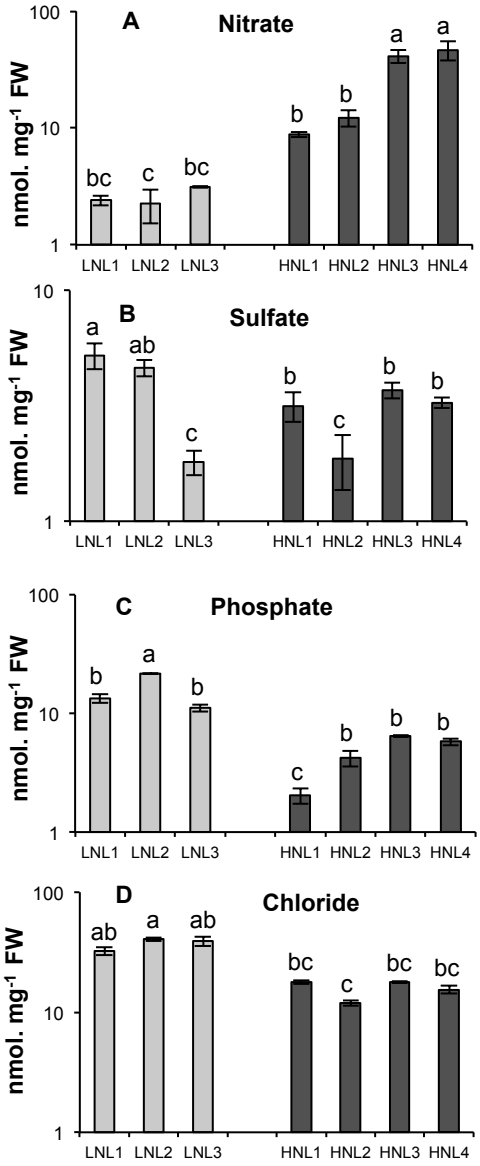

Figure 3. Comparison of anion contents. Nitrate **(A)**, sulfate **(B)**, phosphate **(C)** and chloride **(D)** were measured in leaf ranks of plantlets grown under low (LN light grey) and high (HN dark grey) nitrate conditions. Data represent mean ± SD of 7 biological replicates from two independent cultures. The different letters indicate values significantly different at $P < 0.05$ as determined using XLSTAT ANOVA Newman–Keuls (SNK) comparisons.

in the light, chlorophyll concentrations in darkened leaves were the same as in control before recovery time, while chlorophyll contents in control leaves at T2 were slightly lower than at T1, showing the effect of age-related senescence (Figure 1D).

At T0, flag leaves were still young and kept on growing while at T1 they showed the first symptoms of chlorophyll decrease marking senescence onset. In flag leaves harvested every two days from T1 to T7, chlorophyll content progressively decreased (Figure 1F). Photosystem II efficiency and CO_2 assimilation decreased in parallel (Figure 1G).

Changes in Carbon and Nitrogen contents in barley leaves during senescence

Nitrogen compounds were less abundant in plants grown under LN compared to HN. Nitrogen concentration (N%) decreased significantly with ageing in both leaf ranks and flag leaves; in the oldest leaves N% was close to 50% of that of the youngest (Figures 2A and 2B). By contrast, C% remained stable or decreased slightly with ageing (Figure 2C-D). Therefore, the N% decrease could rather be attributed to nitrogen mobilization than N dilution with ageing. Total amino acids decreased steadily with senescence (Figure 2E-F). Total soluble protein, NH_4^+, Rubisco content and chlorophyll decreased in parallel with ageing (Figure 2G-K) and were higher in HNL3 than HNL4 that was certainly still growing. Similarly, protein patterns in flag leaves showed that the T0 flag leaf is a young developing leaf and that T1 flag leaf is a mature one.

Anion contents

Because it is known that nitrate uptake can modify sulphate or chloride uptake, anion contents were monitored in the leaf ranks of plantlets (Figure 3A-D). Whereas nitrate concentrations were much lower in the LN leaves than in the HN leaves, sulphate, phosphate and chloride ones were significantly higher. Under HN condition, both nitrate and phosphate decreased with ageing meanwhile sulphate and chloride showed a flat pattern, suggesting that all these anions are not mobilized in a similar manner. In LN conditions, the most striking result was the sharp increase of sulphate in older leaves (Figure 3B).

Changes in nitrogen remobilisation enzymes during leaf senescence

Carboxipeptidase, endopeptidase (pH5.4 and pH4.5) and GS activities were monitored in protein extracts of leaf ranks from plantlets grown under LN and HN conditions. Both activities were higher in old leaves compared to young ones under both LN and HN (Figure 4). Surprisingly, and by contrast with other senescence markers, there was no significant difference in protease activity levels between the two nitrate conditions. Total GS activity increased significantly (2 fold) with ageing (Figure 5A) and was also higher in the LN leaves compared to the HN ones. Western blot allowed us to semi quantify the GS1 and GS2 isoforms. GS2 protein was more abundant in leaves of HN plantlets than in those of LN plantlets (Figure 5B). In addition, GS2 protein content decreased with leaf ageing, especially in plants grown under HN (HNL1 and HNL2 compared to HNL3 and HNL4). In parallel, GS1 increased in old leaves in both HN and LN plantlets (Figure 5B).

Changes in metabolite contents during leaf senescence

Changes in metabolite concentrations occurring during leaf senescence were investigated on plantlets (raw data available online in Supplemental Data Set 1 online) and in flag leaves (raw data available online in

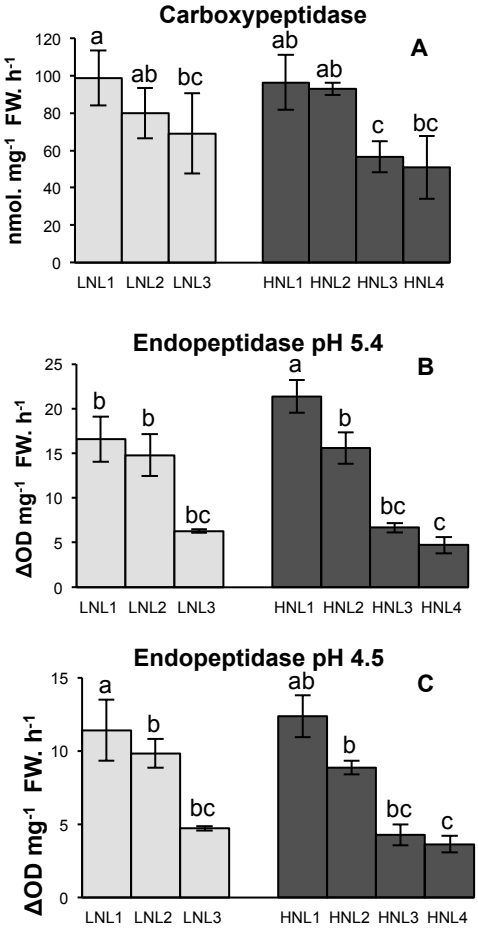

Figure 4. Protease activities are increased in old leaves of plantlets. Carboxypeptidase **(A)** and Endopeptidase at pH5.4 **(B)** and at pH4.5 **(C)** were measured. LN (low nitrate; light grey) and HN (high nitrate; dark grey). Data represent mean ± SD of 3-4 biological replicates. The different letters indicate values significantly different at $P < 0.05$ as determined using XLSTAT ANOVA Newman–Keuls (SNK) comparisons.
Similar results have been obtained on two independent cultures.

Supplemental Data Set 2). For flag leaves, only T1 (95 DAS), T3 (99 DAS) and T5 (103 DAS) samples were used.

In order to obtain a global view of the metabolic changes occurring during leaf senescence, principal component analysis (PCA) of the 110 annotated metabolites detected in barley plantlets and in flag leaves was conducted (Figure 6A and 6B). In plantlets, the first principal component (PC1), accounting for 36.8% of the total variance, resolved the time series of leaf senescence, grouping separately old leaves (L1 and L2) and young leaves (L3 and L4). The second principal component (PC2), accounting for 21.4% of the total variance, resolved the two nitrate treatments LN and HN but only for old leaves (L1 and L2). There was no separation for LNL3, HNL3 and HNL4 showing that nitrate nutrition had no strong effect on metabolite concentrations in young leaves by contrast with old leaves (Figure 6A). In flag leaves harvested at different time points, PC1, accounting for 75.25% of the total variance, separated the young (T1), mature (T3) and senescing (T5) leaves (Figure 6B).

In leaves of plantlets, the most concentrated metabolites were sucrose (50 $nmol.mg^{-1}$ FW) in all leaf ranks and malate (18 $nmol.mg^{-1}$ FW) in HN leaves. Glucose (10 $nmol.mg^{-1}$ FW) in young leaves of both HN and LN, glutamate (2 $nmol.mg^{-1}$ FW) and citrate (5 $nmol.mg^{-1}$ FW) were also abundant (Supplemental Data Set 1). In flag leaves, the most concentrated metabolites were sucrose (100 $nmol.mg^{-1}$ FW), glucose (12 $nmol.mg^{-1}$ FW), fructose (4 $nmol.mg^{-1}$ FW), galactose (2 $nmol.mg^{-1}$ FW) and malate (2 $nmol.mg^{-1}$ FW; Supplemental Data Set 2). Malate and citrate concentrations were lower in flag leaves than in plantlets while sucrose and glucose were higher. Globally metabolite concentrations were different in flag leaves and plantlet leaves (Supplemental Data Set 1 and 2).

In order to investigate the senescence-related metabolic changes, the Log_2 ratios of the metabolite concentrations were computed by normalizing each metabolite concentrations to its concentration in the Leaf 4 (HNL4) of plants grown under HN (Supplemental Data Set 3). Regarding metabolite changes occurring with leaf senescence and depending on nitrate conditions, different classes of metabolites were found (Supplemental Data Set 3; Supplemental Figure 1). Class 1 includes metabolites showing higher concentrations in young leaves under both LN and HN; class 2 includes compounds accumulated in old leaves under both LN and HN; class 3 includes metabolites accumulated in leaves under high nitrate; class 4 includes compounds accumulated in leaves under low nitrate conditions; class 5 includes metabolites accumulated in old leaves but only under HN and class 6 represents compounds accumulated in old leaves only under LN. In order to be more readable, those metabolite changes are represented on a metabolic map using the same false colours as in Supplemental Data Set 3 (Figure 7). In agreement with results reported above, the chlorophyll, protein, anion contents and the glycine/serine ratio are also represented.

In Figure 7 we can see that while glucose, fructose, glucose (-P) and fructose (-P) concentrations decreased steadily with leaf ageing in plantlets, sucrose concentration remained stable. With the exception of galactonate, gluconate, xylose, ribose5P, arabinose and galactose, most of the other minor carbohydrates (minor CHO) increased with leaf senescence. Sedoheptulose (C7 monosaccharide), maltose (disaccharide), which is a product of starch degradation, and melezitose (trisaccharide) sharply increased with leaf ageing. This was also the case of the sugar alcohols arabitol, galactinol and maltitol (Figure 7; Supplemental Data Set 3). For most of these carbohydrates, increases with leaf ageing were similar under LN and HN. Others such as erythritol, threitol, xylitol, ribonate and isomaltose were more specifically accumulated in old leaves of plants grown under LN. By contrast with those carbohydrates and similar to hexoses, most of the amino acid concentrations

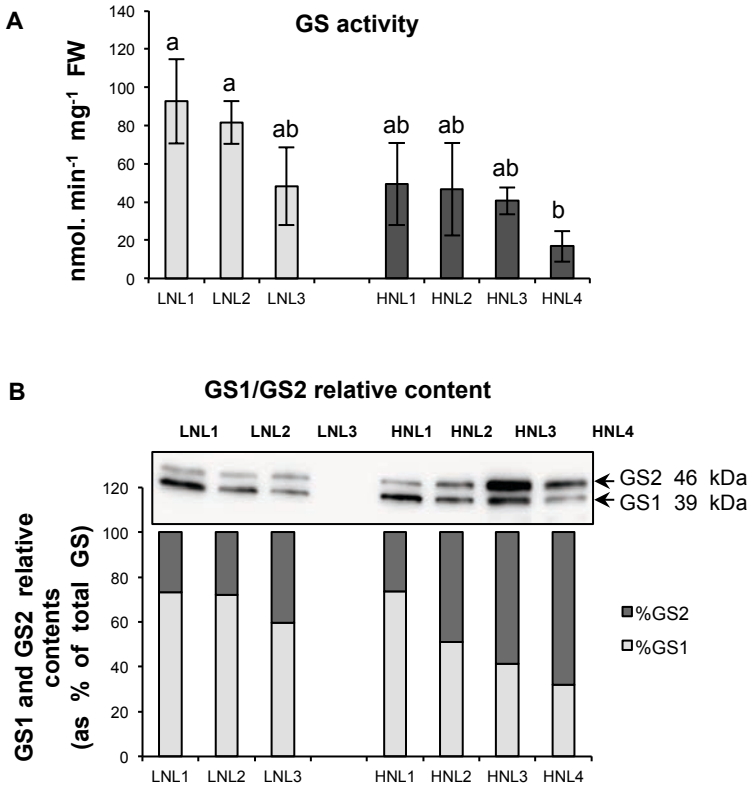

Figure 5. Glutamine synthetase (GS) activity and protein contents in leaf ranks of plantlets. (A) GS activity. Data are mean ± SD of 3-4 biological replicates. The different letters indicate values significantly different at P <0.05 as determined using XLSTAT ANOVA Newman–Keuls (SNK) comparisons. LN (low nitrate; light grey) and HN (high nitrate; dark grey). **(B)** GS1 (39 kDa) and GS2 (46 kDa) were identified on Western blots. GS1 and GS2 proportions were calculated after quantification of signals using densitometry and ImageJ imaging software. Equal protein amounts were loaded in each lane. All experiments were performed on two different cultures giving the same results.

decreased with leaf ageing. This was especially the case of major amino acids (glutamate, Glu; aspartate, Asp and glutamine, Gln) that decreased with leaf senescence whatever the nitrate conditions. Remarkable increases were however observed for cysteine (Cys) and lysine (Lys) in senescing leaves under both LN and HN. Surprisingly, leucine (Leu), proline (Pro) and tyrosine (Tyr) showed contrasted changes, increasing in old leaves under HN and decreasing in old leaves under LN. Serine (Ser) and glycine (Gly) that are both involved in the photorespiratory pathway decreased with senescence, as well as the Gly/Ser ratio, while their upstream precursor glycerate increased in senescing leaves. Globally, amino acid concentrations were lower under LN compared to HN.

The tricarboxylic acid (TCA) cycle intermediates showed more contrasted trends depending on nitrate conditions than other metabolites. Organic acids - except citrate - were more abundant under HN relative to LN and they increased with senescence. It can be noticed that the TCA compound and amino acid decreases with leaf senescence were much more pronounced under LN than HN. This shows that plants sense nitrate limitation as an additive senescence-triggering factor.

All lipids (phytosterols, fatty acids and galactolipids) increased with ageing. Phytol, which is a product of the degradation of chlorophyll decreased in old leaves but only under LN. Regarding oxidative stress related compounds, the picture was also contrasted. The increase of cysteine in old leaves suggested that glutathione pathway was more active. The high increase of both γ and α-Tocopherol in old leaves confirmed higher antioxidant activities in old leaves. However the decrease of both ascorbate and dehydroascorbate showed that antioxidant molecules accumulation was selective.

In flag leaves, the senescence-related metabolic changes were expressed as the Log_2 ratios of the metabolite concentrations normalized to the concentration in the youngest flag leaf (T1) (Supplemental Data Set 4; Figure 8). Two major metabolite classes were found: class 1, with high content of metabolites in T1 young leaf (Supplemental Figure 1G) and class 2 with high content of metabolites in the T5 senescing leaf (Supplemental Figure 1H). Apart from these groups we found that several amino acids like glutamine (Gln), asparagine (Asn), arginine (Arg), isoleucine (Ile), leucine (Leu), phenylalanine (Phe) and tryptophane (Trp) were decreased only in the T3 mature leaf. Metabolite changes occurring with flag leaf senescence are represented on a metabolic map (Figure 8) using the same false colours as in Supplemental Data Set 4.

Globally, despite the fact that metabolite concentrations were different in flag leaves and in plantlet leaves, similar senescence related changes where observed in both leaf types and especially between old flag leaves and leaf ranks of plantlets grown under low nitrate conditions. As such, hexoses and amino acids decreased with leaf senescence while all the minor carbohydrates, galactolipids and some amino acids such as lysine (Lys), cysteine (Cys) and leucine (Leu) increased. The stress related compounds α- and γ-Tocopherol were also sharply increased in senescing flag leaves. Few differences of metabolite profiles between plantlets and flag leaves can however be noticed. We observed that Pro, Tyr, glycerate and galactinol decreased during ageing in the flag leaves while they increased in old leaves of plantlets. Pipecolate, α-aminoadipate, methionine (Met) and β-Ala increased in old flag leaves while they decreased in old leaves of plantlets. It was clear that all the fatty acids accumulated in old leaves of plantlets while they decreased in old flag leaves.

Characterization of Glutamine synthetase (*GS*) and Asparagine synthetase (*ASN*) genes in barley (*Hordeum vulgare*)

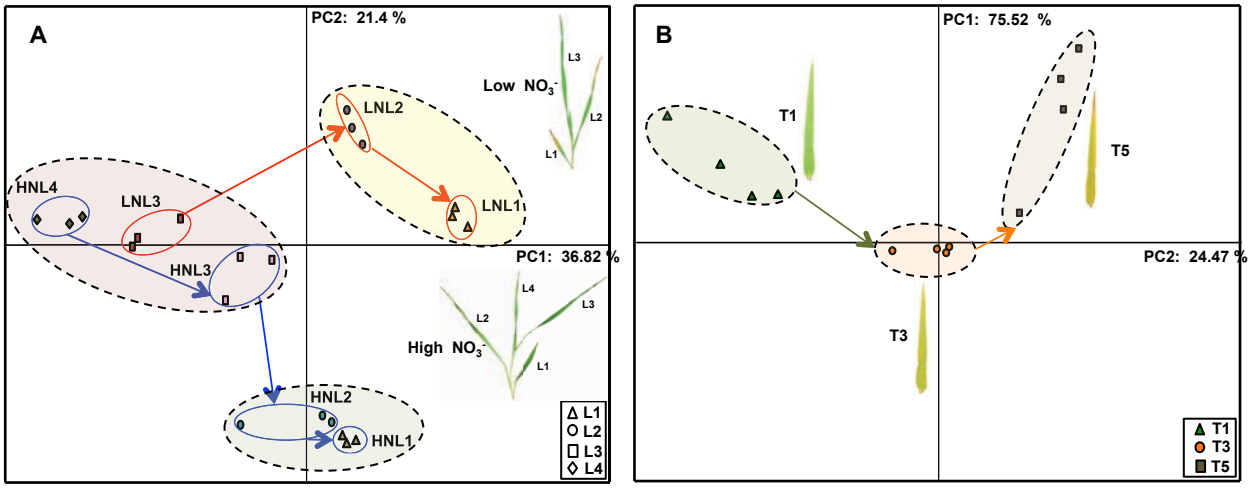

Figure 6. PCA score plot of metabolite profiles. The analysis was performed on 110 annotated metabolites detected in the leaf ranks of plantlets grown in low nitrate (LN; L1 to L3) and high nitrate (HN; L1 to L4) conditions **(A)** and in flag leaves harvested at different stages of senescence, (T1, T3, and T5) **(B)**. PCA was conducted by MultiExperiment Viewer (MeV). In (A), Δ (orange and green), ○ (brown and blue), □ (red and pink) and ◇ (grey) indicate leaf ranks from L1 to L4 of LN and HN plants respectively. Two culture rounds gave similar results (3-4 plant replicates). In (B), Δ, ○ and □ represent T1, T3 and T5 flag leaves. Full line ellipses group samples of the same leaf ranks. Dashed line ellipses group old (L1 and L2) or young (L3 and L4) leaf ranks (A) or time points T1, T3 or T5 (B). Arrows indicate increasing leaf ages.

The barley *HvGS2* sequence encoding the GS2 isoform has been previously reported by Baima *et al.* (1989). Three *HvGS1* genes encoding isoforms of GS1 have been described by Goodall *et al.* (2013). In this report we identify two additional *HvGS1* genes by sequence alignment analysis of barley ESTs with *GS* counterparts from Arabidopsis (*A. thaliana*), rice (*O. sativa*) and maize (*Z. mays*) as queries (Supplemental Table 2). In the phylogenetic tree (Supplemental Figure 2), predicted proteins of these two new isoforms were clustered with the GS proteins of prokaryotes (Swarbreck *et al.,* 2011; Supplemental Tables 3 and 4). Conserved amino acid residues essential for ligand binding specificity of GS1 protein family were found in all GS1 protein sequences (van Rooyen *et al.,* 2011; Supplemental Figure 3). The two supplementary sequences *HvGS1_4* and *HvGS1_5* correspond to two different contigs in the barley genome. Sequences were aligned to the barley genomic sequence in order to establish the *HvGS* gene models (Supplemental Figure 4).

The barley *HvASN1* and *HvASN2* sequences have been described by Moller *et al.* (2003). We found three new *HvASN* genes by alignment analysis using the *ASN* sequences from Arabidopsis, rice and maize as queries. All five *HvASN* correspond to five different contigs in the barley genome (Supplemental Table 3). In the phylogenetic tree, two of these proteins (HvASN1 and HvASN2) were clustered with AtASN1 (class I), two (HvANS3 and HvASN4) with AtASN2 (class II) and the fifth protein (HvASN5) was placed out of the branch of Arabidopsis proteins, nevertheless it was clustered with AS proteins from rice and maize (Supplemental Figure 5). Predicted proteins of all five isoforms showed between 67% and 90% conservation of the amino acid sequence with AS proteins of maize, rice and Arabidopsis (Supplemental Table 6). They conserve amino acid residues from the *purF*-type glutamine binding domain, essential amino acids for glutamate binding and positioning and essential residues for binding of aspartate and ATP (Supplemental Figure 6). *HvASN* sequences were aligned to genomic sequence in order to obtain gene models (Figure 9). Based on the sequences found for *HvGS* and *HvASN* genes, primers were designed for qPCR detection and *HvGS* and *HvASN* transcript levels were monitored during natural and induced senescence.

Changes in *HvGS* and *HvASN* transcript levels in plantlets grown under nitrate limiting conditions

Changes in the transcript levels of *HvGS2*, *HvGS1_1*, *HvGS1_2*, *HvGS1_4* and *HvGS1_5* were measured. As a control the expression of the senescence-associated *HvNAC13* and the senescence repressed *HvLSU* genes was also monitored (Christiansen *et al.,* 2011; Hollmann *et al.*, 2014).

As expected, the *HvNAC13* expression increased with leaf senescence while *HvLSU* decreased (Figure 9). *HvGS2* gene expression also decreased with leaf ageing as expected. By contrast, *HvGS1_1* and *HvGS1_2* expression level increased in old leaves under both HN and LN. *HvGS1_1* transcript level was slightly higher in plants grown under LN. The two prokaryote-like *HvGS1_4 and HvGS1_5* showed different expression patterns. The *HvGS1_4* transcript level increased in younger leaves (L2 and L3) compared to old ones (L1) in LN while in HN it showed a biphasic pattern. The *HvGS1_5* was highly expressed in young L3 in and its transcript level was higher under LN compared to HN (Figure 9). All attempts to measure *HvGS1-3* expression level was unsuccessful for unknown reasons since it was possible to measure it in the samples produced by the dark treatment experiment (see below).

Surprisingly, all the *HvASN* transcripts monitored decreased with ageing under LN and increased under HN. This contrasted effect of leaf ageing was then nitrate-dependent. However, *HvASN4* gene expression was

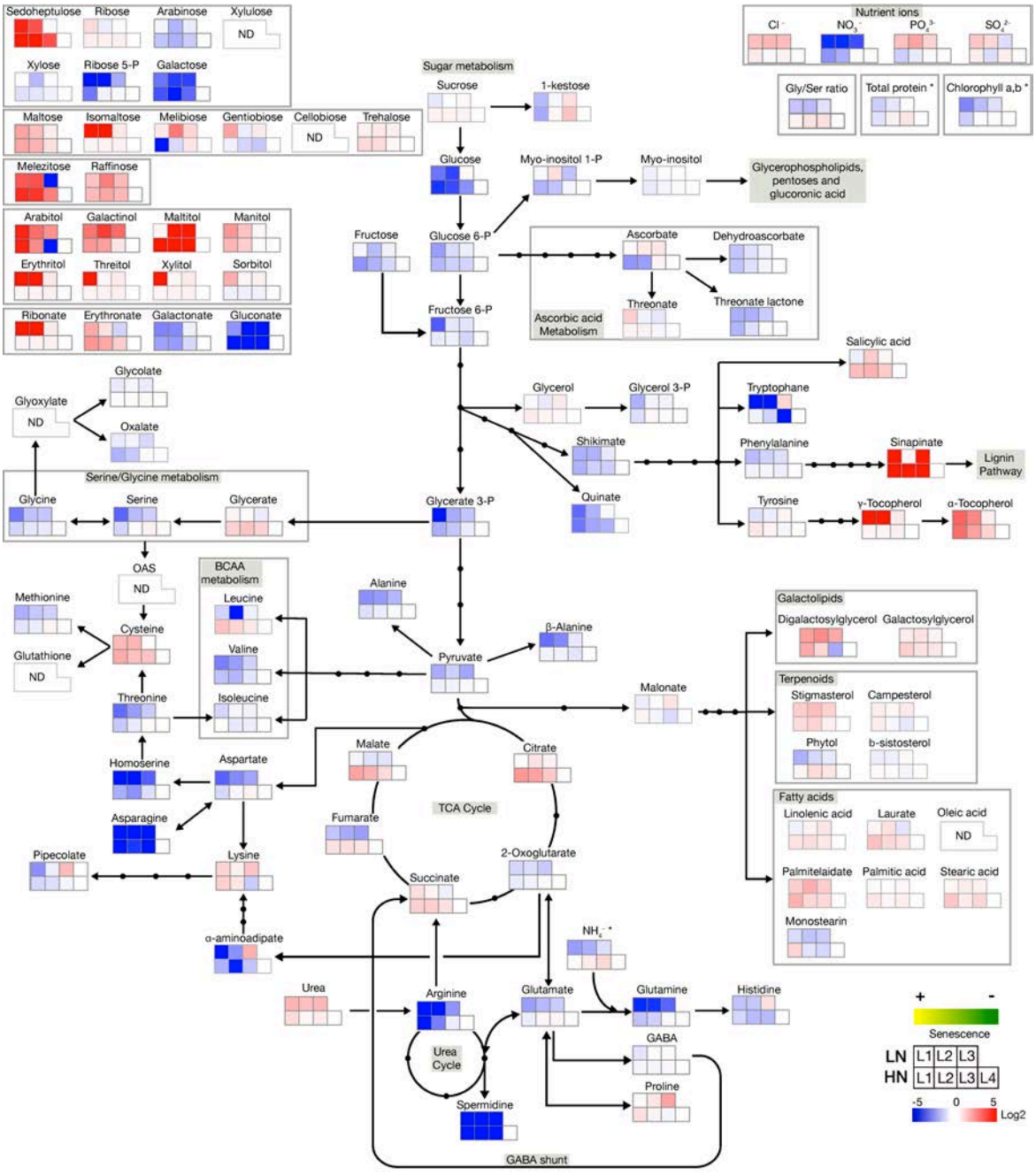

Figure 7. Heat map of metabolite changes in leaf ranks of plantlets grown under LN and HN conditions. Metabolite concentrations were determined according to the fresh weight. Log_2 ratios of metabolite concentrations normalised to the value of the youngest leaf of the high nitrate treatment (HNL4) are displayed as a metabolic pathway representation by shades of red or blue colors according to the scale bar. Stage of senescence of each leaf rank is indicated by shades of colors from yellow (more senescing old leaf) to green (less senescing young leaf) according to the scale bar. Data represent mean values of seven biological replicates for each leaf rank. ND (not determined) was applied to compounds which concentrations were below the detection threshold.

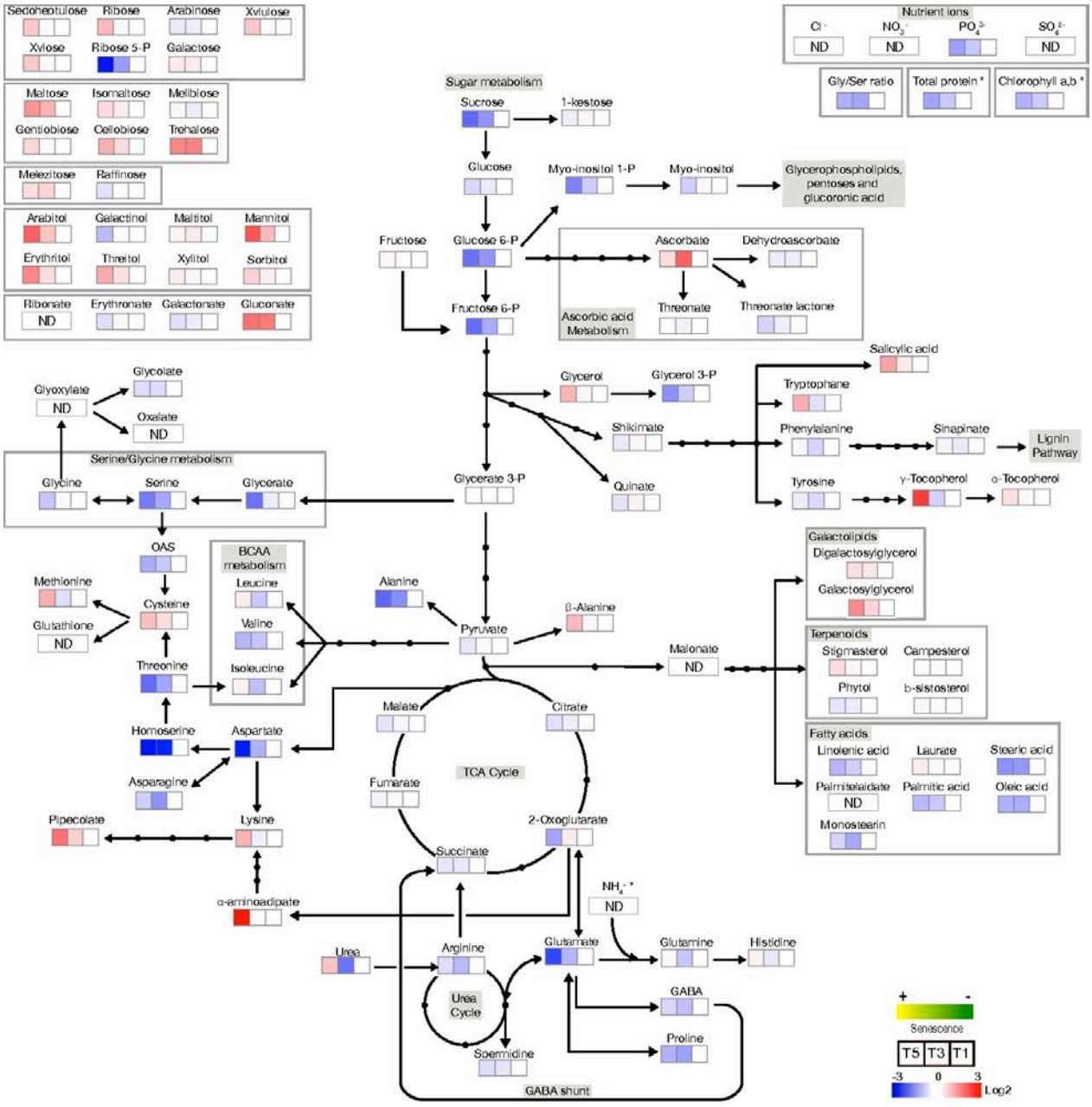

Figure 8. Heat map of metabolite changes in flag leaves during senescence. Metabolite concentrations were determined according to the fresh weight. Log_2 ratios of metabolite concentrations normalised to the value of the youngest leaf (T1) are displayed as a metabolic pathway representation by shades of red or blue colors according to the scale bar. Stage of senescence of each leaf rank is indicated by shades of colors from green (young) to yellow (old leaf) according to the scale bar. Data represent mean values of four biological replicates for each leaf rank. ND (not determined) was applied to compounds, which concentrations were below the detection threshold. Note that T1 to T5 time course is presented from the right to the left in this figure.

different under LN, remaining at the same level in all leaf ranks (Figure 9). *HvASN2* expression level could not be measured since no specific primers were found for this gene.

Changes in *HvGS* and *HvASN* transcript levels in flag leaves during senescence

HvGS and *HvASN* expression was monitored on the young T1 (95 DAS), mature T3 (99 DAS) and senescing T5 (103 DAS) leaves. Only expression of *HvGS1_1*, *HvGS1_4*, *HvGS1_5*, *HvGS2*, *HvASN3* and *HvASN4* could be monitored in flag leaf samples. Due to sequence polymorphism between Carina and Golden Promise genotypes, the primers identified for the other *HvGS* and *HvASN* could not be used for real time RT-qPCR on Carina samples. The *HvGS1_1* and *HvGS1_4* transcript levels gradually increased from T1 to T5 in parallel with *HvNAC13* and opposed to *HvGS2* that decreased with senescence (Figure 10). *HvGS1_5* gene expression did not change during time; *HvASN3* mRNA level showed a slight increase at T3 and T5 compared to T1. *HvASN4* gene expression decreased from T1 to T5 showing a completely opposite pattern.

Changes in *HvGS* and *HvASN* transcript levels in leaf ranks of plantlets grown under dark stress conditions

In order to observe the effect of dark induced senescence on *HvGS* and *HvASN* gene expression, transcript levels were evaluated in the different leaf ranks after 4 d of dark and also after a recovery time of 3 d. Expression in dark treated leaves (DL) was compared to light controls (CL) that had not been transferred to the dark (Figure 1C). *HvNAC13* and *HvSSU* were used as senescence induced and senescence repressed controls (Gregersen *et al.,* 2008). Indeed, *HvNAC13* expression level increased after dark treatment while *HvSSU* decreased (Figure 11).

In leaves from plant controls that remained under optimal light conditions during the whole of this experiment, we observed that the transcript level of all *HvGS1* genes was higher in old leaves of plants harvested at T1. *HvGS1_1*, *HvGS1_2*, *HvGS1_3* expressions levels were also higher in old leaves at T2, but this was not the case for *HvGS1_4* and *HvGS1_5* that remained the same in all leaf ranks. The senescence-related pattern observed on control leaves was mostly similar to that observed in Figure 9. *HvGS1_1* and *HvGS1_2* transcript levels were not modified by dark treatment, while *HvNAC13*, *HvGS1*_3, *HvASN1*, *HvASN4* and *HvASN5* transcript levels were increased after dark treatment. Similarly to *HvGS2* and *HvSSU*, the *HvGS1_4*, *HvGS1*_5 and *HvASN3* transcript levels decreased with dark treatment.

After recovery time (T2), all the transcript levels were similar in dark treated and control leaves with the exception of *HvGS2* and *HvSSU*, which were much higher in the dark treated leaves than in untreated controls (Figure 11).

Discussion

The aim of this study was to provide a picture of the physiological events related to nitrogen management and remobilisation occurring in barley during leaf senescence. Up to now, leaf senescence metabolism has been described in several plant species such as tobacco, Arabidopsis, wheat, maize and rice and different approaches have been used in order to induce and study leaf senescence. For natural senescence studies, plants are usually cultivated under optimal conditions. Stress-induced senescence can be enhanced through nitrate limitation,

b

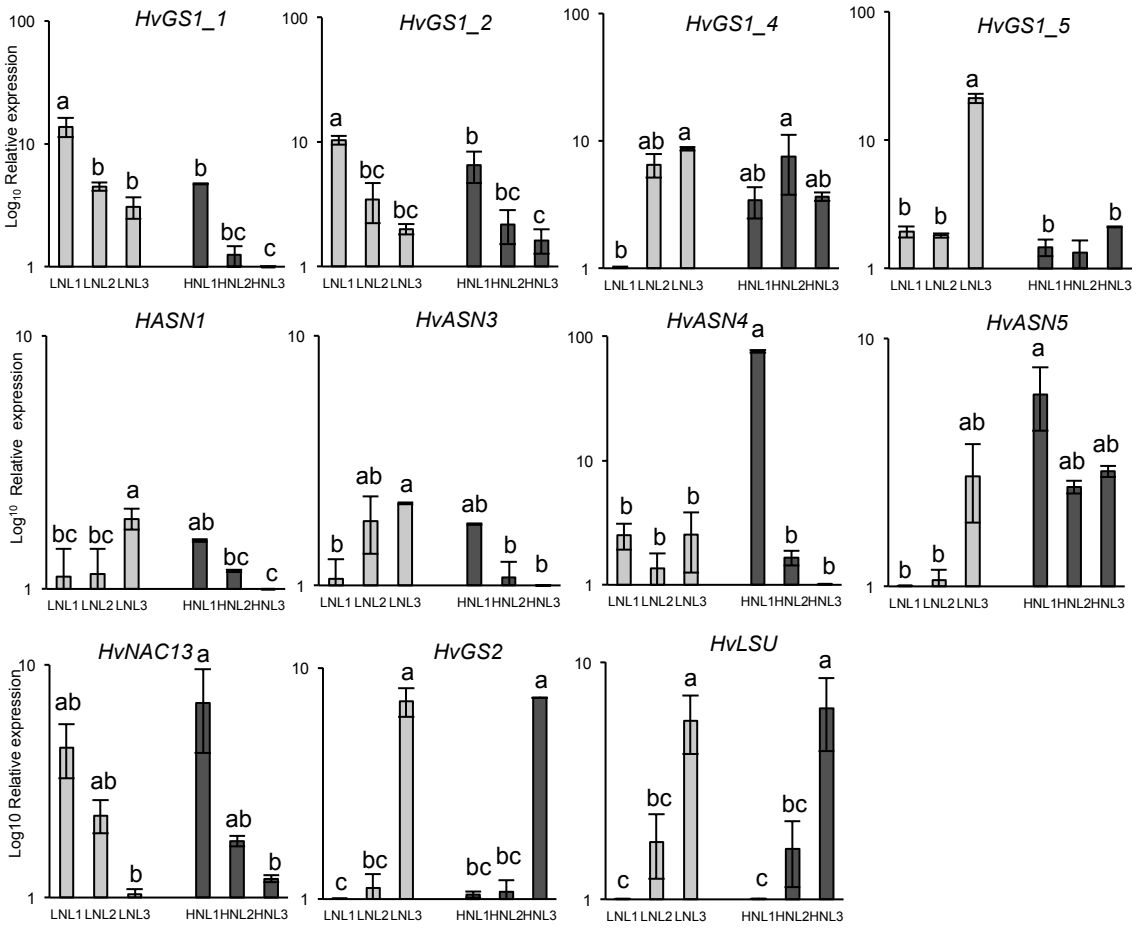

Figure 9. Transcript levels of *HvGS*, *HvASN*, *HvNAC13* and *HvLSU* genes in leaves of plantlets grown under low (LN) and high (HN) nitrate conditions. Only leaf ranks L1, L2 and L3 from LN (grey bars) and HN (black bars) plantlets were analysed. Both line charts and histograms are presented for *HvASN* (LN: light grey line; HN: dark grey line). Log_{10} relative expression values are shown. Data are mean ± SD (n = 3 biological replicates). The different letters indicate values significantly different at P <0.05 as determined using XLSTAT ANOVA Newman–Keuls (SNK) comparisons. *HvGAPDH* was used as reference gene.

carbon starvation through a dark treatment or both, using detached leaves for example. In the case of natural senescence, two experimental designs can be found in literature, as leaf rank comparison at one time-point (Masclaux *et al.,* 2000; Niewiadomska *et al.,* 2009; Hirel *et al.,* 2005a; Hirel *et al.,* 2005b; Orsel *et al.,* 2014), or changes over time, following one leaf rank at different time points (Diaz *et al.,* 2008, 2005). Watanabe *et al.*, (2013) used both models to get a comparison of metabolite contents in Arabidopsis leaves during senescence. Both models present advantages and disadvantages since all leaf ranks cannot be taken into account at all time points and since there are certainly physiological and metabolic differences in leaves depending on vegetative and reproductive stages and on the size and the nature of the sink organs present in the plants (young leaves or seeds) at different time points.

In barley, our aim was to investigate and compare the changes in metabolic and senescence markers using both leaf rank model and flag leaf senescence. We also assayed stress-induced senescence using dark-treated plants and nitrogen limitation. As leaf senescence is mainly considered for its role in nutrient recycling and remobilisation, we focussed mainly on the enzymes related with these processes. Measurements of chlorophyll contents, photosynthesis and senescence-associated gene expressions led to the identification of young, mature and senescing leaves in each experiment. On both flag leaf and leaf rank models, we globally observed the same picture of leaf senescence i.e. a decrease of all the nitrogen compounds, an increase of N remobilisation markers such as GS1 proteins, endoprotease and carboxypeptidase activities and a decrease of the Rubisco and GS2 protein contents (Masclaux-Daubresse *et al.,* 2010 and Avila-Ospina et al., 2014 for reviews). Surprisingly and by contrast with other plant species like Arabidopsis or tobacco, the total GS activity increased significantly with ageing (Diaz *et al.,* 2008; Martin *et al.,* 2006; Masclaux *et al.,* 2000). GS activity was also higher in the LN leaves compared to the HN ones as previously described in Arabidopsis by Lemaître *et al.* (2008). Since GS1 isoforms appear more abundant under LN and in old leaves, it can be concluded that increase in total GS activity during senescence and under low nitrate is mainly due to GS1 activity. We then focused on the expression of the master genes considered to control nitrogen remobilisation from source to sink tissues, namely the glutamine and asparagine synthetase genes. Goodall *et al.* (2013) who identified *HvGS1_1*, *HvGS1_2* and *HvGS1_3* showed that *HvGS1*_3 is more expressed in grain, *HvGS1_1* in stem and *HvGS1_2* in leaves and roots, also that *HvGS1_3* is more highly expressed when ammonium is provided as the sole nitrogen source. While authors have characterized *HvGS1* expressions in response to nitrate and ammonium supply, they do not provide any data about their responses to leaf senescence. Using barley genome sequence, we identified two putative *HvGS1-4* and *HvGS1-5* genes that are more similar to the prokaryotic-like forms (Mathis *et al.,* 1999; Nogueira *et al.,* 2005). Globally all five *HvGS1* genes were more highly expressed in senescing leaves of barley. In response to dark treatment, only *HvGS1_3* was induced while *HvGS1_4* and *HvGS1_5* were repressed. In addition to the two *HvASN1* and *HvASN2* genes already described by Moller *et al.* (2003), we found three more *HvASN3-5* sequences. Then all the *HvASN1-5* identified were surprisingly induced by leaf senescence under HN but repressed under low LN. In flag leaves, senescence effect was more contrasted since *HvASN3* mRNA level increased with ageing while *HvASN4* decreased. Such a difference may have been due to the relative sugar amino acid concentrations and their proportion in leaves, as asparagine synthetase expressions can be modulated by sugar contents (Oliveira *et al.,* 2002; Gaufichon *et al.,* 2010). From phylogeny trees, we found that *HvASN1* and *HvASN2* are more similar to the Arabidopsis *AtASN1*, while *HvASN3*, *HvASN4* are more similar to *AtASN2*. Accordingly we confirmed that *HvASN1* is dark induced (Moller *et al.,* 2003) in a similar

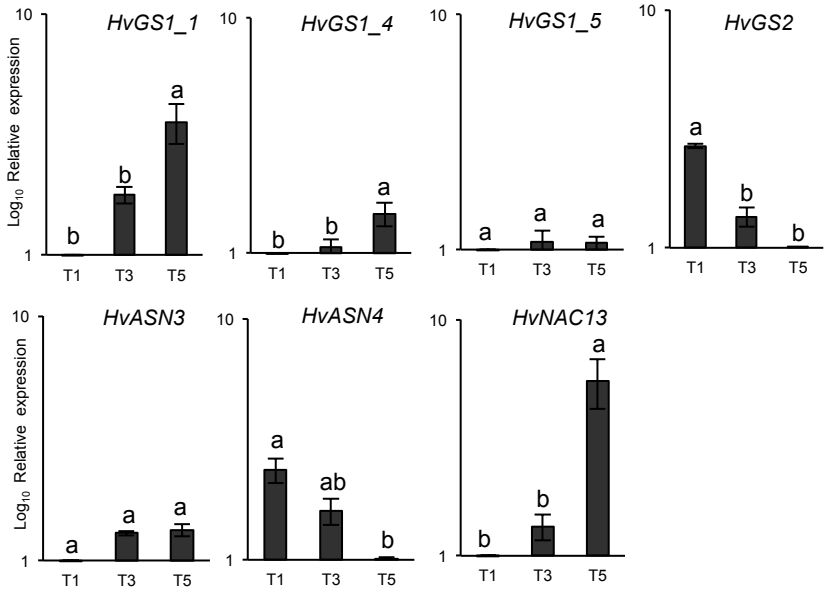

Figure 10. Transcript levels of *HvGS*, *HvASN* and *HvNAC13* genes in flag leaves harvested at different stages of senescence. Young leaf (T1), mature leaf (T3) and senescing leaf (T5) were analysed. Log_{10} relative expression values are shown. Data are mean ± SD (n = 3 biological replicates). The different letters indicate values significantly different at P <0.05 as determined using XLSTAT ANOVA Newman–Keuls (SNK) comparisons. *HvActin* was used as reference gene.

way to *AtASN1* (also called *DIN 6, Dark Inducible 6*; Oliveira *et al.,* 2002; Gaufichon *et al.,* 2010) and that *HvASN3* was dark repressed like *AtASN2*, which is known to be repressed in the dark and to be induced by sugars. This was not however observed for *HvASN4*. The most striking new result is opposite effect of leaf senescence on the expression of *HvASN* genes depending on nitrate conditions. The fact that *HvASN* were induced by senescence only under HN suggests that AS are needed for nitrogen remobilisation specifically under HN, as Asp concentrations are quite high compared to Asn. It also seems that natural and stress-induced senescence do not have the same effect on gene expressions, especially in the case of *HvASN*.

Metabolite profiling provided the best basis to compare leaf senescence models (leaf rank and flag leaf) and plant species (Watanabe *et al.,* 2013; Diaz *et al.,* 2005). The main senescence-related features observed in barley are (i) the increase of carbohydrates (pentoses, sugar derivatives, lipids and fatty acids) certainly released from membrane and cell wall degradations, (ii) the decrease of hexoses and glycolysis compounds, (iii) the increase of organic acids involved in the TCA cycle and (iv) the decrease of most of the amino acids (except cysteine and lysine that increased). Pipecolate and α-aminoadipate that are related to the catabolism of BCAA and lysine, and participate in the anaplerotic respiratory pathway decreased (Boex-Fontvieille *et al.,* 2013; Figure 12). Interestingly, Christiansen and Gregersen (2014) showed that the genes coding the 2-oxoglutarate and succinate dehydrogenase activities involved in TCA pathway are induced with senescence in barley. This is in good accordance with a higher TCA activity in senescing barley leaves. This metabolic picture of barley leaf senescence then suggests that energy sources in senescing leaves are coming from the degradation of cell constituents (cell wall, membranes, proteins and amino acids), pentose phosphate pathway and TCA while photosynthesis and glycolysis activities are decreased.

The senescence features described by Watanabe *et al. (*2013) in Arabidopsis presents several similarities with barley such as the accumulation of secondary metabolites, fatty acids and minor carbohydrates and the decrease of the major amino acids like glutamate, glutamine, aspartate, glycine and serine (Figure 12). However, in contrast to barley, Watanabe *et al.*, (2013) found that sucrose and hexoses, BCAA and AAA accumulate in Arabidopsis senescing leaves, while galactolipids decrease. Apart from the fact that sucrose and hexoses accumulations in Arabidopsis leaves during senescence has been found as a transient feature by Diaz *et al. (*2005), accumulation of BCAA and of the AAA tyrosine observed by Watanabe *et al. (*2013) had also been found by Diaz *et al. (*2005) in senescing leaves of several Arabidopsis genotypes. Regarding to the TCA cycle, Watanabe *et al. (*2013) did not find the same picture as in barley since all the TCA organic acids except citrate decreased with senescence in Arabidopsis. Concerning GABA that can be used through the GABA shunt to provide succinate, Watanabe *et al.* (2013) and Diaz *et al.* (2005) showed that it was highly accumulated in Arabidopsis senescing leaves, in contrast with barley, where we did not detect any GABA modification during leaf senescence. Galactolipids that are specifically from chloroplast membranes can also be used to support respiratory pathway through beta-oxidation in the peroxisomes. While galactolipids decreased in Arabidopsis with senescence (Watanabe *et al.*, 2013), they accumulated in barley old leaves in parallel with the accumulation of saturated fatty acids such as palmitic acid and stearic acid. Both have been proposed as early degradation products of highly unsaturated plastid galactolipids in senescing leaves (Yang and Ohlrogge, 2009). The possibility that metabolic pathways involved in lipid degradation are different between Arabidopsis and barley has to be considered (Wanner *et al.,* 1991). Albeit some metabolite changes occurring in barley and in Arabidopsis during leaf senescence were similar, major differences in the management of glycolysis, TCA and

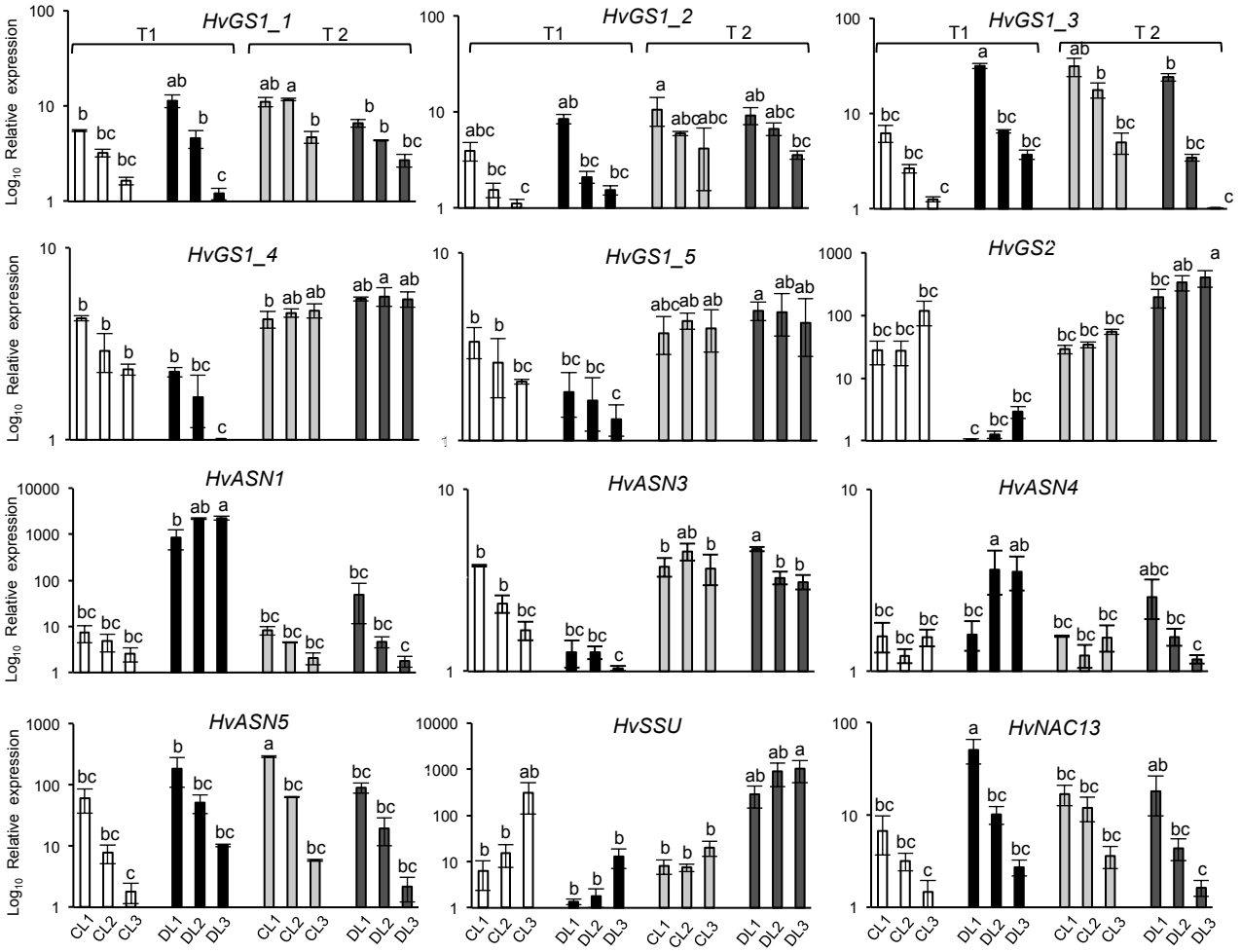

Figure 11. Transcript levels of *HvGS*, *HvASN*, *HvNAC13* and *HvSSU* genes in leaves of plantlets after dark treatment and recovering. CL (control leaves at T1: white; control leaves at T2: light grey); DL (darkened leaves at T1: black; darkened leaves at T2: dark grey). Log_{10} relative expression values are shown. Data are mean ± SD (n = 3 biological replicates). The different letters indicate values significantly different at P <0.05 as determined using XLSTAT ANOVA Newman–Keuls (SNK) comparisons. *HvGAPDH* was used as reference gene.

anabolic/catabolic metabolism of minor amino acids (BCAA and AAA) were identified between the two plant species.

Metabolic changes occurring in the flag leaves - which in cereals are considered as the main contributor to seed filling especially regarding nitrogen management and remobilisation - during leaf senescence were globally the same as in leaf ranks of plantlets, especially when grown under low nitrate conditions (Figure 12). Only few differences (for tryptophane, glycerate, β-alanine and pipecolate) were detected. Compared to HN leaf ranks, we also noticed differences in the free fatty acids and TCA compounds that did not accumulate and were less abundant in flag leaves. Primary leaves contained much more malate and citrate compared to flag leaves. Organic acid concentrations that were strongly modified in plantlet leaves depending on nitrate nutrition were less abundant in leaves of plants grown under low nitrate conditions as shown by Balazadeh *et al. (*2014), thus reaching similar profile as in flag leaves.

From the comparison of the effect of leaf senescence on the chlorophyll and metabolite concentrations, on enzyme activities and transcript levels we can conclude that studying leaf senescence metabolism using leaf rank model is a quite good approximation of what is occurring in flag leaf during monocarpic senescence. By contrast leaf-senescence metabolism appeared more different between barley and Arabidopsis. As the major differences observed in barley compared to Arabidopsis are hexoses and glycolysis, the putative role of glucose and other hexoses in the regulation of leaf senescence that has been proposed in Arabidopsis (Wingler *et al.,* 2006) might have to be considered carefully in the case of barley (Parrott *et al.,* 2005, 2007). Differences in minor amino acid contents in Arabidopsis and barley also raise questions about the mechanisms of catabolism and remobilisation of organic nitrogen in these two plant species. The reason why minor amino acids accumulate in Arabidopsis but not in barley during leaf senescence might be the result of different remobilisation strategies or differential efficiency in the anaplerotic pathways supporting respiration. Indeed, TCA cycle seems to be more active in old leaves of barley than in Arabidopsis ones. The senescence related anaplerotic pathways using amino acid catabolism to support respiration might then also be more efficient in barley. It could also be that nitrogen remobilisation to sinks is more efficient in barley plants, which were bred for this trait, than in Arabidopsis, explaining the fact that Arabidopsis accumulates minor amino acids that it cannot remobilise. Whatever the reason of their metabolic differences, those traits require to be analysed and explored further. We can conclude from this study that several model plants are certainly needed to explore the specificities and the variability of the metabolic changes occurring during leaf senescence.

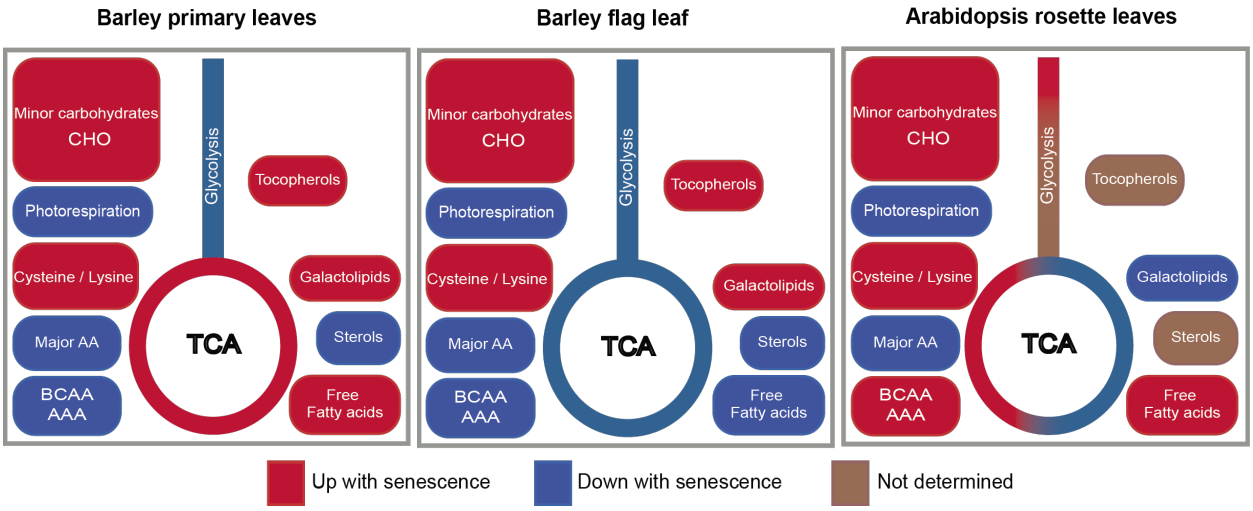

Figure 12. Schematic representation of the metabolic pathways affected during leaf senescence in Arabidopsis and barley. Metabolic pathways in which metabolites accumulate during senescence are represented in red. Metabolic pathways in which metabolites decrease are represented in blue. TCA: tricarboxylic acid cycle; BCAA: branched chain amino acids; AAA: aromartic amino acids. Changes occuring in Arabidopsis leaves during leaf senescence have been interpreted from Watanabe *et al.* (2013).

Supplemental Figures and Tables

Supplemental Figure 1. Metabolite clusters found in leaf ranks of plantlets grown under low nitrate LN and high nitrate HN conditions and in flag leaf at different stages of senescence.

Supplemental Figure 2. Phylogenetic tree of cytosolic Glutamine synthetase 1 gene family.

Supplemental Figure 3. Protein alignment of GS1 family.

Supplemental Figure 4. Description of barley *GS* gene structures (*HvGS*).

Supplemental Figure 5. Phylogenetic tree of Asparagine synthetase gene family.

Supplemental Figure 6. Protein alignment of ASN family.

Supplemental Figure 7. Description of barley *HvASN* gene structures.

Supplemental Table 1.

Supplemental Table 2. Collection of *GS* and *ASN* genes in *A. thaliana, O. sativa* and *Z. mays*.

Supplemental Table 3. Colection of *HvGS* and *HvASN*.

Supplemental Table 4. Intron-Exon sequences of *HvGS* and *HvASN*.

Supplemental Table 5. Percent Identity Matrix - Gluthamine Synthetase proteins.

Supplemental Table 6. Percent Identity Matrix - Asparagine Synthetase proteins.

References

Arnon DI. 1949. Copper enzymes in isolated chloroplasts. Polyphenol oxidase in *Beta vulgaris* L. *Plant Physiology* **24**, 1-15.

Avila-Ospina L, Moison M, Yoshimoto K, Masclaux-Daubresse C. 2014. Autophagy, plant senescence, and nutrient recycling. *J Exp Bot* **doi:10.1093/jxb/eru039**.

Avni R, Zhao R, Pearce S, Jun Y, Uauy C, Tabbita F, Fahima T, Slade A, Dubcovsky J, Distelfeld A. 2014. Functional characterization of GPC-1 genes in hexaploid wheat. *Planta* **239**, 313-324.

Baima S, Haegi A, Stroman P, Casadoro G. 1989. CHARACTERIZATION OF A CDNA CLONE FOR BARLEY LEAF GLUTAMINE-SYNTHETASE. *Carlsberg Research Communications* **54**, 1-9.

Balazadeh S, Schilhauer J, Araujo WL, Munné-Bosch S, Fernie AR, Proost S, Humbeck K, Mueller-Roeber B. 2014. Reversal of senescence by N resupply to N-starved Arabidopsis thaliana: transcriptomic and metabolomic consequences. *Journal of Experimental Botany* **doi:10.1093/jxb/eru119**.

Boex-Fontvieille ERA, Gauthier PPG, Gilard F, Hodges M, Tcherkez GGB. 2013. A new anaplerotic respiratory pathway involving lysine biosynthesis in isocitrate dehydrogenase-deficient Arabidopsis mutants. *New Phytologist* **199**, 673-682.

Brugière N, Dubois F, Masclaux C, Sangwan RS, Hirel B. 2000. Immunolocalization of glutamine synthetase in senescing tobacco (*Nicotiana tabacum* L.) leaves suggests that ammonia assimilation is progressively shifted to the mesophyll cytosol. *Planta* **211**, 519-527.

Buchanan-Wollaston V. 1997. The molecular biology of leaf senescence. *Journal of Experimental Botany* **48**, 181-199.

Christiansen MW, Holm PB, Gregersen PL. 2011. Characterization of barley (Hordeum vulgare L.) NAC transcription factors suggests conserved functions compared to both monocots and dicots. *BMC research notes* **4**, 302-302.

Christiansen MW, Gregersen PL. 2014. Members of the NAC transcription factor gene family show differential co-regulation with senescence-associated genes during senescence of flag leaves. *Journal of Experimental Botany* **doi:10.1093/jxb/eru046**

Diaz C, Lemaitre T, Christ A, Azzopardi M, Kato Y, Sato F, Morot-Gaudry J-F, Le Dily F, Masclaux-Daubresse C. 2008. Nitrogen recycling and remobilisation are differentially controlled by leaf

senescence and development stage in Arabidopsis under low nitrogen nutrition. *Plant Physiology* **147**, 1437-1449.
Diaz C, Purdy S, Christ A, Morot-Gaudry JF, Wingler A, Masclaux-Daubresse C. 2005. Characterization of markers to determine the extent and variability of leaf senescence in Arabidopsis. A metabolic profiling approach. *Plant Physiol* **138**, 898-908.
Distelfeld A, Pearce SP, Avni R, Scherer B, Uauy C, Piston F, Slade A, Zhao R, Dubcovsky J. 2012. Divergent functions of orthologous NAC transcription factors in wheat and rice. *Plant Molecular Biology* **78**, 515-524.
Fischer AM. 2012. The Complex Regulation of Senescence. *Critical Reviews in Plant Sciences* **31**, 124-147.
Gaufichon L, Reisdorf-Cren M, Rothstein SJ, Chardon F, Suzuki A. 2010. Biological functions of asparagine synthetase in plants. *Plant Science* **179**, 141-153.
Goodall AJ, Kumar P, Tobin AK. 2013. Identification and Expression Analyses of Cytosolic Glutamine Synthetase Genes in Barley (Hordeum vulgare L.). *Plant and Cell Physiology* **54**, 492-505.
Gregersen PL, Culetic A, Boschian L, Krupinska K. 2013. Plant senescence and crop productivity. *Plant Molecular Biology* **82**, 603-622.
Guiboileau A, Avila-Ospina L, Yoshimoto K, Soulay F, Azzopardi M, Marmagne A, Lothier J, Masclaux-Daubresse C. 2013. Physiological and metabolic consequences of autophagy defisciency for the management of nitrogen and protein resources in Arabidopsis leaves depending on nitrate availability. *New Phytologist* **199**, 683-694.
Himelblau E, Amasino RM. 2001. Nutrients mobilized from leaves of *Arabidopsis thaliana* during leaf senescence. *J. Plant Physiol.* **158**, 1317-1323.
Hirel B, Andrieu B, Valadier MH, Renard S, Quillere I, Chelle M, Pommel B, Fournier C, Drouet JL. 2005a. Physiology of maize II: Identification of physiological markers representative of the nitrogen status of maize (Zea mays) leaves during grain filling. *PHYSIOLOGIA PLANTARUM* **124**, 178-188.
Hirel B, Martin A, Terce-Laforgue T, Gonzalez-Moro MB, Estavillo JM. 2005b. Physiology of maize I: A comprehensive and integrated view of nitrogen metabolism in a C4 plant. *PHYSIOLOGIA PLANTARUM* **124**, 167-177.
Hollmann J, Gregersen PL, Krupinska K. 2014. Identification of predominant genes involved in regulation and execution of senescence-associated nitrogen remobilisation in flag leaves of field grown barley. *J Exp Bot* **doi:10.1093/jxb/eru094**.
Ishida H, Yoshimoto K, Izumi M, Reisen D, Yano Y, Makino A, Ohsumi Y, Hanson MR, Mae T. 2008. Mobilization of rubisco and stroma-localized fluorescent proteins of chloroplasts to the vacuole by an ATG gene-dependent autophagic process. *Plant Physiol* **148**, 142-155.
Kichey T, Hirel B, Heumez E, Dubois F, Le Gouis J. 2007. In winter wheat (*Triticum aestivum* L.), post-anthesis nitrogen uptake and remobilisation to the grain correlates with agronomic traits and nitrogen physiological markers. *Field Crop Res* **102**, 22-32.
Lemaître T, Gaufichon L, Boutet-Mercey S, Christ A, Masclaux-Daubresse C. 2008. Enzymatic and metabolic diagnostic of nitrogen deficiency in Arabidopsis thaliana Wassileskija accession. *Plant and Cell Physiology* **49**, 1056-1065.
Lothier J, Gaufichon L, Sormani R, Lemaitre T, Azzopardi M, Morin H, Chardon F, Reisdorf-Cren M, Avice JC, Masclaux-Daubresse C. 2011. The cytosolic glutamine synthetase GLN1;2 plays a role in the control of plant growth and ammonium homeostasis in Arabidopsis rosettes when nitrate supply is not limiting. *Journal of Experimental Botany* **62**, 1375-1390.
Martin A, Lee J, Kichey T, Gerentes D, Zivy M, Tatout C, Dubois F, Balliau T, Valot B, Davanture M, Terce-Laforgue T, Quillere I, Coque M, Gallais A, Gonzalez-Moro MB, Bethencourt L, Habash DZ, Lea PJ, Charcosset A, Perez P, Murigneux A, Sakakibara H, Edwards KJ, Hirel B. 2006. Two cytosolic glutamine synthetase isoforms of maize are specifically involved in the control of grain production. *Plant Cell* **18**, 3252-3274.
Martinez DE, Costa ML, Guiamet JJ. 2008. Senescence-associated degradation of chloroplast proteins inside and outside the organelle. *Plant Biol (Stuttg)* **10 Suppl 1**, 15-22.
Masclaux C, Valadier M, Brugière N, Morot-Gaudry J, Hirel B. 2000. Characterization of the sink/source transition in tobacco (*Nicotiana tabacum* L.) shoots in relation to nitrogen management and leaf senescence. *Planta* **211**, 510-518.
Masclaux-Daubresse C, Clément G, Anne P, Routaboul J, Guiboileau A, Soulay F, Shirasu K, Yoshimoto K. 2014. Stitching together the multiple dimensions of autophagy using metabolomic and transcriptomic analyses reveals new impacts of autophagy defects on metabolism, development and plant response to environment. *The Plant Cell* **26**, 1857-1877.

Masclaux-Daubresse C, Daniel-Vedele F, Dechorgnat J, Chardon F, Gaufichon L, Suzuki A. 2010. Nitrogen uptake, assimilation and remobilisation in plants: challenges for sustainable and productive agriculture. *Annals of Botany* **105**, 1141-1157.
Masclaux-Daubresse C, Reisdorf-Cren M, Orsel M. 2008. Leaf nitrogen remobilisation for plant development and grain filling. *Plant Biol (Stuttg)* **10(1)**, 23-36.
Masclaux-Daubresse C, Reisdorf-Cren M, Pageau K, Lelandais M, Grandjean O, Kronenberger J, Valadier MH, Feraud M, Jouglet T, Suzuki A. 2006. Glutamine synthetase-glutamate synthase pathway and glutamate dehydrogenase play distinct roles in the sink-source nitrogen cycle in tobacco. *Plant Physiol* **140**, 444-456.
Mathis R, Grosjean C, de Billy F, Huguet T, Gamas P. 1999. The early nodulin gene MtN6 is a novel marker for events preceding infection of Medicago truncatula roots by Sinorhizobium meliloti. *Molecular Plant-Microbe Interactions* **12**, 544-555.
Mayer KFX, Waugh R, Langridge P, Close TJ, Wise RP, Graner A, Matsumoto T, Sato K, Schulman A, Muehlbauer GJ, Stein N, Ariyadasa R, Schulte D, Poursarebani N, Zhou R, Steuernagel B, Mascher M, Scholz U, Shi B, Madishetty K, Svensson JT, Bhat P, Moscou M, Resnik J, Hedley P, Liu H, Morris J, Frenkel Z, Korol A, Berges H, Taudien S, Groth M, Felder M, Platzer M, Brown JWS, Fincher GB, Sampath D, Swarbreck D, Scalabrin S, Zuccolo A, Vendramin V, Morgante M, Int Barley Genome Sequencing C. 2012. A physical, genetic and functional sequence assembly of the barley genome. *Nature* **491**, 711-+.
Moller MG, Taylor C, Rasmussen SK, Holm PB. 2003. Molecular cloning and characterisation of two genes encoding asparagine synthetase in barley (Hordeum vulgare L.). *Biochimica Et Biophysica Acta-Gene Structure and Expression* **1628**, 123-132.
Niewiadomska E, Polzien L, Desel C, Rozpadek P, Miszalski Z, Krupinska K. 2009. Spatial patterns of senescence and development-dependent distribution of reactive oxygen species in tobacco (Nicotiana tabacum) leaves. *Journal of Plant Physiology* **166**, 1057-1068.
Nogueira ED, Olivares FL, Japiassu JC, Vilar C, Vinagre F, Baldani JI, Hemerly AS. 2005. Characterization of glutamine synthetase genes in sugarcane genotypes with different rates of biological nitrogen fixation. *Plant Science* **169**, 819-832.
Oliveira IC, Brears T, Knight TJ, Clark A, Coruzzi GM. 2002. Overexpression of cytosolic glutamine synthetase. Relation to nitrogen, light, and photorespiration. *Plant Physiology* **129**, 1170-1180.
Orsel M, Moison M, Clouet V, Thomas J, Leprince F, Canoy A-S, Just J, Chalhoub B, Masclaux-Daubresse C. 2014. Sixteen cytosolic glutamine synthetase genes identified in the Brassica napus L. genome are differentially regulated depending on nitrogen regimes and leaf senescence. *J Exp Bot* **doi:10.1093/jxb/eru041**.
Parrott D, Yang L, Shama L, Fischer AM. 2005. Senescence is accelerated, and several proteases are induced by carbon "feast" conditions in barley (Hordeum vulgare L.) leaves. *Planta* **222**, 989-1000.
Parrott DL, McInnerney K, Feller U, Fischer AM. 2007. Steam-girdling of barley (Hordeum vulgare) leaves leads to carbohydrate accumulation and accelerated leaf senescence, facilitating transcriptomic analysis of senescence-associated genes. *New Phytol* **176**, 56-69.
Rosen H. 1957. A modified ninhydrin colorimetric analysis for amino acids. *Archives of Biochemistry and Biophysics* **67**, 10-15.
Schippers JHM, Nunes-Nesi A, Apetrei R, Hille J, Fernie AR, Dijkwel PP. 2008. The Arabidopsis onset of leaf death5 Mutation of Quinolinate Synthase Affects Nicotinamide Adenine Dinucleotide Biosynthesis and Causes Early Ageing. *Plant Cell* **20**, 2909-2925.
Swarbreck SM, Defoin-Platel M, Hindle M, Saqi M, Habash DZ. 2011. New perspectives on glutamine synthetase in grasses. *Journal of Experimental Botany* **62**, 1511-1522.
Tabuchi M, Sugiyama K, Ishiyama K, Inoue E, Sato T, Takahashi H, Yamaya T. 2005. Severe reduction in growth rate and grain filling of rice mutants lacking OsGS1;1, a cytosolic glutamine synthetase1;1. *Plant J* **42**, 641-651.
Taylor SH, Parker WE, Douglas AE. 2012. Patterns in aphid honeydew production parallel diurnal shifts in phloem sap composition. *Entomologia Experimentalis Et Applicata* **142**, 121-129.
Tegeder M. 2014. Transporters involved in source to sink partitioning of amino acids and ureides: opportunities for crop improvement. *Journal of Experimental Botany* **65**, 1865-1878.
Uauy C, Distelfeld A, Fahima T, Blechl A, Dubcovsky J. 2006. A NAC Gene regulating senescence improves grain protein, zinc, and iron content in wheat. *Science* **314**, 1298-1301.
van Rooyen JM, Abratt VR, Belrhali H, Sewell T. 2011. Crystal Structure of Type III Glutamine Synthetase: Surprising Reversal of the Inter-Ring Interface. *Structure* **19**, 471–483.
Wanner L, Keller F, Matile P. 1991. METABOLISM OF RADIOLABELED GALACTOLIPIDS IN SENESCENT BARLEY LEAVES. *Plant Science* **78**, 199-206.

Watanabe M, Balazadeh S, Tohge T, Erban A, Giavalisco P, Kopka J, Mueller-Roeber B, Fernie AR, Hoefgen R. 2013. Comprehensive Dissection of Spatiotemporal Metabolic Shifts in Primary, Secondary, and Lipid Metabolism during Developmental Senescence in Arabidopsis. *Plant Physiology* **162**, 1290-1310.
Wingler A, Purdy S, MacLean JA, Pourtau N. 2006. The role of sugars in integrating environmental signals during the regulation of leaf senescence. *Journal of Experimental Botany* **57**, 391-399.
Yang Z, Ohlrogge JB. 2009. Turnover of Fatty Acids during Natural Senescence of Arabidopsis, Brachypodium, and Switchgrass and in Arabidopsis beta-Oxidation Mutants. *Plant Physiology* **150**, 1981-1989.

Aknowledgements: Authors thanks Dr Bertrand Hirel (INRA Versailles France) for discussion and proofreading and Ekatarina Merkulova for english reading.

Supplemental Figures and Tables

Studying senescence in barley (*Hordeum vulgare* L.) primary leaves and flag leaves reveals specific metabolic shifts in sugar, amino acids and lipid metabolisms

Liliana Avila-Ospina, Gilles Clément, Anne Marmagne, Joël Talbotec, Karin Krupinska and Céline Masclaux-Daubresse

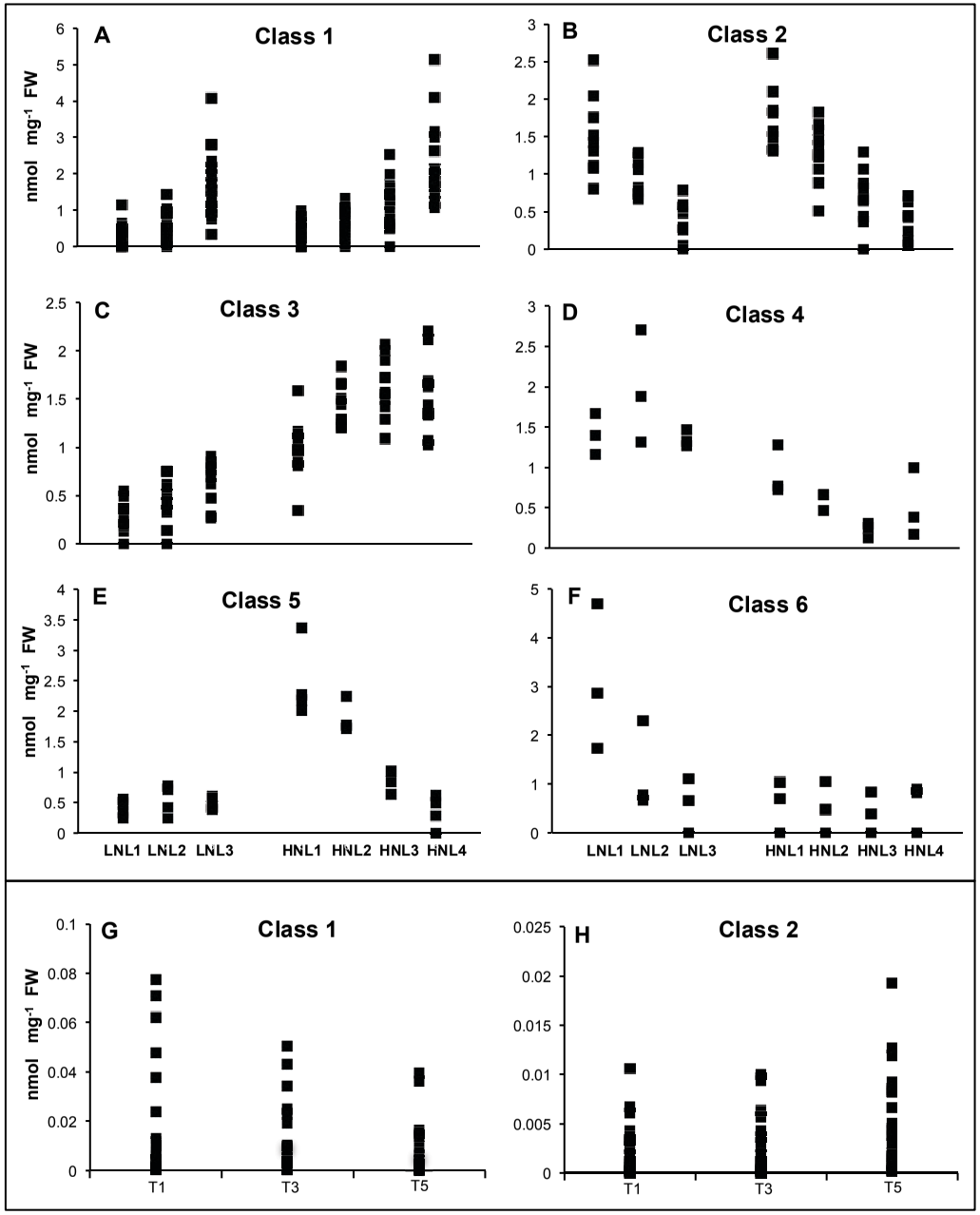

Supplemental figure 1. Metabolite clusters found in leaf ranks of seedlings grown under low nitrate LN and high nitrate HN conditions and in flag leaf at different stages of senescence. Seven classes of metabolites were clustered in leaf ranks of seedlings grown under LN and HN. Class 1 **(A)** includes compounds accumulated in young leaves in both LN and HN. Class 2 **(B)** includes metabolites accumulated in old leaves in both LN and HN. Class 3 **(C)** includes compounds preferentially accumulated in young leaves in plants grown under HN. Class 4 **(D)** includes compounds preferentially accumulated in old leaves in plants grown under LN. Class 5 **(E)** includes metabolites only accumulated in old leaves from HN treatment. Class 6 **(F))** includes metabolites only accumulated in old leaves in old leaves from LN treatment. In flag leaf, two classes of metabolites were clustered. Class 1 **(G)** includes compounds accumulated in the young leaf and Class 2 **(H)** includes compounds accumulated in senescing leaf. Data is shown as the content of each metabolite belonging to each class in nmol mg^{-1} FW. Point charts show the trend of each class. Metabolite clustering was conducted by the MultiExperiment Viewer (MeV4_8_1) (Howe *et al*, 2011).

Supplemental figure 2. Phyllogenetic tree of cytosolic Glutamine synthetase 1 gene family. DNA coding sequences (CDS) were translated to protein and then aligned using ClustalW. Species abreviation are as follows : Hv (*Hordeum vulgare*), Os (*Oryza sativa*), Ta (*Triticum aestivum*), So (*Saccharum officinarum*), Zm (*Zea mays*), At (*Arabidopsis thaliana*), Vv (*Vitis vinifera*), Ps (*Pisum sativum*), Lp (*Lolium perenne*), Sb (*Sorghum bicolor*), Cs (*Chlamydomonas smithii*), Dm (*Drosophila melanogaster*), Hs (*Homo sapiens*), An (*Aspergillus nidulans*), Sf (*Streptomyces filamentosus*), Ec (*Escherichia coli*) and Sa (*Staphylococcus aureus*).

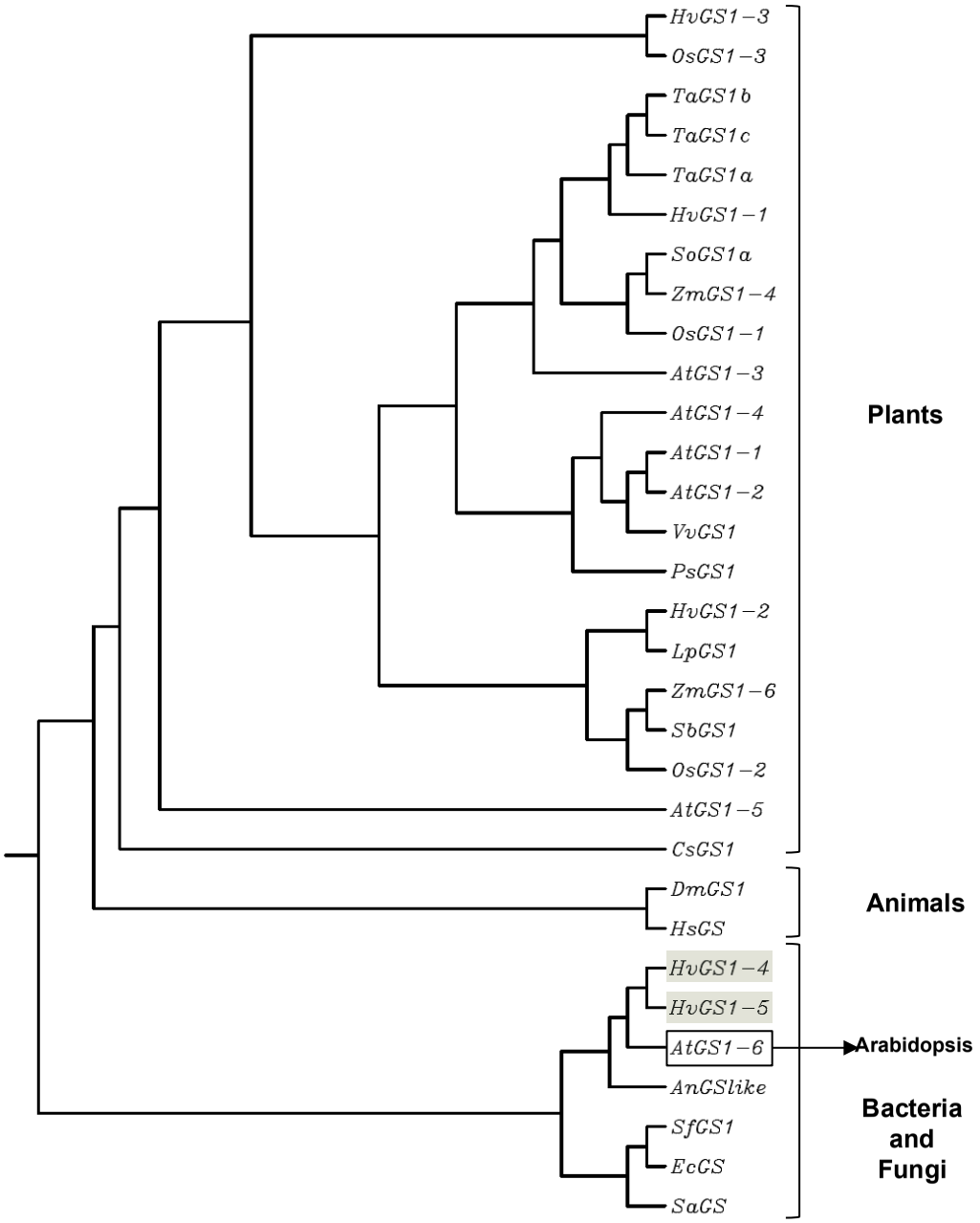

Supplemental figure 3. Protein alignment of GS1 family. GS proteins of different species including prokaryotes and eukaryotes organisms were aligned using ClustalW. Conserved amino acids (aa) are showed by shades of blue colors going from less conserved aa (light blue) to more conserved aa (dark blue). Conserved aa residues found in all species analyzed were indicated by black arrowheads (▼) and aa residues responsable of ligand binding specificity in GS family were indicated by red arrowheads (▼). Species abreviation are as follows : Hv (*Hordeum vulgare*), Os (*Oryza sativa*), Ta (*Triticum aestivum*), So (*Saccharum officinarum*), Zm (*Zea mays*), At (*Arabidopsis thaliana*), Vv (*Vitis vinifera*), Ps (*Pisum sativum*), Lp (*Lolium perenne*), Sb (*Sorghum bicolor*), Cs (*Chlamydomonas smithii*), Dm (*Drosophila melanogaster*), Hs (*Homo sapiens*), An (*Aspergillus nidulans*), Sf (*Streptomyces filamentosus*), Ec (*Escherichia coli*) and Sa (*Staphylococcus aureus*).

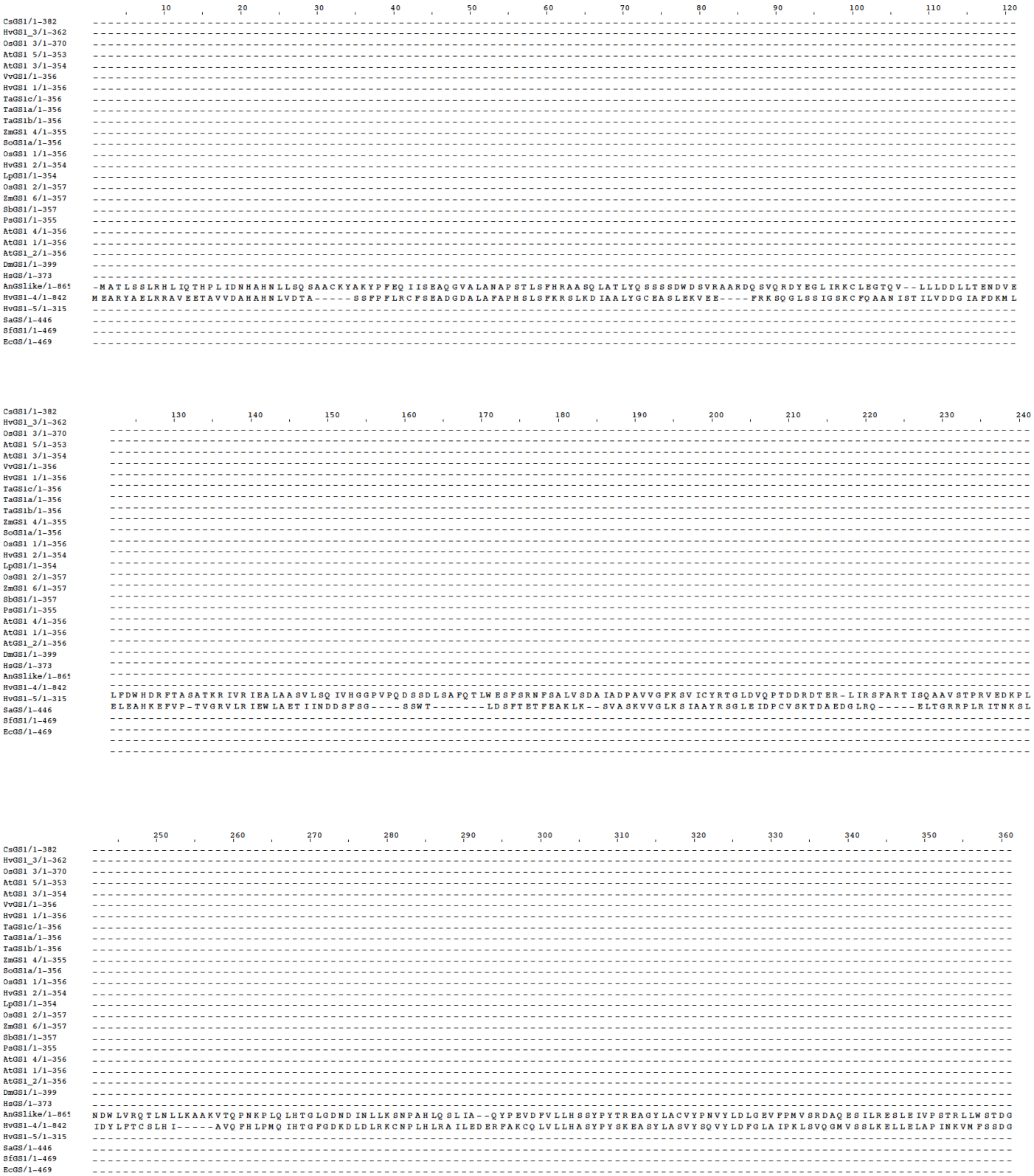

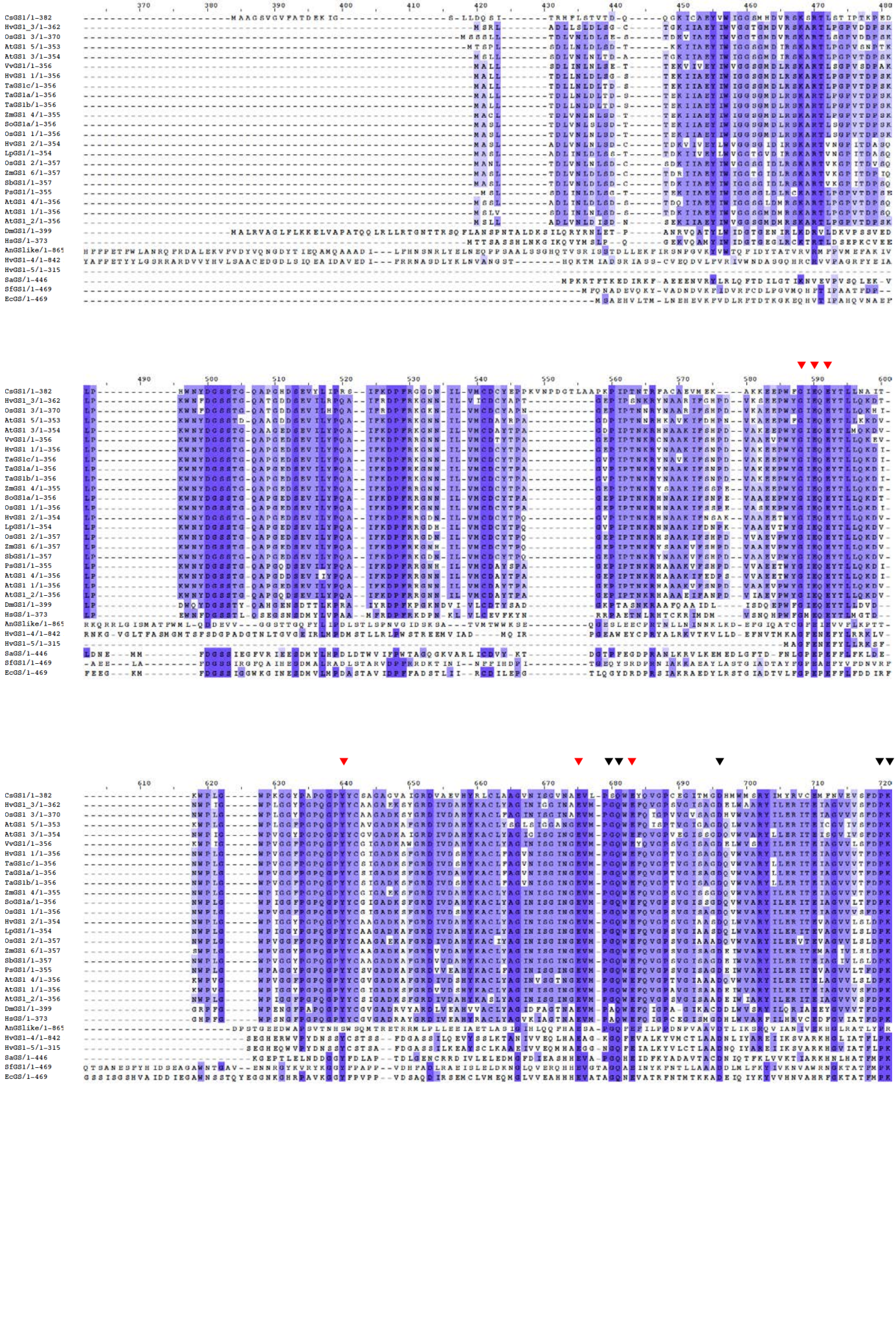

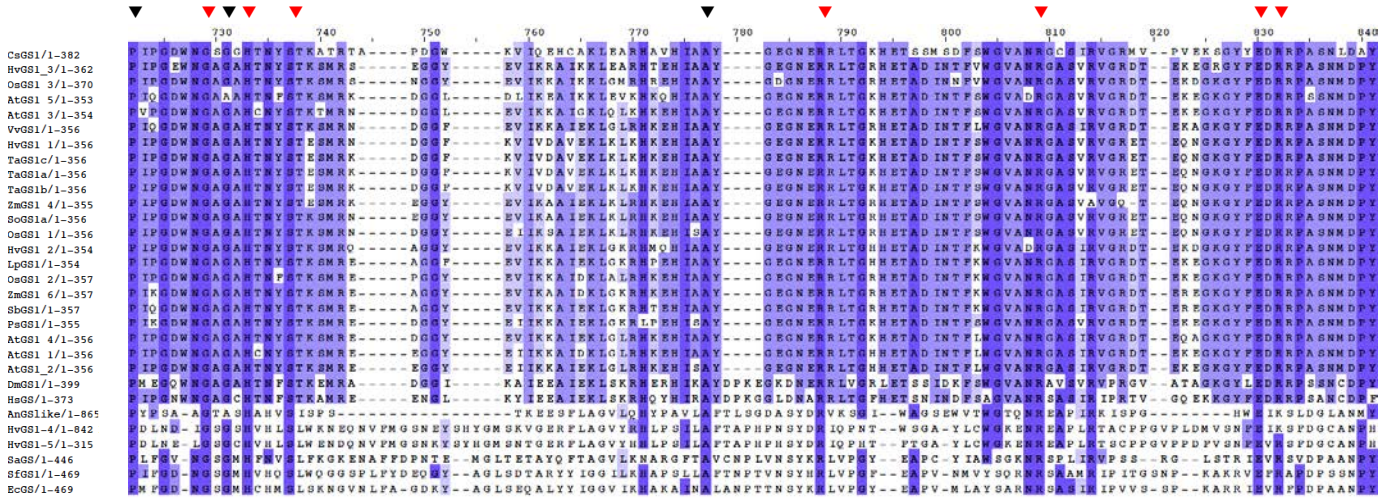
730
740
750
760
770
780
790
800
810
820
830
840
CsGS1/1-382
HvGS1_3/1-362
OsGS1 3/1-370
AtGS1 5/1-353
AtGS1 3/1-354
VvGS1/1-356
HvGS1 1/1-356
TaGS1c/1-356
TaGS1a/1-356
TaGS1b/1-356
ZmGS1 4/1-355
ScGS1a/1-356
OsGS1 1/1-356
HvGS1 2/1-354
LpGS1/1-354
OsGS1 2/1-357
ZmGS1 6/1-357
SbGS1/1-357
PsGS1/1-355
AtGS1 4/1-356
AtGS1 1/1-356
AtGS1_2/1-356
DmGS1/1-399
HsGS/1-373
AnGSlike/1-865
HvGS1-4/1-842
HvGS1-5/1-315
SaGS/1-446
SfGS1/1-469
EcGS/1-469

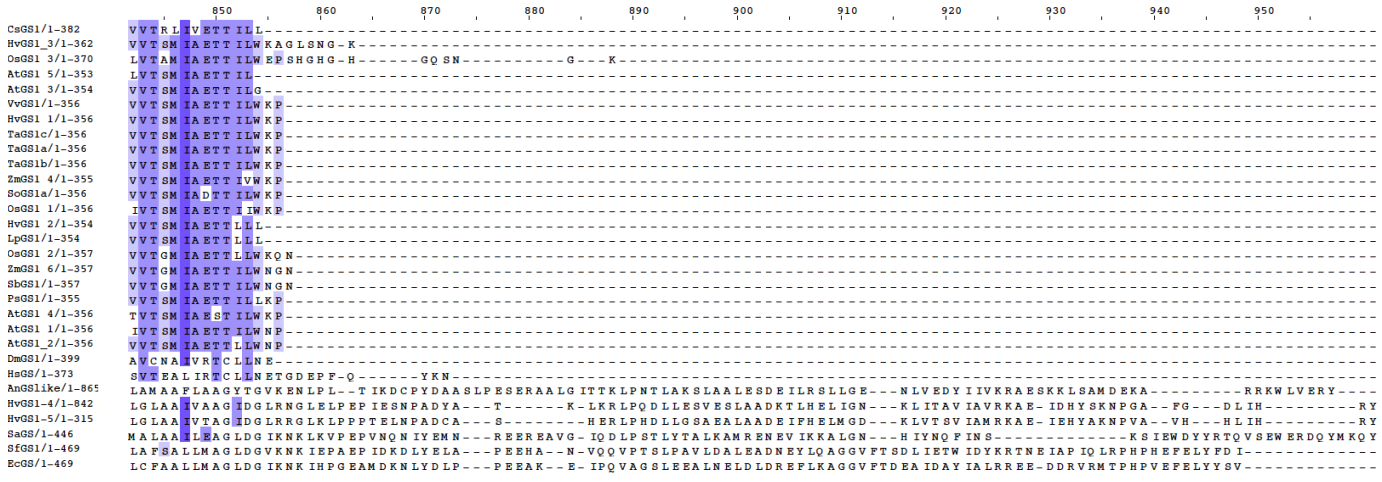
850
860
870
880
890
900
910
920
930
940
950
CsGS1/1-382
HvGS1_3/1-362
OsGS1 3/1-370
AtGS1 5/1-353
AtGS1 3/1-354
VvGS1/1-356
HvGS1 1/1-356
TaGS1c/1-356
TaGS1a/1-356
TaGS1b/1-356
ZmGS1 4/1-355
ScGS1a/1-356
OsGS1 1/1-356
HvGS1 2/1-354
LpGS1/1-354
OsGS1 2/1-357
ZmGS1 6/1-357
SbGS1/1-357
PsGS1/1-355
AtGS1 4/1-356
AtGS1 1/1-356
AtGS1_2/1-356
DmGS1/1-399
HsGS/1-373
AnGSlike/1-865
HvGS1-4/1-842
HvGS1-5/1-315
SaGS/1-446
SfGS1/1-469
EcGS/1-469

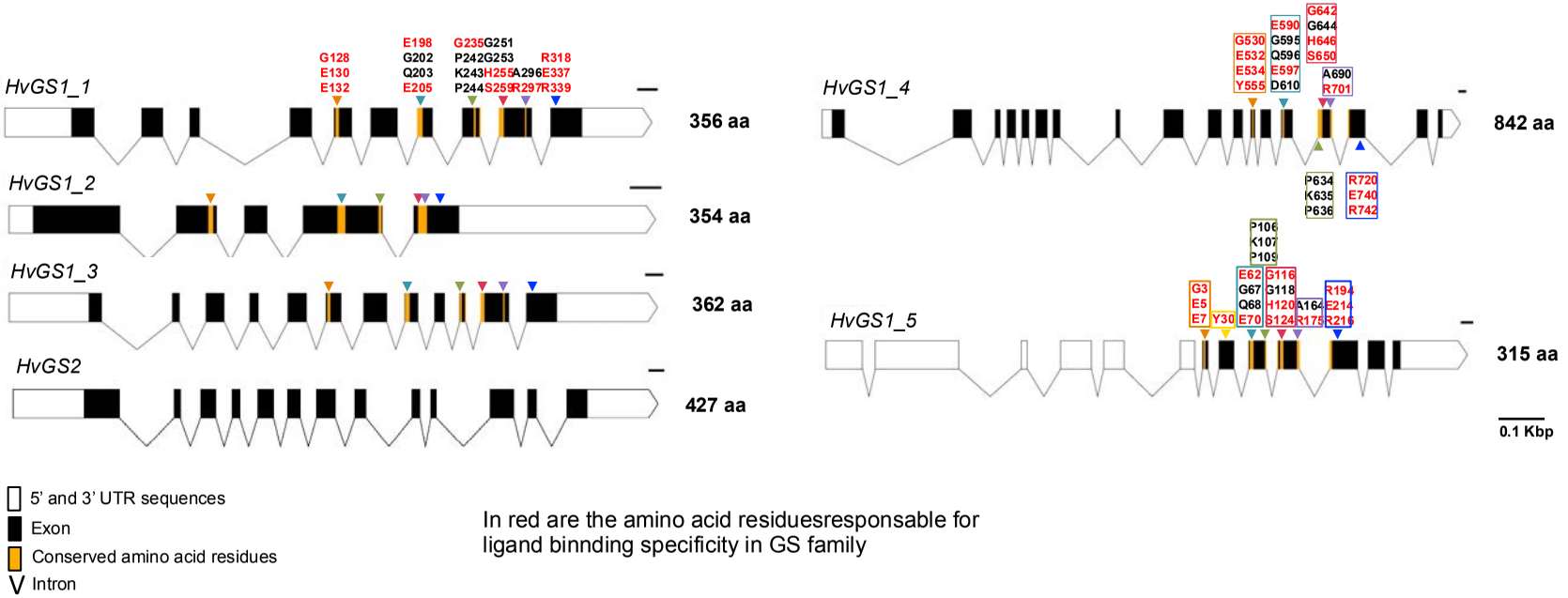

Supplemental figure 4. Description of barley *GS* gene structures (*HvGS*). Diagram of *HvGS*, white boxes (□) represent untranslated regions, black boxes (■) represent coding regions, solid lines (\/) represent introns and yellow boxes (■) indicate the conserved amino acid residues among GS proteins from barley (*H. vulgare*), *Z. mays, O. sativa, A. thaliana*, *T. aestivum, S. officinarum, V. vinifera, P. sativum, L. perenne, S. bicolor, S. smithii, D. melanogaster, H. sapiens, A. nidulans, S. filamentosus, E. coli* and *S. aureus.* Conserved groupes of amino acid residues in all *Hv*GS1 proteins analyzed are indicated in black font and by colored arrowheads. Amino acid residues responsable for ligand binding specificity are indicated in red font and by colored arrowheads. The predicted amino acid (aa) lenght for each of the corresponding proteins is showed at right. See Table 4 and supplemental Table 8 for EST and cDNA sequences supporting each gene.

Supplemental figure 5. Phyllogenetic tree of Asparagine synthetase gene family. DNA coding sequences (CDS) were translated to protein and then aligned using ClustalW. Species abreviation are as follows : Hv (*Hordeum vulgare*), Zm (*Zea mays*), Os *(Oryza sativa*), At *(Arabidopsis thaliana*) and Gm (*Glycine max*).

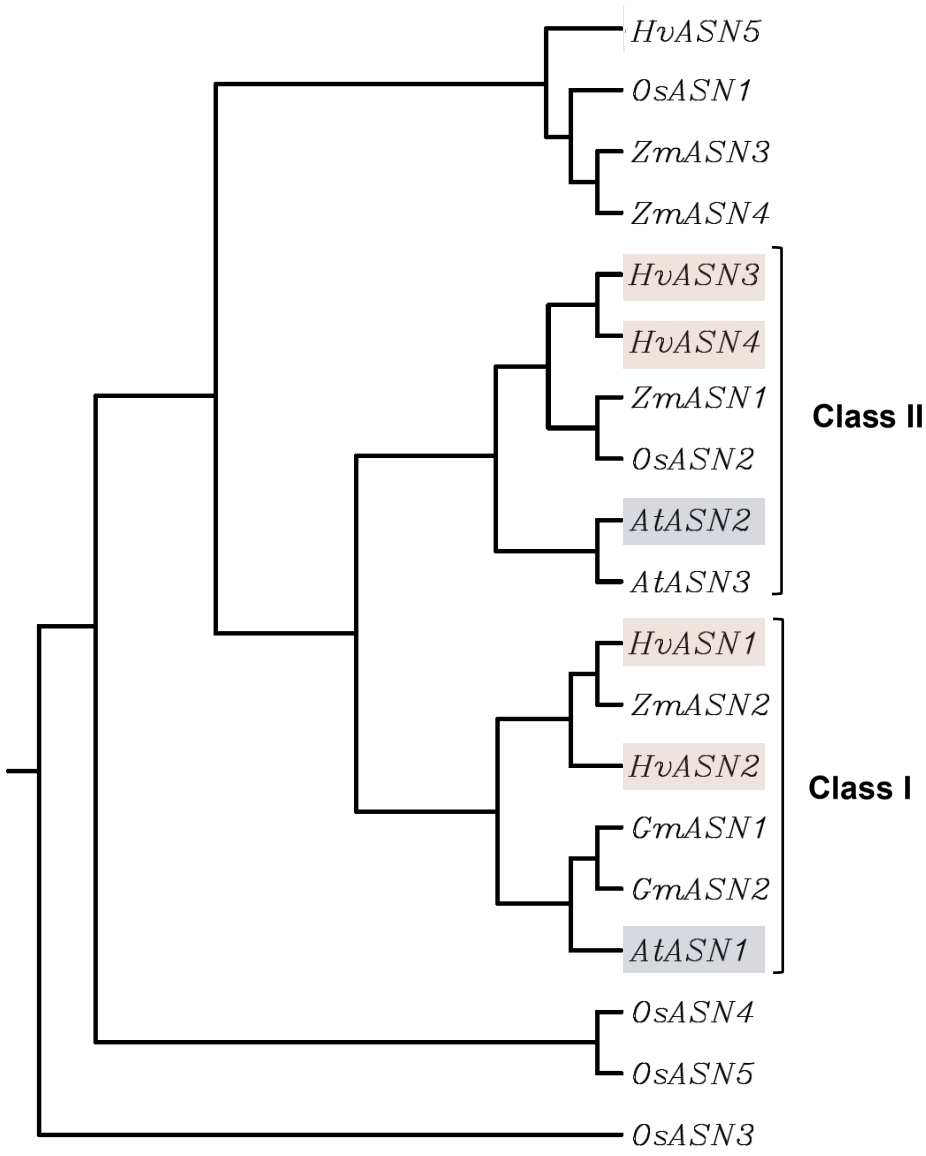

Supplemental Figure 6. Protein alignment of ASN family. ASN proteins of different species were aligned using ClustalW. Conserved amino acids (aa) are showed by shades of blue colors going from less conserved aa (light blue) to more conserved aa (dark blue). Conserved aa residues found in all species analyzed were indicated by orange arrowheads (▼), amino acid residues from *PurF*-type glutamine binding domain are indicated by purple arrowheads (▼), essential residues for the glutamine binding and positioning are marked by green arrowheads (▼) and amino acid residues proposed to facilitate the binding of aspartate and ATP are indicated by light blue arrowheads (▼). Species abreviation are as follows : Species abreviation are as follows : Hv (*Hordeum vulgare*), Zm (*Zea mays*), Os *(Oryza sativa*), At *(Arabidopsis thaliana*) and Gm (*Glycine max*).

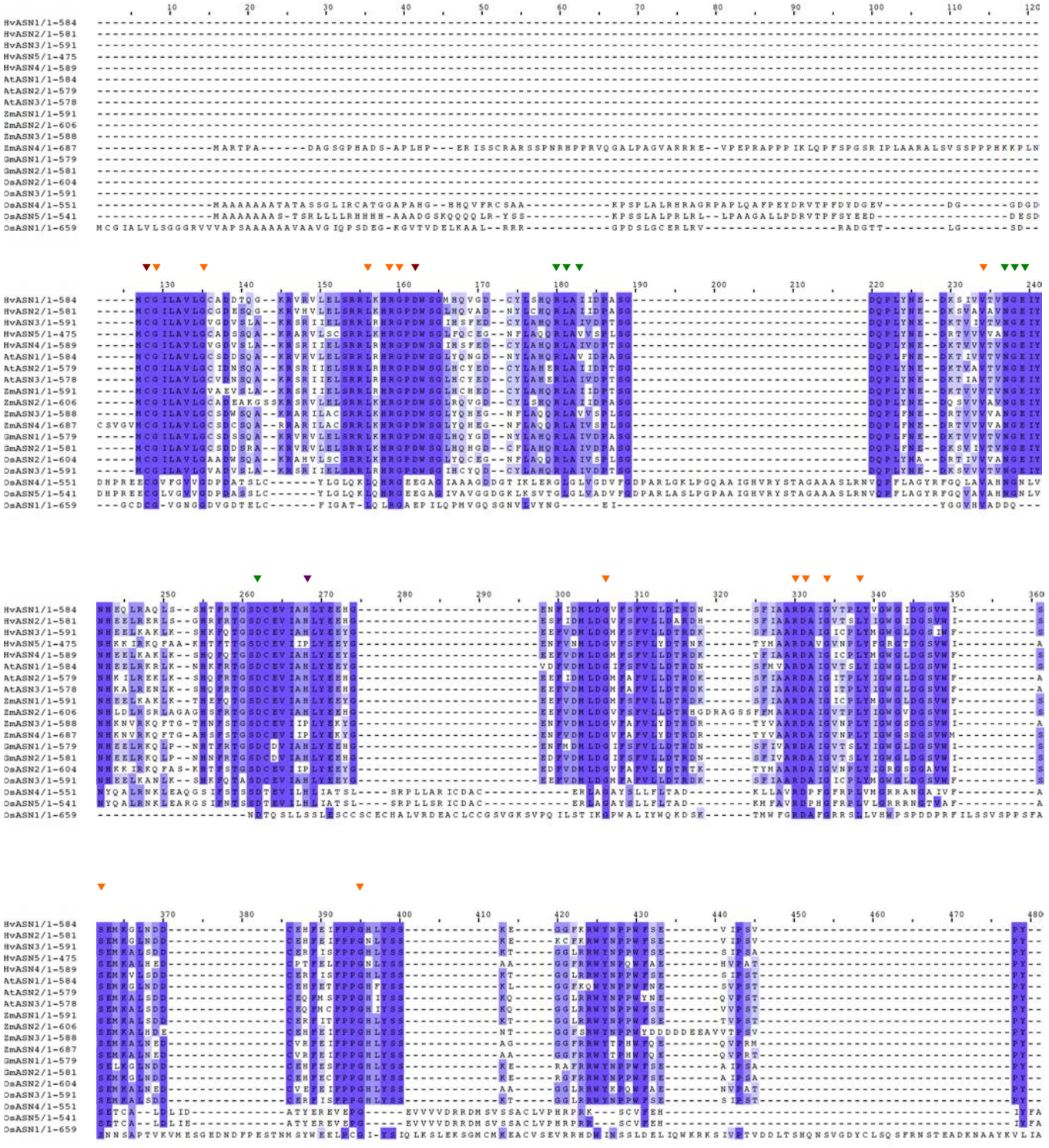

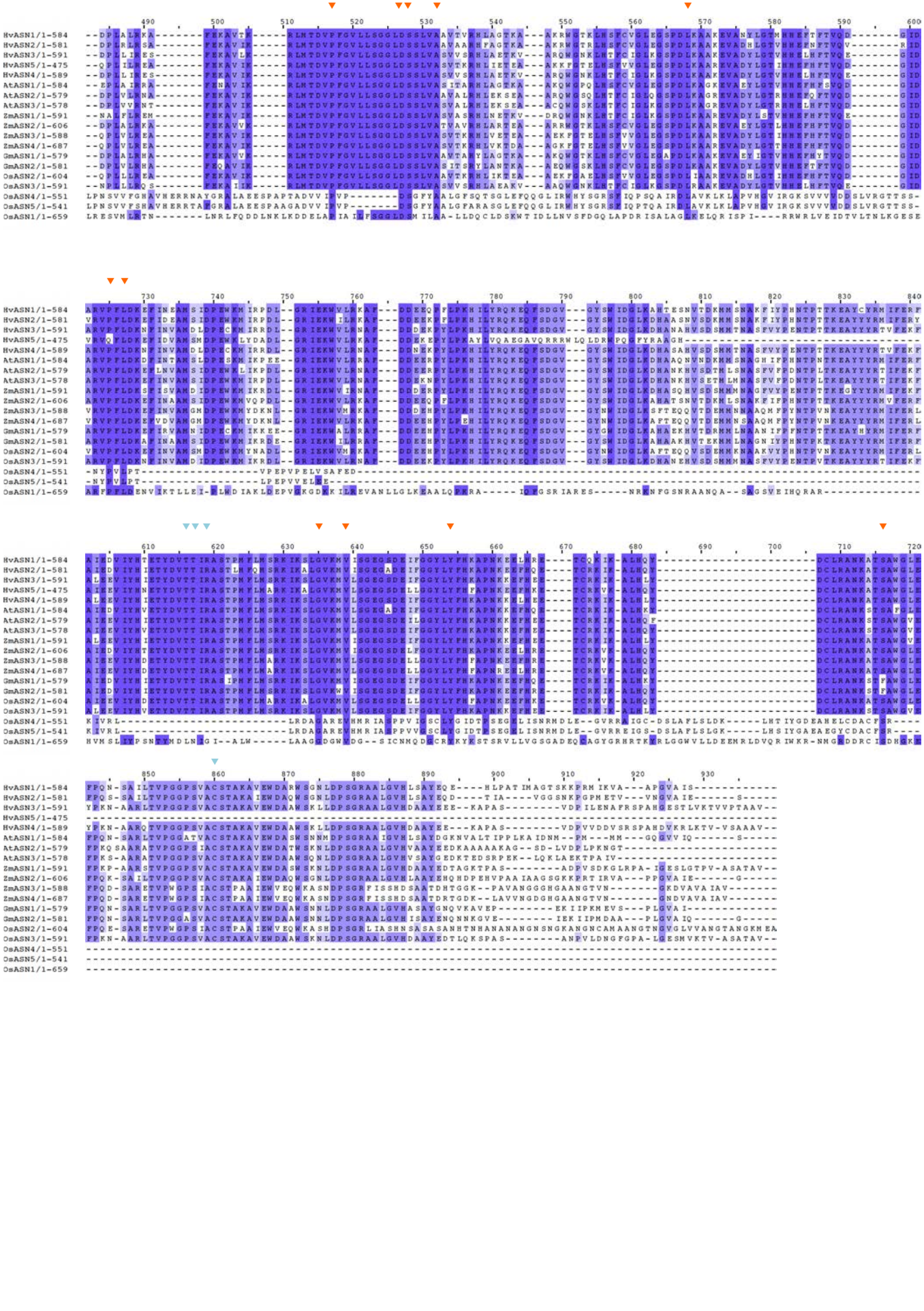

Supplemental Figure 7. Description of barley *HvASN* gene structures. White boxes (□) represent untranslated regions, black boxes (■)coding regions, solid lines (V) introns, grey boxes (■) indicate sequence gaps in coding regions and pink boxes (■) indicate the conserved amino acid residues among ASN proteins from barley (*H. vulgare*), *Z. mays, O. sativa, A. thaliana* and *G. max*. Conserved and essential amino acid (aa) residues in all five isoforms of *HvASN* are indicated by colored arrowheads. Conserved aa residues found in all species analysed were indicated by black font, amino acid residues from *PurF*-type glutamine binding domain are indicated by red font, essential residues for the glutamine binding and positioning are marked by blue font and amino acid residues proposed to facilitate the binding of aspartate and ATP are indicated by orange font. The predicted aa lenght of proteins is showed at right. See Table 2 and supplemental Table 6 for EST and cDNA sequences supporting each gene.

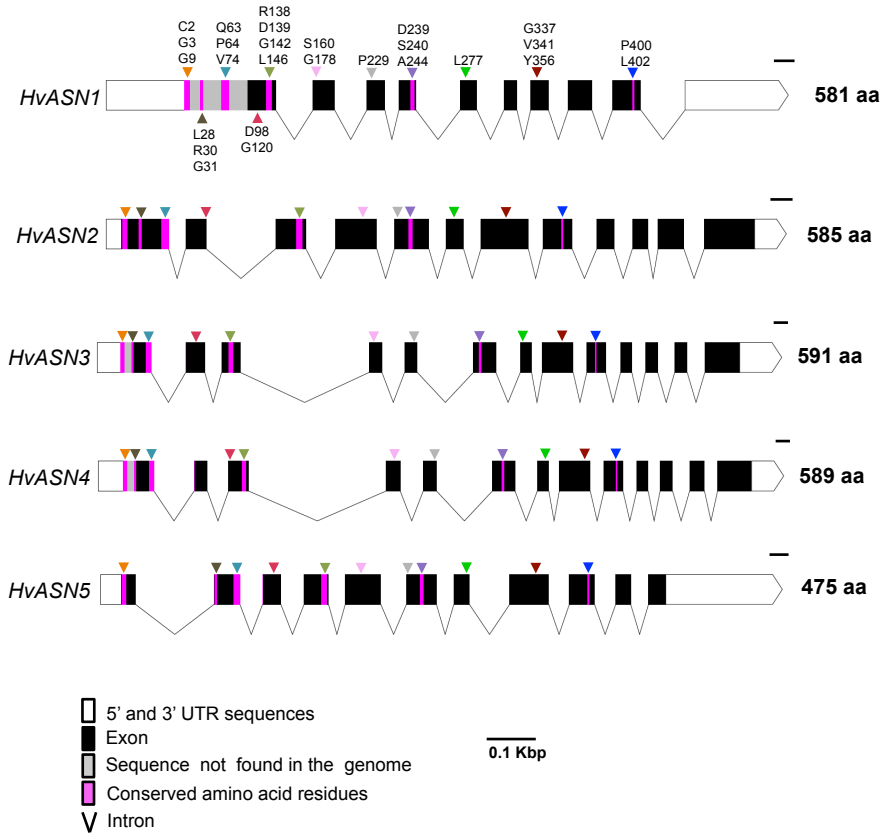

Supplemental Table 1. Primers used for transcript amplification of *HvGS* and *HvASN* genes by RT-qPCR

Gene	Accession	Sequence 5'-3'		Source	Amplification size (bp)
HvGS1_1	JX878489	Fwd Rev	GGACCGTCGGTGATGGGG AAGACGAGAACGAGAAGAGAGACCAGAC	Goodal *et al*, 2013	178
HvGS1_2	JX878490	Fwd Rev	CACTTTGGGCAGGCTCTCGTCTC CAGACTAGACCTTGCAATTGCAAAAGAAAC	Goodal *et al*, 2013	106
HvGS1_3	JX878491	Fwd Rev	CTCCAATGGCAAGTAGAGTTACCTGTG TTATTCAAACCTTGCCAGTCTCATCAC	Goodal *et al*, 2013	107
HvGS2	AK360336	Fwd Rev	AAGCTGGCGCTGAAGGTATGAAGG GACGGAACCACAGGATCAACAAGAATG	Goodal *et al*, 2013	124
HvGS1_4	AK252215	Fwd Rev	AACGGTTCCTTGCTGGAGTA AAGGCCGTTCCTAAGTCCAT	This work	284
HvGS1_5	AK365395	Fwd Rev	GTTGCTCGAAAACACGGAGT CACATGACAACCGGATCCAA	This work	78
HvASN1	AK359770	Fwd Rev	ACGGAGAGAGGTCTTCTAGC ATTCACAGTGACGACGATGG	This work	274
HvASN2	AK357350; AK373732	No primers could be found for this gene			
HvASN3	AK353762	Fwd Rev	CAAGAATGCTGCTAGGCTGA GGGTGGAAGGTTAAACAGCA	This work	266
HvASN4	AK363899	Fwd Rev	TGGTTGTAAATATTTCACCGTGG ACCAAATGCTGAGCAACTCAA	This work	53
HvASN5	AK361923	Fwd Rev	CCTCGGACTGATGAGCCA GACGGATCGATCAATACATCACA	This work	202
HvLSU (Rubisco large subunit)		Fwd Rev	CTCGCGGTATCTTTTTCACTC AGG CGTCCCCAAAGATTTCGGTCAGA	Goodal *et al*, 2013	
HvSSU (Rubisco small subunit)		Fwd Rev	CTACCACCGTCGCACCCTTCC TGATCCTTCCGCCATTGCTGAC	Christiansen *et al*, 2011	
HvNAC13	AK376297	Fwd Rev	ATGCCGCCGCACATGATGTAC ACAGGTCGCCGGAATTAGCG	Christiansen *et al*, 2011	
HvActin	AY145451	Fwd Rev	CGACAATGGAACCGGAATG CCCTTGGCGCATCATCTC	Rapacz *et al*, 2012	
HvGAPDH	AAA32956	Fwd Rev	GCTCAAGGGTATCATGGGTTACG GCAATTCCACCCTTAGCATCAAAG	Hebelstrup *et al*, 2010	98

Supplemental Table 2. *GS* and *ASN* queries. Genes used as queries for barley homologs searching

Gene in *Arabidopsis thaliana*	TAIR locus	No. of amino acid residues	Gene in *Oriza sativa*	TIGR locus	No. of amino acid residues	Gene in *Zea mays*	Gramene locus	No. of amino acid residues
AtGS1_1	At5g37600	356	*OsGS1_1*	Os02g0735200	356	*ZmGS1_1*	GRMZM2G050514	357
AtGS1_2	At1g66200	356	*OsGS1_2*	Os03g0223400	357	*ZmGS1_2*	GRMZM2G024104	368
AtGS1_3	At3g17820	354	*OsGS1_3*	Os03g0712800	370	*ZmGS1_3*	GRMZM2G046601	357
AtGS1_4	At5g16570	356	*OsGS2*	Os04g0659100	428	*ZmGS1_4*	GRMZM5G872068	356
AtGS1_5	At1g48470	353				*ZmGS1_5*	GRMZM2G036464	355
AtGS1_6	At5g35630	845				*ZmGS2*	GRMZM2G098290	423
AtGS2	At3g53180	430						
AtASN1	At3g47340	584	*OsASN1*	Os03g18130	604	*ZmASN1*	GRMZM2G074589	591
AtASN2	At5g10240	578	*OsASN2*	Os06g15420	591	*ZmASN2*	GRMZM2G093175	604
AtASN3	At5g65010	578	*OsASN3*	Os12g38630	561	*ZmASN3*	GRMZM2G053669	588
			OsASN4	Os01g65260	551	*ZmASN4*	GRMZM2G078472	588
			OsASN5	Os05g35580	541			

Supplemental Table 3. Collection of *HvGS* and *HvASN*. *proteins aligned with *AtGS1_1*, *OsGS1_1* and *ZmGS1_1* ; **proteins aligned with *AtGS1_6* ; $^{+}$proteins aligned with *AtASN1* and *ZmASN1* ; $^{++}$proteins aligned with *OsASN3*.

Gene in *Hordeum vulgare*	Gene code	NCBI gene accession number	NCBI protein accession number	BAC clone	Contig	No. of amino acid residues	% Identity *H. vul.* to			
							A. thal.		*O. sat.*	*Z. mays*
HvGS1_1	MLOC_11890	JX878489	AFX60875	-	x_contig_1562081	356	85.67*	14.41**	92.70*	83.15*
HvGS1_2	No gene reported	JX878490	AFX60876	-	x_contig_1569958	354	84.18*	14.78**	84.18*	86.72*
HvGS1_3	MLOC_62030	JX878491	AFX60877	-	x_contig_46131	362	81.97*	15.76**	83.10*	81.69*
HvGS1_4	MLOC_59238	AK252215	-	FLbaf147e20	x_contig_43390	842	15.65*	61.55**	15.94*	16.47*
HvGS1_5	No gene reported	AK365395	BAJ96598	NIASHv2033O14	x_contig_1558692	315	21.97*	57.46**	21.97*	20.98*
HvGS2	MLOC_54057	AK360336	BAJ91545	NIASHv1115P04	x_contig_38845	427	-	-	-	-
HvASN1	MLOC_63089	AK359770	BAJ90979	NIASHv1051G03	X_contig_47260	585	80.90^{+}		77.45^{++}	76.42^{+}
HvASN2	MLOC_75057	AK357350; AK373732	BAJ87368 ; BAK04929	NIASHv1102L13	X_contig_6705	581	79.35^{+}		75.30^{++}	75.47^{+}
HvASN3	MLOC_37219	AK353762	BAJ84981	NIASHv1002J05	X_contig_2547996	591	75.65^{+}		91.17^{++}	88.12^{+}
HvASN4	MLOC_72774	AK363899	BAJ95102	NIASHv2019N19	X_contig_6234	589	75.78^{+}		91.82^{++}	88.78^{+}
HvASN5	MLOC_44080	AK361923	BAJ93127	NIASHv2001E23	X_contig_274144	475	70.68^{+}		68.99^{++}	70.04^{+}

*proteins aligned with *AtGS1_1*, *OsGS1_1* and *ZmGS1_1* ; **proteins aligned with *AtGS1_6* ; $^{+}$proteins aligned with *AtASN1* and *ZmASN1* ; $^{++}$proteins aligned with *OsASN3*

Supplemental Table 4. Intron-Exon sequences of *HvGS* and *HvASN*. Exon sequences (blue), intron (black) and untranslated regions (red) of five isoforms of *HvGS1, HvGS2* and five isoforms of *HvASN*.

Gene	Intron/Exon	Lenght	Sequence
HvGS1_1	5' upstream sequence		AGCGCATCCATCCATCCATCCATCCATTGCGTCGCGCGTATCCGGAACGGGGCGGGGGTAATAAATCACCGCCAAAAACCTCTTCCCGTCGC GCTGCCATGCCGGAAACCTAGTGTATTTCCCGACGAGAAAGGTGGCGTTCACCGCCCGCACGAGGGAGCACCGCCGCCCGCCTCGCTGCGCCCG CGGATCGCGAGGGCGAAAAAGCGTCTGATTAAAAATAAAAAAGGAACACTGCTACGACGAATCTGCACCCCCCATGAATTTAGCATCGAGGAAAAA CGACCCAGCGCTCCGGGCGATCCCGCCTCCTCCTCTCCCCCCCCC
	Exon1	**113 nt**	CTGGCCTTGCTCCTGAGATCCATGCCAGATCCGCCGATCCATATGTACTCGGCGATGATCTTCTCCGTGGAGCCGGAGAGGTCGAGGTTGAGGAG ATCGGTGAGGAGCGCCAT
	Intron1	**236 nt**	TGCACCAACCAGAGCAGCAGCAGCAGCAACAGTTAAAAAATAATACGCACGCTGTTAACCAAAAGGAATCTGGCAACCTCTGATATATAAGCACAAG AACAGCTCAGTGGTGGATAACTAGCTAGCAAAAAGGTGATAGGACACGGCAAGCAAGGTCATGGGAATGATCCATGCCATGCCGGCCGGGGAGGG GAATCTTTATCTGTATATGTATGCCTCTGTATATGCATCTTACC
	Exon2	**105**	TACAGGATGACCTCGCTGTCCTCGCCCGGGGCCTGGCCGGTGCTGGAGCCGTCGTAGTTCCACTTGGGCAGCTTGCTGGGGTCGGTGACCGGGC CGGGGAGGGTC
	Intron2	**133 nt**	CTGCAGCATGGCACATGCCCCAAGGGAAGCAAAAATTACTCCTCGGGTCCAAGGTTAAAAAAAAAAAGGTGATACTAGAATTGCACTTGACAGAGG TAAATAGTTCTGGGGTGGCACGAGAGACGGCACTTAC
	Exon3	**49 nt**	AAGGATGTTGTTTCCCTTCCTGAACGGGTCCTTGAAGATGGCCTGTGGG
	Intron3	**450 nt**	CTGCAAGTGGTTCGAATTTAGTAAGGGGGGATCTTGATTGGCATCAAGGATGTTGACAAGATGATGACCATTGGATTCCCTCTCTACTGTAGTTATTA GGTGGACCAGACAATCACACCTAATTAATAACCAAAAATACGTATAACAATTCATTCACAACCCTGGATGGTCCTTGACTGGGATACAATTTGCGTCA GAAATAGGAGTATCAACAGCTAGTATGAATACTGCACCAAAAAAATCTGCACCAAGTAGTACATGAGAAGATAGTTAAGTTGATCTCCCCTCTTAATG GTGCTCGTTAATCTTCGTAGTTGACCAAAAGAGCTATAGATCAATCGACTACAGTGAAAAACACTCCTACTAGTACTACAGGTGCAGATCACTTGCG CGGCCAGCAGTGCTACAGTCTATTGTACACACGATGATGATAGTGGAGTGGTCACTTAC
	Exon4	**160 nt**	ATGGCTCCTCCTTGGCAACATCGGGGTTGCTAAAGATCTTAGCAGCGTTGTATCTCTTGTTGGTGGGGATTGGCTCTCCAGCTGGGGTGTAGCAAT CGCACATGAC
	Intron4	**112 nt**	TATCATCACAAACAATAGAAAGACCAGTCGATCAATTATGATCATAAAAACAGTTAGACCATTATTCTTTAGCGTTCGTAATCATGGATCAATTTCGTA TATTATATATACC
	Exon5	**87 nt**	GAGGACCAGGGAAGCCACCAACAGGCCAGCCGAGAGGCCAGTTGATGTCCTTCTGTAGGAGGGTGTACTCCTGCTCAATACCGTACC
	Intron5	**96 nt**	ACACACAAAAAAAGTTGTGATTGGTAAGTGTACACTTCACCAAAATTAGGGCCAAATGTCCAAATTCAGCCGGTCAAGCTGAAAGAGACGTACCTG
	Exon6	**131 nt**	CTGTCCGGGCATGACCTCGCCGTTGATGCCACTGATGTTGACGCCGGCAAAGAGGCAAGCCTTGTAGTGGGAGTCAACTATGTCACGCCCAAACG ACTTGTCAGCACCAATACCACAGTAGTAAGGACCCT
	Intron6	**100 nt**	CTGAAAACCAAACATAATAATTCTACTATGGTCAGAAAGACGGTGCTAATTCTGCAAGATACAGAAAATAGGAATGTTCTGCGTTGTAGTGGTGTTTC AC
	Exon7	**75 nt**	CTCAAGAATGTAGCGAGCGACCCACACTTGGTCACCAGCAGAAATGCCAACAGTCGGGCCAACTTGGAACTCCCA
	Intron7	**148 nt**	CTGAAAAACAAAAGGGAAAGTGACATTTAATCACGAGAATTCTAACCGAATGCTAAAGCTATTTGAGCTGTCATTCAACCACAAGGGCCTTATCAGGA TAAGATCACATGACTATTCTAGATCATCTTTAAATGAAGACTATCATTAC
	Exon8	**89 nt**	TAGTTCGTGTGAGCACCAGCACCGTTCCAGTCGCCTGGGATGGGCTTGGGGTCAAACGTGACGACAACTCCGGCGATCTCGGTGATCCT
	Intron8	**92 nt**	GATGCAGCAGAGTCGTTCGCCGTCAGCAAAATAGCACGGTAAGATGAACGGATCATATTCATCGAGTATCTCAATCTCAATTACCTG
	Exon9	**162 nt**	CAGCTGAAGGTGTTGATGTCGGCCGTCTCGTGCTTGCCGGTCAGACGGCGCTCGTTGCCCTCGCCGTAGGCCGCGATGTGCTCCTTGTGCTTCAG CTTGAGCTTCTCGACCGCGTCCACGATGACCTTGAACCCACCGTCATTCCTCATCGACTCGGTACTG
	Intron9	**96 nt**	TGCAGAGCAAGCAACACGTTTTCATTTTAGAACCACTGTTGGAGTAACGAGATTCAGGTGATTCAGGAGCAAGAAGGCGAAGGTGGGGGCGTACC
	Exon10	**154 nt**	TCAGGGCTTCCACAGGATGGTGGTCTCGGCGATCATGGAGGTGACCACGTAGGGGTCCATGTTGGACGCCGGCCGGCGGTCCTCGAAGTAGCCC TTGCCGTTCTGCTCCGTCTCCCGGCCCACGCGCACCGACGCGCCACGGTTTGCCACACCC
	3' downstream sequence		CGGCTGCGGTACGGACCATTTTATTACCATATCAATCGATGATTACACGAGACCATAGCATCCAGACGGCAAGGGAAAACAATCAACCAAATACTGT AGTAATCTTGTGCTTTGACACGCCCCTTGCCACCCATCACCCACCACCCACCCAAAGACGAGAACGAGAAGAGAGACCAGACACCCTGATGAGATG ACCATGATGATGTGACCTACCTAAGCGGACTAGGAGTAGTATGCAACCAAACGTAAAAGGAAAATGCTGGAAGAATTTTCGCCCAAGGCACGAATC CTCCAATGGCCACCACCGGACCCCATCACCGACGGTCCATCACACGGCGATCGGAGCT
HvGS1_2	5' upstream sequence		**GAGCTGCACACCTCATCTCATCATCGTCTTCCCCCCATTGCCATCGACCTCCCTCCCTGCGAGCAGCAGCAGCAGCA**
	Exon1	**279 nt**	**TTACCAATCACAATCTTACACATCAGTTTGTACGTAAAATCTTTACGTAAGCCTTTGTAGGTGTAGCATTACTCGTACCAAAAAGGGTTGAAGGAC CACATAATTTGGAGGTTTTCCACCTTTGTATCCCTGTCCTACCTTATCTGCTTACGTTAAAGCACTGATTGGGCTTATCTCTGAATCCAAACAGGTA TGGTATTGAGCAGGAGTACACACTCCTCCAGAAGGATGTGAACTGGCCTCTTGGCTGGCCAATTGGTGGCTACCCTGGTCCTCAGG**
	Intron1	**183 nt**	**CAAGAAAATTCTCAGCATGCTCTCCAGCTCTTTATGTTTTAAGCTTACATAGAAACATAATAACTGAACATTAAGAAAAAAAAAATCAGAGTCCTC TGAAGATAGTAGGTTCCAGACTGAGCAATAAGAGAGGAAGAACCATACTGAATTACTGATCATGTTGATTCTATGCATTTGCGCAGG**
	Exon2	**128 nt**	GACCATACTACTGCGCCGCCGGTGCCGACAAGGCGTTCGGGCGTGACATCGTGGACGCCCACTACAAGGCGTGCCTCTACGCCGGGATCAACAT CAGCGGCATCAACGGGGAGGTCATGCCCGGCCAG
	Intron2	**91 nt**	GTACTAGAGTCTAGAGATGATCGATCCTCCTCCTGCAACAAGTTGTATAAAAACTCTCTCTGAACCTGATTCTCTGTCCCCTTGGTGACAG
	Exon3	**73 nt**	TGGGAGTTCCAAGTTGGGCCGTCCGTCGGGATCGCCGCCTCCGACCAGCTGTGGGTGGCGCGCTACATCCTCG
	Intron3	**115 nt**	AGGTCCTCCCCTGATACGTAGTGTACTGTAGTATTATTCGCACCTCGTATCGCAACTGCGTGAATCTGGTTAGATGCTGAACTGATTTATTGGATTGG TTTGATCGGTTGATCCTC
	Exon4	**255 nt**	AGAGGATCACAGAGGTTGCCGGGGTGGTGCTGTCCCTGGACCCGAAGCCGATCCCGGGTGACTGGAACGGCGCGGGCGCGCACACCAACTACA GCACCAAGTCCATGAGGCAGGCCGGCGGCTACGAGGTGATCAAGAAGGCCATCGAGAAGCTTGGCAAGCGCCACATGCAGCACATCGCCGCCTA CGGCGAGGGCAACGAGCGCCGCCTCACCGGCCACCACGAGACCGCCGA CATCAACACCTTCAAATGGG
	Intron4	**104 nt**	TACGTGCTGCCACATCTGTTGTACTACTGTGTTGCCTGTCGTGTCTGACTCTTACCTGACGATGATGAATCGATGATGATGATGATGATGCATTT AGG
	Exon5	**146 nt**	GCGTGGCGGACCGCGGCGCGTCCATCCGCGTGGGGCGCGACACGGAGAAGGACGGCAAGGGCTACTTCGAGGACCGCAGGCCGGCCTCCAAC ATGGACCCCTACGTCGTCACCTCCATGATCGCCGAGACCACGCTTCTCCTCTGA
	3' downstream sequence		GCACACGGCCGGCAATGCCTACTCCACCGCCAGATGACACTTTGGGCAGGCTCTCGTCTCGACTCTCTCGATCGAGGGTGGTGATTGATTTCTGCA AAACGTTTCCCGTTTCCATTTCTTTTGCAATTGCAAGGTCTAGTCTGTTTTTGGGGCGTGCCTTTGGTATCTTTCATAGTAGTACGTCTACTGCTCTTC AGGATAAGAAGAGTCTTCAGTGTACTCTGAAAATAATGTTGTTTCCGCATTCTGATAAAATGGAATCATGGAACCGGTTGTGATTCTGTCTGTTCCAT CACATGTCATACACACATACAGTACACGGTTCCATGTTCTCCAGTGCTCTTTCCACGTCACCCTGAGCCTGAGGCGAACAAAATTGACGTGCGGGC GCGAAAGCGGATGCGCCAGTTGCAATTGCCTCTCTGCATTTCGAGCAAGTGTCGTGTCACTAGCTGCGTGCGGCCATGCTGCCTTATGTGTTGCAA CTTGTTGCAGCCTAATCCGTGGGCCAAACGCATCTTATCTTATCTTTCCTCACTCGCTCACGCGACAACTCGACGAATATGATCTCTGGCCCTCTTT GACGTTGGGCCATTCTTTTTTACGCACACCTTTCCGGACGCAGCGTACCGC
HvGS1_3	5' upstream sequence		**GCGAGCTACCCCTCCTCCTCCTTCTTCTNNNNNNNNNNNNNNNNNNNNNNNNNCTCCTCTTCTTCTTCTTCCCCGGAGACGGAGCCTGAGC CGGAGAGGGAGGGGGAGAGCAGGCGGAGGAGGAGGGAGAGGTGTTCTTGTGGGAGGCAAATGGTGGCTAGCTCTCTTGGAAATGCGGGGGG AGGAGGAGGGGCGAGTGGGGGTGGTGTCGCCGTAGCTGGCTCTGCCCCTCTATAAGTAGGTAGGAAGGGAGCAGGGTGGTGACGGGGCCCCC GAAAGGTTGGTGGGCGTTGCGGCCGGGCTGCGTACGTACGGCTGTCCCTCCGCGCGTACGTTTCCGCGGCCCGCGCGCACGCAAGCCTTTTC CACTGCACCACTGCACCGGACGCGAGCGCACTCGACCGGTCGGGTTTCCTCCCTGTCATGTGATGTGATGTGATGTGATGATCC**
	Exon1	**73 nt**	**ATATGTACTCGGCGATGATCTTGCCGGTGCAGCCGGACAGGTCGAGGCTGAGAAGGTCGGCGAGCCGAGACAT**
	Intron1	**402 nt**	**TGAGTTAGGCAAAGCGTAAATGTGAGCAGATTTTCTTGTTTTTGTTCTGAGGGAGTAAATGTGCGCAGATTAGTAATGGCTTTTTTCTTCCTCTTTT GGAAAATGGATGCTGATCGGTGCTATTGCTTCTGTAACTTATCATCAAGACGTGAAGAAGGTGAAGACAGGGGTTTTTACTTGGCTCAAATCTGA GAAACCCAACCAGAAGGAAATTTCAGATGGGATTTGTGGGGAGGAGGAATAATCTGTGGCATGCCTAACTCGGGATAAGAACTAGAGATTTCAA GAAGCGGAAAAGAAAAGGATGAAGTGGATTTTGGTGTGAACTGTGAAGGAAGGTGAGATGGGAGGTTGGGACAGTGGTGAGGGAGGCGGAGG AAGAGGAAGCCGAGCGGTGTTACC**
	Exon2	**40 nt**	**CTGGCTTTGCTCCTGACGTCCATCCCGGTGCCGCCGACCC**
	Intron2	**153 nt**	**TGATTTGTGAACGTCCAAGGGATCCAAAGGGGCAGAAAAAGTGTTAGGAACTTGCTACTACTACTTGCAATGTATTTTTTTAGAGTGATGGTGATT CTCTTTAGGGTAAGGATTAAATGGATGAT TATGAGGGTGGGAGGAACTCGGCCTACC**
	Exon3	**104 nt**	**GGAGGATGACTTCGCTGTCGTCGCCCGTGGCTTGGCCGGTGCTGGAGCCGTCGAAATTCCACTTTGGAAGCTTGCTGGGGTCGTCCACGGGTCC GGGAAGCGTC**
	Intron3	**145 nt**	**TTGGCAGAAGCAAAAAACATGGAGTTCAAATCAGTTTGACCTCAGGCCCAAGGCACGCAAGCCAAGGCAGGGGTTGATTGAAGAGTGCAACCA AGAAGAAGTGCCGGAGGATTATCCTCAAGAAAAAAGGAAAAAAGGTAGTACC**
	Exon4	**49 nt**	**AGGATGTTGTTCCCTTTCCTGAACGGGTCCCTGAAGATGGCTTGGGGTC**
	Intron4	**169 nt**	**TAAAATTTACCATAGGTGAAAAAACAGTCTGGCATTCATGAACAAATTCCAAAGCTGATTCACGCAGACAAAATAAAATAACAATACAAAACTCA TGCCATAACCTTTGTGTGTATATATATATCGTATTTATGAATGAAAAAACAGAGAGGAGGATCCTGAATTTACC**
	Exon5	**107 nt**	**ATGGTTCTTCAGACTTGACATCAGGATGGCCGAATATCCTCGCCGCGTTGTACCGCTTGTTGCTCGGAATCGGCTCTCCGGTAGGCGCATAGCA GTCACAGATGACC**
	Intron5	**110 nt**	**TATATTTCAGGCAACATAAGAGAGGGGGTACAAGATTAATTGCCACATAAATTATGTGCAAAGTTAATTACTTGACTAATTTCTATAGAACGGAGC AACTGATACTGACC**
	Exon6	**86 nt**	**AGGGCCAGGGTAACCCCCTAGTGGCCAGCCAATGGGCCAGTTGGTGTCCTTCTGGAGAAGGGTGTACTCCTGCTCAATCCCATACC**
	Intron6	**129 nt**	**CCACGCACATTTCATCGTTCATCACTTTACTGAAGTATGATGGGCAAGCATTTTTGACAGCAAGTAATTAGCTGAATTTTAGCATTTGCAACTGAA ATGCTGAGTATTGAACATATCTATAGTT ACCTG**
	Exon7	**131 nt**	TGCCCTGGCATGACTTCTGCATTGATGCCGCCGATGTTGATGCCGGCGTAGAGGC AGGCCTTGTAGTGGGCGTCGACGATGTCGCGCCCGTAAGATTTCTCCGCACCCGCGGCGCAGTAGTAAGGCCCCTG
	Intron7	**105 nt**	TGGTTGGTTCAGACAGAAGATCATCAGCCCATGAGCATATTTTTTTCATGGACAAAGGGGC ATCCAAATATGTGAATGTGATCCTGCGCCTGAACCTGAAATTACC
	Exon8	**75 nt**	TCGAGAATGTAGCGAGCCGCCCAGAGCTCGTCGCCGGCGGAGATGCCGACGGAAGGGCCGACTTGGAACTCCCAC
	Intron8	**94 nt**	TGTTGGGTCACACACAAAACAAAGATGTTCTTATCAGCAAAAGTTGCATTTGATTTGATTCATTCAACTAGACGAGGCAGTTTTACAATTTACC
	Exon9	**56 nt**	CCGGGATCGGTTTGGGGTCGAAGGAGACGACGACGCCGGCGATCTCAGTGATCCTC
	Intron9	**88 nt**	CCTGCAATCACAAACATGTAAGAAATGGCTAGCTGGCCAGTGCAGATCAAGTTGAGAATTTTGGTACAACAAG ATGAAGAAATGCTCA

	Exon10	**34 nt**	TAGTTTGTGTGGGCACCGGCACCGTTCCACTCTC
	Intron10	**84 nt**	CATTCAGACATCATCAGGATCATGCCATGACCCATAGCACAAGAGTAGCGATGCATTAGTTTCGCTTGCTCTTTAGATTACCTG
	Exon11	**162 nt**	CATACGAAGGTGTTGATGTCGGCGGTCTCGTGGCGGCCGGTGAGCCGGCGCTCGTTGCCTTCCCCGTAGGCGGCTATGTGCTCCGTGTGCCGCG CCTCGAGCTTCTTGATCGCCCTCTTGATCACCTCGTACCCGCCCTCGCTCCTCATCGAC TTGGTGCTG
	Intron11	**101 nt**	TGGAAGAAACAAGAAAAACAAACAATGTAGACGGAAAAGCAGTAAGAAGAGAGCAATGGTGACGCTCTTGTCTCAAGTCTCAACTCGCCGTATTACT TACC
	Exon12	**172 nt**	CTACTTGCCATTGGAGAGACCGGCCTTCCAGAGGATGGTGGTCTCGGCGATCATGGAGGTGACGACGTAGGGATCCATGTTGGACGCCGGCCTCC GGTCCTCGAAGTAGCCCCTGCCTTCCTTCTC GGTGTCGCGCCCCACCCGCACCGACGCGCCGCGGTTTGCCACGCCC
	3’ downstream sequence		CGTTGCCTATACTGCATACTCTGCTGTGCTGCCGGTACAGTATACGGCCGTAATCTTGTCACAGTGATTGTAATCAAGAGTGCGTTTCTTCATGCAAT ATATTGACGTGTTCCTTTTTTTTTGCCGAGGATTCGTGTACCAATCTTATCTTGAACATCCAAAAGGAAAACATGAAAAACGTAGCAGGAGTTTCTGAA GGATATCATTTCGTGTAGGAAATGTTTCTTTGCTACAGTTTGGAACAGCGGAATTACCATCTTACTTTCCTTTGAAATTCCCTGTGGAATGGGCTACT CCATGGGAACTTTGGAGGAAACCAAATGAATCCTTGTGTTTACAATGGTTTGTCTTGCGATTGAAGAAGACCACAATTAAGTGCCAAACGTAGGTGC CATGACCGCATAACACGAGATGTTTGCAGAAGCGGAACATACATCCAGCAACGGCAAGCGCATCACATCACATCAGTTATTGCTTCATCATTTTTATT CAAACCTTGCCAGTCTCATCACTGCAATGCAGATCACGCACACACAACCACGGGGCGCTTACACATAACACCATCACAGGTAACT
HvGS2	5’ upstream sequence		GGTCGCCCCCCCCTTCCCTCCCTCGCCTCGCCCGCGTCGCCGTCTCTCTGGTTTAGGGGCCGCGGAGTCGCTGTACGTAAGTAAGTAAGTACGTAG AGACG
	Exon1	**239 nt**	ATGGCGCAGGCGGTTGTGCAGGCGATGCAGTGCCAGGTGGGGGTGAGGGGCAGGACGGCCGTCCCGGCGAGGCAGCCCGCGGGCAGGGTGTG GGGCGTCAGGAGGGCCGCCCGCGCCACCTCCGGGTTCAAGGTGCTGGCGCTCGGCCCGGAGACCACCGGGGTCATCCAGAGGATGCAGCAGCT GCTCGACATGGACACCACGCCCTTCACCGACAAGATCATCGCCGAGTACATCTG
	Intron1	**380 nt**	GTACGGTACGCCCGCCGTTGTTTCCGAGTCATATTAGCAGCTTAGGATAGGCCAAACCTGCACTTTTAGGGGATTGCACTAGGTTTGATTAGATTAG CACGTGAGCGAGCACTGCAGTGTGGATTTGCGCCCTTAAAGTGGATATACACTGCTAATAATAGATAAAGCTTCCAAAGGCGTGATGGGTGATTAGT GATTAGTGACGACTCACTGCTTTTGCCTTTGTAGTTCCGGCACTTGAATAAGATTTTGGGCAGTGGACACCCCACTTTTGGGGTGCAACCAGGAATA GATCCTGTCATGTCATGGCACGTACCACTATCATGTAGTCGCATTACTATTAATTAACAAATCTGACTTTCTTTCTTCACACTGTGCAG
	Exon2	**40 nt**	GGTTGGAGGATCTGGAATTGACCTCAGAAGCAAATCAAGG
	Intron2	**140 nt**	GTAAGATCTTCATGGCCATATCGCTGTTTCCTTCCATACATACTACTACATCACACTTGTCTCTGGAGTTGACTGCAGAGCATTGTTTCTGTACTTTCT ATTTCTGCCACTGACAAGAAAATGCAATGCTACTGTTTCAG
	Exon3	**104 nt**	ACGATTTCGAAGCCAGTGGAGGACCCGTCAGAGCTGCCGAAATGGAACTACGACGGATCGAGCACGGGGCAGGCTCCTGGGGAAGACAGTGAAG TCATCCTATA
	Intron3	**114 nt**	GTAAGGGGACAATTACAGTTCATGTGTTCTTCAGCCTTGCACACACAGTCTAATACCGTAATCTCGATATCGACTTTGGCTGACTCTGTTCATGTTTT TCTGTCCTGCTTTCAG
	Exon4	**49 nt**	CCCACAGGCCATATTCAAGGACCCATTCCGAGGAGGCAACAACATACTG
	Intron4	**123 nt**	GTACCTTTCTTCTGGATGTGCTTTATGCTAATCATGAAGAAGTGATTAGTAGTGCTAGTGGTCACTTTACTGGTTACACATAT ACAATTGGCGTGTTAGTTAATACGGAATTTGTTTTTTCAG
	Exon5	**109 nt**	GTTATCTGTGACACCTACACACCACAGGGGGAACCCATCCCTACTAACAAACGCCACATGGCTGCACAAATCTTCAGTGACCCCAAGGTCACTTCA CAAGTGCCATGGT
	Intron5	**95 nt**	AACTACGCATCGAGTACCCGTGCTATATAAAATCCTGCTATTTTCTGATCTCGCTTTTGTTTGCATACGAAACTGAAACATTTGCTTTTCTAGGT
	Exon6	**87 nt**	TCGGAATCGAACAGGAGTACACTCTGATGCAGAGGGATGTGAACTGGCCTCTTGGCTGGCCTGTTGGAGGGTACCCTGGCCCCCAGG
	Intron6	**112 nt**	TACTGCATCGAGAAGCTTGATTTATCAGATGACGATAAACCTTAGGCTGACTGAAATGTACACTTCATT GAACAACAACCAAGTAGTAATATTTGTGCTCAAATGTTGCAGG
	Exon7	**128 nt**	GTCCATACTACTGCGCCGTAGGATCAGACAAGTCATTTGGCCGTGACATATCAGATGCTCACTACAAGGCGTGCCTTTACGCTGGAATTGAAATCAG TGGAACAAACGGGGAGGTCATGCCTGGTCAG
	Intron7	**135 nt**	GTAAGCCTCCGTATTTATATGCGTGCATGTATGCTTGTTATGTGTGAATATGTGTGATGTTTGCGACCTCTTCTTTCTTTCAAAGGAAAATCGAACTGT TTAATAAGTGAAAATTCACAACCTGTATTC ATGCAG
	Exon8	**75 nt**	TGGGAGTACCAGGTTGGACCCAGCGTTGGTATTGATGCAGGAGACCACATATGGGCTTCCAGATACATTCTCGAG
	Intron8	**315 nt**	GTACTTCGAACAACTATCCATGGTTCCCTGATGGCCTGATACCACAGAGCTTTTGTTATTTGCTTTTAGTTAGCTTAGTATGGCTAATAAGTCAACTTT CTTTGTTACATTATTGTAAACCTGATAGGTGCATGTGCTATGAGCTTATGATTTATTCTGACACTTTGAAGAATGCCATTCTTAAATACCATAAAAACA GTTTTCGCTAAAACATCAGAACCCATAAATCCATAACTGACCAGGTGACCATCCTTTGTGATATTAATTTTCTCATTAATAAGCATTTCTAATTAACATC CTACTCACTGTAATCAG
	Exon9	**54 nt**	AGAATCACGGAGCAAGCTGGTGTGGTGCTCACCCTTGACCCAAAACCAATCCAG
	Intron9	**75 nt**	GTATATTTCTGTAAGTTGTTTGATGAAGCAATTTATATATTAGAAGTTCGCAGTCTGAAGATTTATCTGATGTAG
	Exon10	**37 nt**	GTGACTGGAACGGAGCTGGCTGCCACACAAACTACAG
	Intron10	**370 nt**	GTTCCATTCTGTTATGTTAATATTTGTTCATCGTGCGTAACTTTTATAAAGTATATCTTGTCGTTTTCTTTTGAGAAACATATATCTTGCCGCATGTATAT ATTGAAAAAAAGCATCAGAAAACCTATTGCAGCTGACTAGCTGTGTTAGAGTAAATACTAAGGAAAAATATTCTTCGAAATGCAATGTTTCAAACAGG GCATGGATGTTCAGTGCTGGTTATTTTAAAATTACTATAAATGTTATTCCGAATAGACATGTATTTTCTATAGTTAGTTACTAACGGTTTAAGTAGTTTT CTCATTACTCGATAGAGTATCACCTTAAATTGCAAGTGAAAAACTGTGTTTTCTTCTTGTGGTAAATGTAG
	Exon11	**161 nt**	CACATTGAGCATGCGCGAGGATGGAGGTTTCGACGTGATCAAGAAGGCAATCCTGAACCTTCACTTCGCCATGACTTGCACATAGCCGCATATGG TGAAGGAAACGAGCGGAGGTTGACAGGGCTACACGAGACAGCTAGCATATCAGACTTCTCATGGG
	Intron11	**94 nt**	TATGGGTGGAGCAAACCTTTTCTTTCTTTTTTATTTGTATTTTCCTTCCTATTTATTTACAAGTTATACTGATCACAACACTTTGTTTATCAGG
	Exon12	**61 nt**	GTGTGGCGAACC GTGGCTGCTCTATTCGTGTGGGGCGAGACACCGAGGCGAAGGGCAAAGG
	Intron12	**206 nt**	TATGTGCTCTCCCTTGTTCTGCAACCCTACTTGCAATGGTTGGGAATGCAGAAAAAGAACTATGATGTCCCAATTAAAATTCAAATAAAATTATGACAA CCCAAATAAAATTCAAATAAACCTCTTGCCTATGTATATCGGTACTACGTGTCGTAGCTTGGTAATCTGCAATTTCAACTGAAAACAATGCCTTGTTGC CCAACAGG
	Exon13	**139 nt**	ATACCTGGAGGACCGTCGCCCGGCCTCCAACATGGACCCGTACACCGTGACGGCGCTGCTGGCCGAGACCACGATCCTGTGGGAGCCGACCCTC GAGGCGGAGGCCCTCGCTGCCAAGAAGCTGGCGCTGAAGGTATGA
	3’ downstream sequence		AGGACCTGAAAAAAGGACGAATTCTTCTTCCGGGGAAAAGAAAATAAATCGGCGAGCGGCGAGACCGTTGGCCGTCCATTCTTGTTGATCCTGTGG TTCCGTCGGGGCACTGCCTGTACAAAATCCTCACAGTTTGTAGAACCACTCCCGCGTGTGTTTTTCCGCTTGAACTGAGTCCATTTGATCTGTTGGG TCTGTACACTCACTGTACCTGAGTCCATTTGGAGAACTACGTTATTATAAAACGATAATGAATCGCATAGAGGATCTTTTTTTCTTCTTCTTTGCTT TCAGCTTGGTTCGTGTGTAAATCTCGTTGTCCCGTACGAGAGTACGAAGCTGTGGGACGCCACTATGGCCACTGGAGGACGGTGGTCCGTTTGTAG GTGGTGGCTGCCGGCTGCCGGCTGCCATTGTTGCCCGGCGGCACTGCCTCTCTTTCTCTCTCAGCTCGAGGACACACTCTGAAGAAATGGGACAA G
HvGS1_4	5’ upstream sequence		GACAATACTCCGTCCCCAGAGAGACACGCAAGACCGTTCGGGTTTCCGCACGGTCAAACAAGAAGGCGCCGCCCCCGGAAAATCTCCCAGCACTC CCCGGCTGAAGCGTGAGCGAGCGACCGGCGGCGGAGC
	Exon1	**168 nt**	ATGGAGGCCAGGTACGCGGAGCTGCGACGCGCGGTGGAGGAGACGGCGGTGGTGGACGCGCACGCGCACAACCTCGTCGACACGGCGTCCTCC TTCCCCTTCCTCCGCTGCTTCTCCGAGGCCGACGGCGACGCGCTCGCCTTCGCTCCCCACTCCCTCTCCTTCAAG
	Intron1	**1469 nt**	GTACTACTGTACTACGGTGACTAACTGACTGACCGCACGCACCCAAGCTTACACCTCACGCCGCTGCTATGCTCGTCCACGGTCCACTCCCCGGCC GGCCATCCTCGACCGCGCCGTCTTGCTTACATCCTGCTCGAGATCGCAACATTTTCTTTTTCCAAAGTAAGATAGCACTGACATTTACAACGCCATC CTTTAGTCTAGTGTGTATGTGTTTGCCCCTCCCTCTGTTGCTGCCTGCTGGGGAGTGGAGTGTGTGTGCTAGTTTGTGTCGGCCATAGAGTTAGGT GTGCTATCAGGGTCCTATACATGTTGGCGGGTTGATTTACAAATGTGTGCTCTTAAGTTTTGTCTAAGATAAATTGAGCTTTTTGAAGATTGGCCCAT ATCAACATAAGACCTTACGTTCTTGTGTGGTGGGTAAGATGTTGTCAATGATCATGCAGGGCTGGTATGGACATCACAGTTCCGTAAATCAGGAACT AAATTATGGTGCCATTAAAACATGAAGGAAAATAAGGAAATGTATGATTCTAGTTGTTAATGTTATATTTGCTTTCCAATCTTAGTTTTTTTTTCTTTTTT TGCAATTTTTTTTCAATCTGGTTTGGTCACGCTAGATCATACACTATTCGCGTAGACGATGTGGCGTATGTAAGAAATGCACATGAATATACCATGCAC GTGTTTAAAAATACATAAATATGTTAGCTATATATTAATCACATGATTAATTTAGAGAAACTATATTTTTTACATTAGAAACACATACACATAGAAACTAT CATTAGACATACTTAAGTACAAACAACAAAATTATATTTAAGTGGCGTATCATATGTTTTTTCTTCTAAAACCGTGGGATGTCATAAGATTAAGAAAAAA TATAATTCAAGCATAACTGGTTGGTTTTGGAGGGCACAGATGAAAATGAGTCCATATTTATTGTCTATGCTACCATGTTTGATCCGTTAGTTATTACTG ACCGGGGGTATCGGCAGAATATGCGGATGAATGAGTTTGTCTTTTTCCCTTTAACTGGTGGCACGGCGGAGATCGCCAGCTTTATGCCTGCTTGGCC AATCGCCATTGTATGGTGGGGCGCAGTAGGCCTTTTGCCCCGTCTCTTTGCCCTGCTGTGAGGTCCATTCCATGGATGGGCGTGTGTGCTTTTAAT GGCACGCTGCTGGACCCATGGAGGTGCTGGGGCTATTTGGCATGGCTCTTGCTTCTGAGCTTAAGATGTTCATGCCATCATGTGATGTGGGTTAT TTCTTCAGTGCTCTGTCTACCTCTTATGCACCAGTAATTTTTCTGTGGTTCCAATTTCCAAATGCTTGCAATGGGAGTGCTGCTCTTTTGTCTATAAAT AGGAATAATGTGCCAGTTGCTTGTTCCATAGCTATTGCATGGTATCCAAGGATAGATTTTCAGCAACTCATGACATCCTTGCAATATCATTCAATGCA G
	Exon2	**253 nt**	AGAAGCCTCAAGGACATCGCCGCCTTGTACGGCTGTGAAGCCTCACTTGAGAAGGTGGAAGAGTTCAGGAAGTCCCAAGGGCTGTCGTCTATCGG TTCGAAATGCTTCCAAGCTGCCAATATATCCACCATCCTCGTGGACGACGGCATAGCATTTGATAAAATGCTAGAGCTGGAAGCCCACAAGGAATTT GTTCCCACAGTCGGCAGAGTTCTGAGAATCGAATGGCTGGCGGAAACAATTATTAATGATG
	Intron2	**317 nt**	TGAGCCTCTCTGTACTCAACGATAAAATCTTTTTTTGGGGCCACCCTTGCAATAACTAGATTCTAATAATGGTAAATGACATTTAAGAATATTTTCT GTACGAATTAGTTGCCCACATTTTCTCCACAAAAAGATGTTGCCCACCGTTCATCATCTACCAGCACAATGGTTGATTTACATGACATTGTGAGCCTG AAATAACAGAATAACTAGGGTAGTTAAATATCCATGTTTGATTCATTTCTATGTTGGCGTACTCCCTTTGCAGCTAAAGATTATGATGAGCTACTGATG AAATTACTTACTGCTTTCAGG
	Exon3	**68 nt**	ATTCATTCAGTGGATCAAGCTGGACGTTGGACTCATTCACTGAAACTTTTGAGGCTAAGCTCAAATCA
	Intron3	**94 nt**	TATCCTCCAGATTTTTTATTTGGGACAAAGTGGAAGTTTTTTTTTCTCTTTTTGTTCTTTCAACTACATGGATATCCTTGACCAAGTTCTCACA
	Exon4	**117 nt**	GTTGCCAGTAAAGTTGTTGGGTTGAAAAGCATTGCTGCATACAGAAGTGGCTTAGAGATTGATCCATGTGTTAGCAAGACAGATGCAGAGGATGGTC TTCGTCAGGAGCTAACAGGT
	Intron4	**81 nt**	GAAACAGATCAAACATGTTGCCGCCTATGATTATAAGATCTATTTTATGCTTACAATCCATATTTTTCAGGTCGAAGACCT
	Exon5	**95 nt**	CTTCGGATTACAAATAAAAGCCTGATTGACTATCTATTTACTTGTAGTCTTCATATTGCTGTACAGTTTCACTTGCCAATGCAGATCCACACAGG
	Intron5	**94 nt**	GTAATGACTGGCATTTCAGATTTTATGAAAGCACTTTCCTGTCTGATCTTTTTAAGATCTCAAGTATATACATCTTCCTTCTACACAATTTTAG
	Exon6	**158 nt**	CTTTGGAGATAAAGACCTTGACTTGCGGAAGTGCAATCCTCTACATCTCCGTGCTATTCTTGAGGATGAAAGATTCGCTAAGTGCCAACTGGTCCTT TTACATGCTTCTTATCCATATTCTAAGGAAGCATCCTATCTTGCATCTGTTTACTCTCAGG
	Intron6	**75 nt**	TTGGAGGCTCGTCTTCATGCAATTATTCACCCATTCTGTTTTAAGTTAAGTTAATGATCACAAACAATCCACAAA
	Exon7	**99 nt**	CAGGTCTATCTTGATTTTGGTTTGGCGATTCCAAAACTTAGTGTTCAAGGAATGGTGTCATCACTTAAAGAGCTTCTGGAGCTAGCTCCCATAAACAA G
	Intron7	**756 nt**	GTACATATCCGTCGTTTGGATAATTGCTTCTATAAAATCTGAAGAAGTTATTAATAATATGAAAACATATTTTGCTTTTCCATGGTGCAGAAAAACTGAA CTAATTAATATTCTCCCACAACTCAATAACGTATTATCCTCCATTGTGCCATCACATGTACATTTTTGCCATAGTCCTCCTTCCAGTGACAAAGATTGC

			TAATGTGGACACTGACGCTCAATATTACTGATGCAGTTTACTGATAAGACTTAGTAGCATTATAATATTACAAAATAATAAATTGAGATGGATATAATC GTATTTTTCATATGTTCATTTGGAGGCCCTCAATATTCATAGAGAATCAATAGTCAAAGTTTAGAAAGTTTGACTGCACATATCCCAAAATGTCACTTT CTTTACTGGAAGGAGACTACTAGACACAGAGATTACTGCAGTAAAACATATGGTCCATGTTCTTGAATGGAAAAGTAGCACACATGGTCCAGGATCC AGGTCCGAGCAGTATTCGGTGCTTAGTATAGATTACTGTTGGCTTTTGATATTCGATGTTTGAGAATCTCTCGCTTATTTTTGTCTTGCAATGCATCTG ATTTACTATCTTGTCTGAAATAGTTACTCTTAAGTTTCCTTTCTAATAGCACTCTTGATGTATGTCTCATTGTCAGTCACATATGTTCATTCTCATCTTCT GTTGCTTCTGGAGATACTATGTGCATGATGTTTTTATTTGTTAACTGTTAACCATTGGCAG
	Exon8	**51 nt**	GTCATGTTTAGTTCAGATGGATACGCTTTTCCGGAGACATACTATCTAGGT
	Intron8	**593 nt**	ACAATAATCAGTTTTAACTCTTTCATAAGATGATGAAAGATCATTGTAAGTCAGTACAAATGTTAGTTATATTATCATAAATTAAGTAGGTCAAATAGTA TCCTCTCATGGTAGGAAAACAAACTTTTGGGCCAATAGAAAATACAAAAAACAGAAAGATTTGGCACAGGATCTAGACCTTCAGATATACCACCTCTG TTCCAAAATACTACTCCCTTCGTCCCATAATATAAGACGCTTTTTAACACTACACTAGTGTCGAAAAACGTCTTACATTATGGGACGGGGGGAGTACA TGATTTCCTAAAAAGTGTACACTCAACCTTTTCTATCTTTGACAACTAATTAACAAAAGGTTGTTCAGATTTGTTTGGTAACAACTGTGACGTTAGATTT GTCATGAAAAAATAATTTCAAAATATTTTTTACTAACATAAGTATATGAAAAATAGCGTCAAAGTTACGTATTTTGTAGTGGAGGGAGTATATAAATAAG TAGTGCAGACAAGGAAAGTTATCCAAAAACCACACAAGAGTGTCCATTTAGTTGTTGATTTTAAGTGATAATACATGGTTTGTACTGATTTGCAGGT
	Exon9	**266 nt**	TCAAGAAGGGCACGTGATGTTGTTTACCATGTCCTATCAGCTGCATGTGAAGATGGTGATCTTAGCATTCAGGAAGCTATTGATGCAGTTGAGGACA TCTTTAGAAGAAATGCATCGGATCTATACAAGTTGAACGTTGCCAATGGGTCAACTCACCAGAAAACTATGATAGCTGACAGTAGGATAGCATCATCT TGTGTTGAACAAGATGTCCTCTTTGTTCGCA TCGTCTGGAATGATGCTTCAGGTCAACATAGATGCCGCGT
	Intron9	**339 nt**	AAGCACATCTTTCCAAGCACATGCTGCATTGTTTACATTGTGTGATGTAGTTTTCTCACTGATCATTTCTCTTCTTTTTTATTGACAAAAAATTCTCTTTT AGAAAATTGTCTTAAATAAATTACCAACTAGACACAATAGTTAACATGAACTTTGTTTGAAGATTACCTACAAGTTGTTTCGTTTCAATAGATGGTCAAC TTAGCACGTATAAAACTACTGATAATTGCATGGTGTTGACTGTGTTGACGGTCAGCTTACCCACCTGAACAACGGCATTGTTTTTAGAATTGCTAATG CCAAATCCAATTTTGAGAAAATAGAACTTCACTTTCAGGT
	Exon10	**173 nt**	TGTCCCAGCCGGAAGGTTTTATGAGATTGCAAGGAATAAGGGTGTCGGCCTGACTTTTGCATCAATGGGAATGACTTCCTTTTCTGATGGCCCAGCT GATGGGACAAACCTTACTGGTGTAGGAGAGATCAGGCTTATGCCAGATATGTCAACGCTTTTGAGACTACCATGGT
	Intron10	**168 nt**	AAAGTTAATTCATTTAACGTTTTCTCTGTACTTTGTATCGAACCACCCCTTAGAATCCCATAACTTAGGATCGTATATGAATAGTTTCTTGTTTGTTAAC AGCAGGTCAATTCTCTGAACTTATTAAGGCATCATTGAACTAATGATAGTTTACTCACATTGCAAGGT
	Exon11	**119 nt**	CAACACGTGAGGAAATGGTGATAGCTGACATGCAAATTAGGCCTGGAGAAGCCTGGGAATACTGTCCTAGATATGCCTTAAGAAAAGTCACAAAAGT TCTGCTGGATGAATTCAATGTG
	Intron11	**115 nt**	GTAAGAATAATCCCAGAATGTTGCCTACATGACTCTGAGAAGATCATTTTCGTCTCATGAGTTCTTTCTGTGCACTTGTTTTTTGTATTTATGCTTAGTT GTTTGTTCTTTGTAG
	Exon12	**53 nt**	ACAATGAAGGCAGGTTTCGAGAATGAATTTTATCTGCGGAGAAAATTAGTAAG
	Intron12	**83 nt**	GTAGCTTTTTCCCGACTCTCCAAAATAAATTATGATAAAGGCCATGTTGTTCTGTATGTGACCCAAATCAGAAAACTCTACAG
	Exon13	**130 nt**	TGAGGGGCATGAGCGTTGGGTTCCATATGATAATAGCAGTTACTGCTCAACCTCATCATTTGATGGTGCCTCATCTATACTACAAGAAGTGTATTCTT CTCTTAAAACGGCAAATATTGTGGTTGAGCAG
	Intron13	**147 nt**	TAAGACTTTATTTTACCACCAAAAAGATGTCAAAACTCGTGATGTTATATATCAAACTGTTTACCTTTTTGATTGTATGTCATGATTTAGTGATTGATCA TTTTTTCTATGTTTACATTCACTTTCTTGCTCAACAAAATATAAAAG
	Exon14	**146 nt**	CTGCATGCCGAAGCTGGGAAAGGGCAGTTCGAGGTTGCCTTAAAGTATGTGATGTGCACTCTTGCTGCTGACAATTTGATATATGCTCGCGAGATTA TTAAATCTGTTGCTCGAAAGCACGGGTTGATAGCAACATTTCTTCCAAA
	Intron14	**350 nt**	GTAAGCCAATGGATCTACAGTCTGTTTTTTCATTAGCATGCTCTATAGTTTGAATTGTATTGTGTACACTGCTTTGTGTTAACAGCAAATCAGAACACC AGAGAGTGTGTCCAGGCAACATTACTGGCTTGTAAAAGAATTGACTTTTTACTTAGAAGCTTAAGAGAACTGAAATGAGCTGCGGTTGATCAAATAAT ACTTCTATTTGCTGATATCCCTATGTTATACTCTGATGCATTATGCAAATATCAGGTTTTAGCAATACAAATGTGTGATTTGAAAACATAAAATATTGCC AATAAGTGAAACTTGCCTTTCTGGTGCCTGATGCTTTATTCTGCTGGACACAG
	Exon15	**189 nt**	ACCTGACCTGAATGATATTGGATCGGGTTCCCATGTGCATCTGAGTTTATGGAAGAATGAGCAGAATGTTTTTATGGGATCAAATGAATATAGCCACT ATGGAATGTCAAAAGTTGGAGAACGGTTCCTTGCTGGAGTATACCGTCACCTTCCATCAATCTTGGCATTTACTGCTCCTCACCCTAACAG
	Intron15	**217 nt**	GTAACATCTTCCTGAAAAGCTTCGAAGAATACATGTTAATTCGATAATAGCTTTGATAACTGATTTTGGTATTTGTTTTTTTGCATAAACTCTCTGATGT CAGCGTATTTTTTATTATCTAGAATCTGGATAACACAGTTTTCTACTTGTTGGAAAAATGCCAGAACATCAAAGTAACCATTTTAACAATCATTATTATT GGTTTCTCTATATGTAG
	Exon16	**233 nt**	CTATGATCGAATTCAACCAAATACATGGAGTGGAGCTTACCTATGCTGGGGAAAAGAAAACCGGGAGGCTCCATTGAGAACCGCATGCCCACCTGG TGTGCCTCTCGACATGGTCAGCAACTTCGAAATTAAATCATTTGATGGGTGCGCAAATCCGCACTTGGGGCTTGCTGCTATTGTCGCTGCTGGGATT GATGGACTTAGGAACGGCCTTGAGTTGCCTGAACCAATTG
	Intron16	**697 nt**	GTAGGAAAAAAAACCCGTTGCTTGACCTTTTTTATATTACTCTCATGCATTACTGATACTCCCTCCGTTCCTAAATATAAGACCTTGTAGAGATACTAC ATACGGAGCAAAATGAATNNNNNNNNNNNNNNNNNNNNNNNNNNNNNNNNNNNNNNNNNNNAGTTCATAGTGAAATCTCTAAAAGGAGTATTTGTCATG CTGCCATGGTGTCTGAAAATGCCCTAGGAACATATTGAGCATGTTCGGTGATCCTTGCAGGAACATGTACAACATGATAGAAAGTTGTCGAAAAACA CAACTGAAGGTCCTGAAAATTCTGGGGAAAACTATCATGACATGGACACAATGCACATCTGTTATGCCCACATAGTGTCAAATCCAAATGAAATTCAT AGCTTGATAAAAGGAAAGAGCTCAGGCTGGTACTATTCTGTCGGATTTGTCTTCTTTTTTTGTTGATCTGTGGGATGAAATTTGGAGACATGGTAGAT GTTGTGTAATGTTGTGAAAGAAAGTCAGATTTCCTCATTATCGTTAAAGTTGCTAATCAATAATCTAACACATTACTATAACTTATGTGCCTAATGGATC TGGCATGCCCCTAAACATGTTATGCTATATGTCTGGATTAGATTATTTCTGCCGACTAGCTTTTGGTTTCCTCAGTGCAAATGTTACATGTGTCTTGTG TCTCTTCCAG
	Exon17	**144 nt**	AATCAAATCCTGCAGATTATGCTACCAAGCTCAAAAGGCTACCGCAGGACTTGCTGGAATCTGTAGAATCACTTGCTGCAGACAAAACTTTGCATGA GCTAATCGGGAATAAGCTTATTACAGCTGTTATCGCTGTACGCAAGG
	Intron17	**144 nt**	TTAGTACTCATAAGTTGCTCCCTCCCAAAGTGTCTTGGGAGGGGGTATTATTTTCCTTCACGTGATATAACTCGACAGATTTGTCAGAAATGAAATGA AAGCATGAGCGCGACTAACATCTTAGGTTCTATTTTATTTTTCAGG
	Exon18	**59 nt**	CGGAGATTGATCATTACTCGAAGAACCCTGGGGCATTTGGCGATCTCATTCACCGTTAC
	3' downstream sequence		TAAGACAGAATACTTGTTTCAAGACCACTTTCTCTGTCGCTTGGAAGGTTAAGCCGACGAATAATGTTGCCCACGAGTTACTGATCCTCATGACTGAA TTTGCGTGTTTTTCAGTTAATAATAAAGTGCTTAGAATATGAAATCTGTCATCGGACATTCTTTTTTATCTGACGAAAAATCGAACAGAAAAGATAAGA CTTGATGCCTTCGTCTCTTGCTTGAACCCCCAAAAAAAAAAAAAAA
HvGS1_5 Fragment	5' upstream sequence		AGGAGTCACTTTCTGGATCAAGCTGGACACTAGACTCATTCACTGAAGCTTTTGTGGCAAAGCTCAAATCATATCCTACACAATTTCGGATGTTGTCT GTTTGTGACTATGTGTGTGCGCGCAAGTGCATGTGTGTCTCTTTGTTTGTTTGTTTGAACTCTGTAAATAACTAAATATCCTTAAAAAATTCCTCACAG TTACCAACAAAATTGTTGGATTGAAAAGCATAGCTGCACACAGAAGTGGATTGGATATTGATCCAAGTGTTAGCAAGGTGGATGCAGAGGATGGTCT TCAGAAGGACCTAGCAAGTAAGCATATTTCTTTGTTGGGAGATAGAAATGTGTAAGCCGATAAAATAGGGTTGCTAGTTAATAATGACAATGGCCCAT TAAGCTTATTAGTCGTCAATACTTTTCAGCACGGAGGCCTCTTCGGATTACAAACAAAAACCTGGTTGACTATATATTTATTCGTAGTCTTGAAATTGC TGTGGAGTTTCACTTGCCAATGCAAATTCATACAGGGTAAGGACAACATTTTAAATCCTATATATCAAAACACGGTGGATTAATTTCAATATGTATCTC TAGTATAAATATGGTTGTGTGCATCAGACAATCAGAGGCCAAGGATCATCCCCTCTTTTTAAAAAAAAAATCTCCAATGTATATGGCATATGATTTCCA AGCAATTTCAGGTTTGGAGACAGGGACGTGGAATTACGAAATTGCACCCCTTTTCATCTGCGTTCTCTTCTTGAAGACAAAAGATTTGCCAAGTGCC AAATAGTTCTACTAAATGCTTCATATCCATTTTCAAGGGAAGCATCCTATCTTGCATCTGTTTACTCCCAGGTGGAACCCCATTTTTACTACTCCCTCC GATCCATATTAATCATCGCAGCTTTAGTAGAAAGTTGTACTAAAGCTGCGATAATAAATATGGATCGAAGTGAGTAACAAATTACACATTGTCCGTTTT AATTATTTTCTTCATTTTAAGTTATTAACCATCTTACACAAACCACAATAGGTCTACCTTGATTTTGGCTTTGCATTTCCAAAACTTAGTGTTCAAGGAA TAACATCATCACTTAAAGAGCTCCTAGAGCGAGCTCCCATAAAGAAGGTAAAGTATCTGTCTTCTGAATAGCTGTTTCTAGGAAGGTCATTGTTACGA ATACATATTTTACTTTACTTTTCATGGATAGTGCTGAATACAAACTGAGGATTCTCATGCTGTTGGAACCAAAAACAACTCAAAGGTAGTACTCCTTCT AGTCACCACTTGTCTTAGTGGATACCGACATAGTGCCAAAACTCCTTTGACCCTGTGAAATATTTATAAATACAGTACGGTTACAATATTAAGAAAATA TTTGTGAAGGCAAATCACCTCACACTTTATCCAGATGCTCAATTTTAAGTTTATAATATTCACACAGATATTTATAGATAAATTAATTAATTAAAATTGAC TGCATCTATATCAAGACCCTTGTCAATCCTTGTCTAGTATTCACTCTCATGATTCCTCTGAACAGAAGTCCATTGCTATCAATTCTGCTCATATTTGAT GCATGTATTATTTTTATCTGAAGTTTGCCACCTCTGGAAATACTATACTCTCATACACCTAGCAATTTTTAACATTAATTTCAGGTCATGTTCAGCACAG ATGGATATGCTTTTCCCGAGACATACTATCTAGGTATGTTTATCCATCTTATCTATATGAAGTACTATTAAATAAGGTGAATCTTATAAGTCAATACGAA TGTATATGCTTATAAAGAATAAGGGACTTTGAACTGAATAAGTTAGGGAGCAATAATTTTTAAGTTTGTCACAAATAAAAGTTAAAAAAGTGGAATATA TATTTGATGTGATACAGAGCCTATTGATATACATATTTCCTAGTTCATTTAGGAGTTTAGGACCGTAGACGTACAGTTATTTCTTTTAGGTATTGAGTTT TAGCTTGGGCTGATTTACAGGTGCAAAATGGGCACGTGATATCGTTTACCGTGTCCTCTTAGCTGCATGTGAAGATGGTGATCTTACCATTCAGGAA GCTATCGAAGCAGTTGAGGATATCTTGAGAAGAAATGCACTGCATCTTTACAAGTTGGATGTCGTCCATGAAAAAGTTATTAATATTGATGATAATAG CACATCATCGTCATCCTGTGTCAAGAAAGATGATGTGATTCTTGTTCGAATGGTTTGGAATGATGCTTCAGGTCAACATAGATGCCGTGTAAGCATAT CTTCCAGACCACATACAACATTGTTAAGTTTTTTTTTCCTTAGAATTGTTACTATTTTAGTAGGTAGTCTTGAGAAATGGAAACTTTACTTTCAGGCCTT GCCAGCCGAGAGATTTTACGGCATTGCACGGAATAAGGGTGTTGGTCTGGGTATTGCAGCAGTGGGGTTTACTTCCTTTAGAGATGCCCCAGCAGC TGGGACAAATCTTACTTGTGCAGGAGAGGAAATCAGGCTTGTGGCAGATATGTCAACACTTTTGAGGATCCCATGGTGAATGTCCTTAATTAATTTAT TTTTGAACAAATTATTGTTATTTTTTATATATAAATTGGGTCAAACCTTAATTTTTGAACAATTTACTTATTTCTTATTATCGTTTCTCTCTCACACAGACC CAACTTTCCTTTTAGATCAACCACCCCAACTTGTACATAAGCATGCCGATTTGTTGCTTATACCTGGCGAAGGATATCCTTATGGTTTCTGTTCTGTAC ATAACTACTAGTCCCTCTGTATCACAATATAAGAGGGTTTTTTATAATCCCTTTGTATCAAAAAAAAGTATATTTCGATATAGAGGGAGTAATTACTTGG TTCTTATCAGGCATATGCATTTCCAGATTGTTCACAACCTATCCGGACAAACCGAGAATTCACTACGACATAGTCTTAACAATGGCAACCTTAAATTTT TGAAGGAAAAACATTAGCTTGTGATTGTACTAATCGCACTTTACACTTCTTACAAGGTCAAGAAACGAAGAAATGGTGATGGCTGACATGATAACCGG TTCCGGCGAAGCCTCCGAATACTGTCCTAGAAATGCTTTAAGAAAAGTGATAAAAGTTCTGCTAGATGAATTCAATGTGGTAAGAATAAACCTATAAA AATGTAGTTGATGTCTTTTTGTTGATGCTTAGTTTTTTTTCCTAGACAGTG
	Exon1	**45 nt**	ATGGCAGGTTTCGAGAATGAATTTTATCTCCTCAGGAAATCATTC
	Intron1	**93 nt**	AGGTAGCTTTGCCTGACTCTGTAGTCTGTGTAAAATTAATCGTGGTAGGAAGGATCTATCCGCTCGTTCTTTATATGTACTGAAAACTCATGC
	Exon2	**129 nt**	AGTGAGGGCCATGAACAGTGGGTACCATATGATAATAGCAGTTACTGCTCGACTTCAGCATTTGATGGTGCATCATCTATACTGAAAGAAGCATATT CCTGTCTTAAAGCTGCAGAAATTGTGGTTGAG
	Intron2	**126 nt**	CAGGTAACAAGTGACTTTTGTAGATGTGAAGAACTTCTGGTGTCAAATTGGTTACCCTTTTTTTGTGTATTGATTTAGTGATCTTTTTTTCTGTTTTCAC CTATATTCTTCCTCCTGCAAGTATAA
	Exon3	**149 nt**	CAGATGCATGCTGAAGGTGGTAATGGGCAGTTCGAGATAGCCTTAAAGTATGTGTTATGCACTCTTGCTGCTGATAATCAAATATATGCCCGAGAAA TTATTAAATCCGTTGCTCGAAAACACGGAGTGATAGCAACATTTCTACCAAA
	Intron3	**95 nt**	GTAAGTCAACAGATTAACATATCGTAATCCATCTTGTTCAATGACACAAGCAGGTATCTAGTATATGATGCAATGTTTTCATTGGCAATTTCCAG
	Exon4	**186 nt**	ACCAGACCTGAATGAACTTGGATCCGGTTGTCATGTGCACCTGAGCTTATGGGAGAATGACCAAAATGTTTTTATGGGCTCAAATAAATATAGTTACC ATGGGATGTCAAATACCGGTGAACGGTTCCTTGCTGGAGTTTATCATCATCTTCCATCGATACTGGCATTTACTGCCCCTCACCCACA
	Intron4	**260 nt**	CAGGTATTACTTCAATCATAAGCAGGAGATTTTGTAAATATAGTCTCCAATGCGATTGAATACCCAATCACTACTTTTTTAGGCATATGTTGCTAGACA TTTATGGTTTTTGCTATCCTGAAAGTAGTTTTCATGGCAAGGTTATTGATTTTTTTAGGATTACCAATCCAAATATTTTTTGTAAATACATATAGTTTTTT ATTTGTTTACCGAAGATGAGGGGTATGATGATTGTGATTTTATTTCTGTGCATACATATA
	Exon5	**236 nt**	CAGCTATGACCGAATTCAGCCACACACATTTACTGGAGCATATCTTTGCTGGGGGAAAGAGAACCGGGAGGCTCCGTTGAGGACCTCCTGCCCACC GGGCGTGCCTCCTGATTTTGTCAGCAACTTCGAGGTCAGATCTTTCGACGGGTGCGCGAACCCTCACCTTGGCCTCGCCGCCATCGTCACCGCCG GCATCGACGGATTAAGGAGAGGCCTGAAGCTGCCTCCACCAACTG
	Intron5	**91 nt**	GTAAACACTAATTTCTCATTGCTTTCTTGAGCTTTCAACATCTTAACCACGAGTGTTTCACTCGGGGAAATGTGTCTCTTGGCTCTTGCAG
	Exon6	**141 nt**	AACTGAATCCTGCAGATTGCGCTTCACACGAGAGGCTACCGCACGACTTGCTGGGATCTGCAGAGGCACTTGCGGCGGACGAGATTTTTCATGAAC TGATGGGTGATAAACTTGTTACTTCTGTTATAGCTATGCGAAAGG
	Intron6	**71 nt**	TAACTAGTAGACACACTCCAGTGTACTGTTTCCATCTGCTCTTCATATTACTAATCTTCGTGATCTACAGG

	Exon7	**62 nt**	CTGAGATCGAGCATTACGCGAAGAACCCAGTGGCAGTCCACCATCTCATTCACCGTTACTAG
	3' downstream sequence		CGATGCCTATTTGCCTTGCTTGGTGATCGATCGGGATCGGGTTGAAAAAGTACTGCTCTGCTTTCAGACGTTGCTCTGTTCTCAGCACTTCACATGT ATGTGGATGAGTAAATGTTGTCCAGATGATTGCTCATGATCTCGGCAATGCACTTGCCGTTGTCAGACTTTTTCAGTTAATAAGTGGTAGAGACCAAG GTTTAGATGATTGCTCACCGACAAAGCTGCGCCAGGCCCTGGGATGGTGGCAGCAGGGCCATTTTCACCCTCCGCCCTTCCCCCAGATCTGGTCC CCGGCAGCACCGCCAGCTTCCACCGACGACGGGGGCGGCCTCCCCGGCCATCCCGTCCTCGAGGTGCTGCTCCCGTCGGTTGCATGTTCAAAAG TTTGATTTGTCAGTACCGGAGCTTGATGTGTCGATGTGTTGGATCTTCAGGCTATGAGCAACCCTTACACCTGATAAAACTGATATGTGGATGTGGAT TCACACATGTGAGTGGCTTGATGTATACAATGGACATATCTATCTTTCTTTGACAAATCTGTGCATATATAAATGTCGTACAATTGATGC
HvASN1	5' upstream sequence		GATATGCTCAGACTGCTATGCTTTCCTCTGCTTCGCTGGATATCGTCGTCGTCGATCGTTGTCTACAGCCAACAGCGAGGTACGTAGTCGATCTGAA TTGTGCATCTAGTATATACGAGTATTACAGATGCACAGCGTTGAGACTTCCTTTGCAGGAAGCCTATTATAATCCGTGTCTGGACACTGAAAAATCAG AGAAAGAGAAAAGAAGAAAAGAAAGAAAAAGGAAGAAGGTGTTGGGAGCTCGATACTTTGAATTCTCATTACAAAGAATCGATCATCCGTGACGACG GCTGGGGAAAATTTCGAGAGGAGTCACTTGACAGGGCAATGCCGCTGTGGGGGGCGTTCACTTCCATTGGTTGGCGACGATGTCGGCGAGGTCG ACGACC
	Exon1 (no match in genome seq)	314	AGATGGGCGATGACCTCGCAGTCACTGCCGGTCCGGAACCTGTGGCCGGAGAGCCGTTCCCGGAGCTCCTCATGGTTGTAGATCTCCCCGTTGAC GGCAACAGCAACGGACTTGTCCTCGTTGTAGAGCGGCTGGTCGCCGGAGGCCGGGTCGATGATGGCGAGGCGCTGGTGGCAGAGGTAGTTGTCG GCGACCTGGTGCAGGCCGCTCCAGTCCGGGCCGCGGTGCTTGAGCCTGCGCGAGAGCTCGAGCACATGCACCCTCTTCCCCTGCGACTCGTCGC CGCACCCCAGCACCGCCAGTATGCCGCACAT
	Exon1	144 nt	CCATCGATTCCCCAGCCAATGTAGAGAGACGTGACACCAATGGCATCACGAGCAGCAATGAAGCTGTGATCTCGTGCGTCAAGCAACACGAACGA GAAAACACCATCCAACATGTCAATGAAGCTTTCTCCATGTTCCTCATAC
	Intron1	100 nt	CCTGACAATTTTTCAGAGACGTGCATGTTTAGAAACGCAGTGCAAATGATATAGGTTTGTTTCATGAAAAGATTCCTCAAGCACTTTTGAGAGTGTTA TA
	Exon2	188 nt	TTTCAAATGCCGATCTGAGACGTAGTGGGTCATAGGGAACCGAGGGGATGACCTCAGAGAACCAAGGAGGGTTATACCATCTCTTGAAGCATTTTT CTTTGCTGGAGTAAAGATTACCAGGTGGGAAGATCTCGAAGTGCTCACAATCATCGTTTAGTCCTTTCATCTCCGAAGATATCCACACTGAA
	Intron2	108 nt	GAATGAAGAACATGAAGAATCATGGCCATGAGTCCGAAATTTTATTACATCTCTGTTTTTCAAAGATACTAGATGATGGTTAGTTGAGGCCGTTACAG TTTGCGACCT
	Exon3	162 nt	CAAGCCCAACACAGAAGGAGTGGAGCCTAGTTCCCCAGCGCTTTGCAGCCTTCGTCCCTGCGAAATGACGGGCTGCGACGGCTGCCACCAGTGAT GAGTCGAGGCCACCAGAGAGGAGGACACCGAATGGAACATCTGTCATGAGCCTCTTGATGACAGCCT
	Intron3	90 nt	ACAATATAAATTGAGATAACAGCATGGATTCAAGTTCTATTACTCCGAAACTTCAATAAACGTGTACATGTTCCTTTCAATTTCACACCT
	Exon4	71 nt	GAACTGTGAAGTTGAACTCATTACTCCGAAACTTCAATAAACGTGTACATGTTCCTTTCAATTTCACACCT
	Intron4	85 nt	ACAGCAATTTGTGCAACTAAAATAAGTGATTGTGTACAAATAAGATAGGATCGTTATACTTCTTAGTGGTACTACTACCGTACCT
	Exon5	222 nt	TCCGACATGTTTCTTGGTGGAACTCCTCCTTGTTGGGGGCCTTGTGGAAATACAAGTACCCCCCGAAGATTTCATCAGCACCCTCACCAGAGATGAC CATCTTGACACCAAGCGCCTTGATCTTGCGTGACATCTGGAACATTAGTGTGCTTGCCCTGATCGTCGTCACATCATATGTTTCAATGTGATATATCA CGTCTTCAATTGCATCGATGCCGTCCT
	Intron5	84 nt	GCAAAACAAATCATGTTAGAGCAGAGTGTTATGTGTCCTATATATTGTTTCTGCTCCTGTGAAATGTTTGTATTTTAAAGACCT
	Exon6	136 nt	ATCTTCCATTCAGGATCTATGCTCATAGCCTCATCGATGAACTCCTTGTCCAAGAATGGCACACGAACCTCAAGGCCCCATGCAGATGTTGCTTTATT GGCCCTCAAGCAATCGTACTGATGGAGAGCTTTGATCT
	Intron6	65 nt	TGTGTGATTAAATTTAGAAAACAATGCAGTGCACTCCCATTCTTGTGAAATATTTTGTTCTTACC
	Exon7	69 nt	GGTTTCTCCTCATCGTCGAACGCTTTCCTCAGTATCCATTTTTCAATTCTTCCAAGATCAGGCCGGATC
	Intron7	89 nt	CATAGATCACACAGAAGAACGTGTTAATAACTCCACTACTCCAGCTGGATCTGACTGTTGAGTCGAAAATGTTACCTTCGGCAAGAAG
	Exon8	100 nt	ATTTGATGCTGCATGATCCTTAAGGCCATCAATCCAGCTATACCCAACACCATCACTAAACTGCTCCTTCTGCCTGTACAGAATGTGCTTCGGCAAGAA AC
	Intron8	118 nt	CTGCAGTCAGTGATTTCATTTCATATCAGTTAGATATTGCAATCACATACTCGTATCGAGGAACGTACGTATTAGTTTTACCAAAACTAATTAACATGG AAAATATTTGTTTATTTAC
	Exon9	104 nt	GGGAAGTACCTCTCGAAGATCATCCTGTAATAGTAGGCCTCTTTAGTTGTTGGGGTGTTGTGTGGGTAGATGAACTTTGCATTGGACATCATCTTAT CACTCAC
	Intron9	141 nt	AACAAGGTCAAGCAACCAACATTGCTTCCATTAAACATTGCTCCAATGGTATTGAAGTTAAGGTATCTATTTCATTCCTTTACGCAAAAGGATAATGTC CATGTTGCTCAACATTTCTTTTGTATTTACTCACTCACCTGG
	Exon10	223 nt	GCTCTCTATGGCAACACCATTCACCACGGTCTCCATCGGCCCAGGCTTATTGCTACCACCCACAGCGATCGTGTCCTGCTCGTAGGCTGAGAGATG GACTCCAAGCGCTGCTCTCCCAGAGGGGTCCAGGTTCCCAGACCACTGCGCGTCCCACTCTATTGCCTTGGCTGTGCTGCACGCCACGCTTGGCC CGCCTGGCACCGTGAGGATCGCCGAGCTCTGA
	3' downstream sequence		GAGTATCATATCATGATACCGTATCATATTAAATGTTGTGCTAGTATGTGTTATGCATGGCAATAAATGATATATCATATGATACTATGCATTACGGGT GTAGTATCATATGCATGATATTAGTATATGATACTCTCCATTACAACCAGCCTAACCGGATACACCATAAATTTCACCATCATATTTAGCTTATATATGC GGGCTATAAAAAGGACAAGTAACGACCAAACAGACCGGACCCACCATAAATTTCAGCAAATCCCGCTCCCCTAAGCTTGCCGGACAAGCCCCACTT TTCTTCTCCACTCACCTCCCTCGTCCACGCCGGCTCTCACCTAGCTTTGCTTGCCATCCTAGCTCACCGACCCCTCCAATCTAGATTTTCCAATTCAT AGGCCAGGCCAAGAGAATCTTTTAAATTAAACAGGAGAAACATAGGCCTGTCTTATTACAACACCGACAAGAACTTATGCATCATATATGTCTTTAGT AGGACACGATATACGTGTCATTCATCA
HvASN2	5' upstream sequence		TTTCGCTGGATCGACGGCTACAGTATGTAGCTAGAAGACCTCTCTCCGTTCTTCCGAATGAGGATGGTTGTC
	Exon1	219 nt	AGTGACGACGATGGACTTGTCCTCGTTGTAAAGTGGCTGGTCGCCTGAGGCAGGGTCGATGATGGCGAGGCGCTGGTGGGAGAGGTAGCAGTCA CCGACCTGGTGCATGCCACTCCAGTCGGGGCCGCGGTGCTTGAGCCTGCGCGAGAGCTCGAGCACGCGCACTCTCTTCCCCTGGGTGTCATCGG CGCAGCCCAGCACTGCCAGTATGCCACACAT
	Intron1	79 nt	CTGCAAGGAGAAGCTTGTTTTAGCAGAAAGAAGCAAGCTACAATAGTGGCAGAGAAATTCACACAGAAGGTAAACATAC
	Exon2	96 nt	CAGGTGTGCGATGACCTCGCAGTCGCTGCCTGTCCTGAATGTGTGGGAGGAGAGCTGCGCCCGGAGCTGTTCATGGTTGTAGATCTCTCCATTCA C
	Intron2	324 nt	CTATACAATGGTAAAATTAAGTTATGCATCCACTTGTTAATCACATATATTTCCAGTTTGGTTAATTGTCTTTTTATCTTCATGTTTATCGATGACATGG AATCATTTCTCTGTTTACGGTGGTCAAGGACTACAAATGCAGGAAATGTCATTCTGGTGTTATTCGTGCCTTTCCCGTACCAGAGGTGTTCTTTTTTT GACTTGTGATAGATATGTTAGTGTCTCGCAACTTGGCATATCTTAATGATATCATGACTAGTAATTATTGTTAAGGAGGAGGAAGAGGAGAGTTGACA TTTGAGTGTTGTCATGTAGGTGACTTAC
	Exon3	141 nt	ATCAATTCCCCAGCCAACATACAGGGGTGTGACACCAATGGCATCACGGGCAGCAATGAAGCTGTTGTCGCGTGTGTCGAGCAAGACGAAGGAGA AGACACCATCCAGCATGTCGATGAAATTCTCCCCATGCTCCTCGTA
	Intron3	138 nt	TGGCAATTTGCAGAACATGAGCAGGTATGTTAGACAGATTTTACTTGTCCTTGACTAGGTAGTATTACTACTGTGTGACAAGATTGTCTGAGGGTAGG TATTGTGTGTCATTATTGAGTAAAATTAACATGACTCACC
	Exon4	192 nt	CTTTTCGAAAGCTTTCCTGAGAGCAAGTGGATCATATGGCACTGAAGGAATGACCTCCGAGAACCAAGGTGGGTTGTACCATCTCTTGAAGCCTCC CTCCTTGCTGGAGTAGAGATGACCAGGTGGAAAGATCTCAAAGTGCTCACAATCATCATTCAGGCCCTTCATCTCTGATGATATCCACACCGACCC
	Intron4	83 nt	CTGAAAGAAGACTACACAGTTAGACCATGGTGGGATCTTAAAATTGTTTTTTTTTTTAATTTCAGGCAATGGTCTCGTCTGAC
	Exon5	160 nt	CAAGTCCGACACAAAAAGAGTGAAGCTTAGTCCCCCAGCGCTTTGCAGCCTTTGTCCCTGCCAGGTGACGAACTGTAACCGCTGCAACCAATGATG AGTCAAGGCCACCAGAGAGTAGAACACCGAATGGAACGTCTGTCATAAGCCTCTTGGTGACAGC
	Intron5	80 nt	GCGTAATAGTAATGTGGTGCAATTTGTTGGAAATCTGCTAAAGGTTACAGTCATTGATGATCTTTTTCAGTTCCATACCT
	Exon6	82 nt	TGAACAGTGAAGGTGAACTCATGGTGCATGGTGCCCAGGTAATTGGCTACCTCCTTTGCAGCCTTCAGATCAGGTGACCCCT
	Intron6	81 nt	TGCAATGCTTTGTGCTATTAGTACAACAACTAGTCTGGTATGATCGACAGATGAAGCATGCAGCTTCTCATGCTTGCTACC
	Exon7	221 nt	TTTGACATGTCTCACGGTGGAGCTCCTCTTTGTTGGGTGCCTTGTGGAAGTAGAGGTACCCTCCAAAAATCTCATCGGAACCCTCACCAGAGATGAC CATCTTGACCCCAAGTGACTTGATCTTTCGTGACATCAGGAACATTGGTGTGCTTGCCCTGATTGTTGTCACATCATATGTTTCGGTGTGATAAATCA CATCCTCAATTGCATCAATGCCATCC
	Intron7	68 nt	ACAGTGTAATCATTATGTCAGGGTGTCTGAATCCGCCATTTTTCTGAACATTTCTATCTTATTCACCT
	Exon8	136 nt	ATCTTCCACTCAGGATCAATGCTCATTGCCTCATTGATAAACTCCTTGTCCAAGAATGGCACACGTGCTTCGAGGCCCCATGCAGATGTTGCCTTGT TGGCCCTCAAGCAATCGTACTGATGCAGAGCTTTGATCT
	Intron8	115 nt	TGTAACATCAGATATAGTAATTGTCTAAAAGTAGAAACTGGGAAGACATTTTACAACAATATGGTATGTTCTTTCTCAAGTTTCTAGATTCGTAAGGTT TGAGCTTCAGCATACC
	Exon9	80 nt	TCGGCAGGAATGGTTGCTCCTCGTCATCAAATGCTTTCCTCAGAACCCACTTCTCAATTCTTCCAAGATCAGGCCGGATC
	Intron9	86 nt	GCAATTGCCACACAATAGAAACTGTTAATTCCACTTCTCTATTAACATATTGATGTAGCACAAATTTGAATTAAAAACTGTTACCT
	Exon10	73 nt	GCCTTTAGGCCATCAATCCAGCTGTAGCCAACACCATCACTGAACTGCTCTTTCTGCCTGTACAGAATGTGCT
	Intron10	47 nt	TGTTGACCATGAGAGGCAGCAATGTTTTTACATTTGATTCTGTGTGA
	Exon11	120 nt	GGGAAGAACCTCTCAAATATCATCCTGTAACAGTAGGCCTCTTTTGTAGTCGGGGTGTTGTGTGGGTAAATGAACTTCGCATTTGACATCATCTTATC GGTCACATTTGATTCTGTGTGG
	Intron11	95 nt nt	TACAAGAGCAACAGATATGCTTGCATCAACATAGTTATTCCATGGAAAAGTGAGTTTTCTGTTTCATGTTCTTGCTGTTTTATTTGCTCACCTGG
	Exon12	235 nt	ACTCTCAATTGCGACACCAGGTGCCGCAACCTTGATCATCCTCGGCTTCTTGCTGGTTCCTGCCATGATGGTTGCTGGGAGATGCTCCTGCTCATA GGCCGAGAGATGGACTCCAAGTGCTGCTCTCCCTGAGGGATCCAGGTTCCCCGACCACCGAGCATCCCACTCTACTGCCTTCGCCGTGCTGCATG CGACGCTTGGCCCGCCTGGCACTGTCAGGATTGCCGAGTTCTGG
	3' downstream sequence	148 nt	CAGAAATCATCCGGTCTCTGATTTCATAAGAACTATAGAAACATTAATGCACAATCTTCACTCAACCTTAGGTCTGCATCACTCTAATGGCAAGACTA GGTACATCTTATTTCTTATCAGAAACGGCAAGCAGGACAGGACACCATCA
HvASN3	5' upstream sequence		GAGCCGCCGTTCCGTTCCGCCCGTACCTTACCCCTCCCCCCCACCACCACCCGCGCCCGTCCCTCCTCGTCGGGGCGTCGCCGCCTCCGCCTCC GCCTCCGCCCCGCTCGTCCGCGGCGTCTGGTCGGTCCAGCGACCGAGGCCTGAGGTCCCGCCGGCCGCCACC
	Exon1 (no match in genome seq)	79 nt	ATGTGCGGCATCCTCGCCGTCCTCGGCGTCGGCGACGTCTCCCTCGCCAAGCGCTCGCGCATCATCGAGCTCTCCCGCC
	Exon1	142 nt	GATTACGGCACAGAGGCCCTGATTGGAGTGGTATACACAGCTTTGAGGACTGCTATCTTGCACACCAGCGGTTGGCTATTGTTGATCCCACATCTG GGGACCAGCCATTGTACAATGAGGACAAAACAGTTATTGTGACGGT

	Intron1	249	CAGTATCTGGAGTGAGAATGACACTTCACTGTTTCCATTTATCTTATTTCTGCTTTCATGATTCATTTCCACGTACAACACATGATTATGTCTCACCATT CTGCTTTTAGTGACTAGCATTTGCTAGTATAATTTTGTGATGGGATTTTTGAAATGTTGTGTATCGAGCTCCGCTCAATACATCTTTTGAGACACAACC TACCCACCATATTTTTGTAACTAAACTAATTATGTTTTACATTTCCAGGT
	Exon2	137 nt	GAATGGGGAGATCTATAATCATGAAGAACTGAAAGCTAAGCTGAAATCACATAAATTCCAAACTGGTAGTGATTGTGAAGTTATTGCTCACCTAGTAA GTTTGTATTCTTATTTCTATGTTCAGCTTCTCTTAGTGC
	Intron2	121 nt	TCTATTGTCTAACTTGGCTTCTGCCAATACTTTCAAATGTCTTCTCCTAAGCATCATCCTCCAGTACATATATTTTATATGTTAACATCTGTACTTCCAA ATTCTATTGTTTTCACAGTAC
	Exon3	134 nt	GAGGAATATGGGGAAGAATTTGTGGATATGTTGGATGGCATGTTCTCATTTGTGCTTCTTGACACACGTGATAAAAGCTTCATAGCTGCCCGTGACG CTATTGGCATCTGTCCTTTATACATGGGCTGGGGCCT
	Intron3	927 nt	GACGGTATGCATGGAATCTGTTCTTGTAGCTACTTGTCTGTTTGATCAAAATCACAACCATGAAGTTATAGCTTTTTTCCTCTCAAATTTATCTTGGTC TGGACTTTGTGTATGGTTTGCTTGGTTATTCAACTTTTTCAACGGTCAGTCAATGTATCATGGGGAGGTGCAAAGCAGGCTGCGTTTAGGTTCATTTA AATTGAAGTTAAGATTAGAAGTAGATATATCATTGCTTGCCTACTTCATTAGAATAGAACTGGATAAGGCCAATTCATTTGCAAAAATAACAATAAAAG ATAATAACCCTGGATCTATCGTCGGCTCACATCCCACAAAATCGGAGTGATATCTCTCACCATTTGCAAAGAATATAGAGGTGTTACTCCCTCTGTCT TGATTTATAAGGCGTATTGTGATTGTAAAAGTTTAATCTTTGACCATATTTTTTTATAATATTTGCTATGAGTTAAAAAATCGCAATCAAGAGAAAGAGC TTTTGTATTTGAATCTAAAGGTATAAATTCTGTGTCACATAGCTCACGTATCATGAGATTAAATTTTGGGTCAGATCTTTAGACAATCAAAATATGCCTT ATATACCTGCACGAAGGAAGTATCTAGGTTGTGATGACGCCCATGATATATGTGCAACGGGAATGTCTGATGGGAAAGATGTGGATATAGACATAATAT TTGCCAAGCTGACTGTTAAATTTGCAATACGGAGTTAGCTATGCAAAGATTCTGAGATGTTCCGTGAGCTGTTGAAAACTATGGTTGGCTGTCTGCAT TTGCAAGTGCACAGTTCTGGAACATTAGACACTGTAGTGTTTGCATGTTTCACAACTTGTTACAGTTATATGGATTTAAGTAGCTGCTACAAATCTACT ATGCATTAATCTGTACATTCATTGTTATTCCAGGATCCG
	Exon4	92 nt	TTTGGTTCTCTTCGGAGATGAAGGCGTTGAGTGATGATTGCGAGCGCTTCATATCGTTCCCCCCTGGACACTTGTACTCAAGCAAAACAGGT
	Intron4	163 nt	TCAAATGTCTTGCTGTAACATATTGACGATCTCATCAGGCATTATACTAGAAATGCAGAGTTGCAAAGTCTGAAGGCAAAAATAGTATAAGTTACCAT GTATGTTGCAAATATCCGTTTGTCTTGCCTACTAATCTGCTTTCTAACATTTATCCTAGGTGGCT
	Exon5	91 nt	TAAGGAGGTGGTACAACCCTCCATGGTTTTCAGAAAGCATTCCCTCAGCCCCCTATGATCCTCTTCTCATCCGAGAGAGTTTTGAGAAGGC
	Intron5	404 nt	ACGCCTTTTCTTATGCTCTGTTACATTTCATACCTTTTGATGCATAAATTGTATGTTTATAATTATTTAATGATAATCTCTTTTTTATTTTGTTTCATGTTG ATATGATGTATACACGCCTCTGATTAAGTGATGCTTGTTTGGAATACCCTTGTTGATAATTCATGAGTCGTAATAGACTAATAGGTTATTGTAGCTCCC TGCAATCACATTTATGTCTTAGTGCGATGATTTCTATATTAATATCTTAGATATATGGCATTTTATTCGGAATCATGCTAATTGGTTATTAAGTATGTAC GGAGTATAAATAAATTATTGTGTCTGACGCATATTTTGTAAGCTAAGTTTCTTTACGTATGTCATCTACTATATTTCTTAGATGAATTGTAAAATTCGCA GGC
	Exon6	161 nt	TGTTCTCAAGAGGCTAATGACTGATGTGCCATTTGGTGTTCTCTTGTCTGGTGGGCTTGACTCTTCTTTGGTGGCTTCTGTTGTTTCACGCCACTTGG CAGAAACAAAAGTTGCCAGGCAGTGGGGAAACAAACTGCACACCTTTTGCATTGGTTTGAAGG
	Intron6	176 nt	TACATTTCTTAATGTTGTTTACTGGTGTATCCCCATTGCTGGGAATCTTTCAAATTTAAGTTGTTTTCTTGCTCTTATGAGTGTTTTTTACAATAAAAAA GAAGGTTTTTCAGTGGAGTAACATAAGCAGAGGATAAAATATGATAGAAGTTCTAACACATTCCAATTTTTATAGG
	Exon7	81 nt	GTTCTCCTGATCTTAAAGCTGCTAAGGAAGTTGCTGACTACCTTGGCACAGTCCATCATGAATTACACTTCACAGTGCAGG
	Intron7	78 nt	TTCGTTATTTTTATTTGTCCTTCGCATAGAGGAAGAGACATTTTGAAGTTATTAAATCATCTGAAAAAAAATTGCAGG
	Exon8	221 nt	AGGGCATTGATGCTTTGGAAGAAGTTATTTATCACATTGAGACGTATGATGTAACGACCATTAGAGCAAGTACCCCAATGTTTCTAATGTCTCGGAAA ATCAAATCGTTGGGTGTGAAGATGGTTCTTTCGGGAGAAGGTTCCGATGAAATATTTGGTGGTTATCTTTATTTTCACAAGGCACCAAACAAAAAGGA ATTCCATGAGGAAACATGTCGGAAG
	Intron8	98 nt	GTAATTAATGATAACATTGCTCCTTCTGGTTTATATCTGCTAAGTTGTTTAGATGGTCAGCTGATTAATTTATTTGAGTTCTCTTGTCTGGCGTTTAG
	Exon9	135 nt	ATAAAGGCTCTCCATTTATATGATTGTTTGAGAGCAAACAAAGCAACTTCTGCCTGGGGTCTCGAGGCTCGTGTTCCATTCCTCGACAAAAACTTCAT CAATGTAGCAATGGACCTGGATCCGGAATGTAAGATG
	Intron9	108 nt	GTATGTAATTTCTTGCTATAATACACTAATCTCACTCTAGCTCTATCCATGTATTACAATTTACAACTAGCATTCTCATCTTATATTTGTCATCTTGAAAA AAATTAG
	Exon10	81 nt	ATAAGACGTGATCTTGGCCGGATCGAGAAATGGGTTCTGCGTAATGCATTTGATGATGATGAGAAGCCCTATTTACCCAAG
	Intron10	97 nt	GTTGGAGAAGTTGATCTTTTTATGGTGTTATATTTGCTCTGTTACTTTCACAAGCTTGCGTCTATGCTCATAAGGAAGATTTTTTTTCTGTGAACAG
	Exon11	89 nt	CACATTCTTTACAGGCAAAAAGAACAGTTCAGCGATGGTGTTGGGTACAGTTGGATTGATGGATTGAAGGACCATGCTAATGCACATGT
	Intron11	122 nt	ATGCCATCTTTTCTTTGTCAAACCATTCATAACTTGACAATTGTTTACTTAGTCGACTTGCGATGGTTTCATATTACTTTACCCCCATTAGAATTAACGT TTGCTCCCATTCATGTTCAGGT
	Exon12	90 nt	GTCAGATTCCATGATGACAAACGCCAGCTTTGTTTACCCTGAAAACACACCCACAACAAAAGAAGCCTACTATTATAGGACAGTATTTGA
	Intron12	127 nt	AAAGTTTTATCCCAAGGTCCATAAGCTACAACCAGCATTTACTTTTATCATGATATTCCAAGCTATTTCATTTGCGTGGTAAAAGAATTAATGCCTGCT CTCCACTTAACTAACAATTCAATTGTGC
	Exon13	251 nt	AGAATGCTGCTAGGCTGACGGTGCCAGGAGGTCCCAGCGTTGCATGCAGCACCGCGAAAGCTGTTGAATGGGACGCCGCCTGGTCCAAGCTCCT CGACCCGTCTGGCCGTGCTGCTCTCGGTGTGCATGACGCAGCATACGAAGAGGAAAAGGCTCCCGCATCGGTCGATCCCATCTTGGAGAATGCCT TCCGTTCACCAGCCCATGGAGAGAGCACCCTAGTCAAAACCGTTGTTCCAACAGCTGCTGTT
	3' downstream sequence		TAACCTTCCACCCCATGGTTTCATATAGAATGCTCGAGAAAATGTTGTCACTTAGTTTAATTCTAGCTTCATTGCAGCTTGTCTGTAGCTTCAATCATT CAGTGTAGAAATTGCTTTCCTCTATTTTCCTTGACGCTTGCTGTTATGTTTTGCTTTCGCATGTATGTACTAAGTTTGTTTATGTGGTGAGCATTGCAT TTGTAAATATTTCACCATTGTTGTGCTATCCTTGAGTTGCTCAACGGTTGGTTTTCAAACTGCAAAGTTCCATTAATAACTTCCAATGTTGGTTTCTAG ATTAC
HvASN4	5' upstream sequence		GCGCCGCCGTAGAACGCCGTACCTCCACCACCACCCGCGTCGCCGCCGTCGCCGTCGTCGTCGCCCGTCCGTCGGGGCATCGCCGCCGCCGAC GTTGCCCGTTCGTCCGCGGCGTCTGGCCACCGAGGCTTGAGGTCCCGCCGGCCGCAACC
	Exon1 (no match in genome seq)	78 nt	ATGTGCGGCATCCTCGCCGTCCTCGGCGTCGGCGACGTCTCCCTCGCCAAGCGCTCGCGCATCATCGAGCTCCCCGCC
	Exon1	142	GATTACGGCACAGAGGCCCTGATTGGAGCGGTATACACAGCTTTGAGGATTGCTACCTTGCGCACCAGAGGTTGGCTATTGTTGATCCCACATCTG GAGACCAGCCATTGTACAATGAGGACAAAACAGTTGTTGTGACGGT
	Intron1	289 nt	CTGTATCTGGAGTGAGAATAAGATTTCACCGTTTTCATCCATCTCATTGCTTTCCATGATTCATTTCAACGTGTAACACATGACTATGTCTCACTATTC TGCTTTTGGCAACTAGAATTTCTTTGTGGATAATTTTGTGATGGGATTTTATAAATGTTGTCTTCGATCTCTGCTCATTGCATCTCTGGAGACACAACC TTTAATCCACTATTTCTGTACCAATTGAGAAAATATGTTTTGTTCTTTTATTTTATTTTAACCACATCTTGTCTGTTTGACTTTTCCAGGT
	Exon2	94 nt	GAATGGTGAGATCTATAATCATGAAGAACTGAAAGCTAAGCTGAAATCTCATCAGTTCCAAACTGGTAGTGATTGTGAAGTTATTGCTCACCTA
	Intron2	152 nt	GTAAGTTTGTACTCTTATTTCTCTAATCATCGTCCTCGTGATTGTGTAGCTTCGCTTCTGCCAACACTTTTTAGGGTCTTCACCCAAGCATCGTCCTTG TGCATATATTTTATTTGTTAACATTTGTGTTTCAAACTATATTGTGTTCACAG
	Exon3	141 nt	TATGAGGAATATGGGGAAGAATTCGTGGATATGTTGGATGGCATGTTCTCTTTTGTGCTTCTTGACACACGTGATAAAACCTTCATCGCTGCACGCG ATGCTATTGGCATCTGTCCTTTATACATGGGCTGGGGTCTTGAT
	Intron3	987 nt	GGTATGCACAGATTCCATTCTTATAGCTACTTTGTCCCTTCGATCAAAATCAGGAATGTGAAGTTATTATCTTTTATCTCTAAATTTATCTTGGTCTGTA CTTTTGTATGGTTTCCTTGGTTATGCAACTGTTTTCAGTGGTCAATACATATAACACGACAAGGAGAAAAGCAGGTTGCATGTAGGCCTATTTAAATT GAGGTTGAGATTAGAAGTAGATATATCACTGCTTGCCTATTTCCTTAGAATAGAATTGGACAAGGCCAATTAATCTGGAAAAATAACAGTAAAAGATG ATAACCCTAGAGTATAGAGGTGCTACTCCCTCTATCTGGATCCCTCTATCTGGATATTTAAGACGTATTATAATTGTCGAAGTTCAATCTTTGACCATA TTTTTCCATAATATTTGTTACTGGTTACAGAATCACGATCATAGGAAGCTTTTGAATTCGACTCAAACAGTAACAATTTTGTGTCGCATAACTCACATAT CGTAGGAGTAAAATCTTTAGCCAATCCAGACGAAGGTTGTGATGCCTATGATAGTGTGCAATTTGAATGTCTGATGTGAAAGATGTGGATAGACACA ATATTTCCCAAGCTGACTGTTAAATTCGTTATACGGAGTTAGCTATGCCGAAGTTTCTGAGTTGTTCTGTGAATTGTCGAAACATATAGTTGGCTATTT GTATTTGCAAGTACACCCTTATGGAACAAGTAGGTACTGTAGTGTTTGTATCTGTTACAACTTGGCACAACTCTGCATTTGTGTAGTTGCTACTACTC CCTCCGTTCCTAAANNTAAGTATTTTAAGAGATTTTACTAGGAGTCTACATACGGAGCAAANNNNNNNNNNNNNNNNNNNNNNNNNNNNTGTCTATATAC ATCTGTATGTACTCTACTAATGAAATCTCTAGAAAGACTCATATTTAGGAACAGAGGGAGTAGTGTACTATGCATTAATTCGTATGTTCACTTTTATTC CA
	Exon4	99 nt	GGGTCAGTATGGTTTTCTTCAGAGATGAAGGTATTGAGTGATGATTGCGAGCGCTTCATATCGTTCCCCCCTGGACACTTGTACTCAAGCAAAACAG GT
	Intron4	165 nt	TCAAATGTCTTACTGAGTTTGTGACAAATTGACGATCTTATCAGACATTATACCAGAAATGTAGATTTGCAAACTCTGAAGGCAAAAATAGTATAAGCT ACTATTAGTTGTTTCAGATATCAAATTGTCTTGCCTGGTAATTTGTTTCTAACATTTATGCTAGGT
	Exon5	94 nt	GGCCTAAGGAGGTGGTACAACCCCCCATGGTTTTCAGAAAGCATTCCCTCAACCCCTTACGATCCTCTCCTCATCCGAGAGAGTTTTGAGAAGG
	Intron5	401 nt	TCACACCTTTCCTTATGCTCTCTGTCAAATTTTTGTACCTTTTGATGCATAAAGTATACATTTATAGTTATTTCATGTTAATCTCTTCTTGATTTGCTTCA TGTTGATATGATGTATTGATGCCTCTGAATAGGCGATGCTTGTATGGAATACCCTGGTTGATAATTCATGAGTACTAATAGGTTATTGCAGCTGCCTG CAATCACATTTATGTCTTAGTGCGACGATCCCTATATTGAGATCTTAGATAGATGGCATGTTATTCAAAACCATGCTAATTGGTTATTATGTATGTGAA GCGTATAAATAAGCTATTGTGTCTGACGGTATATTTCATAAGCTAAGTTTCTTTACGTATATCATCTACTACATTTTCTTAGATGAATTGCAAATTTTGC AGG
	Exon6	161 nt	CTGTTATTAAGAGGCTAATGACTGATGTGCCATTTGGCGTTCTCTTGTCTGGTGGACTTGACTCTTCCTTGGTGGCTTCTGTTGTTTCACGGCACTTG GCAGAAACAAAAGTTGCCAGGCAGTGGGGAAACAAACTGCACACCTTTTGCATCGGTTTGAAG
	Intron6	160 nt	GTACACCTCATTGCTGAGACTCACTTTAGGTCATCTTTCAAAATTTAAGTTGTTTTCTTGCTCTTATGAGTATCTTTTATAAGAAAAGGAGGGATGTTTA GTTGAGTGATACAAGCAGAGGATACAGTAGGACAAACTTAACAAGTTCCATTTTTTGTAG
	Exon7	82 nt	GGTTCTCCTGATCTTAAAGCTGCTAAGGAAGTTGCTGACTACCTTGGCACTGTCCATCATGAATTACACTTCACAGTGCAGG
	Intron7	75 nt	TTCGTTATTTTTTTCATCCTTTACATAGAGGAAGGGTCATTTTGTAGTTATTAATTCATCTGACGAAATCCCAGG
	Exon8	221 nt	AGGGTATTGATGCATTGGAAGAAGTTATTTACCACATCGAGACATACGACGTAACGACCATTAGAGCAAGTACCCCAATGTTTCTAATGTCTCGGAA AATCAAATCATTGGGTGTGAAGATGGTTCTTTCAGGAGAAGGTTCCGATGAAATATTTGGTGGTTATCTTTACTTTCATAAGGCACCAAACAAGAAGG AACTCCATGAGGAGACGTGTAGGAAG
	Intron8	99 nt	GTAATTAAAGACATAATTGCTCTTTTGGTTTATCATAATCTATATGCACAACATGGTCAGCTGATGAACTTACTAGAGTTGTTTTGCCCTGACATTTAG
	Exon9	135 nt	ATAAAAGCTCTTCATTTATATGATTGTTTGAGAGCAAACAAAGCAACTTCTGCCTGGGGTCTTGAGGCTCGTGTTCCATTCCTCGACAAAAACTTCAT CAATGTAGCAATGGACCTGGATCCCGAATGTAAGATG
	Intron9	99 nt	GTATGTAATATCTTGCGATAATACACTAATTTCACTCTGGCTCTACTCATTTATTATAACCAGCATTATCATCTTATATTTATCATCTTGAAAAAATAG
	Exon10	81 nt	ATAAGACGTGATCTTGGCCGGATTGAGAAATGGGTTCTGCGTAATGCATTTGATGATAATGAGAAGCCCTATTTACCCAAG
	Intron10	86 nt	GTTGGAGAAGGCTCATCTTTTAATTGCTCTGTTACTTGTGCAAGCTTGCTTGTATCTCATAATGAATATTTATTTTCTGTGAACAG
	Exon11	89 nt	CACATTCTTTACAGGCAAAAGGAACAATTCAGCGATGGTGTTGGGTACAGTTGGATTGATGGACTGAAGGACCATGCTAGTGCACATGT
	Intron11	122 nt	ATACCATTTTTTCTTCGTTATACCATTCATAAGCTGACAGCTGTTTATTTATTTGACTTACAATGGTTTTGTATCACTTTACCCCAATCAGAATTCACAG TTTCTCCTACTCATGTTCAGGT

	Exon12	106 nt	GTCGGATTCCATGATGACGAACGCTAGCTTTGTTTACCCTGAGAACACACCCACAACTAAGGAGGCCTACTATTACAGGACTGTGTTCGAGAAATTC TATCCCAAG
	Intron12	94 nt	GTCCAGAAGCCACAACCAGCCTTTAATCTGCATCATGATATTCCAAGCTATTTCATCTGCATCGTGAATCTTAATTATCGTTCTAATTGTGCAG
	Exon13	243 nt	AATGCTGCTAGGCAAACGGTGCCAGGAGGTCCCAGCGTCGCATGCAGCACCGCTAAAGCTGTCGAATGGGATGCTGCCTGGTCCAAGCTCCTCGA CCCGTCTGGCCGCGCCGCTCTTGGCGTGCATGATGCGGCGTACGAAGAAAAGGCTCCTGCATCGGTCGATCCTGTCGTGGATGACGTCTCCCGTT CACCTGCACATGACGTCAAAAGACTGAAAACCGTCGTTTCAGCAGCTGCTGTA
	3’ downstream sequence		TAACCTTCCATTCCATGGTTCTACAAATGTCGTCGTTTAGTTTAATTCTAGCTTTCCTTGCAACCTGTCTGTAGTTCCTTCAATCACGCCAGTGCGGAA ATTGCTTTGCTCTACTTTCGTTCATGTTTTGCTTTCACATTTATGTACCAATTTTGTTTATGCAGTGAGCATTTTGGTTGTAAATATTTCACCGTGGTTG ATATCCTTGAGTTGCTCAGCATTTGGTTTGC
	5’ upstream sequence		GGCATCTCTCTCTCTCTCTCTCTCAACACGAGCATCATTCACTCCTCCTTCCTCTTCTTCAACCTCATCCGCCCCCCGAACCCCGCGTCGTCCGT CGCCGCGTCCACC
	Exon1	94 nt	GTGACCTGCTGCTCGGTAAAAGCCTTGAGGCCATCGATCCAGTTGTAGCCAACGCCGTCGCTGAACTGCTCCTTCTGCCTGTACAAGATATGCT
	Intron1	96 nt	GTGGACGGCAGTTGCAGACAGCATTAGTTCAGAACGCCCTGTGCATGCTACGCTGGATATCTGATCTGAAAACTCAAAGAAGGTGGTGTCTGTACC
	Exon2	81 nt	TTTGGCAGGTATGGCTCCTTCTCGTCGTCGAAAGCCTTCCTCAACACCCACTTCTCGATGCGGCCAAGATCGGCATCGTAC
	Intron2	114 nt	TGCGTCGCAGCAAACAACAAGAAAACGTCAGCAAATTCAGGGCCAAAACAAATCAGACATGCGCTTAGCACACCATTTCTCCTTTCACGGCAGAGAT GAGTGAGAGCTTGTACC
	Exon3	136 nt	AGTTTCCACTCGGGGTCCATGCTCATGGCGACGTCGATGAACTCCTTGTCGAGGAACTGCACGCGGACTTCCAGCCCCCAAGCGGACGTCGCCTT GTTGGCGCGCAGGCAGTCATACTGATGAAGCGCTTTCACCT
	Intron3	111 nt	GCGGGTTTCACCACATCAGTTTCGCGTCAAACCTGAGGGAATCCGACGAGTGTGTCTTGGTTGTTTGTGCAGTATTATTAATTAGGTATGATGTAGT TTCAGTTAGCACCT
	Exon4	211 nt	TGCGGCAGGTCTCCTTGTGGAACTCCTCCTTGTTGGGGGCGAAGTGGAAGTAGAGGTAGCCGCCAAGGAGCTCGTCGGAGCCTTCCCCTGACAG CACCATCTTAACACCGAGCGCCTTGATCTTGCGCGCCATCAGGAACATCGGCGTGCTCGCACGTATCGTCGTCACGTCGTACGTCTCGTTGTGGTA GATCACCTCCTCGATGGCGTC
	Intron4	217 nt	CATCCTAAACAGGACAAAATGACTCATCACTACCTCTGAATCTCTGATCCCCCGCTGTCTGTAGTGAGCAGTCTTTTCATTTATTATATGCCGAGATG TCTTAAGGCTTAAGGTTTCAATCTCAAATTTCTGGGGTTGTCAGTGTGAGCGTTCTGCAAATTTATTATGCCAAGCATCAAGATGTCCTGAGGCTTGA GGTTTTATTTGCTTTTCTTTA
	Exon5	84 nt	CCTGGACAGTGAAATGGAACTCGTGATGGATGGTTCCCAGATAGTCAGCAACCTCTCTCGCGGCCTTCAGGTCAGGTGACCCCT
	Intron5	94 nt	ACAATGTTCAGCAACATGTTAGAATCATCAGAATTCCATGGTTCTTGAATAAGAAGAAAGAGTAGGACAAAAACATGTGAAGAAAAACAAACCT
	Exon6	84 nt	CCTGGACAGTGAAATGGAACTCGTGATGGATGGTTCCCAGATAGTCAGCAACCTCTCTCGCGGCCTTCAGGTCAGGTGACCCCT
HvASN5	Intron6	217 nt	CATCCTAAACAGGACAAAATGACTCATCACTACCTCTGAATCTCTGATCCCCCGCTGTCTGTAGTGAGCAGTCTTTTCATTTATTATATGCCGAGATG TCTTAAGGCTTAAGGTTTCAATCTCAAATTTCTGGGGTTGTCAGTGTGAGCGTTCTGCAAATTTATTATGCCAAGCATCAAGATGTCCTGAGGCTTGA GGTTTTATTTGCTTTTCTTTA
	Exon7	211 nt	TGCGGCAGGTCTCCTTGTGGAACTCCTCCTTGTTGGGGGCGAAGTGGAAGTAGAGGTAGCCGCCAAGGAGCTCGTCGGAGCCTTCCCCTGACAG CACCATCTTAACACCGAGCGCCTTGATCTTGCGCGCCATCAGGAACATCGGCGTGCTCGCACGTATCGTCGTCACGTCGTACGTCTCGTTGTGGTA GATCACCTCCTCGATGGCGTC
	Intron7	111 nt	GCGGGTTTCACCACATCAGTTTCGCGTCAAACCTGAGGGAATCCGACGAGTGTGTCTTGGTTGTTTGTGCAGTATTATTAATTAGGTATGATGTAGT TTCAGTTAGCACCT
	Exon8	136 nt	AGTTTCCACTCGGGGTCCATGCTCATGGCGACGTCGATGAACTCCTTGTCGAGGAACTGCACGCGGACTTCCAGCCCCCAAGCGGACGTCGCCTT GTTGGCGCGCAGGCAGTCATACTGATGAAGCGCTTTCACCT
	Intron8	114 nt	TGCGTCGCAGCAAACAACAAGAAAACGTCAGCAAATTCAGGGCCAAAACAAATCAGACATGCGCTTAGCACACCATTTCTCCTTTCACGGCAGAGAT GAGTGAGAGCTTGTACC
	Exon9	81 nt	TTTGGCAGGTATGGCTCCTTCTCGTCGTCGAAAGCCTTCCTCAACACCCACTTCTCGATGCGGCCAAGATCGGCATCGTAC
	Intron9	114 nt	TGCGTCGCAGCAAACAACAAGAAAACGTCAGCAAATTCAGGGCCAAAACAAATCAGACATGCGCTTAGCACACCATTTCTCCTTTCACGGCAGAGAT GAGTGAGAGCTTGTACC
	Exon10	81 nt	TTTGGCAGGTATGGCTCCTTCTCGTCGTCGAAAGCCTTCCTCAACACCCACTTCTCGATGCGGCCAAGATCGGCATCGTAC
	Intron10	96 nt	GTGGACGGCAGTTGCAGACAGCATTAGTTCAGAACGCCCTGTGCATGCTACGCTGGATATCTGATCTGAAAACTCAAAGAAGGTGGTGTCTGTACC
	Exon11	94 nt	GTGACCTGCTGCTCGGTAAAAGCCTTGAGGCCATCGATCCAGTTGTAGCCAACGCCGTCGCTGAACTGCTCCTTCTGCCTGTACAAGATATGCT
	3’ downstream sequence		TGACGAGATGATGAAGAACGCCGCAGAGGAGTACCCGTACAACACGCCCATCAACAAGGAGGCCTACTACTACCGGATGATCTTCGAGAGGCTCT ACCCTCAGGAGTCGGCGAGGGAGACGGTGCCGTGGGGTCCGAGCATCGCGTGCAGCACGCCGGCGGCCATCGAGTGGGTGGCCCAGTGGAAG GCCTCCAACGACCCCTCCGGCCGGCTCATCGCCTCCCACAACGATGCCACCCCCGCTCATGCCCACGCCAACGGCAACGGTAACGGGGCGGTGG CCAACGGGAAAGCCAACGGGAACGGCACGGCGAACGGGAACGGGAACGCCAACGGGACTCTGGTCCCGTGCTAGCCGTCGCCGCTCGCGCTAG CTGGTTCGGCCGTGGTGGGTGCGTGTGCGTGTGCGCGTGTCCTCGGACTGATGAGCCATATGCCATTGGCGCCGCGGCCGGTGCTGTTGTTGTG TACGTGTTGTAGTACGTTTCTTCAGTGTTGTTGTGTGTGCGTGTGCGTGGGATGGAGCTCGCGGTCCGAGCATGTGGCGGGGGTGATGGATCGCC TGTAGAACAAGAACGTGAATCAAGTGAACTTGTGATGTATTGATCGATCCGTCTCATATTTCCTC

Supplemental Table 5. Percent Identity Matrix - Gluthamine Synthetase proteins

	HvGS1_3	*OsGS1_3*	***ZmGS1_2***	***TaGS1b***	***TaGS1c***	***TaGS1a***	*HvGS1_1*	*ZmGS1_4*	*ZmGS1_5*	*SoGS1a*	*OsGS1_1*	***AtGS1.4***	*PsGS1*	***AtGS1.1***	***AtGS1.2***	*HvGS1_2*	*LpGS1*	***ZmGS1_1***	*ZmGS1_3*	*SbGS1*	*OsGS1_2*	*VvGS1*	***AtGS1.3***	***AtGS1.5***	*CsGS1*	*DmGS1*	*HsGS*	***HvGS1_4***	***HvGS1_5***	*AtGS1.6*	*AnGS*like	*SfGS1*	*EcGS*	*SaGS*
HvGS1_3	100.00	87.85	84.49	81.41	81.13	81.69	82.54	83.62	83.62	83.38	83.10	79.44	80.79	81.97	83.38	79.66	80.51	81.69	82.82	83.10	80.85	82.25	81.64	78.98	61.08	53.85	54.08	16.43	22.67	15.76	13.66	17.99	16.03	16.92
OsGS1_3	87.85	100.00	85.56	82.02	81.74	82.30	82.87	82.54	82.54	83.71	83.99	80.34	80.85	82.02	82.02	80.79	80.51	81.79	82.35	83.47	80.67	82.58	81.07	78.47	59.60	53.98	54.14	17.18	23.38	15.97	13.35	17.39	16.62	17.22
ZmGS1_2	84.49	85.56	100.00	80.85	80.56	80.85	81.97	81.92	81.92	83.10	83.10	80.00	80.79	83.10	81.97	79.60	80.17	80.06	81.46	81.74	80.62	83.10	81.59	78.92	60.97	53.71	52.78	15.34	21.30	14.69	14.00	16.86	15.80	17.27
TaGS1b	81.41	82.02	80.85	100.00	99.72	99.72	98.31	90.99	90.99	91.01	91.57	84.83	84.23	84.83	85.11	80.79	81.64	82.58	82.58	84.27	82.30	85.39	87.01	80.97	63.07	53.56	54.55	15.36	21.97	14.70	14.20	16.22	16.32	17.55
TaGS1c	81.13	81.74	80.56	99.72	100.00	99.44	98.03	90.70	90.70	90.73	91.29	84.55	83.94	84.55	84.83	80.51	81.36	82.30	82.30	83.99	82.02	85.11	86.72	81.25	62.78	53.56	54.55	15.36	21.97	14.70	14.20	16.22	16.32	17.55
TaGS1a	81.69	82.30	80.85	99.72	99.44	100.00	98.03	91.27	91.27	91.29	91.29	84.55	84.51	84.55	85.39	81.07	81.92	82.87	82.87	84.55	82.58	85.67	87.29	81.25	63.07	53.85	54.83	15.36	21.97	14.70	14.20	16.22	16.32	17.55
HvGS1_1	82.54	82.87	81.97	98.31	98.03	98.03	100.00	91.55	91.55	92.13	92.70	85.67	85.07	85.67	85.39	80.79	81.92	83.15	83.15	84.83	82.87	86.80	86.72	80.97	62.50	54.13	55.11	15.07	21.97	14.41	13.91	16.52	16.32	17.55
ZmGS1_4	83.62	82.54	81.92	90.99	90.70	91.27	91.55	100.00	100.00	96.06	93.80	85.07	85.03	86.76	87.32	83.85	83.00	85.07	84.51	85.92	86.20	87.32	85.84	79.77	61.25	54.00	54.42	15.12	21.62	14.16	14.54	15.66	16.07	16.35
ZmGS1_5	83.62	82.54	81.92	90.99	90.70	91.27	91.55	100.00	100.00	96.06	93.80	85.07	85.03	86.76	87.32	83.85	83.00	85.07	84.51	85.92	86.20	87.32	85.84	79.77	61.25	54.00	54.42	15.12	21.62	14.16	14.54	15.66	16.07	16.35
SoGS1a	83.38	83.71	83.10	91.01	90.73	91.29	92.13	96.06	96.06	100.00	95.22	86.52	86.48	87.36	88.20	85.31	85.03	85.96	86.24	87.36	86.52	89.04	86.72	80.40	61.93	54.70	56.25	15.65	21.97	14.41	14.50	15.62	16.02	16.30
OsGS1_1	83.10	83.99	83.10	91.57	91.29	91.29	92.70	93.80	93.80	95.22	100.00	86.80	86.20	87.64	87.64	84.18	83.05	85.11	85.11	86.80	85.67	88.48	87.01	80.97	61.36	54.99	55.11	15.94	21.97	14.41	14.20	15.62	15.43	16.61
AtGS1.4	79.44	80.34	80.00	84.83	84.55	84.55	85.67	85.07	85.07	86.52	86.80	100.00	86.20	88.48	86.52	84.46	84.75	83.71	83.71	84.55	85.39	85.39	83.33	80.40	60.23	53.28	53.41	16.23	22.42	15.56	15.09	16.52	16.32	16.93
PsGS1	80.79	80.85	80.79	84.23	83.94	84.51	85.07	85.03	85.03	86.48	86.20	86.20	100.00	86.48	86.76	83.00	84.99	85.63	85.35	86.48	82.82	85.07	83.29	79.77	61.54	54.29	55.27	15.70	21.97	14.16	13.35	15.32	15.73	17.55
AtGS1.1	81.97	82.02	83.10	84.83	84.55	84.55	85.67	86.76	86.76	87.36	87.64	88.48	86.48	100.00	92.13	84.18	85.03	86.52	85.96	87.36	85.67	88.20	86.16	79.55	61.36	52.71	53.41	15.65	21.97	15.27	14.50	15.92	16.32	17.24
AtGS1.2	83.38	82.02	81.97	85.11	84.83	85.39	85.39	87.32	87.32	88.20	87.64	86.52	86.76	92.13	100.00	84.46	85.31	84.27	84.55	85.96	86.24	87.08	84.18	79.55	60.80	52.42	54.26	16.52	22.42	15.27	14.20	16.52	17.21	18.18
HvGS1_2	79.66	80.79	79.60	80.79	80.51	81.07	80.79	83.85	83.85	85.31	84.18	84.46	83.00	84.18	84.46	100.00	94.63	86.72	87.01	89.27	89.27	84.46	81.36	77.84	60.51	53.71	53.14	16.33	21.27	14.78	15.18	16.31	15.22	16.40
LpGS1	80.51	80.51	80.17	81.64	81.36	81.92	81.92	83.00	83.00	85.03	83.05	84.75	84.99	85.03	85.31	94.63	100.00	88.14	87.29	89.55	88.70	85.31	80.79	77.27	60.23	53.43	53.71	15.74	21.27	14.78	14.88	16.31	15.22	17.03
ZmGS1_1	81.69	81.79	80.06	82.58	82.30	82.87	83.15	85.07	85.07	85.96	85.11	83.71	85.63	86.52	84.27	86.72	88.14	100.00	95.80	96.64	89.92	85.11	81.92	77.84	61.65	52.71	52.97	16.47	20.98	14.94	13.86	15.27	15.68	16.88
ZmGS1_3	82.82	82.35	81.46	82.58	82.30	82.87	83.15	84.51	84.51	86.24	85.11	83.71	85.35	85.96	84.55	87.01	87.29	95.80	100.00	95.52	89.64	85.39	81.36	77.56	61.65	52.99	52.69	16.47	21.43	15.23	14.45	15.87	15.98	16.56
SbGS1	83.10	83.47	81.74	84.27	83.99	84.55	84.83	85.92	85.92	87.36	86.80	84.55	86.48	87.36	85.96	89.27	89.55	96.64	95.52	100.00	91.04	86.80	83.62	78.69	62.50	52.71	53.54	15.90	20.54	14.66	14.16	15.27	15.68	16.88
OsGS1_2	80.85	80.67	80.62	82.30	82.02	82.58	82.87	86.20	86.20	86.52	85.67	85.39	82.82	85.67	86.24	89.27	88.70	89.92	89.64	91.04	100.00	85.39	82.49	77.56	60.51	52.99	54.11	15.90	21.88	15.52	15.34	17.07	15.98	16.56
VvGS1	82.25	82.58	83.10	85.39	85.11	85.67	86.80	87.32	87.32	89.04	88.48	85.39	85.07	88.20	87.08	84.46	85.31	85.11	85.39	86.80	85.39	100.00	85.59	80.11	60.80	54.99	54.26	15.36	21.52	14.99	14.20	16.22	16.02	16.93
AtGS1.3	81.64	81.07	81.59	87.01	86.72	87.29	86.72	85.84	85.84	86.72	87.01	83.33	83.29	86.16	84.18	81.36	80.79	81.92	81.36	83.62	82.49	85.59	100.00	83.24	61.93	53.43	55.71	16.03	22.17	14.49	13.99	15.71	17.01	17.03
AtGS1.5	78.98	78.47	78.92	80.97	81.25	81.25	80.97	79.77	79.77	80.40	80.97	80.40	79.77	79.55	79.55	77.84	77.27	77.84	77.56	78.69	77.56	80.11	83.24	100.00	59.54	55.01	56.86	16.08	21.82	15.12	14.63	16.11	16.22	16.83
CsGS1	61.08	59.60	60.97	63.07	62.78	63.07	62.50	61.25	61.25	61.93	61.36	60.23	61.54	61.36	60.80	60.51	60.23	61.65	61.65	62.50	60.51	60.80	61.93	59.54	100.00	49.44	51.68	14.02	21.17	12.06	13.22	14.53	16.47	16.27
DmGS1	53.85	53.98	53.71	53.56	53.56	53.85	54.13	54.00	54.00	54.70	54.99	53.28	54.29	52.71	52.42	53.71	53.43	52.71	52.99	52.71	52.99	54.99	53.43	55.01	49.44	100.00	61.05	15.72	21.88	15.38	15.26	15.68	17.94	18.10
HsGS	54.08	54.14	52.78	54.55	54.55	54.83	55.11	54.42	54.42	56.25	55.11	53.41	55.27	53.41	54.26	53.14	53.71	52.97	52.69	53.54	54.11	54.26	55.71	56.86	51.68	61.05	100.00	14.96	21.37	13.22	14.65	17.29	17.48	17.31
HvGS1_4	16.43	17.18	15.34	15.36	15.36	15.36	15.07	15.12	15.12	15.65	15.94	16.23	15.70	15.65	16.52	16.33	15.74	16.47	16.47	15.90	15.90	15.36	16.03	16.08	14.02	15.72	14.96	100.00	79.05	61.55	32.63	21.51	21.68	21.38
HvGS1_5	22.67	23.38	21.30	21.97	21.97	21.97	21.97	21.62	21.62	21.97	21.97	22.42	21.97	21.97	22.42	21.27	21.27	20.98	21.43	20.54	21.88	21.52	22.17	21.82	21.17	21.88	21.37	79.05	100.00	57.46	34.48	27.54	27.87	28.81
AtGS1.6	15.76	15.97	14.69	14.70	14.70	14.70	14.41	14.16	14.16	14.41	14.41	15.56	14.16	15.27	15.27	14.78	14.78	14.94	15.23	14.66	15.52	14.99	14.49	15.12	12.06	15.38	13.22	61.55	57.46	100.00	31.86	20.09	20.26	23.80
*AnGS*like	13.66	13.35	14.00	14.20	14.20	14.20	13.91	14.54	14.54	14.50	14.20	15.09	13.35	14.50	14.20	15.18	14.88	13.86	14.45	14.16	15.34	14.20	13.99	14.63	13.22	15.26	14.65	32.63	34.48	31.86	100.00	18.37	15.99	19.10
SfGS1	17.99	17.39	16.86	16.22	16.22	16.22	16.52	15.66	15.66	15.62	15.62	16.52	15.32	15.92	16.52	16.31	16.31	15.27	15.87	15.27	17.07	16.22	15.71	16.11	14.53	15.68	17.29	21.51	27.54	20.09	18.37	100.00	54.09	35.55
EcGS	16.03	16.62	15.80	16.32	16.32	16.32	16.32	16.07	16.07	16.02	15.43	16.32	15.73	16.32	17.21	15.22	15.22	15.68	15.98	15.68	15.98	16.02	17.01	16.22	16.47	17.94	17.48	21.68	27.87	20.26	15.99	54.09	100.00	40.00
SaGS	16.92	17.22	17.27	17.55	17.55	17.55	17.55	16.35	16.35	16.30	16.61	16.93	17.55	17.24	18.18	16.40	17.03	16.88	16.56	16.88	16.56	16.93	17.03	16.83	16.27	18.10	17.31	21.38	28.81	23.80	19.10	35.55	40.00	100.00

Supplemental Table 6. Percent Identity Matrix - Asparagine Synthetase proteins

	OsASN4	*OsASN5*	*HvASN5*	***OsASN2***	*ZmASN3*	*ZmASN4*	*HvASN3*	*HvASN4*	*ZmASN1*	***OsASN3***	***AtASN2***	***AtASN3***	*HvASN1*	*ZmASN2*	*HvASN2*	*GmASN1*	*GmASN2*	***AtASN1***	*OsASN1*
OsASN4	100.00	82.62	11.21	11.32	11.17	10.99	11.59	11.42	12.31	12.69	12.31	12.34	12.50	12.27	11.94	12.13	11.94	12.50	8.04
OsASN5	82.62	100.00	10.31	10.75	10.61	10.42	11.57	11.57	11.95	12.33	11.55	11.57	11.76	11.91	11.57	11.95	11.95	12.52	8.38
HvASN5	11.21	10.31	100.00	86.11	83.79	82.32	69.56	70.34	70.04	68.99	71.25	71.88	72.36	73.05	70.68	71.10	70.89	70.68	12.50
OsASN2	11.32	10.75	86.11	100.00	86.22	84.86	66.78	67.52	67.97	67.80	70.02	69.15	70.74	71.23	70.40	69.43	70.00	68.61	12.95
ZmASN3	11.17	10.61	83.79	86.22	100.00	95.24	68.44	68.56	69.57	68.55	70.54	69.84	70.91	71.92	69.54	71.16	71.38	69.81	12.31
ZmASN4	10.99	10.42	82.32	84.86	95.24	100.00	67.41	68.21	68.21	67.69	69.67	68.98	70.74	71.58	69.36	70.81	70.52	68.95	12.31
HvASN3	11.59	11.57	69.56	66.78	68.44	67.41	100.00	95.93	88.12	91.17	82.35	83.22	77.07	75.17	75.95	77.30	78.47	75.65	12.87
HvASN4	11.42	11.57	70.34	67.52	68.56	68.21	95.93	100.00	88.78	90.82	82.15	83.36	77.03	75.13	75.74	76.91	77.74	75.78	12.89
ZmASN1	12.31	11.95	70.04	67.97	69.57	68.21	88.12	88.78	100.00	90.19	83.39	82.70	76.42	75.09	75.47	75.82	77.51	75.56	12.65
OsASN3	12.69	12.33	68.99	67.80	68.55	67.69	91.17	90.82	90.19	100.00	83.39	84.78	77.45	74.40	75.30	76.68	78.55	76.08	13.86
AtASN2	12.31	11.55	71.25	70.02	70.54	69.67	82.35	82.15	83.39	83.39	100.00	90.83	76.82	77.16	76.22	76.52	77.22	76.43	13.04
AtASN3	12.34	11.57	71.88	69.15	69.84	68.98	83.22	83.36	82.70	84.78	90.83	100.00	77.51	76.30	75.87	76.87	78.61	76.78	11.85
HvASN1	12.50	11.76	72.36	70.74	70.91	70.74	77.07	77.03	76.42	77.45	76.82	77.51	100.00	88.01	87.59	83.74	84.26	80.90	12.67
ZmASN2	12.27	11.91	73.05	71.23	71.92	71.58	75.17	75.13	75.09	74.40	77.16	76.30	88.01	100.00	83.48	78.93	79.69	77.05	12.41
HvASN2	11.94	11.57	70.68	70.40	69.54	69.36	75.95	75.74	75.47	75.30	76.22	75.87	87.59	83.48	100.00	81.28	81.83	79.35	13.04
GmASN1	12.13	11.95	71.10	69.43	71.16	70.81	77.30	76.91	75.82	76.68	76.52	76.87	83.74	78.93	81.28	100.00	90.14	83.59	12.52
GmASN2	11.94	11.95	70.89	70.00	71.38	70.52	78.47	77.74	77.51	78.55	77.22	78.61	84.26	79.69	81.83	90.14	100.00	83.99	12.20
AtASN1	12.50	12.52	70.68	68.61	69.81	68.95	75.65	75.78	75.56	76.08	76.43	76.78	80.90	77.05	79.35	83.59	83.99	100.00	12.31
OsASN1	8.04	8.38	12.50	12.95	12.31	12.31	12.87	12.89	12.65	13.86	13.04	11.85	12.67	12.41	13.04	12.52	12.20	12.31	100.00

Annex 1: Complement to methods.

Studying senescence in barley (*Hordeum vulgare* L.) primary leaves and flag leaves reveals specific metabolic shifts in sugar, amino acids and lipid metabolisms

Liliana Avila-Ospina, Gilles Clément, Anne Marmagne, Joël Talbotec, Karin Krupinska and Céline Masclaux-Daubresse

Plant growth

In nitrogen stress experiments, barley (Hordeum Vulgare L.) Cultivar Golden promise, a two-rowed spring barley cultivar was used due to its routine usage in biotechnological applications. Plants were grown in a growth chamber with controlled photoperiod, temperature and humidity (16h – 25°C/ 8h – 17°C). Seeds were sown on a seedbed and five days seedlings were transferred into polyvinyl chloride (PVC) tubes containing sand as a substrate. The experimental unit was a tube (6 ø – 45 cm units) containing 3 seedlings. Plants were watered eight times per day with a nutritive solution containing 5 mM NO3- (124 mM KH2PO4, MgSO4 ; 19.95 mM KNO3 ; 2.49 mM CaN2O6, 1mM NaCl ; 0.04 μM (NH4)6Mo7O24, 24.3 μM H3BO3, 11.8 μM MnSO4, 3.48 μM ZnSO4, 1 μM CuSO4 ; 0.001% Sequestrene 138 FE 100 Syngenta) named high nitrate treatment (HN) or a 0.5 mM NO3- (124 mM KH2PO4, K2SO4, MgSO4, KNO3 ; 0.625 mM CaN2O6, CaCl2 ; 0.04 μM (NH4)6Mo7O24, 24.3 μM H3BO3, 11.8 μM MnSO4, 3.48 μM ZnSO4, 1 μM CuSO4 ; 0.001% Sequestrene 138 FE 100 Syngenta) named low nitrate treatment (LN).

In field experiments, spring barley (Hordeum Vulgare L.) Cultivar Carina was used. The experiments were performed at *Hohenschulen research farm at 15.5 km west of Kiel* during the 2013 growing season, June being nearly wet and July warm and relatively dry. Spring barley was sown using a drill on April 2 of 2013. The barley was managed organically and organic manure equal to 70 kg N ha−1 was added. There were four replicate plots 150 m2 each. Plants were grown in a concentration of 300 plants/m2 with 12.5 cm of row distance. Crop was spreaded with 1.5 L/ha of Ariane C (Dow agrosciences) and 20 g/ha of Trimmer SX (FCS) [herbicides] on May 14 of 2013. Subsequently, it was added 0.3 L/ha of Moddus (Syngenta) and Ethephon (Bayer CropSc.) [growth regulators], 0.5 L/ha of Gladio (Syngenta) [fungicide], 5 kg/ha of MgSO4 and 10 L/ha of Mn-EDTA on June 5 of 2013. At last, 150 kg/ha Kierserit (KALI) [25% MgO, 20% S) and 30 kg/ha KAS (76% NH4NO3, 24% CaCO3] were added on June 7 of 2013.

Metabolite profiling using GC-MS

The ground frozen leaf samples (20 mg) were resuspended in 1 ml of frozen (-20°C) water:chloroform:methanol (1:1:2.5) and extracted for 10 min at 4 °C with shaking (1400 rpm) in an Eppendorf Thermomixer. Insoluble material was removed by centrifugation and 900 µl of the supernatant were mixed with 20 µl of 200 µg ml^{-1} ribitol in methanol. Water was

then added and 50 µl of polar phase were collected and dried in a Speed-Vac and stored at -80°C. For derivatization, 10 µl of 20 mg ml^{-1} methoxyamine in pyridine were added to the samples. The reactions were performed for 90 min at 28°C with continuous shaking in an Eppendorf thermomixer. A 90 µl aliquot of N-methyl-N-trimethylsilyl-trifluoroacetamide (MSTFA) was then added and the reaction continued for 30 min at 37°C. After cooling, 50 µl of the reaction were transferred to an Agilent vial for injection. For the analysis, 1 µl of the derivatized samples was injected in the Splitless mode onto an Agilent 7890A gas chromatograph (GC) coupled to an Agilent 5975C mass spectrometer (MS). The column used was an Rxi-5SilMS from Restek (30 m with 10 m Integra-Guard column). The liner (Restek # 20994) was changed before each series of analyses and 10 cm of the column were removed. Oven temperature ramp was 70°C for 7 min, then 10°C min^{-1} up to 325°C for 4 min. Helium flow was maintained at 1.5231 ml min^{-1}. GC temperatures were: injector, 250°C; transfer line, 290°C; source, 250°C; and quadripole, 150°C. Samples and blanks were randomized, amino acid standards were injected at the beginning and end of the analyses for monitoring of the derivatization stability. An alkane mix (C10, C12, C15, C19, C22, C28, C32, and C36) was injected in the middle of the analyses for external retention index calibration. Five scans per second were acquired. For data processing, Raw Agilent data files were converted into the NetCDF format and analysed with AMDIS http://chemdata.nist.gov/mass-spc/amdis/. A home retention indices/mass spectra library built from the NIST, Golm, and Fiehn databases and standard compounds were used for metabolite identification. Peak areas were then determined using the quanlynx software (Waters) after conversion of the NetCDF file into the masslynx format. Analyzed metabolites were annotated and their levels on a fresh weight basis were normalized with respect to the ribitol internal standard.

Metabolomic Data processing

For nitrate limiting conditions, samples from two independent plantings were used. From each one, three (culture 1) and four (culture 2) biological repeats were analyzed for each leaf rank. For field experiments, four biological repeats consisting of four plant plots harvested at 3 different stages of senescence were analyzed.

Statistical analysis was made with TMEV (http://www.tm4.org/mev.html); univariate analysis by permutation (1 way-anova and 2 way-anova) was firstly used to select the significant metabolites. Multivariate analysis (hierarchical clustering ; HCA and principal component analysis ; PCA) was then made in order to establish the metabolite clusters. Only metabolites showing repeatable and significant differences (based on T-test) according to leaf rank, nitrate treatment and senescence stage are reported.

A heat map was made showing major primary metabolic pathways. Results are shown as Log_2 ratio of metabolite concentrations normalized to the metabolite content of the youngest leaf.

Chlorophyll measurements adapted from Arnon (1949):

50 μl of crude leaf extract, obtained grinding fresh material in 50 mM Tris-HCl pH7.5 buffer (100 mg FW / 1 ml buffer) were homogenised in 950 μl of Acetone 80% and kept overnight at 4°C in the dark. Acetone extract was then centrifuged to remove cell debris and absorbance

was measured spectrometrically at 652 nm on the whole volume. Calculation is: [mg of chlorophyll / cuvette = 36xDAbsorbance].

Glutamine synthetase essay:

According to O'Neal and Joy (1973)

BUFFERS:	Stock solutions concentration (mM)
Extraction buffer Tris-HCl pH 7.6 $MgC1_2$ Na-EDTA	 250 10 10
Reaction buffer Tris-HCl pH 7.6	 50
AMIX (X5) pH 7.6 MgS04 Glutamate Hydroxylamine EDTA	 150 600 45 30
ATP (X5) pH 7.6	60
STOP buffer FeC13 (28% solution) TCA HCl	 370 200 1.79 M
Gamma-glutamylhydroxamate	20

AMIX and ATP are prepared in the 50mM Tris-HCl pH7.6 reaction buffer. Gamma-glutamylhydroxamate is dissolved in H20.

150 mg FW are grinded in 1 mL extraction buffer containing 2X protease inhibitor cocktail complete EDTA-free (Roche), 0.5% polyvinyl pyrrolidone (w/v) and 0.1% beta-mercaptoethanol (v/v) added just before extraction.
After homogenisation, extract was centrifuge 13000g for 10 min and supernatant used for protein quantification using Coomassie Protein assay reagent from BioRad, Hercule, California, USA, abd GS assays.

For GS activity measurement in 96-well plates, 50 μl of extract is added to 60 μl of reaction buffer, 20 μl of AMIX and 20 μl of ATP. No ATP is added in blank control; ATP is replaced by reaction buffer.

Standard is obtained with successive dilutions of gamma-glutamylhydroxamate (from 0 to 20 mM).

After 30 min incubation at 30°C and under shaking, 150 μl of STOP solution is added in each well. Plates are then centrifuged (4000g for 10 min) and 200 μl of each well transferred to clean plate. Absorbance is then measured at 540 nm. Activity is expressed as nmol gamma-glutamylhydroxamate formed per min and per mg protein or mg FW.

PAPER 2

The nineteen autophagy genes found in barley (*Hordeum vulgare* L.) are differentially regulated during leaf senescence, chronic nitrogen limitation and in response to dark treatment.

Liliana Avila-Ospina[1,2] and Céline Masclaux-Daubresse[1,2,*]

(1) INRA, UMR1318, Institut Jean-Pierre Bourgin, RD10, F-78000 Versailles, France
(2) AgroParisTech, Institut Jean-Pierre Bourgin, RD10, F-78000 Versailles, France

*Corresponding author:
Dr Céline Masclaux-Daubresse
Institut Jean-Pierre Bourgin (IJPB), UMR 1318, INRA 78026 Versailles Cedex, France
phone +33 (0)1 30 83 30 88
fax +33 (0)1 30 83 30 96
e-mail celine.masclaux@versailles.inra.fr

Financial supports:
This work was supported by the FP7 Marie Curie Actions – Networks for Initial Training Project FP7-MC-ITN N° 264394 acronym CropLife for L.A-O.

SUMMARY

- **Research Conducted**

In Arabidopsis, autophagy participates to nitrogen remobilisation and grain filling. Barley is a cereal of primary importance and a useful model for wheat. Autophagy genes have never been described in barley so far.

- **Methods**

HvATG sequences were identified in BAC, CDNA and EST libraries. *HvATG g*ene models were computed from alignments between genome and transcript sequences. Transcripts levels were quantified using real time RT-qPCR.

- **Key Results**

A total of 19 barley *HvATG* genes were found from alignments with the transcript and cDNA sequences identified in barley libraries. All the genomic sequences found, except *HvATG5*, completely match with the cDNA sequences. The functionality of the *HvATG5* transcript sequence was then verified through Arabidopsis *atg5* mutant complementation. All *HvATG* genes were induced by leaf senescence, nitrogen starvation and dark-treatment. Specific responses were however identified among members of gene families. Regulation of *HvATG5* by leaf ageing was mainly observed in flag leaves.

- **Main conclusion.**

The present report gives the first characterization of *ATG* genes in barley. Barley sequences will be useful for transcriptome studies and to investigate further the role of autophagy in barley and wheat for nitrogen remobilisation and grain yield and quality.

Keywords: Autophagy, *Hordeum vulgare* L., leaf senescence, nitrogen limitation, dark treatment

INTRODUCTION

Plants have a fundamental dependence for inorganic nitrogen. The million metric tons of nitrogenous fertilizers used worldwide annually represent the major cost in plant production. Furthermore, there is serious concern regarding the inorganic nitrogen loss occurring in the fields that pollutes soils and water. The possibility of lowering fertilizer input is considered for a long time and breeding plants with better nitrogen remobilisation efficiency is certainly one of the main issues for sustainable agriculture (Hirel *et al.*, 2007; Masclaux-Daubresse *et al.*, 2008; Masclaux-Daubresse *et al.*, 2010).

NRE is defined as the ability of plants to recycle and reuse all along its lifespan organic nitrogen at the whole plant level. Nitrogen recycling and remobilisation certainly occurs all along plant development and cycle, however it is especially needed during senescence to improve nitrogen use efficiency i.e. plant performance for yield and grain protein content. Numerous studies have indeed shown that a large part of the nitrogen contained in grain proteins is provided by the recycling and remobilisation of organic nitrogen from the vegetative organs like leaves, stems and even roots (Cliquet *et al.*, 1990; Coque *et al.*, 2008; Malagoli *et al.*, 2005; Kichey *et al.,* 2007). Due to the strong impact of nitrogen remobilisation on plant biomass, yield and grain quality, many studies aimed at improving this process engineering plants and breeding new varieties. Mechanisms involved in nitrogen recycling at cellular levels during leaf senescence were the main targets considered for plant engineering and a special focus was for enzymes involved in organic nitrogen management during leaf senescence (Chardon *et al.,* 2012).

It is well known for many years that the main organic nitrogen resources available in leaves and used during leaf senescence for remobilisation are located inside the chloroplast (Peoples & Dalling, 1988). Despite the numerous studies on this topic, the main question that remains to be elucidated is how chloroplast proteins are degraded. Lot of enzymes induced during leaf senescence are located within the central vacuole or in senescence associated vacuoles (Roberts *et al.,* 2012; Otegui *et al.,* 2005; Avila-Ospina *et al.,* 2014 for a review). Although thylakoid proteins are certainly degraded within the chloroplast by specific proteases (Roberts *et al.,* 2012), the recent advances suggest that stromal proteins would be expulsed out of the chloroplast in Rubisco Containing Bodies (RCB) dedicated to degradation in the central vacuole (Chiba *et al.,* 2003; Wittenbach *et al.,* 1982). Ishida *et al.,* (2008) then showed that RCB degradation in the vacuole is autophagy dependent, suggesting a

specific role of macro-autophagy (named autophagy further in the text) in N recycling and remobilisation during leaf senescence (Avila-Ospina *et al.,* 2014).

Autophagy is a vesicular process, present in all eukaryotic cells, that consists in the formation of small double membrane vacuoles that engulf portions of cytosol and organelles to be degraded after fusion with lysosomes or lytic vacuoles. The *AuTophaGy* (*ATG*) genes were first discovered in yeast. There is 30 *ScATG* genes in yeast and homologous have been described in animal and plants including Arabidopsis (Doelling *et al.,* 2002; Hanaoka *et al.,* 2002; Xiong *et al.,* 2005), rice (Xia *et al.,* 2011) and maize (Chung, T *et al.,* 2009). The central autophagy machinery that is necessary for autophagosome formation consists of 18 *ATG* genes involved in the regulation of autophagy, the nucleation of pre-autophagosomal structures, the recruitment of lipids to expand the membrane and form autophagosome and the enclosure of the membrane around the cargo to be degraded (see Mizushima & Komatsu, 2011 for a review). From the knowledge of yeast model, the molecular machinery and the roles of each ATG proteins in the autophagosome formation is now more understood and many recent paper review those molecular aspects in plant (Thompson & Vierstra, 2005; Yoshimoto, 2012; Li & Vierstra, 2012; Liu & Bassham, 2012).

The functional analysis of the role of the different autophagy genes in plant has only been investigated in Arabidopsis up to now. Several autophagy mutants (*atg*) have been isolated and characterized (Doelling *et al.,* 2002; Hanaoka *et al.,* 2002; Thompson *et al.,* 2005). Autophagy mutants are characterized by the absence of autophagosome formation in the cytosol and absence of autophagic bodies in their vacuole. Both can be verified using microscopy, the first by over-expressing *35S::GFP::ATG8* protein fusions in plants, the second by treating plants with drugs like concanamycin-A that through blocking autophagic body degradation in the vacuole facilitate their observation (Merkulova *et al.,* 2014). All the Arabidopsis *atg* mutants also show hypersensitivity to nitrogen deficiency and early leaf senescence even though symptoms' severity varies (Guiboileau *et al.,* 2012). We used several of the well-characterized mutants in order to investigate nitrogen remobilisation and management at the whole plant level in Arabidopsis. This study allowed us to show that nitrogen remobilisation to the seeds is impaired in *atg* mutants compared to wild type and that all sort of nitrogen compounds that cannot be degraded or mobilized accumulate in mutants' leaves with ageing (Guiboileau *et al.,* 2012; Guiboileau *et al.,* 2013; Masclaux-Daubresse *et al.,* 2014). Little is currently known about the role of autophagy in other plant species than Arabidopsis, and given our recent finding about the role of autophagy in nitrogen

remobilisation and grain filling, we aim at studying autophagy machinery in barley, which is a cereal of primary importance and a useful model system for the study of wheat due to its smaller and simpler genome (2n =2x=14) for which assembly and an integrated physical map are available (Mayer *et al.*, 2012).

This report present all the *HvATG* genes that can be identified in the barley genome published recently (Consortium, 2012). Analysis of EST and cDNA sequences allowed us to find the functional splice variants and to characterize *HvATG* gene structures and mRNA more accurately. Thanks to their sequences, the regulation of the 19 *HvATG* genes identified was investigated during natural and dark-induced leaf senescence. Response to nitrogen limitation was also monitored. All the results presented in this report are necessary to the further studies aiming at investigating autophagy process in barley including the manipulation of autophagy pathway through plant engineering and the plant breeding approaches using quantitative trait locus mapping or genome wide association approaches.

MATERIALS AND METHODS

Plant material and growth conditions

In nitrate limitation experiments, barley plants (*Hordeum Vulgare* L.) Cultivar Golden promise, a two-rowed spring barley cultivar, were grown in a growth chamber with controlled photoperiod, temperature and humidity (16h – 25°C/ 8h – 17°C). Seeds were sown on a seedbed and five days seedlings were transferred into polyvinyl chloride (PVC) tubes containing sand as a substrate. The experimental unit was a tube (6 ø – 45 cm units) containing 3 seedlings. Plants were watered eight times per day with a nutritive solution containing 5 mM NO_3^- (124 mM KH_2PO_4, 124 mM $MgSO_4$, 19.95 mM KNO_3, 2.49 mM CaN_2O_6, 1mM NaCl; 0.04 µM $(NH_4)_6Mo_7O_{24}$, 24.3 µM H_3BO_3, 11.8 µM $MnSO_4$, 3.48 µM $ZnSO_4$, 1 µM $CuSO_4$, 0.001% Sequestrene 138 FE 100 Syngenta) named high nitrate treatment (HN) or a 0.5 mM NO_3^- (124 mM KH_2PO_4, 124 mM K_2SO_4, 124 mM $MgSO_4$, 124 mM KNO_3, 0.625 mM CaN_2O_6, 0.625 mM $CaCl_2$, 0.04 µM $(NH_4)_6Mo_7O_{24}$, 24.3 µM H_3BO_3, 11.8 µM $MnSO_4$, 3.48 µM $ZnSO_4$, 1 µM $CuSO_4$, 0.001% Sequestrene 138 FE 100 Syngenta) named low nitrate treatment (LN). 20 days after sowing (DAS) the leaves were harvested individually, leaves L1 to L4 in HN and leaves L1 to L3 in LN. L1 representing the bottom and older leaf and L3 and L4 the upper and younger leaf under low or high nitrate conditions respectively. For plants grown under LN and HN, three (in the first culture) and four (in the second and third culture) independent groups containing 18 leaves of each leaf rank were

harvested between 10:00 h and 12:00 h and stored at -80°C for further experiments. A total of 3 plantings were performed and the following analyses were carried out on at least two plant cultures.

In dark stress experiments, plants were grown in the same growth chamber as describe above, with the same controlled photoperiod, temperature and humidity. Seeds were sown in sand and seedlings were grown in PVC tubes watered eight times per day with a nutritive solution containing 5 mM NO_3^- (described above). 14 DAS, the whole plants were covered from the light during 4 days in a period called (Dark Treatment). At the end of the dark stress, plants were harvested and leaf ranks collected as described above, this first harvest was called T1. The remaining plants were left growing in the light during 3 more days in a period called (Recovery treatment). After this recovery period, plants were harvested and leaf ranks collected, this second harvest was called T2. At each harvesting time, three independent groups containing 12 leaves of each leaf rank were harvested between 10:00 h and 12:00 h and stored at -80°C until further experiments. Leaves from plants growing in optimal light conditions throughout the experiment were also harvested at T1 and T2 and used as untreated controls.

In field experiments, spring barley (*Hordeum Vulgare* L.) Cultivar Carina was used. The experiments were performed at *Hohenschulen research farm at 15.5 km west of Kiel* during the 2013 growing season, June being nearly wet and July warm and relatively dry. Spring barley was sown using a drill on April 2 of 2013. The barley was managed organically and organic manure equal to 70 kg N ha^{-1} was added. There were four replicate plots 150 m^2 each. Plants were grown in a concentration of 300 plants/m2 with 12.5 cm of row distance. Crop was spreaded with 1.5 L/ha of Ariane C (Dow agrosciences, St Quentin en Yvelines, France) and 20 g/ha of Trimmer SX (FCS) [herbicides] on May 14 of 2013. Subsequently, it was added 0.3 L/ha of Moddus (Syngenta, Guyancourt, France) and Ethephon (Bayer CropSc., Puteaux, France) [growth regulators], 0.5 L/ha of Gladio (Syngenta, Guyancourt, France) [fungicide], 5 kg/ha of MgSO4 and 10 L/ha of Mn-EDTA on June 5 of 2013. At last, 150 kg/ha ESTA® Kierserit (KALI, Kassel, Germany) [25% MgO, 20% S) and 30 kg/ha KAS (76% NH_4NO_3, 24% $CaCO_3$] were added on June 7 of 2013. 30 flag leaves from the main shoots were harvested from each plot between 10:00 and 12:00 and immediately stored at -80°C for further experiments. 3 whole plants were taken from each plot and dark adapted for 30 to 45 min for further photosynthesis and CO_2 assimilation measurements on the flag leaf.

Samples were harvested at several time points representing different stages of leaf senescence and grain maturity, the first time point (T1) was 95 DAS, second time point (T2) was 99 DAS and time point 3 (T3) was 203 DAS. Senescence stage was monitored in flag leaves in the field by measuring chlorophyll contents (SPAD), photosystem II efficiency using a photosynthesis yield analyzer (Mini-PAM, H. Walz Effeltrich, Germany) and CO_2 assimilation using a portable gas exchange fluorescence system GFS-3000 (H. Walz Effeltrich, Germany). After harvesting, all plant material was immediately frozen using liquid nitrogen and ground to obtain a fine homogenous powder. This powder was stored at -80°C for further analysis.

A. thaliana wild type (Col-0), *atg5* mutant (SAIL_129B07) and complemented *atg5* p35S::HvATG5 mutant (this work) were grown on soil in both glass house and growth chamber at 60% relative humidity with a 16/8 light/dark cycle at 21/17 °C and light intensity 150 µmol $m^{-2}s^{-1}$. Plants were watered three times a week with either, a complete nutrient solution (10mM NO_3^-) containing 5mM KNO_3, 2.5mM $Ca(NO_3)_2$, 0.25mM $MgSO_4$, 0.25mM $KH2PO_4$, 0.42mM NaCl, 0.1mM FeNa–EDTA, 30 µM H_3BO_3, 5 µM $MnSO_4$, 1 µM $ZnSO_4$, 1 µM $CuSO_4$, and 0.1 µM $(NH_4)6Mo_7O_{24}$. Or a nitrate deficient solution (2 mM NO_3^-) containing 1.75mM KNO_3, 0.125mM $Ca(NO_3)_2$, 0.25mM $MgSO_4$, 0.25mM $KH2PO_4$, 0.42mM NaCl, 0.1mM FeNa–EDTA, 30 µM H_3BO_3, 5 µM $MnSO_4$, 1 µM $ZnSO_4$, 1 µM $CuSO_4$, and 0.1 µM $(NH_4)6Mo_7O_{24}$.

DNA and protein sequence analysis

Barley *ATG* genes were identified using homologous protein sequences from Arabidopsis and rice (*Oryza sativa*) as queries. Arabidopsis and rice *ATG* gene and protein sequences were obtained from The Arabidopsis Information Resource, TAIR (http://www.arabidopsis.org/) and GRAMENE (http://www.gramene.org/) databases (Supplemental table 1). Arabidopsis and rice protein sequences were then used to search by TBLASTN and TBLASTX (Altschul & Lipman, 1990) in different cDNA, EST, BAC clone libraries, protein and genomic assembly databases: GeneBank, http://www.ncbi.nlm.nih.gov/; European nucleotide Archive, ENA, http://www.ebi.ac.uk/ena/; UniProt, http://www.uniprot.org/; European Bioinformatic institute, EBI, http://www.ebi.ac.uk/ (last searched November 2013). The identified *HvATG* cDNA sequences were then used as BLASTN query sequences against full barley genome sequence found in EnsemblPlants (http://plants.ensembl.org/) database in order to obtain the gene models and to assign each cDNA to a genomic locus.

Sequence alignments between individual cDNA and genomic sequences were manually inspected for consensus coding regions, introns and exons. Sequence alignments between *Hv*ATG and other species ATG protein sequences were also manually inspected for conserved and essential for function amino acids. These protein sequences were also used to perform phylogenetic analysis. ATG protein sequences for other species different to Arabidopsis and rice were found through GeneBank database. Multiple protein sequence alignments and phyllogenetic trees were generated using ClustalW algorithm (Thompson *et al.,* 1994). The *HvATG* gene model figures were generated by Exon-Intron graphic maker (http://wormweb.org/exonintron). Splice variants predicted by EnsemblPlants database and the corresponding accession numbers are found in the Table 1.

RNA purification and RT-qPCR analysis

400 mg of frozen ground material was used for RNA isolation with TRIzol reagent (Ambion) according to manufacture specifications. RNA was suspended in nuclease free water, the purity and concentration were spectrophotometrically determined with a Nanodrop 1000 (Thermo Scientific) and stored at -80°C. cDNA synthesis was performed with 1µg of RNA using the first strand cDNA synthesis kit (Thermo Scientific) at 37°C for 50 min. cDNA was diluted 1:2 (v/v) in nuclease free water and stored at -20°C. qPCR mix was composed by 10 µL of MESA FAST qPCR master mix plus for SYBR assay (Eurogentec), 3.8 µL water, 1.2 µL of 10 mM specific forward and reverse primers and 5 µL diluted cDNA 1:30 (v/v) in nuclease free water. Reactions were carried out in triplicate in a 96-well plates in a Bio-Rad CFX connect thermocycler on the following cycle, 94°C for 5 min followed by 94°C for 5 s, 72°C for 20 s and a melt curve from 50°C to 95°C increasing by 0.5°C every 30 s. Fluorescence readings were taken during the elongation step (72°C). Ct values were calculated by the CFX connect software.

Genes and primers are listed in Supplemental Table 2. Several reference genes (including GADPH, Actin, SAMd, CHS90, α-Tubulin, β-Tubulin, EF1a, ADPrf1, CDC48 and Ubiquitin) were trialled and only GADPH was validated across all samples in nitrate limitation and dark stress assays and Actin was validated across all senescence stages in samples from field experiments in accordance with geNorm algorithm (Vandesompele *et al.,* 2002). Results are shown as Log_{10} fold changes of the transcript levels of samples compared to the youngest leaf.

***HvATG5* cloning and *Agrobacterium tumefaciens*-mediated transformation**

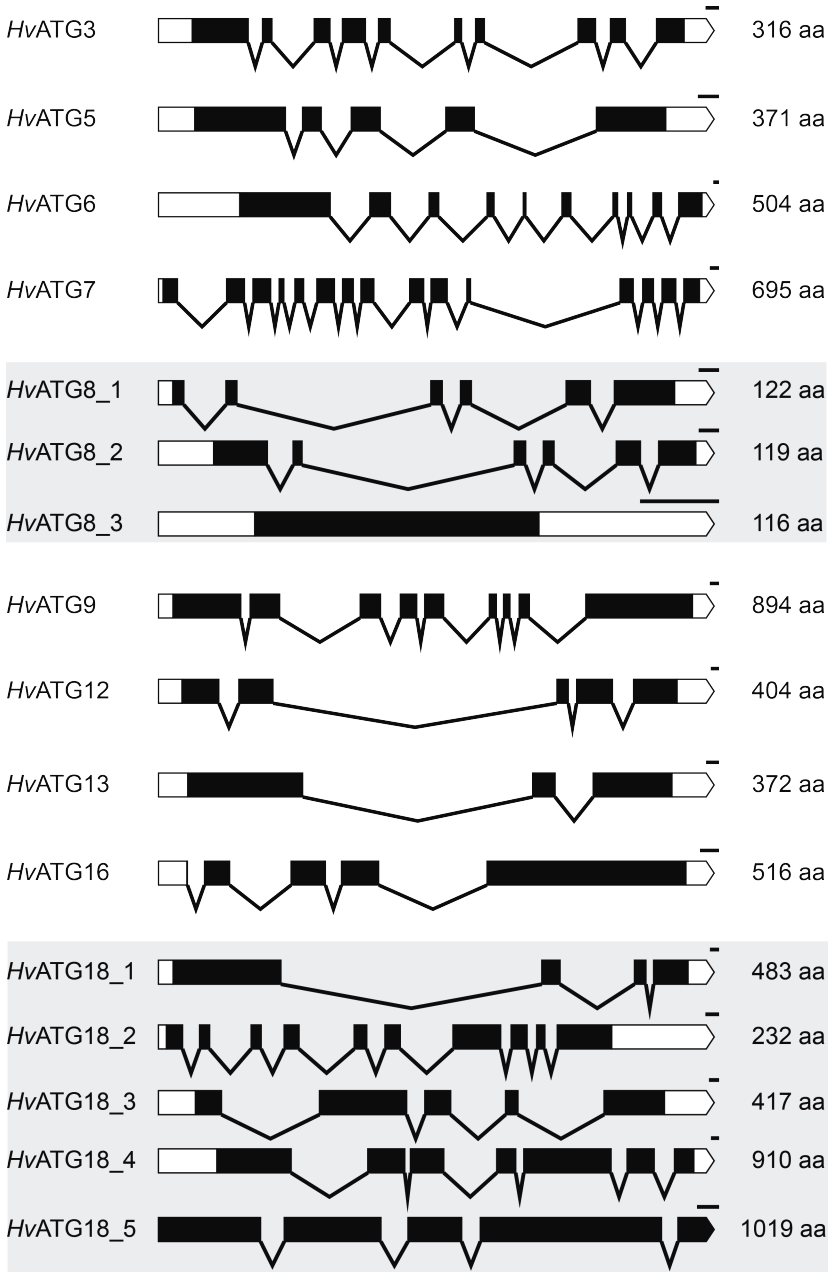

Figure 1. Diagram of barley *HvATG* genes. Gene structures were deduced from the sequences of cDNA, EST, BAC clone libraries and alignments with genomic sequences (see Methods) using genome assembly database Ensemblplants (http://plants.ensembl.org/index.html). White boxes (□) represent untranslated regions, black boxes (■) represent coding regions and solid lines (\) represent introns. The predicted amino acid (aa) lenght for each of the corresponding proteins is shown at right. HvATG gene families are highlighted in grey. Upper bars correspond to 0.1 Kbp.

HvATG5 coding DNA sequence (CDS) was amplified from the BAC clone NIASHv2006J04 (provided by the National Institute of Agrobiological Sciences, NIAS) using the primers attB1 *HvATG5* (5'-GGGGACAAGTTTGTACAAAAAAGCAGGCTTCGAAGGAGATAGAACCATGGCGGC GGCGGCGCCGT) and attB2 *HvATG5* (5'-GGGGACCACTTTGTACAAGAAAGCTGGGTTTCAAGCGCTGACGTATACAC). Then, the PCR product was recombined into pDONR207 (Invitrogen). The insert in pDONR-*HvATG5* was then transfered into the destination binary vector pMDC32 (Invitrogen) by LR recombination. The fragment generated by PCR and the cloned fragments were verified by sequencing in all vectors. Subsequently, these plasmid was transferred into the *A. tumefaciens* strain GV3101::PMP90 (C58C1) by electroporation and *atg5* (SAIL_129B07) *Arabidopsis thaliana* was transformed by floral dipping.

Chlorophyll content determination

Chlorophyll content was determined in seedlings leaves and flag leaf crude extracts according to (Arnon, 1949).

Concanamycin A Treatment

Primary roots of wild-type (Col-0), *atg5* mutant and complemented *atg5 p35S::HvATG5* plants vertically grown on MS medium for 1 week were cut and then incubated in MS-N liquid medium containing 1μM concanamycin A (C-9705;Sigma-Aldrich, St. Louis, MO) under gentle agitation at 23°C for 6 h in the dark. The roots were mounted in MS medium and observed by conventional transmission light microscopy (ZEISS Axioplan) (Merkulova *et al.,* 2014).

RESULTS

Identification of *ATG* genes in Barley

In order to find the barley *HvATG* homolog sequences, we used rice (*OsATG*), Arabidopsis (*AtATG*) and yeast (*ScATG*) equivalents as queries. Yeast equivalents are single genes for each function while in Arabidopsis and rice, some ATG functions are encoded by gene families. This is the case of *ATG1* (three genes in Arabidopsis and four in rice), *ATG3* (two genes in rice), *ATG4* (two genes in both Arabidopsis and rice), *ATG8* (nine genes in

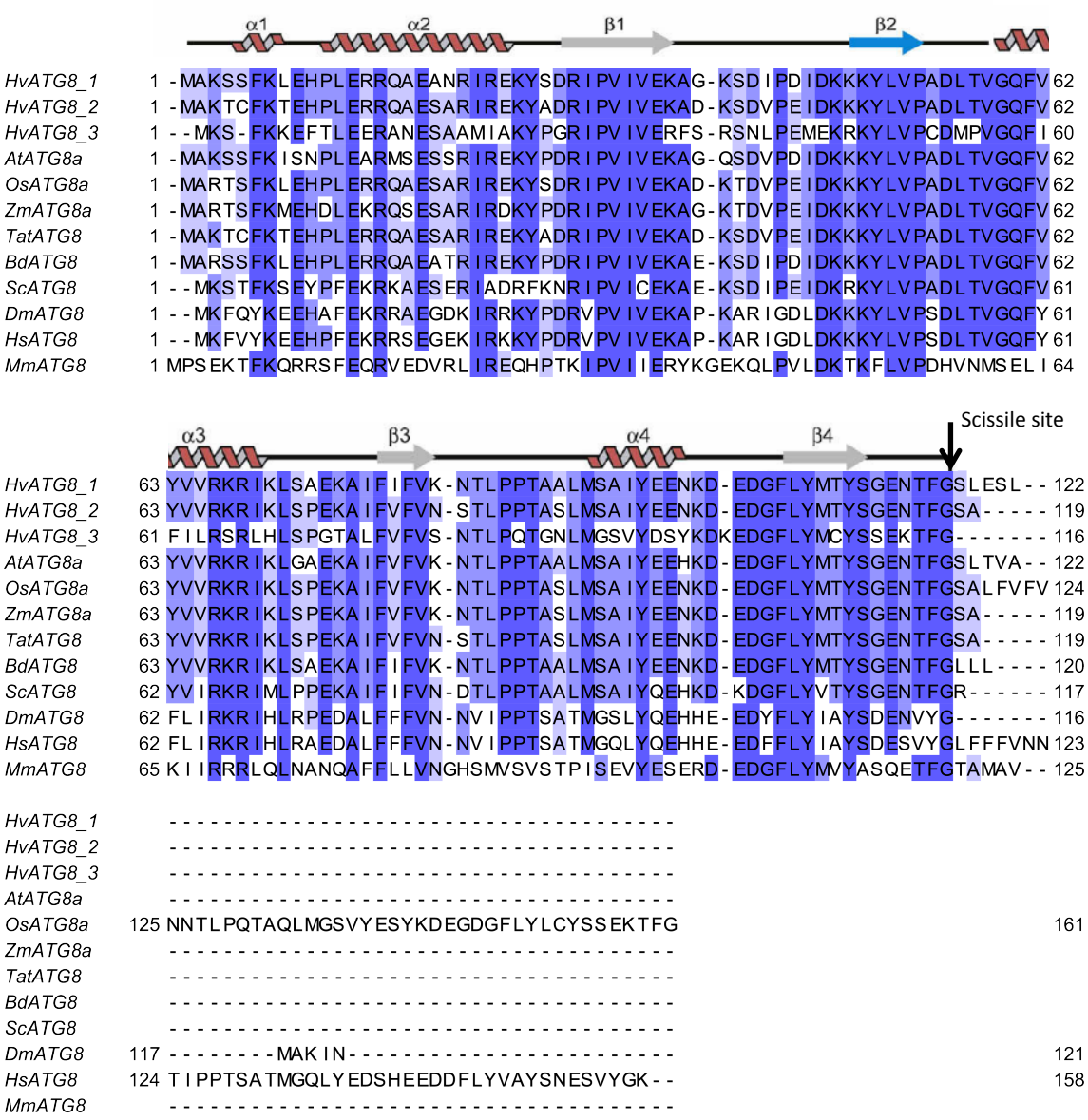

Figure 2. Protein alignment of ATG8 family. ATG8 proteins of different species including the three isoforms of HvATG8 were aligned using ClustalW. Only one isoform of ATG8 protein in other species was used for the alignment. Conserved amino acids (aa) are showed by shades of blue colors going from less conserved aa (light blue) to more conserved aa (dark blue). The secondary structural elements of *S. cerevisiae* ATG8 are shown above the alignment (Noda *et al.*, 2010). Scissile site of cleavage by ATG4 is shown by arrow. Species abreviation are as follows : Hv (*Hordeum vulgare*), At (*Arabidopsis thaliana*), Os (*Oryza sativa*), Zm (*Zea mays*), Ta (*Triticum aestivum*), Bd (*Brachypodium distachium*), Sc (*Saccharomyces cerevisiae*), Dm (*Drosophila melanogaster*), Hs (*Homo sapiens*), Mm (*Mus musculus*).

Arabidopsis and five genes in rice), *ATG9* and *ATG10* (2 genes of each in rice), *ATG12* (two genes in Arabidopsis and three genes in rice), *ATG13* (two genes in both Arabidopsis and rice) and *ATG18* (eight genes in Arabidopsis and six genes in rice). The Arabidopsis, rice and yeast *ATG* collections (Supplemental Table 1) were used as queries in BLASTX and TBLASTN searches of different DNA and protein sequence databases including cDNA, EST (e.g. GeneBank and ENA), genomic assembly databases (e.g. EnsemblGenomes) and protein sequence database (e.g. Uniprot, EBI). Gaps in the sequences were eliminated by sequence analysis of corresponding bacterial artificial chromosome (BAC) clone sequences available in the databases previously mentioned. Finally, all cDNA sequences found were aligned with genomic sequences in order to establish the *HvATG* gene models (Figure 1).

A total of nineteen *HvATG* genes were found in our study (Table 1). We found that single genes encode *HvATG3*, *HvATG5*, *HvATG7*, *HvATG9*, *HvATG12*, *HvATG13 and HvATG16*, while *HvATG1*, *HvATG8* and *HvATG18* are encoded by gene families (three genes in both *HvATG1* and *HvATG8* and five genes in *HvATG18*; Table 1 and Supplemental Data Set 1). For many putative proteins, high amino acid sequence conservation was observed when they were compared with their homologs in rice, but less homology with their Arabidopsis and yeast equivalents. For example HvATG5 has 72% homology with OsATG5, 48% with AtATG5 and 13% with ScATG5. Other proteins showed high homology with all counterparts, for example HvATG8_1 has 87% homology with OsATG8a, 86% with AtATG8a and 71% with ScATG8a. This protein shows also high homology with other ATG8 proteins from organisms such as drosophila, mouse and human and represents one of the most conserved proteins of all HvATG collection (Figure 2). On the other hand, some loci showed low similarity with all their three equivalents, for example HvATG1_2, that showed a 5% homology with OsATG1a, 4% with AtATG1a and 2% with ScAtg1.

In phylogenetic analysis carried out using HvATG family predicted protein sequences (HvATG1_1 to 3, HvATG8_1 to 3 and HvATG18_1 to 5) and homologous protein sequences of different eukaryotic species (Supplemental figure 1), we could observed that predicted proteins of HvATG1 family are clustered with OsATG1 like and animal proteins (Supplemental Figure 1A). Predicted proteins from HvATG18 family were clustered with Arabidopsis homologues with exception of HvATG18_4 and HvATG18_5, which were clustered with other ATG18 like proteins from other plants (Supplemental Figure 1B). Predicted proteins from *Hv*ATG8 family were all branched with Arabidopsis proteins (Supplemental Figure 1C). In all cases, the gene and protein names were given according to their phylogenetic proximity with each Arabidopsis isoform. Furthermore, key amino acids

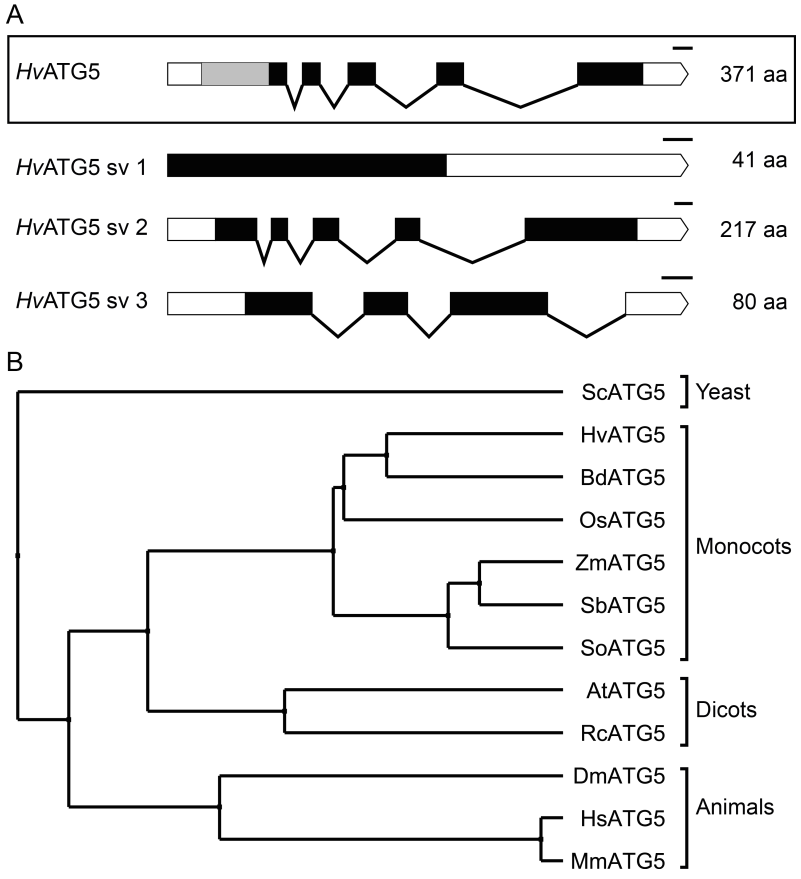

Figure 3. Sequence gap in the coding region of *HvATG5* genome sequence codifies for amino acids essential for the monocots clustering. The gene model of the long *HvATG5* sequence analyzed in this study is showed into a square in **A**. Predicted splice variants from the short sequence available in the genome assembly database Ensemblplants (http://plants.ensembl.org/index.html) are also shown. White boxes (□) represent untranslated regions, black boxes (■) represent coding regions, solid lines (\/) represent introns, grey boxes (■) indicate sequence gaps in coding regions. A phyllogenetic tree shows that the predicted protein encoded by the long sequence of *HvATG5* was clustered with other ATG5 proteins of monocots **B**. Phyllogenetic analysis were performed using ClustalW. Species abreviation are as follows : Hv (*Hordeum vulgare*), Os (*Oryza sativa*), Zm (*Zea mays*), Bd (*Brachypodium distachium*), So (*Saccharum officinarum*), Sb (*Sorghum bicolor*), At (*Arabidopsis thaliana*), Rc (*Ricinus communis*), Sc (*Saccharomyces cerevisiae*), Dm (*Drosophila melanogaster*), Hs (*Homo sapiens*), Mm (*Mus musculus*).

necessary for the function of most of the HvATG proteins were detected (Supplemental Figure 2A-H), these residues include the catalytic Cys residues in ATG3 and ATG7 essentials for their interaction with ATG8 (Yamada *et al.,* 2007; Noda *et al.,* 2011), the Lys residue in ATG5 considered as conjugation site for ATG12 (Otomo *et al.,* 2013), high conserved amino acids from BARA domain in ATG6 essentials for autophagy (Noda *et al.,* 2012), amino acids from C-terminal domain in ATG7 responsible for the recognition of ATG8 (Noda *et al.,* 2011; Figure 2), amino acid residues from the ATG8-family interacting motif crucial for selective autophagy (Noda *et al.,* 2010), the Ser residues of ATG9, targets of ATG1 phosphorylation (Papinski *et al.,* 2014), the Arg residue belonging to the HORMA domain in ATG13 and required for autophagy and PI-3 kinase recruitment (Jao *et al.,* 2013) and the amino acid residues from the coiled-coil domain (CCD) in ATG16 essentials for the interaction with the ATG5-ATG12 conjugate (Fujioka *et al.,* 2010). No essential amino acid residues were found in predicted proteins of HvATG1 and *Hv*ATG18 families.

In the light of this, due to the low homology of HvATG1_1, HvATG1_2, HvATG1_3, HvATG18_4 and HvATG18_5 amino acid sequences to other species counterparts and the fact that no key amino acid essential for their function could be found in these sequences, we cannot assure that these genes encode for ATG functions in barley. Further studies are needed to validate these sequences as truly HvATG.

Our gene models have been performed aligning the EST, BAC and cDNA sequences collected on the genome sequence available (Consortium, 2012). We then compared our models to the putative ones published by the genome assembly database EnsemblPlants *(http://plants.ensembl.org/index.html)*. We could observe that many genes had several predicted splice variants that did not always correspond to the one we have found (*HvATG5*, *HvATG7*, *HvATG16* and *HvATG18_5*; Supplemental Figure 3). The number of genes with *in silico* found splice variants in barley (7 of 11) was higher than in Arabidopsis (8 of 14), however only one of these *in silico* predicted splice variant matched with the cDNA and EST sequences identified, suggesting than only one of them was real (Supplemental Figure 3).

HvATG5 **description and functional complementation**

The *HvATG5* gene we found aligning *HvATG5* EST sequences is contained into a BAC clone library and codifies for a 371 amino acids protein (Supplemental Figure 2B). However, analysing the *HvATG5* genomic sequence provided by the barley genome, we found a shorter version of *Hv*ATG5 that codifies a 217 amino acids protein (Supplemental Figure 3

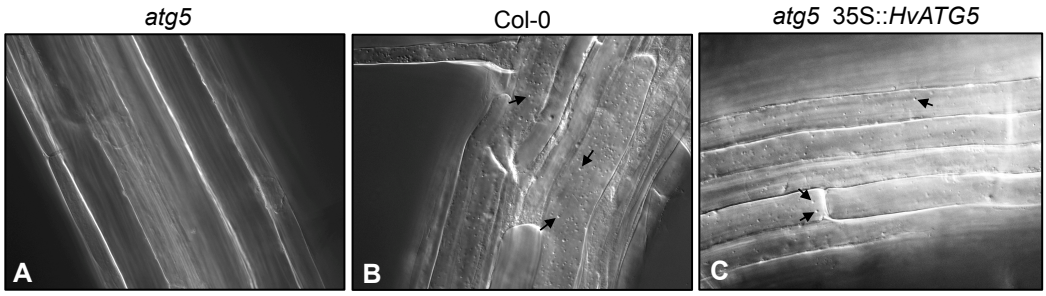

Figure 4. Accumulation of autophagic bodies in Arabidopsis *atg5* mutant complemented with the *HvATG5* cds. Roots of *atg5* (**A**), wild type (**B**) and *atg5* 35S::*HvATG5* transformant (**C**) were incubated with MS medium containing concanamycin A for 6h and then observed by conventional transmision light microscopy. Black arrows indicate autophagic bodies located inside the vacuole.

and Figure 3). Comparing the two sequences (the long and the short) we found a gap in the published genome sequence which matched with the first 462 nucleotides of the CDS of *HvATG5* EST sequence, and encodes the first 154 amino acids of the H*v*ATG5 protein we initially found (Figure 3). Alignments of the HvATG5 protein sequences from different species showed that the missing part includes sequences coding for several conserved amino acids in all the species as the essential Lys residue considered as the conjugation site for ATG12. The long HvATG5 protein found from EST sequence analysis was cluster with the monocots ATG5 in a phylogenetic tree while the shorter version deduced from the published genomic sequence is excluded even from the cluster of plants. Altogether, this show that the genomic sequence in the 5' region of *HvATG5* is missing. This gap in the genome sequence could be due to the high GC content of its 5' end which makes it difficult to amplify and sequence as it was also described by Chung *et al.,* (2009) for *ZmATG5*.

In order to test the *HvATG5* gene/mRNA sequence we identified was able to encodes a functional protein (Figure 3), the cds sequence was cloned in order to over-express *HvATG5* in Arabidopsis *atg5* mutant and test complementation. Arabidopsis *atg5* mutant phenotype includes the total absence of autophagosome and autophagic body when treated with concanamycin-A, early leaf senescence, small rosette size and sensitivity to nitrogen limitation (Doelling *et al.,* 2002; Hanaoka *et al.,* 2002; Guiboileau *et al.,* 2012). Complemented Arabidopsis *atg5* mutants recovered the same capacity as wild type plants to accumulate autophagic bodies when treated with concanamycin-A (Figure 4), which indicates that the expression of *HvATG5* transgene rescued autophagy. Complemented Arabidopsis *atg5* mutants also showed a bigger rosette size and longer stems than *atg5* mutants (Figure 5a). Other phenotypes such as early leaf senescence and sensitivity to NO_3^- limitations were also recovered by the expression of *HvATG5* (Figure 5b).

Expression patterns of *HvATG* genes during leaf senescence and nutritional stress.

The transcript levels of *HvATG* genes was estimated using RT-qPCR in two different plant models: plantlets grown in growth chambers under high (HN) or low (limiting; LN) nitrate conditions (Figure 6A) and flag leaves from plants grown in the field (Figure 8A). Dark treatment was also performed in order to determine the response of *HvATG* genes to carbon starvation (Figure 7AB). For seedlings, we analysed each leaf rank separately: L1, L2 and L3 representing old, mature and young leaves respectively. In all conditions, plant senescence was determined comparing the chlorophyll contents (Figures 6A, 7C and 8A) and the

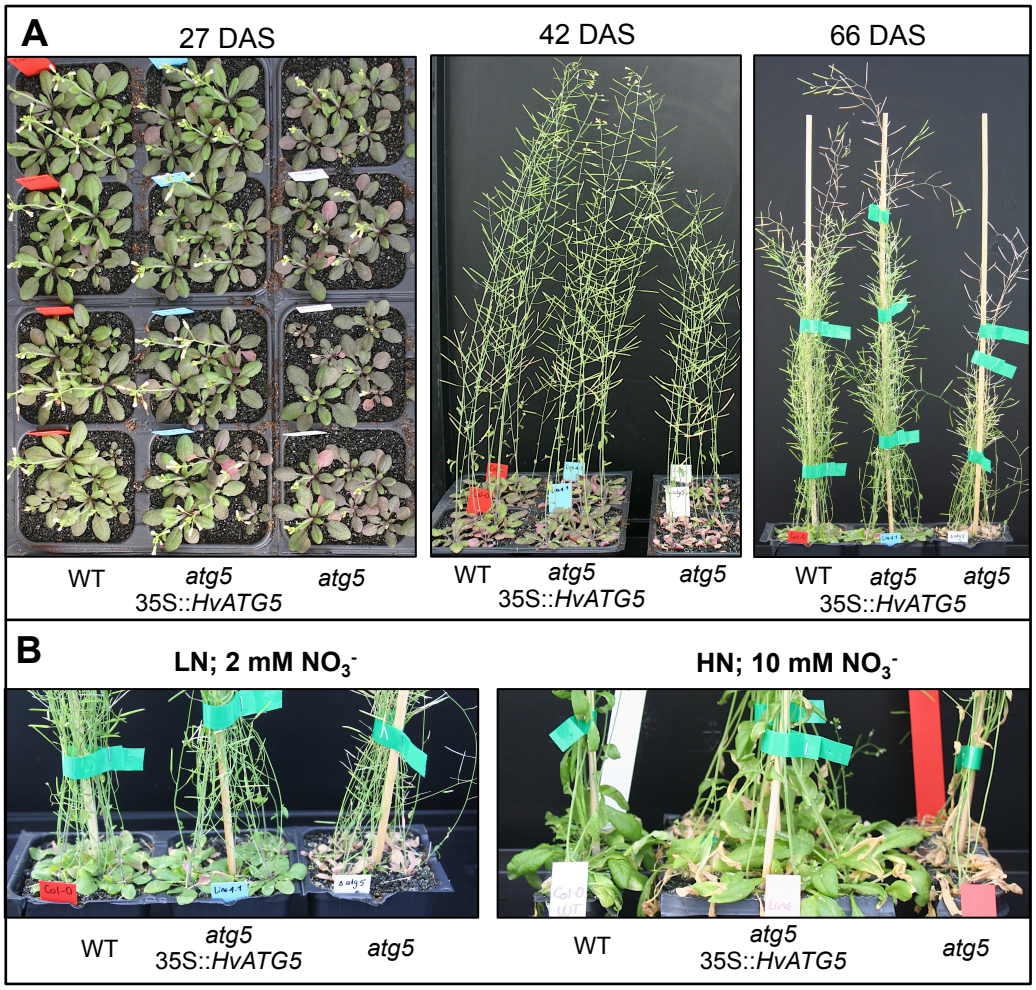

Figure 5. The *atg5* 35S::*HvATG5* transformants are less senescing and less sensitive to nitrate limitation than *atg5* mutants. Wild type, *atg5* mutant and *atg5* 35S::*HvATG5* transformant were grown under low (A and B left panel) and high (B right panel) nitrate conditions. In A, phenotypes of plants 27, 42 and 66 days after sowing (DAS) are shown. Early leaf senescence was observed in *atg5* but not in *atg5* 35S::*HvATG5* plants under both low and high nitrate conditions. Planting was repeated two times including three independent transformants that showed similar recovery phenotypes. Only one is shown here.

expression of the senescence-associated gene *HvNAC13* and the senescence-repressed gene *HvGS2* (Figures 6B, 7D and 8B). Based on the *HvATG* sequences found, specific primers were designed for each gene in order to evaluate their expression during senescence and under stress conditions. The expression of almost all genes described in this study could be estimated with exception of *HvATG1_1, HvATG9, HvATG12* and *HvATG18_4* as it was not possible to find efficient primers.

HvATG *transcript levels in leaf ranks of plants grown under low or high nitrate conditions.*

The three leaf ranks of plantlets grown under low (LN) or high (HN) nitrate conditions were analysed. For most of the *HvATG*, with the exception of the regulatory *HvATG1-1, HvATG1-2* and *HvATG13* genes and *HvATG5*, the highest mRNA abundances were observed in the old leaf (L1) compared to the young one (L3) (Figure 6D). In addition, expression levels were higher in plants grown in LN compared to HN, with the only exception of *HvATG8_3*, which transcripts showed a decrease in plants grown in LN (Figure 6D).

HvATG *transcript levels in leaf ranks of plants submitted to dark treatment.*

In order to perform carbon limitation, barley plants were submitted to dark treatment for 4 d (T1; Figure 7A). Few darken plants were then let growing during 3 more days in normal day/night conditions for a period called recovery treatment (T2). Dark treated plants exhibited higher chlorosis than control plants (Figure 7B). Chlorophyll content that decreased in plants during the dark period, increased after the recovery time (Figure 7C) indicating that senescence process was reversed after that light was restored. In good agreement, *HvNAC13* transcripts increased during dark treatment and decreased during recovery time, while *HvGS2* transcript levels decreased dramatically during the dark treatment and then they highly increased during the recovery time (Figure 7D).

In all samples from the dark treated and control plant harvested after dark treatment or after recovery time, we observed that all *HvATG* genes were more expressed in old leaves than in young ones (Figure 7E). We also observed that most of the *HvATG* transcript levels were higher in darken leaves than in control leaves after dark treatment. The positive effect of dark treatment on *HvATG* transcript levels was transient and completely abolished after 3 days of recovery in normal day/night photoperiod. Surprisingly for some genes like *HvATG3*, *HvATG8_2*, *HvATG8_3*, *HvATG18_2* and *HvATG18_3* transcripts levels were even lower after recovery time in darken leaves than in control ones. This suggests a strong effect of the C/N status of the plant on autophagy gene regulation.

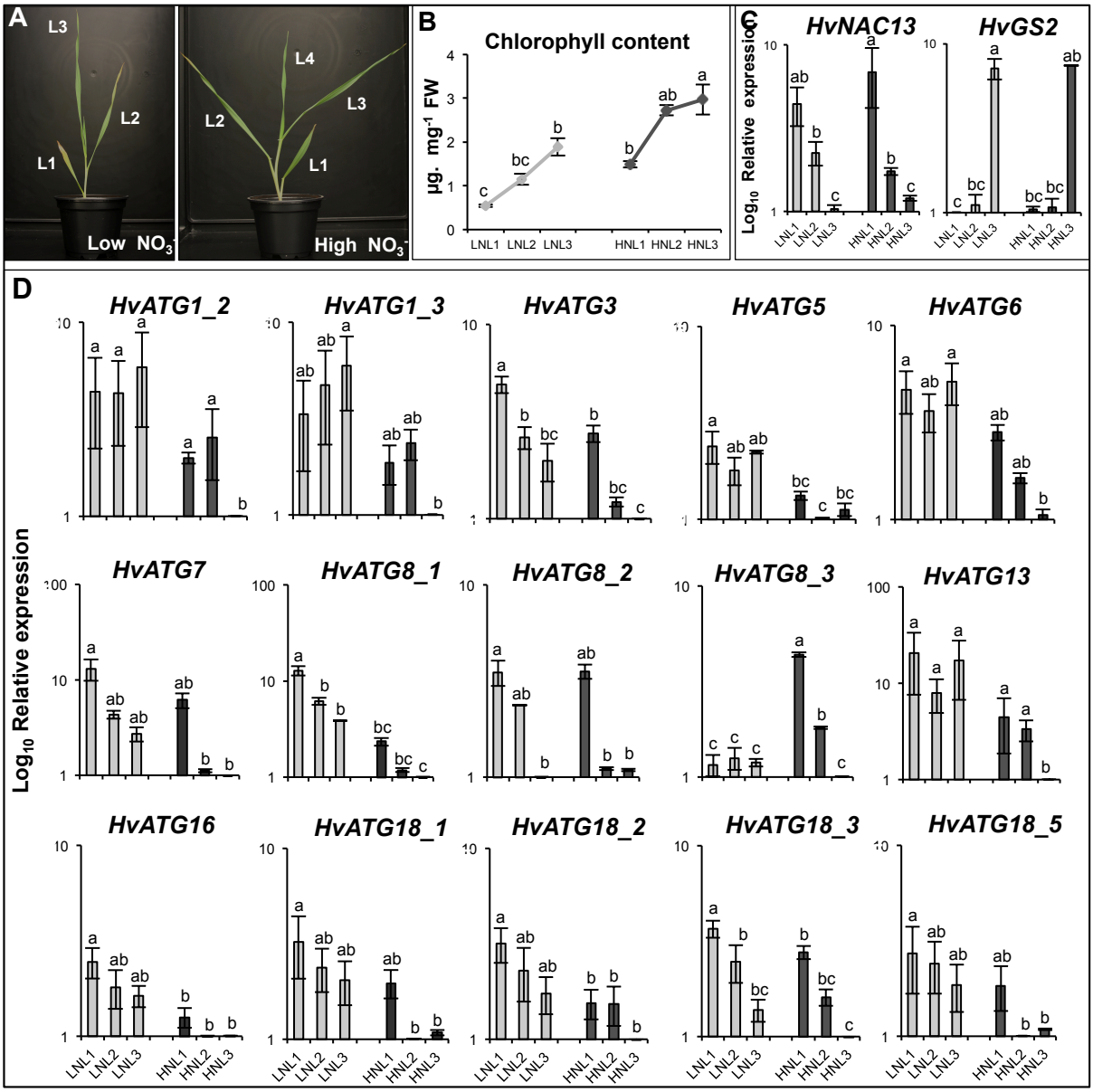

Figure 6. Transcript levels of *HvATG* genes are higher in leaves of plantlets grown under low nitrate (LN) compared to high nitrate (HN) conditions. A: Leaf ranks of 20 days old plants grown under low (0.5 mM NO_3^-) and high (5 mM NO_3^-). **B**: Chlorophyll content of L1, L2 and L3 from LN (light grey bars) and HN (dark grey bars). **C:** Transcript levels of *HvNAC13* (Senescence Associated Gene) and *HvGS2* (Senescence Repressed Gene) show opposite patterns. **D:** Transcript levels of *HvATG.* Transcript levels were measured by RT-qPCR. Only leaf ranks L1, L2 and L3 from both LN and HN plants were analysed. Results are shown as Log_{10} relative expression values. Data are mean ± SD of three independent biological replicates. *HvGAPDH* was used as reference gene. The different letters indicate values significantly different at P <0.05 as determined using XLSTAT ANOVA Newman–Keuls (SNK) comparisons.

HvATG *transcript levels in in flag leaf during senescence.*

Barley cv. Carina was sown in the field under conditions previously described in materials and methods. Flag leaf was harvested from plants at three different time points: T1 (96 DAS), T2 (99 DAS) and T3 (105 DAS) (Figure 8A). Senescence was determined by chlorophyll content (Figure 8B) and by the expression of the *HvNAC13* and *HvGS2* marker genes (Figure 8C). Both showed that T1 represents a young leaf, T2 represents a mature leaf and T3 represents a senescing leaf.

Unfortunately, all the primers used to monitor the expression of *HvATG* in the golden promise cultivar, could not be used on leaf samples from Carina cv., probably due to polymorphism of these two genotypes. Only six of the fifteen genes analysed in golden promise could be analysed in Carina samples.

In good agreement with previous finding on plantlet leaf ranks, the *HvATG* transcript levels were increased in the senescing leaves (T3) compared to the young leaves (T1) and mature leaves (T3). More interestingly, the *HvATG5* showed a clear increment related with leaf senescence, characteristic that was not so clearly observed in leaf ranks and that could indicate that *HvATG5* is more related to N remobilisation to the grain during barley flag leaf senescence than to sequential leaf senescence at vegetative stage.

DISCUSSION

In all organisms, recycling of intracellular constituents is critical for growth, survival under nutrient limiting conditions and for quality control of cell proteins and organelles. In plants that are not moving organisms, recycling is especially important. Plants have adapted to poor environments storing nutrients when available and remobilizing them when needed, to support the growth of new organs and the formation and filling of seeds. We recently showed that autophagy is important for nitrogen use efficiency and remobilisation of nitrogen from the rosette leaves to the seeds in Arabidopsis (Guiboileau *et al.,* 2012). Using several autophagy mutants we showed that they stored and kept nitrogen compounds and especially soluble proteins they cannot degrade properly in their leaves (Guiboileau *et al.,* 2013). In addition to a role in nutrient remobilisation we also showed that autophagy is important for the metabolic and redox homeostasis in leaves, especially under nutrient limitation (Masclaux-Daubresse *et al.,* 2014). Links between autophagy, redox and stress resistance has been described in Arabidopsis in several reports (Phillips *et al.,* 2008; Slavikova *et al.,*

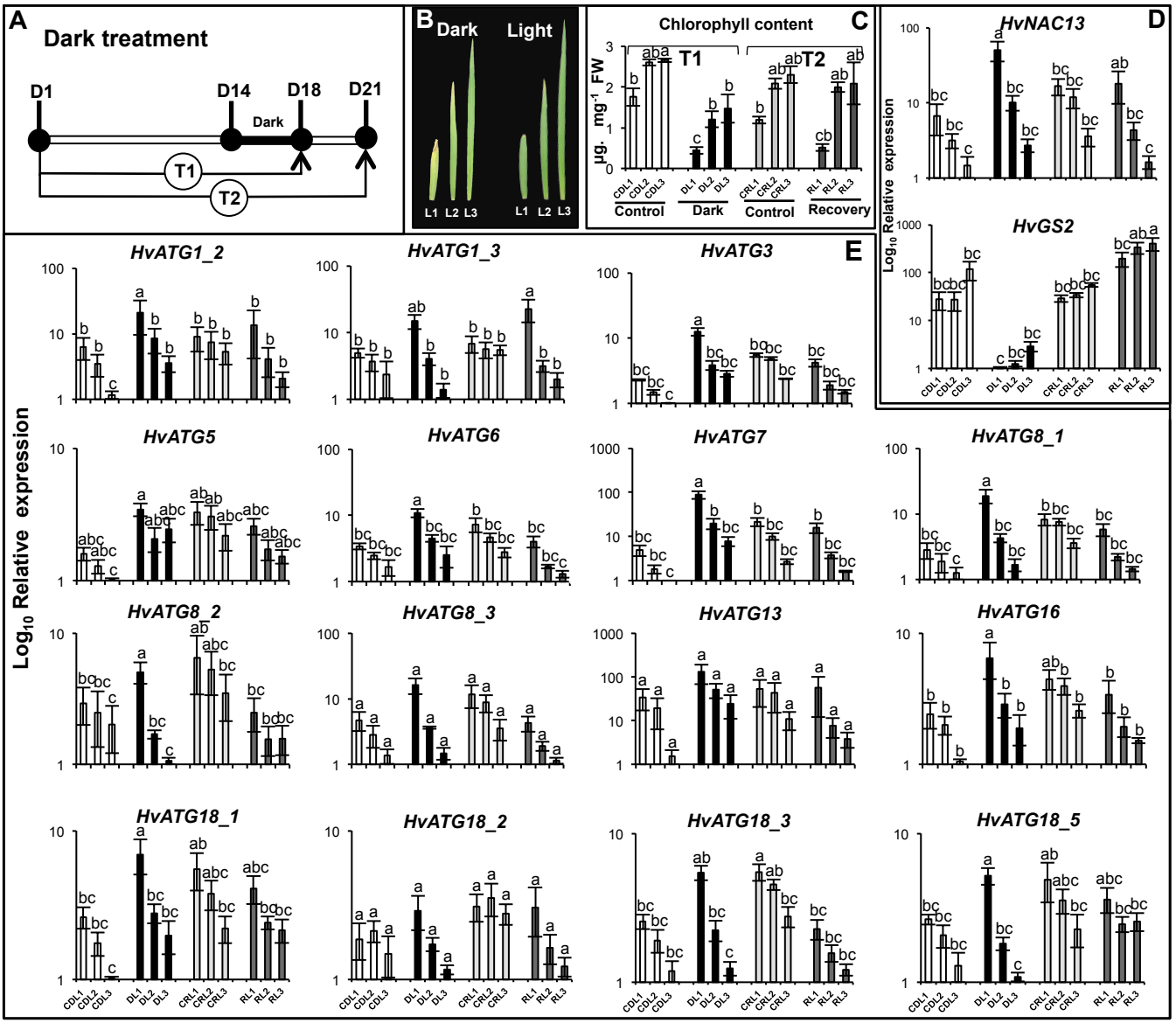

Figure 7. Transcript levels of *HvATG* genes in plantlets after dark treatment. A: *H. vulgare* cv. golden promise plantlets were kept (Darken Leaves, DL; dark bars) or not (Control of Darken Leaves, CDL; white bars) in the dark for 4 days and harvested 18 days afetr sowing (T1; D18). After the dark period, plants were kept growing three more days (from D18 to D21) to test recovering under normal day/night photoperiod. Leaves of control plants (CRL; light grey bars) and of recovering plants after dark treatment (RL; dark grey bars) were harvested at T2. **B:** Leaf ranks L1, L2 and L3 harvested after dark treatment, at T1 on control and treated plants. **C:** Chlorophyll content of leaves from controls (CDL and CRL) and treated plants (DL and RL) at T1 and T2. **DE:** Transcript levels of *HvNAC13*, *HvSSU* (**D**) and *HvATG* (**E**) were measured by RT-qPCR in leaf ranks of plantlets submitted or not to dark treatment. Results are shown as Log_{10} relative expression for each gene. Data are mean ± SD of three independent biological replicates. *HvGAPDH* was used as reference gene. The different letters indicate values significantly different at P <0.05 as determined using XLSTAT ANOVA Newman–Keuls (SNK) comparisons.

2008; Xiong *et al.,* 2007; Liu *et al.,* 2009). Autophagy seems to play also a role - direct or indirect - in plant immunity (Yoshimoto *et al.,* 2009; Lai *et al.,* 2011). Albeit all Arabidopsis *atg* mutant studied so far present phenotypes as early leaf senescence, sensibility to N or C starvations and sensibility to stresses, we found that some of them exhibit stronger phenotypes than others. For example, it seems that knock out mutants in single genes like *atg2*, *atg5* or *atg7* are highly affected. Regarding all the process in which autophagy pathway is involved, and the little things known about its role in other plant species than Arabidopsis, we aimed at dissecting autophagy genes in barley in order to prepare transfer of knowledge to cereals.

Barley genes identified in this report have been found searching *ATG* homologous cDNA, EST and BAC sequences in barley libraries, and then aligning the cDNA sequences found with genomic sequence in order to establish the *HvATG* gene models. The use of rice (*OsATG*), Arabidopsis (*AtATG*) and yeast (*ScATG*) *ATG* as queries was large enough to ensure the finding of a maximum of genes. In addition, proceeding this way ensured that all the nineteen *HvATG* genes described in this report (Figure 1) are translated to mRNA and are giving proteins that share all the characteristics and essential amino acids of the other known homologues in plants, animals and yeast. In addition, starting from cDNA identifications allowed us to identify splice variants that are actually not proposed by the genome assembly database EnsemblPlants *(http://plants.ensembl.org/index.html)* available online and that are certainly the true ones since they are supported by the existence of transcripts. New splice variants were then found for *HvATG5*, *HvATG7*, *HvATG16* and *HvATG18_5* (Figure 1 and Supplemental Figure 1). Albeit the splice variant we found for these genes were different from those proposed by EnsemblPlants, we were able to identify in the genomic sequence all the introns and exons in our gene models (Figure 1), except in the case of *HvATG5*. For *HvATG5*, the 5' sequence region found in the cDNA sequences of barley cannot be found in the genome sequence available online. This was certainly due to the difficulty to sequence the high GC content of this 5' end, leading to a gap in the genomic sequence. Because such high GC region is difficult to amplify using RT-PCR, and to verify that *HvATG5* cDNA was coding functional ATG5 protein, we cloned the cds sequence to transform Arabidopsis *atg5* mutant. Arabidopsis *atg5* mutants have been described for a long time by both Pr. Ohsumi and Pr. Viestra groups (Thompson *et al.,* 2005; Inoue *et al.,* 2006). We have also used them in our previous studies (Guiboileau *et al.,* 2013; Guiboileau *et al.,* 2012; Masclaux-Daubresse *et al.,* 2014). These mutants present slightly smaller rosette size and early leaf senescence than wild type especially when grown under low nitrate nutrition. They cannot produce autophagosome or autophagic body, and such defect can be observed in their roots

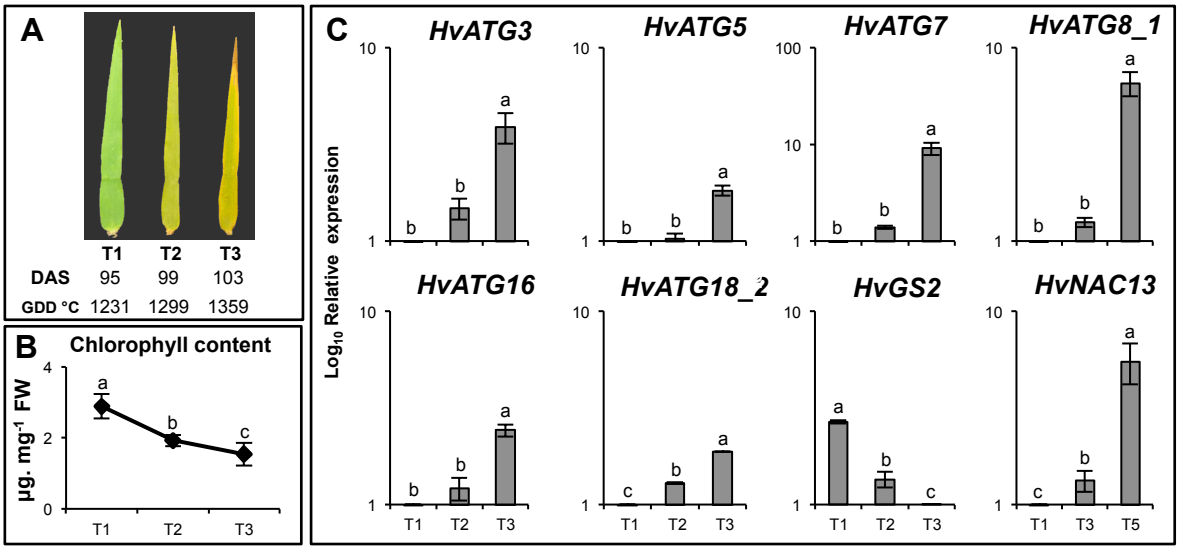

Figure 8. Transcript levels of *HvATG* were increased in flag leaves during senescence. A: *H. vulgare* cv. carina flag leaves were harvested at different time points (T1: 95 DAS; T2: 99 DAS; T3: 103 DAS; DAS days after sowing). **B:** chlorophyll content decrease with leaf ageing. **C:** Transcript levels of *HvNAC13*, *HvGS2* and *HvATG* genes were measured by RT-qPCR. Results are shown as Log_{10} relative expression for each gene. Data are mean ± SD of three independent biological replicates. *HvActin* was used as reference gene. The different letters indicate values significantly different at P <0.05 as determined using XLSTAT ANOVA Newman–Keuls (SNK) comparisons.

after concanamycin-A treatment. Conacanamycin-A drug inhibits tonoplast ATPases and modify the pH of the lumen; this blocks autophagic body degradation within the vacuole. After treating with concanamycin-A, autophagic bodies accumulated in the roots of type plants, and in the roots of the *atg5* mutants over-expressing *HvATG5*, but not in *atg5* mutants. Complementation of Arabidopsis *atg5* by the *HvATG5* cds was then operational. In addition we observed that complemented 35S::*HvATG5 atg5* plants were bigger and greener than *atg5*, recovering wild phenotype.

From our splice variants and cDNA sequence analyses, we concluded that for all the genome loci identified in barley, we can only find one functional splice variant per loci. The functional gene models presented in Figure 1 is supported by the existence of transcript sequences. In their reports, Chung et al 2009 discussed the number of *ATG* splice variants in maize and Arabidopsis. They interpreted the meaning of splice variant diversity as an adaptation of plants to the complex response of autophagy activity to developmental and environmental cues. Our finding is not in agreement with their interpretation, and our results suggest that barley have adapted duplicating some *ATG* genes like *HvATG8* or *HvATG18* – like other plant and animal have done – thus providing protein isoforms coded by different genes. The developing RNAseq study will help resolving this question in the future facilitating the identification of rare splice variants in barley if they exist.

Although we did not identified more than one functional splice variants per *HvATG* gene, in we found both single *ATG* genes and *ATG* gene families, like in other plant species. Gene families were found for *HvATG1* (3 genes), *HvATG8* (3 genes) and *HvATG18* (5 genes). For *HvATG8* and *HvATG18* members of families were less than in Arabidopsis where there are 9 *AtATG8* and 9 *AtATG18*. The reason why plants have conserved these gene families in the case of few autophagy functions is certainly due to role specificities in the adaptation to environment. We can indeed see that the three *HvATG8* and five *HvATG18* do not present the same responses to ageing, nitrogen limitation or carbon limitation. *HvATG8_1* is highly induced by leaf senescence but more specifically under low nitrate conditions while *HvATG8_3* is highly induced by leaf senescence but more specifically under high nitrate conditions. *HvATG8_2* is equally induced by leaf senescence under high or low nitrate conditions. Similarly *HvATG18* genes showed specific response to leaf senescence depending on nitrate conditions. The reason why plants and animals have several ATG8 isoforms by contrast with yeast is certainly inherent to their multicellular organisation and also to the role of the ATG8 protein in the selectivity of autophagy for cargos (Noda *et al.,* 2010). As ATG8 would participate to cargo recognition, we can imagine that the different isoform present

different cargo selectivity. They also certainly differentially regulated post-transcriptionally. Regarding the three *HvATG8*, we can indeed see that *HvATG8_1* and *HvATG8_2* present the canonical sessile site of cleavage by ATG4 activity at Gly^{117} and a C-terminal sequence that need to be removed to allow ATG8 lipidation, whereas *HvATG8_3* does not. The presence of C-term sequence on two of the *HvATG8* suggests then that a HvATG4 protease is needed to mature HvATG8. However we have not found any cDNA or genomic sequence potentially coding such HvATG4. Improving barley genomic sequence annotation and completing discontinuous structure assembling will certainly facilitate the finding of *HvATG4*.

Thanks to all the cDNA and genomic sequences found for nineteen *HvATG* genes, we were able to design primers to perform transcript level analysis through RT-qPCR for almost all of them. Globally, the responses of *HvATG* genes to N or C limitation and to leaf ageing were similar. Consistently with Arabidopsis studies (Breeze *et al.,* 2011; Avila-Ospina *et al.,* 2014) for a review), all of them were highly induced by leaf senescence in plants grown under low or high nitrate, except *HvATG5*, and under low nitrate *HvATG18_3, HvATG13 and HvATG6.* All of them were also globally more expressed under low nitrate than under high nitrate conditions (Hollmann *et al.,* 2014). Dark treatment also sharply enhanced *HvATG* gene expression due to carbon starvation (Rose *et al.,* 2006). The lowest responsive gene to C starvation was again *HvATG5*. Interestingly ageing was more efficient in enhancing *HvATG5* expression in flag leaf than in leaf ranks of plantlets. In flag leaves, *HvATG5* transcript levels doubled while they remain stable in the three leaf ranks of plantlets grown under low or high nitrate conditions. As flag leaves are the major sources for nutrient remobilisation and grain filling, such results sound consistent with the role of *ATG5* in nitrogen remobilisation to the seeds reported by Guiboileau *et al.,* (2012). This is also consistent with the late expression of *AtATG* during leaf senescence described by (Avila-Ospina *et al.,* 2014) in Arabidopsis.

Interestingly phylogeny trees showed that for genes of the *ATG1*, *ATG8* and *ATG18* families, a mix of monocot and dicot sequences could be found in each cluster. In the case of *ATG5*, sequences clustered to form a dichotomy between monocot sequences and dicots' ones. Such speciation between monocot ad dicot suggests a specialisation of ATG5 proteins in these two angiosperm groups. Specificities of monocot and dicot proteins remain to be investigated.

The present report gives the first characterization of *ATG* genes in cereals. Barley sequences will be useful for transcriptome studies and to investigate further the role of autophagy in barley and wheat for nitrogen remobilisation and grain yield and quality (Hollmann *et al.,* 2014). The possibility to transform barley efficiently and the existence of tilling mutant collections will facilitate such study. While mutations in autophagy genes affect plant yield

and nutrient use efficiency, two reports indicate that over-expressing autophagy genes can improve plant performance and tolerance to stress (Slavikova *et al.,* 2008; Xia *et al.,* 2012). All the results presented in this report will be useful to test whether such beneficial effects can be reached manipulating autophagy genes in barley.

Acknowledgements

Authors warmly thanks Joël Talbotec (INRA Versailles, France) for taking care of plants, Pr Karin Krupinska (University of Kiel, Kiel, Germany) for facilitating plant material harvest during field experiment, Dr Kohki Yoshimoto (INRA Versailles, France) and Dr Anne Marmagne (INRA Versailles, France) for advises on cloning. Authors thanks the National Institute of Agrobiological Sciences, NIAS for providing the BAC clone NIASHv2006J04 containing the *HvATG5* coding DNA sequence (CDS).

Financial supports:

This work was supported by the FP7 Marie Curie Actions – Networks for Initial Training Project FP7-MC-ITN N° 264394 acronym CropLife for L.A-O.

REFERENCES

Altschul SF, Lipman DJ. 1990. Protein database searches for multiple alignments. *PNAS* **87**: 5509-5513.

Arnon DI. 1949. Copper enzymes in isolated chloroplasts. Polyphenol oxidase in *Beta vulgaris* L. *Plant Physiology* **24**: 1-15.

Avila-Ospina L, Moison M, Yoshimoto K, Masclaux-Daubresse C. 2014. Autophagy, plant senescence, and nutrient recycling. *Journal of Experimental Botany* doi:10.1093/jxb/eru039.

Breeze E, Harrison E, McHattie S, Hughes L, Hickman R, Hill C, Kiddle S, Kim Y-s, Penfold CA, Jenkins D, Zhang C, Morris K, Jenner C, Jackson S, Thomas B, Tabrett A, Legaie R, Moore JD, Wild DL, Ott S, Rand D, Beynon J, Denby K, Mead A, Buchanan-Wollaston V. 2011. High-Resolution Temporal Profiling of Transcripts during Arabidopsis Leaf Senescence Reveals a Distinct Chronology of Processes and Regulation. *Plant Cell* **23(3)**: 873-894.

Chardon F, Noël V, Masclaux-Daubresse C. 2012. Manipulating NUE in Arabidopsis and crop plants to improve yield and seed quality. *Journal of Experimental Botany* **63(9)**: 3401-3412.

Chiba A, Ishida H, Nishizawa NK, Makino A, Mae T. 2003. Exclusion of ribulose-1,5-bisphosphate carboxylase/oxygenase from chloroplasts by specific bodies in naturally senescing leaves of wheat. *Plant Cell Physiol* **44(9)**: 914-921.

Chung TJ, Suttangkakul A, Vierstra RD. 2009. The ATG autophagic conjugation system in maize: ATG transcripts and abundance of the ATG8-lipid adduct are regulated by development and nutrient availability. *Plant Physiology* **149(1)**: 220-234.

Cliquet J-B, Deléens E, Mariotti A. 1990. C and N mobilization from salk to leaves during kernel filling by ^{13}C and ^{15}N tracing in *Zea mays* L. *Plant Physiology* **94**: 1547-1553.

Consortium TIBGS. 2012. A physical, genetic and functional sequence assembly of the barley genome. *Nature* **491**: 711-717.

Coque M, Martin A, Veyrieras JB, Hirel B, Gallais A. 2008. Genetic variation for N-remobilisation and postsilking N-uptake in a set of maize recombinant inbred lines. 3. QTL detection and coincidences. *Theor Appl Genet* **117(5)**: 729-747.

Doelling JH, Walker JM, Friedman EM, Thompson AR, Vierstra RD. 2002. The APG8/12-activating enzyme APG7 is required for proper nutrient recycling and senescence in Arabidopsis thaliana. *Journal of Biological Chemistry* **277(36)**: 33105-33114.

Fujioka Y, Noda NN, Nakatogawa H, Ohsumi Y, Inagaki F. 2010. Dimeric Coiled-coil Structure of Saccharomyces cerevisiae Atg16 and Its Functional Significance in Autophagy. *Journal of Biological Chemistry* **285(2)**: 1508-1515.

Guiboileau A, Avila-Ospina L, Yoshimoto K, Soulay F, Azzopardi M, Marmagne A, Lothier J, Masclaux-Daubresse C. 2013. Physiological and metabolic consequences of autophagy defisciency for the management of nitrogen and protein resources in Arabidopsis leaves depending on nitrate availability. *New Phytologist* **199(3)**: 683-694.

Guiboileau A, Yoshimoto K, Soulay F, Bataillé M, Avice J, Masclaux-Daubresse C. 2012. Autophagy machinery controls nitrogen remobilisation at the whole-plant level under both limiting and ample nitrate conditions in Arabidopsis. *New Phytologist* 194**(3)**: 732-740.

Hanaoka H, Noda T, Shirano Y, Kato T, Hayashi H, Shibata D, Tabata S, Ohsumi Y. 2002. Leaf senescence and starvation-induced chlorosis are accelerated by the disruption of an Arabidopsis autophagy gene. *Plant Physiology* **129(3)**: 1181-1193.

Hirel B, Le Gouis J, Ney B, Gallais A. 2007. The challenge of improving nitrogen use efficiency in crop plants: towards a more central role for genetic variability and quantitative genetics within integrated approaches. *J Exp Bot* **58(9)**: 2369-2387.

Hollmann J, Gregersen PL, Krupinska K. 2014. Identification of predominant genes involved in regulation and execution of senescence-associated nitrogen remobilisation in flag leaves of field grown barley. *J Exp Bot* doi:10.1093/jxb/eru094.

Inoue Y, Suzuki T, Hattori M, Yoshimoto K, Ohsumi Y, Moriyasu Y. 2006. AtATG genes, homologs of yeast autophagy genes, are involved in constitutive autophagy in Arabidopsis root tip cells. *Plant and Cell Physiology* **47(12)**: 1641-1652.

Ishida H, Yoshimoto K, Izumi M, Reisen D, Yano Y, Makino A, Ohsumi Y, Hanson MR, Mae T. 2008. Mobilization of rubisco and stroma-localized fluorescent proteins of chloroplasts to the vacuole by an ATG gene-dependent autophagic process. *Plant Physiology* **148(1)**: 142-155.

Jao CC, Ragusa MJ, Stanley RE, Hurley JH. 2013. What the N-terminal domain of Atg13 looks like and what it does A HORMA fold required for PtdIns 3-kinase recruitment. *Autophagy* **9(7)**: 1112-1114.

Kichey T, Hirel B, Heumez E, Dubois F, Le Gouis J. 2007. In winter wheat (*Triticum aestivum* L.), post-anthesis nitrogen uptake and remobilisation to the grain correlates with agronomic traits and nitrogen physiological markers. *Field Crop Res* 102**(1)**: 22-32.

Lai Z, Wang F, Zheng Z, Fan B, Chen Z. 2011. A critical role of autophagy in plant resistance to necrotrophic fungal pathogens. *Plant Journal* 66(6): 953-968.

Li F, Vierstra RD. 2012. Autophagy: a multifaceted intracellular system for bulk and selective recycling. *Trends in Plant Science* **17(9)**: 526-537.

Liu Y, Bassham DC. 2012. Autophagy: pathways for self-eating in plant cells. *Annual Review of Plant Biology* **63**: 215-237.

Liu Y, Xiong Y, Bassham DC. 2009. Autophagy is required for tolerance of drought and salt stress in plants. *Autophagy* **5(7)**: 954-963.

Malagoli P, Laine P, Rossato L, Ourry A. 2005. Dynamics of nitrogen uptake and mobilization in field-grown winter oilseed rape (Brassica napus) from stem extension to harvest. II. An 15N-labelling-based simulation model of N partitioning between vegetative and reproductive tissues. *Ann Bot (Lond)* **95(7)**: 1187-1198.

Masclaux-Daubresse C, Clément G, Anne P, Routaboul J, Guiboileau A, Soulay F, Shirasu K, Yoshimoto K. 2014. Stitching together the multiple dimensions of autophagy using metabolomic and transcriptomic analyses reveals new impacts of autophagy defects on metabolism, development and plant response to environment. ***The Plant Cell*** http://www.plantcell.org/cgi/doi/10.1105/tpc.114.124677**.**

Masclaux-Daubresse C, Daniel-Vedele F, Dechorgnat J, Chardon F, Gaufichon L, Suzuki A. 2010. Nitrogen uptake, assimilation and remobilisation in plants: challenges for sustainable and productive agriculture. *Annals of Botany* **105(7)**: 1141-1157.

Masclaux-Daubresse C, Reisdorf-Cren M, Orsel M. 2008. Leaf nitrogen remobilisation for plant development and grain filling. *Plant Biol (Stuttg)* **10(1)**: 23-36.

Mayer KFX, Waugh R, Langridge P, Close TJ, Wise RP, Graner A, Matsumoto T, Sato K, Schulman A, Muehlbauer GJ, Stein N, Ariyadasa R, Schulte D, Poursarebani N, Zhou R, Steuernagel B, Mascher M, Scholz U, Shi B, Madishetty K, Svensson JT, Bhat P, Moscou M, Resnik J, Hedley P, Liu H, Morris J, Frenkel Z, Korol A, Berges H, Taudien S, Groth M, Felder M, Platzer M, Brown JWS, Fincher GB, Sampath D, Swarbreck D, Scalabrin S, Zuccolo A, Vendramin V, Morgante M, Int Barley Genome Sequencing C. 2012. A physical, genetic and functional sequence assembly of the barley genome. *Nature* **491(7426)**: 711-+.

Merkulova EA, Guiboileau A, Naya L, Masclaux-Daubresse C, Yoshimoto K. 2014. Assessment and optimization of autophagy monitoring methods in Arabidopsis roots indicate direct fusion of autophagosomes with vacuoles. *Plant Cell Physiology* **55(4)**: 715-726.

Mizushima N, Komatsu M. 2011. Autophagy: Renovation of Cells and Tissues. *Cell* **147**: 728-741.

Noda NN, Kobayashi T, Adachi W, Fujioka Y, Ohsumi Y, Inagaki F. 2012. Structure of the Novel C-terminal Domain of Vacuolar Protein Sorting 30/Autophagy-related Protein 6 and Its Specific Role in Autophagy. *Journal of Biological Chemistry* **287(20)**: 16256-16266.

Noda NN, Ohsumi Y, Inagaki F. 2010. Atg8-family interacting motif crucial for selective autophagy. *FEBS Letters* **584(7)**: 1379-1385.

Noda NN, Satoo K, Fujioka Y, Kumeta H, Ogura K, Nakatogawa H, Ohsumi Y, Inagaki F. 2011. Structural Basis of Atg8 Activation by a Homodimeric E1, Atg7. *Molecular Cell* **44(3)**: 462-475.

Otegui MS, Noh YS, Martinez DE, Vila Petroff MG, Staehelin LA, Amasino RM, Guiamet JJ. 2005. Senescence-associated vacuoles with intense proteolytic activity develop in leaves of Arabidopsis and soybean. ***Plant J*** **41(6)**: 831-844.

Otomo C, Metlagel Z, Takaesu G, Otomo T. 2013. Structure of the human ATG12 similar to ATG5 conjugate required for LC3 lipidation in autophagy. *Nature Structural & Molecular Biology* **20(1)**: 59-U79.

Papinski D, Schuschnig M, Reiter W, Wilhelm L, Barnes CA, Maiolica A, Hansmann I, Pfaffenwimmer T, Kijanska M, Stoffel I, Lee SS, Brezovich A, Lou JH, Turk BE, Aebersold R, Ammerer G, Peter M, Kraft C. 2014. Early Steps in Autophagy Depend on Direct Phosphorylation of Atg9 by the Atg1 Kinase (vol 53, pg 471, 2014). *Molecular Cell* **53(3)**: 515-515.

Peoples M, Dalling M 1988. The interplay between proteolysis and amino acid metabolism during senescence and nitrogen reallocation. In: Noodén L, Leopold A eds. *Senescence and aging in plants*. San Diego: Academic Press, 181–217.

Phillips AR, Suttangkakul A, Vierstra RD. 2008. The ATG12-conjugating enzyme ATG10 is essential for autophagic vesicle formation in Arabidopsis thaliana. *Genetics* **178(3)**: 1339-1353.

Roberts IN, Caputo C, Criado MV, Funk C. 2012. Senescence-associated proteases in plants. *PHYSIOLOGIA PLANTARUM* **145(1)**: 130-139.

Rose TL, Bonneau L, Der C, Marty-Mazars D, Marty F. 2006. Starvation-induced expression of autophagy-related genes in Arabidopsis. *Biology of the Cell* **98(1)**: 53-67.

Slavikova S, Ufaz S, Avin-Wittenberg T, Levanony H, Galili G. 2008. An autophagy-associated Atg8 protein is involved in the responses of Arabidopsis seedlings to hormonal controls and abiotic stresses. *Journal of Experimental Botany* **59(14):** 4029–4043.

Thompson AR, Doelling JH, Suttangkakul A, Vierstra RD. 2005. Autophagic nutrient recycling in Arabidopsis directed by the ATG8 and ATG12 conjugation pathways. *Plant Physiology* **138(4)**: 2097-2110.

Thompson AR, Vierstra RD. 2005. Autophagic recycling: lessons from yeast help define the process in plants. *Curr Opin Plant Biol* **8(2)**: 165-173.

Thompson JD, Higgins DG, Gibson TJ. 1994. CLUSTAL-W - IMPROVING THE SENSITIVITY OF PROGRESSIVE MULTIPLE SEQUENCE ALIGNMENT THROUGH SEQUENCE WEIGHTING, POSITION-SPECIFIC GAP PENALTIES AND WEIGHT MATRIX CHOICE. *Nucleic acids research* **22**: 4673-4680.

Vandesompele J, De Preter K, Pattyn F, Poppe B, Van Roy N, De Paepe A, Speleman F. 2002. Accurate normalization of real-time quantitative RT-PCR data by geometric averaging of multiple internal control genes. ***Genome biology* 3(7)**: RESEARCH0034-RESEARCH0034.

Wittenbach VA, Lin W, Hebert RR. 1982. VACUOLAR LOCALIZATION OF PROTEASES AND DEGRADATION OF CHLOROPLASTS IN MESOPHYLL PROTOPLASTS FROM SENESCING PRIMARY WHEAT LEAVES. *Plant Physiology* 69**(1)**: 98-102.

Xia K, Liu T, Ouyang J, Wang R, Fan T, Zhang M. 2011. Genome-wide identification, classification, and expression analysis of autophagy-associated gene homologues in Rice (Oryza sativa L.). *DNA Research* **18**: 363-377.

Xia T, Xiao D, Liu D, Chai W, Gong Q, Wang NN. 2012. Heterologous Expression of ATG8c from Soybean Confers Tolerance to Nitrogen Deficiency and Increases Yield in Arabidopsis. *Plos One* **7(5).**

Xiong Y, Contento AL, Bassham DC. 2005. AtATG18a is required for the formation of autophagosomes during nutrient stress and senescence in Arabidopsis thaliana. *Plant Journal* **42(4)**: 535-546.

Xiong Y, Contento AL, Nguyen PQ, Bassham DC. 2007. Degradation of oxidized proteins by autophagy during oxidative stress in Arabidopsis. *Plant Physiology* **143(1)**: 291-299.

Yamada Y, Suzuki NN, Hanada T, Ichimura Y, Kumeta H, Fujioka Y, Ohsumi Y, Inagaki F. 2007. The crystal structure of Atg3, an autophagy-related ubiquitin carrier protein (E2) enzyme that mediates Atg8 lipidation. *Journal of Biological Chemistry* **282(11)**: 8036-8043.

Yoshimoto K. 2012. Beginning to Understand Autophagy, an Intracellular Self-Degradation System in Plants. *Plant and Cell Physiology* **53(8)**: 1255-1365.

Yoshimoto K, Jikumaru Y, Kamiya Y, Kusano M, Consonni C, Panstruga R, Ohsumi Y, Shirasu K. 2009. Autophagy Negatively Regulates Cell Death by Controlling NPR1-Dependent Salicylic Acid Signaling during Senescence and the Innate Immune Response in Arabidopsis. *Plant Cell* **21(9):** 2914-2927.

Table 1. Collection of barley *HvATG* sequences. cDNA sequences obtained from retranscription of transcripts are found in BAC clones, EMBL-EBI and NCBI accessions. Genomic sequences are represented as X_contig sequences.

Gene	BAC clones	Gene ID EMBL-EBI	Accession No. NCBI	*H.vulgare* Genomic seq.	No. of Amino Acid Residues	Identitiy to		
						S. cerevisiae	*A. thaliana**	*O. sativa***
HvATG1_1	NIASHv2067A10	MLOC_70360	AK368043	x_contig_57832	509	11%	15%	79%
HvATG1_2	NIASHv3128P13	MLOC_67740	AK376609	x_contig_53539	827	2%	4%	5%
HvATG1_3	FLbaf163a20	MLOC_10262	AK252590	x_contig_1558709	450	12%	14%	14%
HvATG3	FLbaf179k14	MLOC_66486	AK252967	x_contig_51626	316	26%	71%	89%
HvATG5	NIASHv2006J04	MLOC_70253	AK362511	x_contig_57680	371	13%	48%	72%
HvATG6	NIASHv2011D22	MLOC_71271	AK362923, AM075824	x_contig_59463	504	19%	37%	85%
HvATG7	NIASHv2065A17	MLOC_20377	AK367931	x_contig_158944	695	28%	34%	49%
HvATG8_1	FLbaf129h07	MLOC_74964	AK251678	x_contig_66871	122	71%	86%	87%
HvATG8_2	FLbaf5e12	MLOC_18032	AK248733	x_contig_1578994	119	73%	81%	93%
HvATG8_3	FLbaf77m18	MLOC_62061	AK250515	x_contig_46162	116	48%	47%	50%
HvATG9	NIASHv2013F07	MLOC_54359	AM085509, AK363183	x_contig_39071	890	13%	48%	79%
HvATG12	NIASHv3020L01	MLOC_54496	AK373086	x_contig_39173	404	5%	3%	51%
HvATG13	NIASHv2035H08	MLOC_12860	AK365609	x_contig_1564279	540	10%	24%	76%
HvATG16	NIASHv1141N15	MLOC_66915	AK361491	x_contig_52278	516	6%	50%	77%
HvATG18_1	NIASHv2028H07	MLOC_56544	AK364793	x_contig_40934	483	16%	58%	77%
HvATG18_2	NIASHv2141H12	MLOC_74982	AK371787	x_contig_6690	232	16%	17%	17%
HvATG18_3	NIASHv2025P14	MLOC_56913	AK364502	x_contig_41239	385	19%	42%	38%
HvATG18_4	NIASHv2073H03	MLOC_4865	AK368421	x_contig_135595	912	7%	6%	6%
HvATG18_5	NIASHv2002C04, NIASHv2139D21	MLOC_24797	AK362065, AK371649	x_contig_1655679	1019	6%	6%	5%

Sequences compared with the single gene product in yeast and the a isoform of Arabidopsis* and rice**

Legends of Figures

Figure 1. Diagram of barley *HvATG* genes. Gene structures were deduced from the sequences of cDNA, EST, BAC clone libraries and alignments with genomic sequences (see Methods) using genome assembly database Ensemblplants (http://plants.ensembl.org/index.html). White boxes (□) represent untranslated regions, black boxes (■) represent coding regions and solid lines (\/) represent introns. The predicted amino acid (aa) lenght for each of the corresponding proteins is shown at right. HvATG gene families are highlighted in grey. Upper bars correspond to 0.1 Kbp.

Figure 2. Protein alignment of ATG8 family. ATG8 proteins of different species including the three isoforms of HvATG8 were aligned using ClustalW. Only one isoform of ATG8 protein in other species was used for the alignment. Conserved amino acids (aa) are showed by shades of blue colors going from less conserved aa (light blue) to more conserved aa (dark blue). The secondary structural elements of *S. cerevisiae* ATG8 are shown above the alignment (Noda *et al.*, 2010). Scissile site of cleavage by ATG4 is shown by arrow. Species abreviation are as follows: Hv (*Hordeum vulgare*), At (*Arabidopsis thaliana*), Os (*Oryza sativa*), Zm (*Zea mays*), Ta (*Triticum aestivum*), Bd (*Brachypodium distachium*), Sc (*Saccharomyces cerevisiae*), Dm (*Drosophila melanogaster*), Hs (*Homo sapiens*), Mm (*Mus musculus*).

Figure 3. Sequence gap in the coding region of *HvATG5* genome sequence codifies for amino acids essential for the monocots clustering. A. The *HvATG5* gene model obtained from the EST sequence analyzed in this study (showed into square) is different from the predicted splice variants (*HvATG5* sv1; sv2 and sv3) provided by the genome assembly database Ensemblplants (http://plants.ensembl.org/index.html). White boxes (□) represent untranslated regions, black boxes (■) represent coding regions, solid lines (\/) represent introns, and the grey box (■) indicates the sequence missing in the genome sequence but found in EST coding region of X-contig-57680. **B**. The HvATG5 protein sequence deduced from the *HvATG5* sequence of X-contig-57680 cluster with the ATG5 proteins of monocots. Phyllogenetic analysis was performed using ClustalW. Species abreviation are as follows: Hv (*Hordeum vulgare*), Os (*Oryza sativa*), Zm (*Zea mays*), Bd (*Brachypodium distachium*), So (*Saccharum officinarum*), Sb (*Sorghum bicolor*), At (*Arabidopsis thaliana*), Rc (*Ricinus communis*), Sc (*Saccharomyces cerevisiae*), Dm (*Drosophila melanogaster*), Hs (*Homo sapiens*), Mm (*Mus musculus*).

Figure 4. Accumulation of autophagic bodies in Arabidopsis *atg5* mutant complemented with the *HvATG5* cds. Roots of *atg5* (**A**), wild type (**B**) and *atg5* 35S::*HvATG5* transformant (**C**) were incubated with MS medium containing concanamycin A for 6h and then observed by conventional transmision light microscopy. Black arrows indicate autophagic bodies located inside the vacuole.

Figure 5. The *atg5* 35S::*HvATG5* transformants are less senescing and less sensitive to nitrate limitation than *atg5* mutants. Wild type, *atg5* mutant and *atg5* 35S::*HvATG5* transformant were grown under low (A and B left panel) and high (B right panel) nitrate conditions. In A, phenotypes of plants 27, 42 and 66 days after sowing (DAS) are shown. Early leaf senescence was observed in *atg5* but not in *atg5* 35S::*HvATG5* plants under both low and high nitrate conditions. Planting was repeated

two times including three independent transformants that showed similar recovery phenotypes. Only one is shown here.

Figure 6. Transcript levels of *HvATG* genes are higher in leaves of plantlets grown under low nitrate (LN) compared to high nitrate (HN) conditions. A: Leaf ranks of 20 days old plants grown under low (0.5 mM NO_3^-) and high (5 mM NO_3^-). **B**: Chlorophyll content of L1, L2 and L3 from LN (light grey bars) and HN (dark grey bars). **C:** Transcript levels of *HvNAC13* (Senescence Associated Gene) and *HvGS2* (Senescence Repressed Gene) show opposite patterns. **D:** Transcript levels of *HvATG.* Transcript levels were measured by RT-qPCR. Only leaf ranks L1, L2 and L3 from both LN and HN plants were analysed. Results are shown as Log_{10} relative expression values. Data are mean ± SD of three independent biological replicates. *HvGAPDH* was used as reference gene.

Figure 7. Transcript levels of *HvATG* genes in plantlets after dark treatment. A: *H. vulgare* cv. golden promise plantlets were kept (Darken Leaves, DL; dark bars) or not (Control of Darken Leaves, CDL; white bars) in the dark for 4 days and harvested 18 days afetr sowing (T1; D18). After the dark period, plants were kept growing three more days (from D18 to D21) to test recovering under normal day/night photoperiod. Leaves of control plants (CRL; light grey bars) and of recovering plants after dark treatment (RL; dark grey bars) were harvested at T2. **B:** Leaf ranks L1, L2 and L3 harvested after dark treatment, at T1 on control and treated plants. **C:** Chlorophyll content of leaves from controls (CDL and CRL) and treated plants (DL and RL) at T1 and T2. **DE:** Transcript levels of *HvNAC13*, *HvSSU* (**D**) and *HvATG* (**E**) were measured by RT-qPCR in leaf ranks of plantlets submitted or not to dark treatment. Results are shown as Log_{10} relative expression for each gene. Data are mean ± SD of three independent biological replicates. *HvGAPDH* was used as reference gene.

Figure 8. Transcript levels of *HvATG* were increased in flag leaves during senescence. A: *H. vulgare* cv. carina flag leaves were harvested at different time points (T1: 95 DAS; T2: 99 DAS; T3: 103 DAS; DAS days after sowing). **B:** chlorophyll content decrease with leaf ageing. **C:** Transcript levels of *HvNAC13*, *HvGS2* and *HvATG* genes were measured by RT-qPCR. Results are shown as Log_{10} relative expression for each gene. Data are mean ± SD of three independent biological replicates. *HvActin* was used as reference gene.

Legends of Supplemental Material

Supplemental Figure 1. Phyllogenetic trees of HvATG1, HvATG18 and HvATG8 gene families.
Supplemental Figure 2. Alignment of HvATG proteins.
Supplemental Figure 3. Diagram of predicted splice variants of barley ATG genes.
Supplemental Table 1. Collection of yeast, Arabidopsis and rice ATG genes used as queries
Supplemental Table 2. Primers used for transcript amplification of HvATG genes by RT-qPCR
Supplemental Data Set 1: Fasta sequences of HvATG CDS and cDNA.

Supplemental Figure 1. Phyllogenetic trees of *HvATG1* (A), *HvATG18* (B) and *HvATG8* (C) gene families. DNA coding sequences (CDS) were translated to protein and then aligned using ClustalW. Species abbreviation are as follows: At (*Arabidopsis thaliana*), Tc (*Theobroma cacao*), Rc (*Ricinus communis*), Gm (*Glycine max*), Os *(Oryza sativa*), Hv (*Hordeum vulgare*), Sc (*Saccharomyces cerevisiae*), Dm (*Drosophila melanogaster*), Hs (*Homo sapiens*), Mm (*Mus musculus*), Ce (*Caenorhabditis elegans*), Tu (*Triticum urartu*) Zm (*Zea mays*), Bd (*Brachypodium distachium*), Cv (*Chlorella variabilis*), Gm (*Glycine max*), Lb (*Laccaria bicolor*), Vv (*Vitis vinifera*).

A

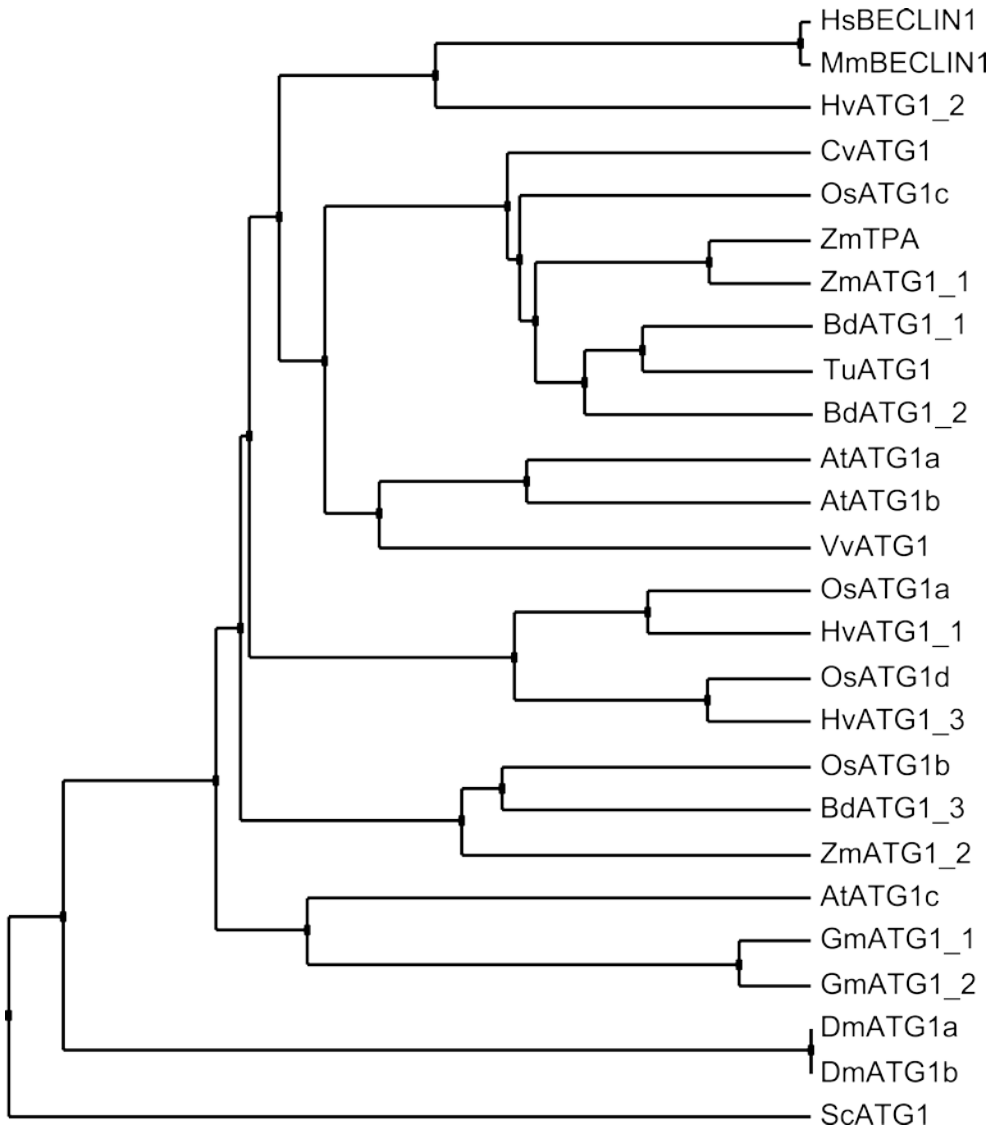

B

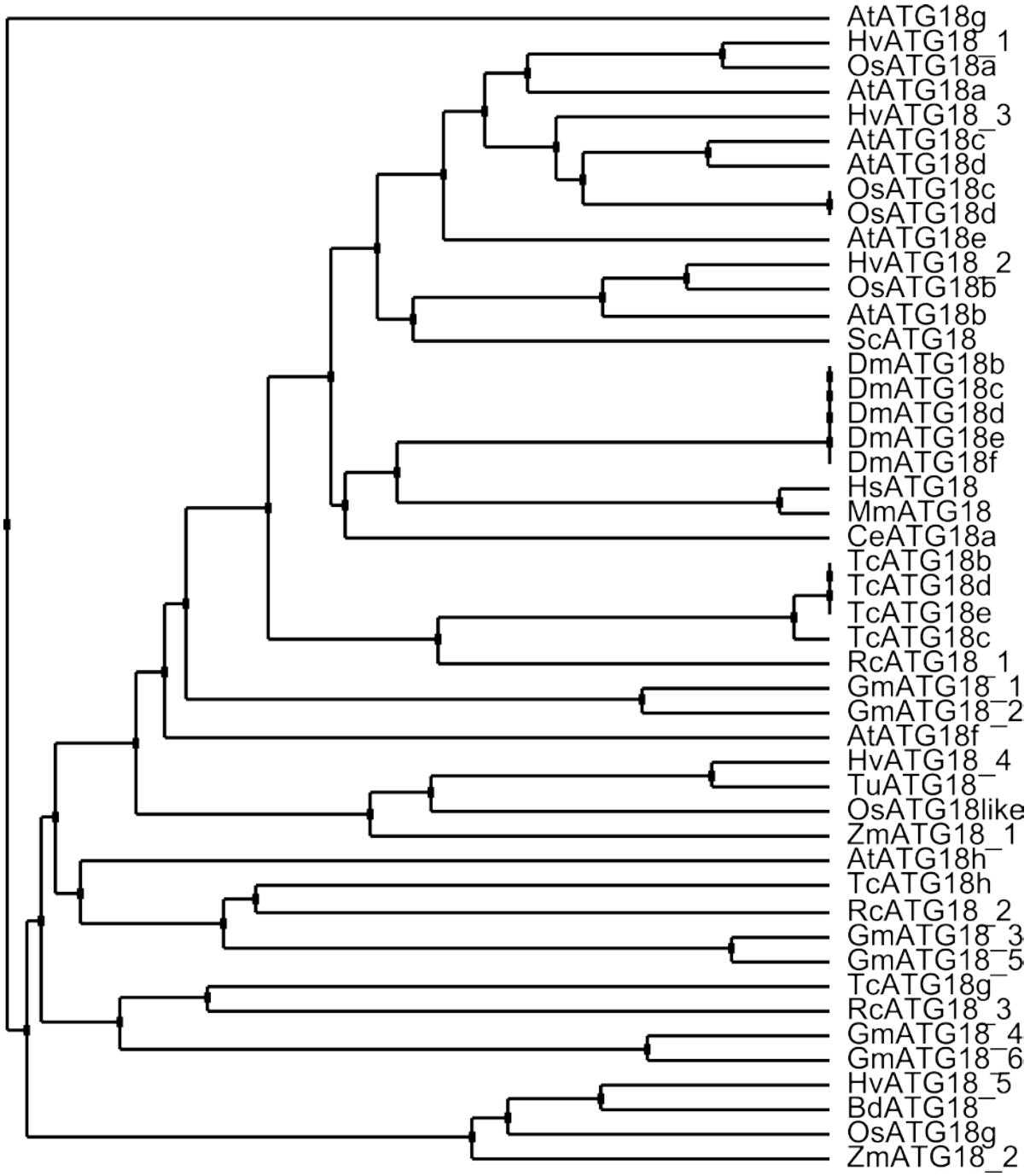
AtATG18g
HvATG18_1
OsATG18a
AtATG18a
HvATG18_3
AtATG18c
AtATG18d
OsATG18c
OsATG18d
AtATG18e
HvATG18_2
OsATG18b
AtATG18b
ScATG18
DmATG18b
DmATG18c
DmATG18d
DmATG18e
DmATG18f
HsATG18
MmATG18
CeATG18a
TcATG18b
TcATG18d
TcATG18e
TcATG18c
RcATG18_1
GmATG18_1
GmATG18_2
AtATG18f
HvATG18_4
TuATG18
OsATG18like
ZmATG18_1
AtATG18h
TcATG18h
RcATG18_2
GmATG18_3
GmATG18_5
TcATG18g
RcATG18_3
GmATG18_4
GmATG18_6
HvATG18_5
BdATG18
OsATG18g
ZmATG18_2

C

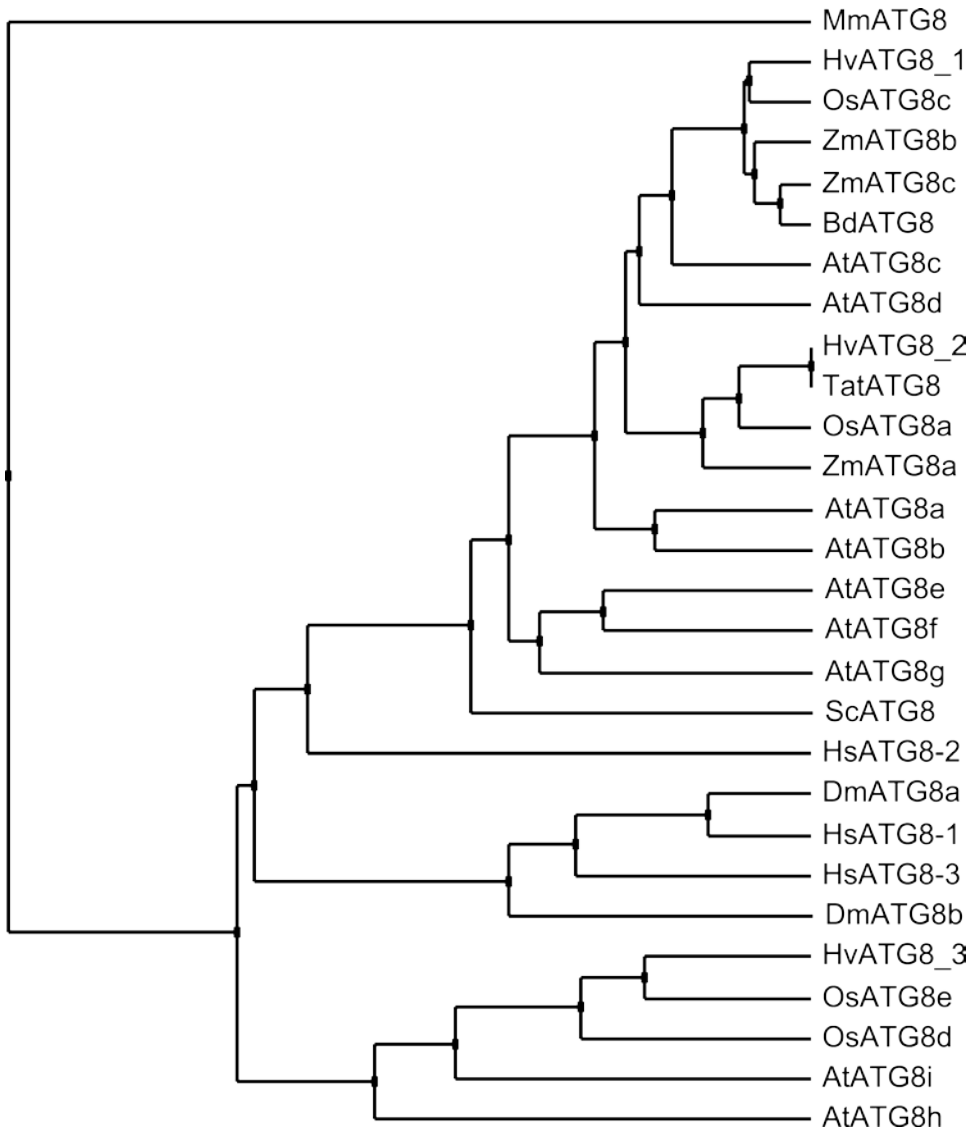
MmATG8
HvATG8_1
OsATG8c
ZmATG8b
ZmATG8c
BdATG8
AtATG8c
AtATG8d
HvATG8_2
TatATG8
OsATG8a
ZmATG8a
AtATG8a
AtATG8b
AtATG8e
AtATG8f
AtATG8g
ScATG8
HsATG8-2
DmATG8a
HsATG8-1
HsATG8-3
DmATG8b
HvATG8_3
OsATG8e
OsATG8d
AtATG8i
AtATG8h

Supplemental Figure 2. Alignment of HvATG proteins. HvATG3 (**A**), HvATG5 (**B**), HvATG6 (**C**), HvATG7 (**D**), HvATG9 (**E**), HvATG12 (**F**), HvATG13 (**G**) and HvATG16 (**H**) proteins of different species were aligned using ClustalW. Conserved amino acids (aa) are showed by shades of blue colors going from less conserved aa (light blue) to more conserved aa (dark blue). Species abreviation are as follows: Hv (*Hordeum vulgare*), Os *(Oryza sativa*), Ta (*Triticum aestivum*), Sc (*Saccharomyces cerevisiae*), At (*Arabidopsis thaliana*), Cr (*Caenorhabditis remanei*), Hs (*Homo sapiens*), Mm (*Mus musculus*), Dm (*Drosophila melanogaster*), Xl (*Xenopus laevis*), Dr (*Danio rerio*), Bd (*Brachypodium distachium*), So (*Saccharum officinarum*), Zm (*Zea mays*), Sb (*Sorghum bicolor*), Rc (*Ricinus communis*).

A

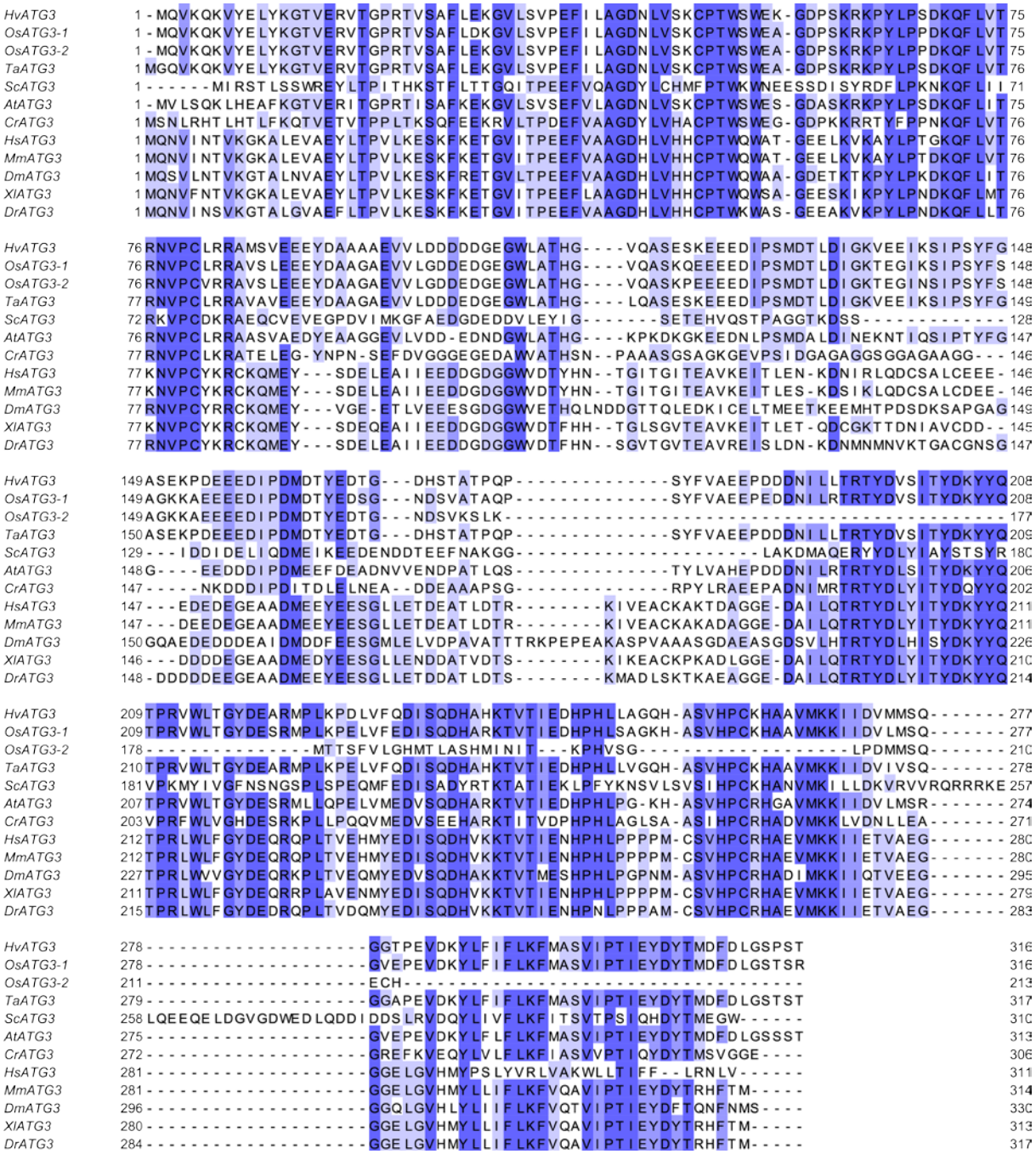

B

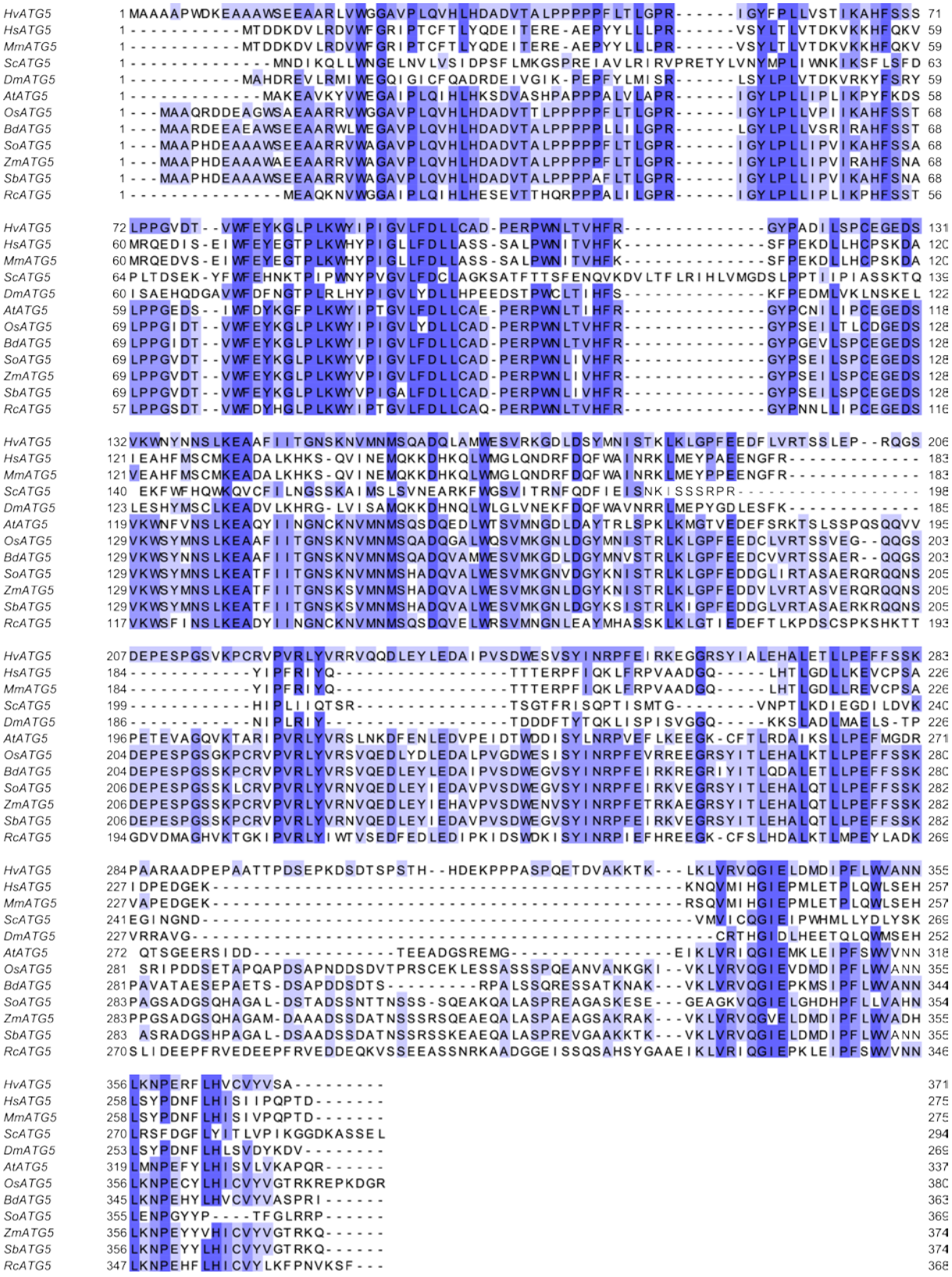
HvATG5
HsATG5
MmATG5
ScATG5
DmATG5
AtATG5
OsATG5
BdATG5
SoATG5
ZmATG5
SbATG5
RcATG5

C

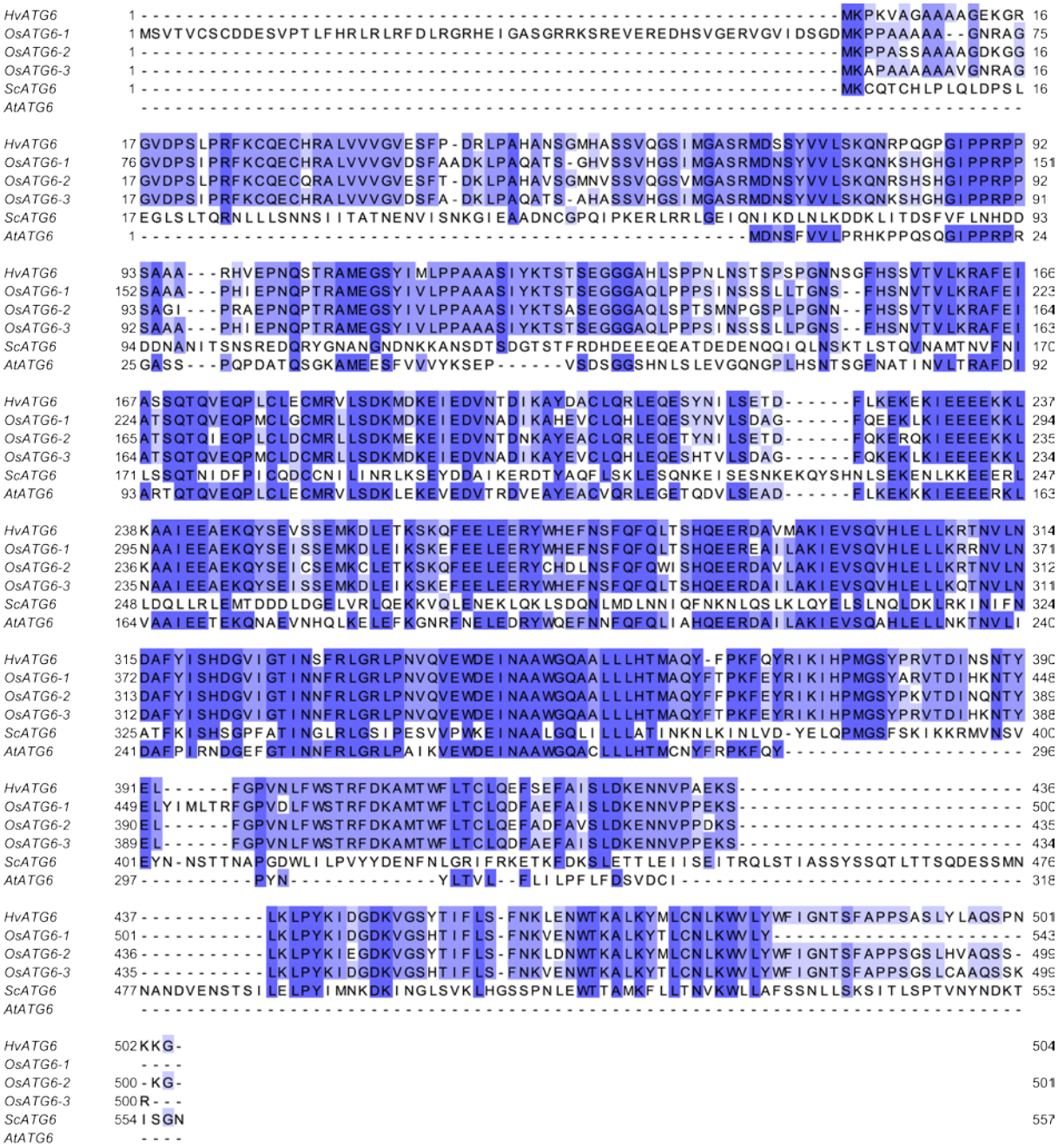

D

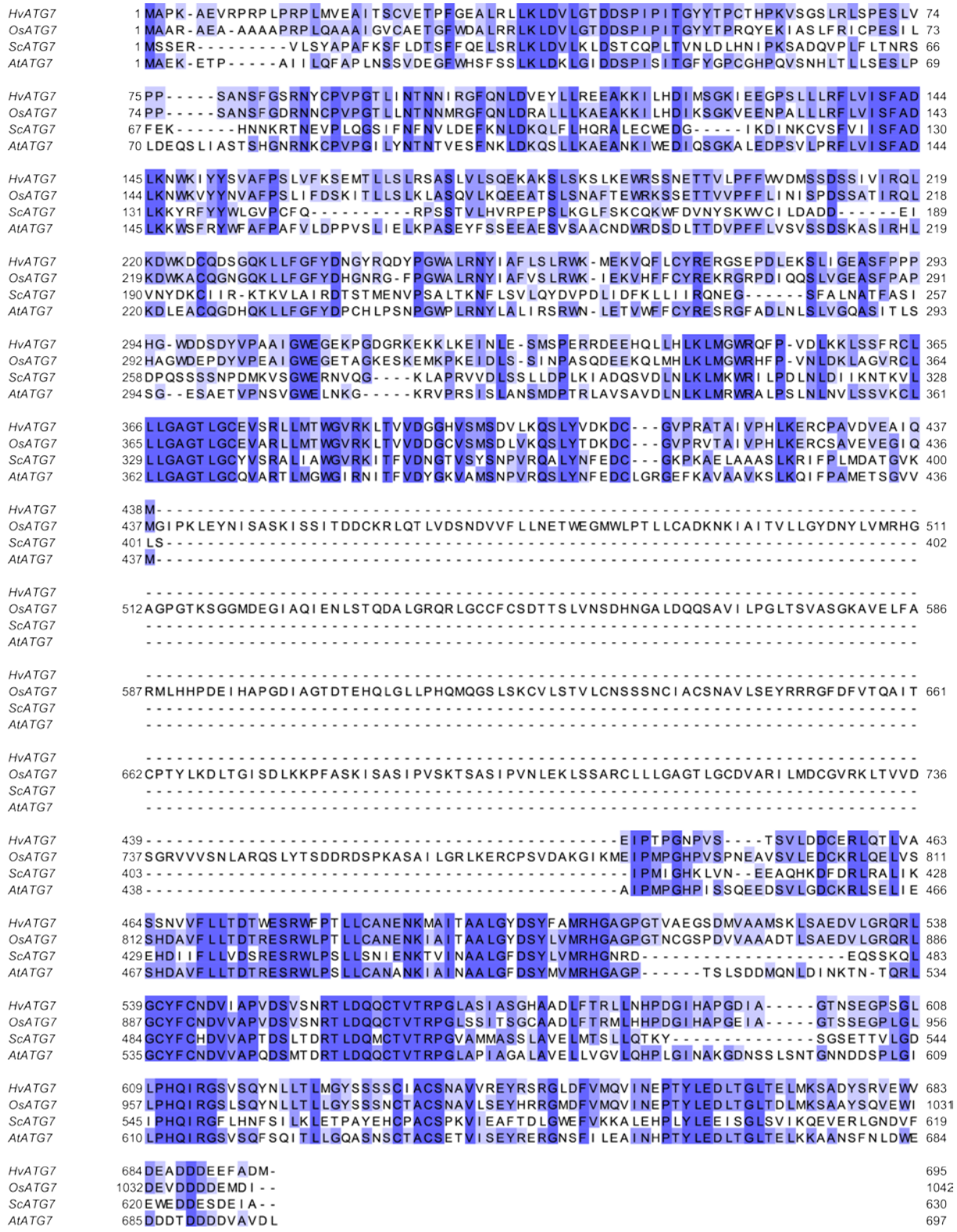

E

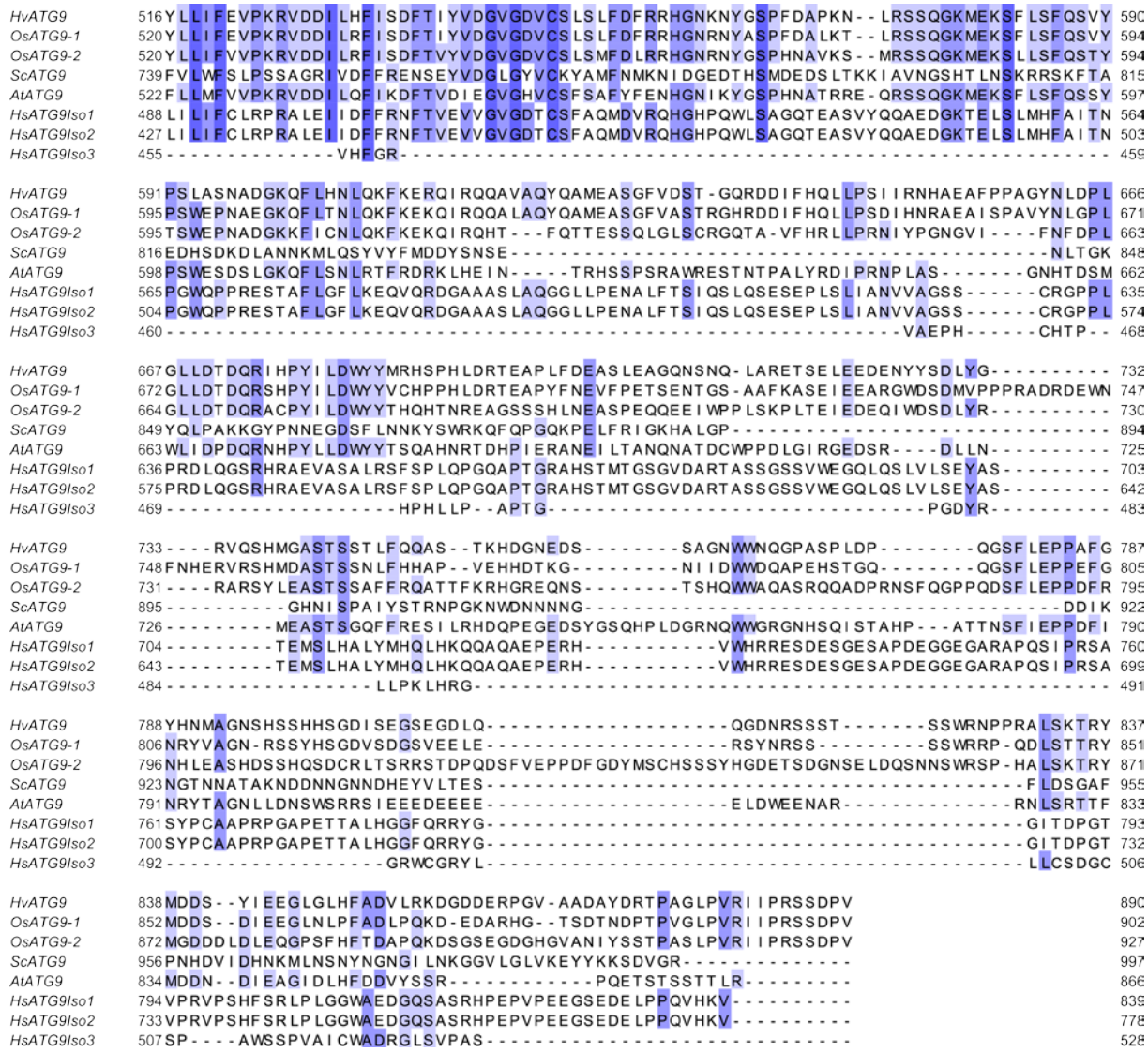
HvATG9 516 YLLIFEVPKRVDDILHFISDFTIYVDGVGDVCSLSLFDFRRHGNKNYGSPFDAPKN--LRSSQGKMEKSFLSFQSVY 590
OsATG9-1 520 YLLIFEVPKRVDDILRFISDFTIYVDGVGDVCSLSLFDFRRHGNRNYASPFDALKT--LRSSQGKMEKSFLSFQSVY 594
OsATG9-2 520 YLLIFVVPKRVDDILRFISDFTVYVDGVGDVCSLSMFDLRRHGNRNYGSPHNAVKS--MRSSQGKMEKSLLSFQSTY 594
ScATG9 739 FVLWFSLPSSAGRIVDFFRENSEYVDGLGYVCKYAMFNMKNIDGEDTHSMDEDSLTKKIAVNGSHTLNSKRRSKFTA 815
AtATG9 522 FLLMFVVPKRVDDILQFIKDFTVDIEGVGHVCSFSAFYFENHGNIKYGSPHNATRRE-QRSSQGKMEKSFLSFQSSY 597
HsATG9Iso1 488 LILIFCLRPRALEIIDFFRNFTVEVVGVGDTCSFAQMDVRQHGHPQWLSAGQTEASVYQQAEDGKTELSLMHFAITN 564
HsATG9Iso2 427 LILIFCLRPRALEIIDFFRNFTVEVVGVGDTCSFAQMDVRQHGHPQWLSAGQTEASVYQQAEDGKTELSLMHFAITN 503
HsATG9Iso3 455 ----------VHFGR---------- 459
HvATG9 591 PSLASNADGKQFLHNLQKFKERQIRQQAVAQYQAMEASGFVDST-GQRDDIFHQLLPSIIRNHAEAFPPAGYNLDPL 666
OsATG9-1 595 PSWEPNAEGKQFLTNLQKFKEKQIRQQALAQYQAMEASGFVASTRGHRDDIFHQLLPSDIHNRAEAISPAVYNLGPL 671
OsATG9-2 595 TSWEPNADGKKFICNLQKFKEKQIRQHT---FQTTESSQLGLSCRGQTA-VFHRLLPRNIYPGNGVI----FNFDPL 663
ScATG9 816 EDHSDKDLANNKMLQSYVYFMDDYSNSE---------- 848
AtATG9 598 PSWESDSLGKQFLSNLRTFRDRKLHEIN-----TRHSSPSRAWRESTNTPALYRDIPRNPLAS-------GNHTDSM 662
HsATG9Iso1 565 PGWQPPRESTAFLGFLKEQVQRDGAAASLAQGGLLPENALFTSIQSLQSESEPLSLIANVVAGSS------CRGPPL 635
HsATG9Iso2 504 PGWQPPRESTAFLGFLKEQVQRDGAAASLAQGGLLPENALFTSIQSLQSESEPLSLIANVVAGSS------CRGPPL 574
HsATG9Iso3 460 ----------VAEPH------CHTP-- 468
HvATG9 667 GLLDTDQRIHPYILDWYYMRHSPHLDRTEAPLFDEASLEAGQNSNQ-LARETSELEEDENYYSDLYG---------- 732
OsATG9-1 672 GLLDTDQRSHPYILDWYYVCHPPHLDRTEAPYFNEVFPETSENTGS-AAFKASEIEEARGWDSDMVPPPRADRDEWN 747
OsATG9-2 664 GLLDTDQRACPYILDWYYTHQHTNREAGSSSHLNEASPEQQEEIWPPLSKPLTEIEDEQIWDSDLYR---------- 730
ScATG9 849 YQLPAKKGYPNNEGDSFLNNKYSWRKQFQPGQKPELFRIGKHALGP---------- 894
AtATG9 663 WLIDPDQRNHPYLLDWYYTSQAHNRTDHPIERANEILTANQNATDCWPPDLGIRGEDSR----DLLN---------- 725
HsATG9Iso1 636 PRDLQGSRHRAEVASALRSFSPLQPGQAPTGRAHSTMTGSGVDARTASSGSSVWEGQLQSLVLSEYAS--------- 703
HsATG9Iso2 575 PRDLQGSRHRAEVASALRSFSPLQPGQAPTGRAHSTMTGSGVDARTASSGSSVWEGQLQSLVLSEYAS--------- 642
HsATG9Iso3 469 ----------HPHLLP--APTG---------- 483
HvATG9 733 ----RVQSHMGASTSSTLFQQAS--TKHDGNEDS--------SAGNWWNQGPASPLDP--------QGSFLEPPAFG 787
OsATG9-1 748 FNHERVRSHMDASTSSNLFHHAP--VEHHDTKG---------NIIDWWDQAPEHSTGQ--------QGSFLEPPEFG 805
OsATG9-2 731 ----RARSYLEASTSSAFFRQATTFKRHGREQNS--------TSHQWWAQASRQQADPRNSFQGPPQDSFLEPPDFR 795
ScATG9 895 ----------GHNISPAIYSTRNPGKNWDNNNNG---------- 922
AtATG9 726 ----------MEASTSGQFFRESILRHDQPEGEDSYGSQHPLDGRNQWWGRGNHSQISTAHP---ATTNSFIEPPDFI 790
HsATG9Iso1 704 ----------TEMSLHALYMHQLHKQQAQAEPERH----------VWHRRESDESGESAPDEGGEGARAPQSIPRSA 760
HsATG9Iso2 643 ----------TEMSLHALYMHQLHKQQAQAEPERH----------VWHRRESDESGESAPDEGGEGARAPQSIPRSA 699
HsATG9Iso3 484 ----------LLPKLHRG---------- 491
HvATG9 788 YHNMAGNSHSSHHSGDISEGSEGDLQ--------QGDNRSSST--------SSWRNPPRALSKTRY 837
OsATG9-1 806 NRYVAGN-RSSYHSGDVSDGSVEELE---------RSYNRSS----------SSWRRP-QDLSTTRY 851
OsATG9-2 796 NHLEASHDSSHQSDCRLTSRRSTDPQDSFVEPPDFGDYMSCHSSSYHGDETSDGNSELDQSNNSWRSP-HALSKTRY 871
ScATG9 923 NGTNNATAKNDDNNGNNDHEYVLTES---------FLDSGAF 955
AtATG9 791 NRYTAGNLLDNSWSRRSIEEEDEEEE---------ELDWEENAR----------RNLSRTTF 833
HsATG9Iso1 761 SYPCAAPRPGAPETTALHGGFQRRYG---------GITDPGT 793
HsATG9Iso2 700 SYPCAAPRPGAPETTALHGGFQRRYG---------GITDPGT 732
HsATG9Iso3 492 ----------GRWCGRYL---------LLCSDGC 506
HvATG9 838 MDDS--YIEEGLGLHFADVLRKDGDDERPGV-AADAYDRTPAGLPVRIIPRSSDPV 890
OsATG9-1 852 MDDS--DIEEGLNLPFADLPQKD-EDARHG--TSDTNDPTPVGLPVRIIPRSSDPV 902
OsATG9-2 872 MGDDDLDLEQGPSFHFTDAPQKDSGSEGDGHGVANIYSSTPASLPVRIIPRSSDPV 927
ScATG9 956 PNHDVIDHNKMLNSNYNGNGILNKGGVLGLVKEYYKKSDVGR---------- 997
AtATG9 834 MDDN--DIEAGIDLHFDDVYSSR----------PQETSTSSTTLR---------- 866
HsATG9Iso1 794 VPRVPSHFSRLPLGGWAEDGQSASRHPEPVPEEGSEDELPPQVHKV---------- 839
HsATG9Iso2 733 VPRVPSHFSRLPLGGWAEDGQSASRHPEPVPEEGSEDELPPQVHKV---------- 778
HsATG9Iso3 507 SP----AWSSPVAICWADRGLSVPAS---------- 528

F

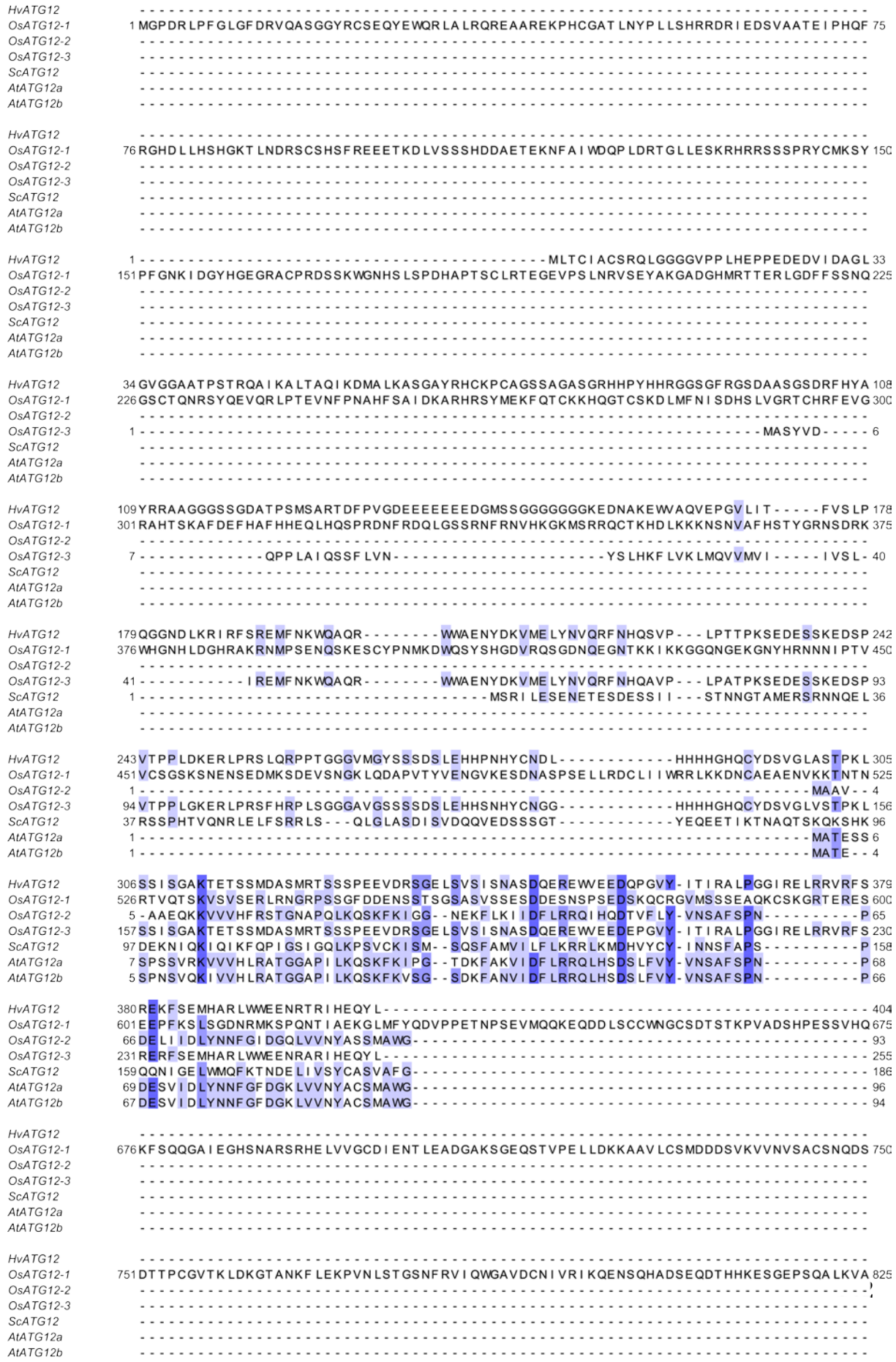
HvATG12
OsATG12-1
OsATG12-2
OsATG12-3
ScATG12
AtATG12a
AtATG12b


HvATG12
OsATG12-1 826 SNQQIPHQFDSDRDNPCTTRQADWDSCSSIPDLNCLPNMNTDDELEPVENVTFQVNEDGTNPQNNIKSLSASSCK 900
OsATG12-2
OsATG12-3
ScATG12
AtATG12a
AtATG12b
HvATG12
OsATG12-1 901 PTLQKEQSKQPEPIELTGGICERKDGNRFQSPNSHSGPSQQSIVEESSMSIDVFKCNLCEFIKNIIKPLWEDGLL 975
OsATG12-2
OsATG12-3
ScATG12
AtATG12a
AtATG12b
HvATG12
OsATG12-1 976 SREVHKIIVRKAVEKVTTVLGSKVPLTEIDACRFLLEESQNLEKLVQGYLDLYVGREVLKKKHDR 104C
OsATG12-2
OsATG12-3
ScATG12
AtATG12a
AtATG12b

G

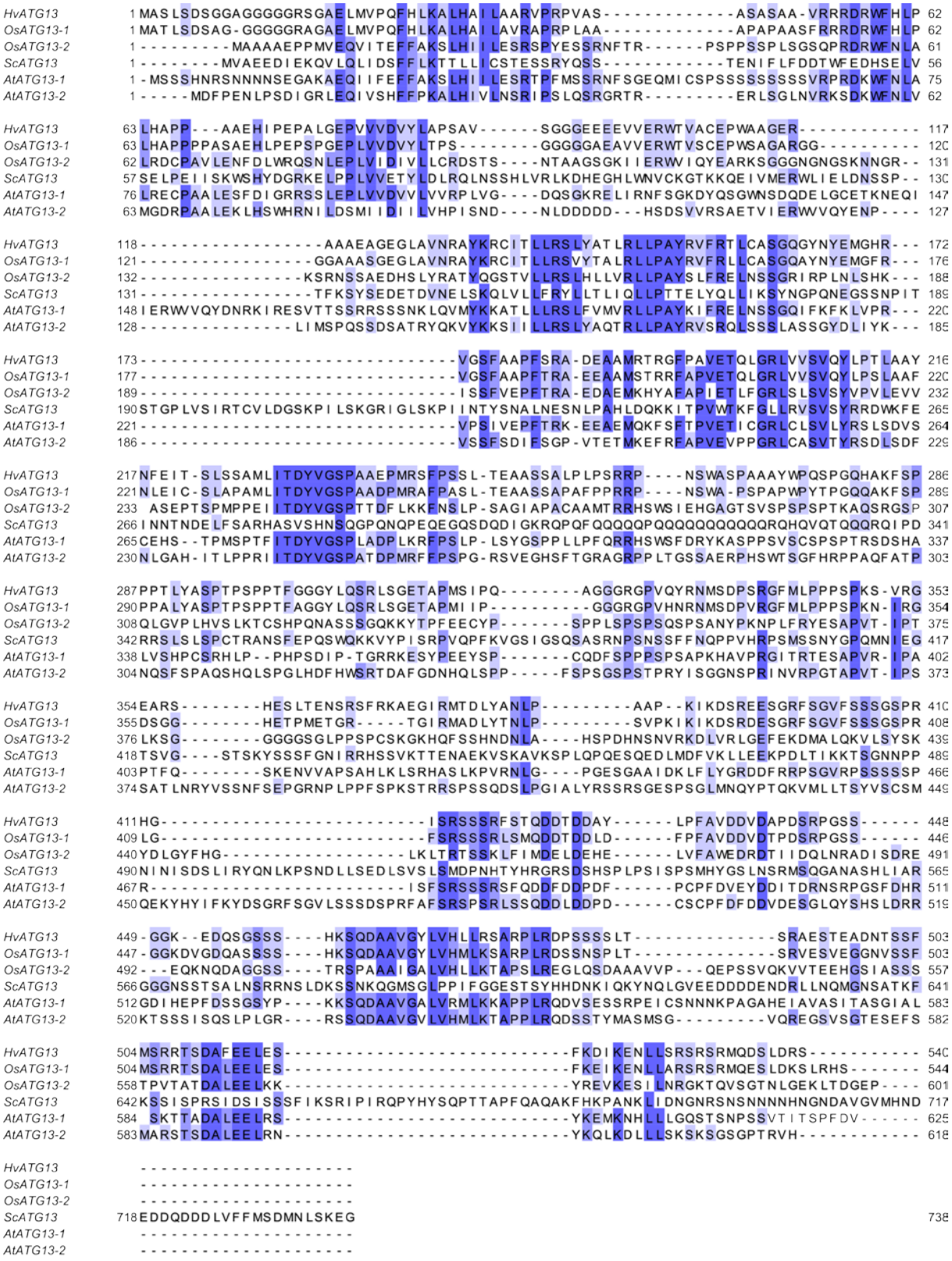

H

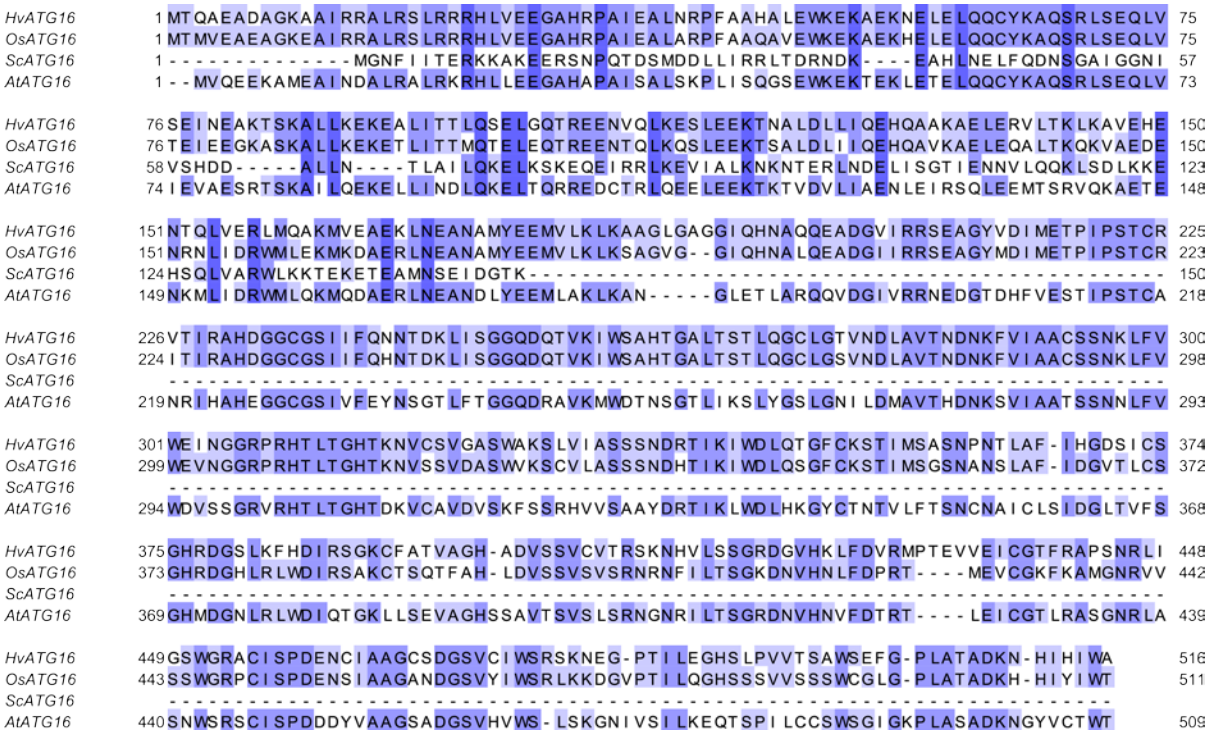
HvATG16 1 MTQAEADAGKAAIRRALRSLRRRHLVEEGAHRPAIEALNRPFAAHALEWKEKAEKNELELQQCYKAQSRLSEQLV 75
OsATG16 1 MTMVEAEAGKEAIRRALRSLRRRHLVEEGAHRPAIEALARPFAAQAVEWKEKAEKHELELQQCYKAQSRLSEQLV 75
ScATG16 1 ---------------MGNFIITERKKAKEERSNPQTDSMDDLLIRRLTDRNDK----EAHLNELFQDNSGAIGGNI 57
AtATG16 1 --MVQEEKAMEAINDALRALRKRHLLEEGAHAPAISALSKPLISQGSEWKEKTEKLETELQQCYKAQSRLSEQLV 73
HvATG16 76 SEINEAKTSKALLKEKEALITTLQSELGQTREENVQLKESLEEKTNALDLLIQEHQAAKAELERVLTKLKAVEHE 150
OsATG16 76 TEIEEGKASKALLKEKETLITTMQTELEQTREENTQLKQSLEEKTSALDLIIQEHQAVKAELEQALTKQKVAEDE 150
ScATG16 58 VSHDD-----ALLN----TLAILQKELKSKEQEIRRLKEVIALKNKNTERLNDELISGTIENNVLQQKLSDLKKE 123
AtATG16 74 IEVAESRTSKAILQEKELLINDLQKELTQRREDCTRLQEELEEKTKTVDVLIAENLEIRSQLEEMTSRVQKAETE 148
HvATG16 151 NTQLVERLMQAKMVEAEKLNEANAMYEEMVLKLKAAGLGAGGIQHNAQQEADGVIRRSEAGYVDIMETPIPSTCR 225
OsATG16 151 NRNLIDRWMLEKMKDAERLNEANAMYEEMVLKLKSAGVG--GIQHNALQEADGIIRRSEAGYMDIMETPIPSTCR 223
ScATG16 124 HSQLVARWLKKTEKETEAMNSEIDGTK---------- 150
AtATG16 149 NKMLIDRWMLQKMQDAERLNEANDLYEEMLAKLKAN-----GLETLARQQVDGIVRRNEDGTDHFVESTIPSTCA 218
HvATG16 226 VTIRAHDGGCGSIIFQNNTDKLISGGQDQTVKIWSAHTGALTSTLQGCLGTVNDLAVTNDNKFVIAACSSNKLFV 300
OsATG16 224 ITIRAHDGGCGSIIFQHNTDKLISGGQDQTVKIWSAHTGALTSTLQGCLGSVNDLAVTNDNKFVIAACSSNKLFV 298
ScATG16 ----------
AtATG16 219 NRIHAHEGGCGSIVFEYNSGTLFTGGQDRAVKMWDTNSGTLIKSLYGSLGNILDMAVTHDNKSVIAATSSNNLFV 293
HvATG16 301 WEINGGRPRHTLTGHTKNVCSVGASWAKSLVIASSSNDRTIKIWDLQTGFCKSTIMSASNPNTLAF-IHGDSICS 374
OsATG16 299 WEVNGGRPRHTLTGHTKNVSSVDASWVKSCVLASSSNDHTIKIWDLQSGFCKSTIMSGSNANSLAF-IDGVTLCS 372
ScATG16 ----------
AtATG16 294 WDVSSGRVRHTLTGHTDKVCAVDVSKFSSRHVVSAAYDRTIKLWDLHKGYCTNTVLFTSNCNAICLSIDGLTVFS 368
HvATG16 375 GHRDGSLKFHDIRSGKCFATVAGH-ADVSSVCVTRSKNHVLSSGRDGVHKLFDVRMPTEVVEICGTFRAPSNRLI 448
OsATG16 373 GHRDGHLRLWDIRSAKCTSQTFAH-LDVSSVSVSRNRNFILTSGKDNVHNLFDPRT----MEVCGKFKAMGNRVV 442
ScATG16 ----------
AtATG16 369 GHMDGNLRLWDIQTGKLLSEVAGHSSAVTSVSLSRNGNRILTSGRDNVHNVFDTRT----LEICGTLRASGNRLA 439
HvATG16 449 GSWGRACISPDENCIAAGCSDGSVCIWSRSKNEG-PTILEGHSLPVVTSAWSEFG-PLATADKN-HIHIWA 516
OsATG16 443 SSWGRPCISPDENSIAAGANDGSVYIWSRLKKDGVPTILQGHSSSVVSSSWCGLG-PLATADKH-HIYIWT 511
ScATG16 ----------
AtATG16 440 SNWSRSCISPDDDYVAAGSADGSVHVWS-LSKGNIVSILKEQTSPILCCSWSGIGKPLASADKNGYVCTWT 509

Supplemental Figure 3. Diagram of predicted splice variants of barley *ATG* genes. Data is according to genomic assembly database EnsemblPlants (http://plants.ensembl.org/). White boxes (□) represent untranslated regions, black boxes (■) represent coding regions and solid lines (\⁄) represent introns. The predicted amino acid (aa) lenght for each of the corresponding proteins is shown at right. See table 1 for EST and cDNA sequences supporting each gene. The upright bars represent a scale of 0.1 Kb. Asterisks and red boxes indicate gene models found in this study. sv1 to sv9 name extension indicate the different splice variants described on *Ensemblplants* web site. *HvATG5**, *HVATG7** and *HvATG16** have not been described by *EnsemblPlants*.

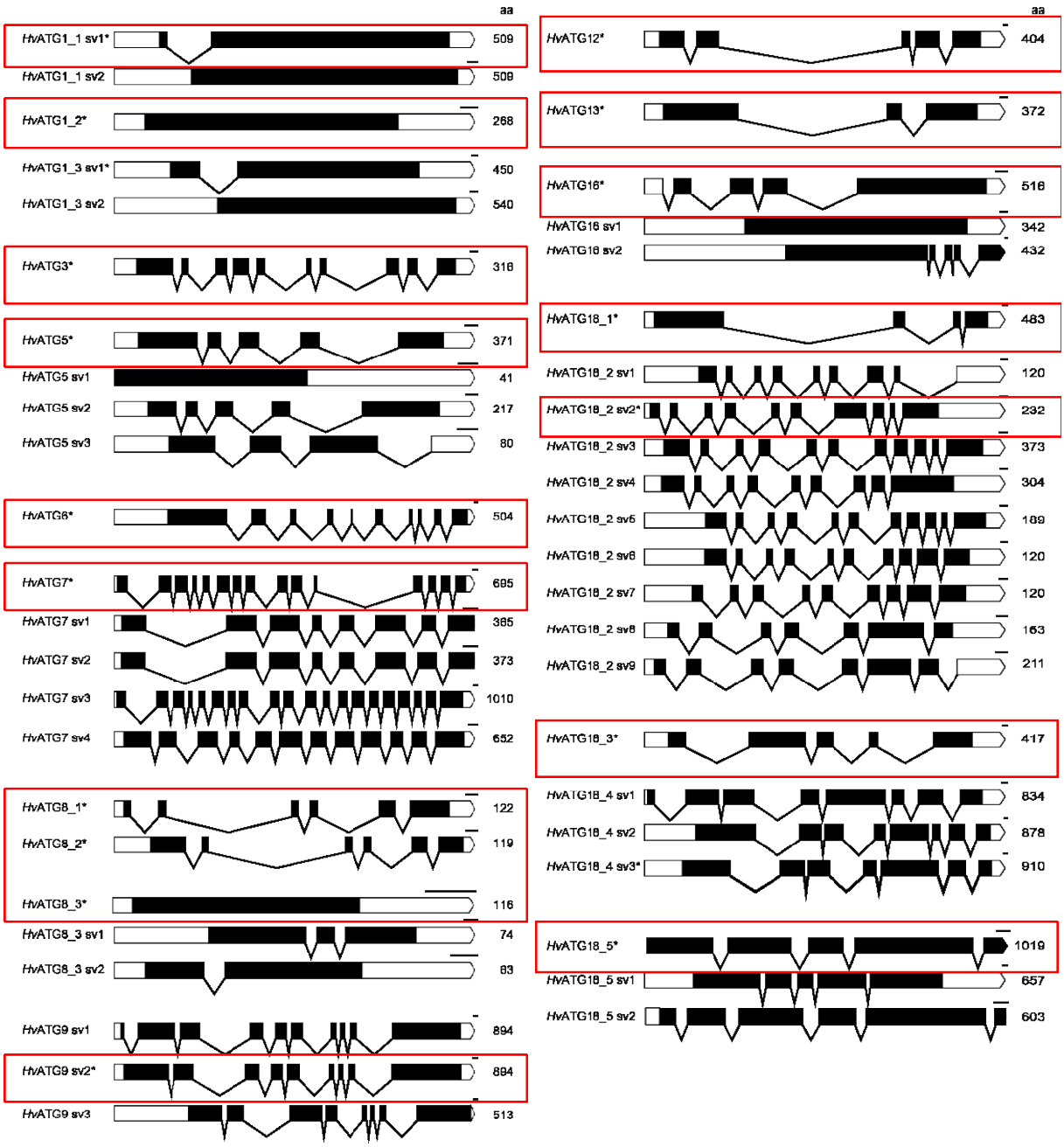

Supplemental Table 1. Collection of yeast, Arabidopsis and rice ATG genes used as queries

Gene in *S. cerevisiae*	Systematic gene name	No. of Amino acid residues	Gene in *A. thaliana*	TAIR locus	No. of Amino acid residues	Gene in *O. sativa*	TIGR locus	No. of Amino acid residues	Identity *O. sat.* to	
									Sacc.	*A. thal.**
				AT2G37840	733		*Os*01g60910	503	11%	16%
ATG1	YGL180W	897	**ATG1**	AT3G53930	711	**ATG1 like**	*Os*03g02980	464	14%	30%
				AT3G61960	626		*Os*03g16130	715	15%	47%
							*Os*07g48100	444	12%	14%
ATG2	YNL242W	1592	**ATG2**	AT3G19190	1839	**ATG2**	*Os*06g15700	1920	12%	32%
ATG3	YNR007C	310	**ATG3**	AT5G61500	313	**ATG3a**	*Os*01g10290	314	27%	72%
						ATG3b	*Os*10g41110	314	13%	36%
ATG4	YNL223W	494	**ATG4a**	AT2G44140	467	**ATG4a**	*Os*03g27350	474	18%	45%
			ATG4b	AT3G59950	477	**ATG4b**	*Os*04g58560	478	19%	48%
ATG5	YPL149W	294	**ATG5**	AT5G17290	337	**ATG5**	*Os*02g02570	380	12%	48%
							*Os*03g15290	544	15%	32%
ATG6	YPL120W	557	**ATG6**	AT3G61710	517	**ATG6**	*Os*03g44200	502	19%	36%
							*Os*01g48920	501	17%	36%
ATG7	YHR171W	630	**ATG7**	AT5G45900	697	**ATG7**	*Os*01g42850	1043	20%	34%
			ATG8a	AT4G21980	137					
			ATG8b	AT4G04620	122					
			ATG8c	AT1G62040	133	**ATG8a**	*Os*07g32800	120	71%	82%
			ATG8d	AT2G05630	164	**ATG8b**	*Os*04g53240	120	72%	83%
ATG8	YBL078C	117	**ATG8e**	AT2G45170	122	**ATG8c**	*Os*08g09240	121	71%	84%
			ATG8f	AT4G16520	121	**ATG8d**	*Os*11g01010	119	33%	31%
			ATG8g	AT3G60640	121	**ATG8e**	*Os*02g32700	87	51%	51%
			ATG8h	AT3G06420	119					
			ATG8i	AT3G15580	115					
ATG9	YDL149W	997	**ATG9**	AT2G31260	866	**ATG9**	*Os*03g14380	903	13%	48%
						ATG9	*Os*10g07994	927	14%	47%
ATG10	YLL042C	167	**ATG10**	AT3G07525	226	**ATG10a**	*Os*04g41990	199	15%	40%
						ATG10b	*Os*12g32210	223	14%	42%
						ATG12	*Os*06g10340	94	2%	1%
ATG12	YBR217W	186	**ATG12a**	AT1G54210	96	**ATG12 like**	*Os*09g27230	256	16%	70%
			ATG12b	AT3G13970	94	**ATG12 like**	*Os*03g37140	458	8%	5%
ATG13	YPR185W	738	**ATG13**	AT3G49590	618	**ATG13**	*Os*11g06320	602	10%	24%
			ATG13	AT3G18770	625	**ATG13 like**	*Os*02g43040	544	10%	32%
ATG16	YMR159C	150	**ATG16**	AT5G50230	509	**ATG16**	*Os*03g53510	510	5%	54%
			ATG18a	AT3G62770	425					
			ATG18b	AT4G30510	312	**ATG18a**	*Os*01g70780	458	7%	6%
			ATG18c	AT2G40810	393	**ATG18b**	*Os*02g54910	375	17%	61%
ATG18	YFR021W	500	**ATG18d**	AT3G56440	391	**ATG18c**	*Os*01g07400	418	20%	49%
			ATG18e	AT5G05150	374	**ATG18g**	*Os*05g33610	769	20%	49%
			ATG18f	AT5G54730	763	**ATG18 like**	*Os*01g57720	871	21%	21%
			ATG18g	AT1G03380	959	**ATG18 like**	*Os*05g07710	383	6%	6%
			ATG18h	AT1G54710	927					

Sequences compared with the single gene product in yeast and the a isoform from Arabidopsis*

Supplemental Table 2. Primers used for transcript amplification of *HvATG* genes by RT-qPCR

Gene	Accession	Sequence 5'-3'		Source	Amplification size (bp)
HvATG1_2	AK376609	Fwd Rev	CTACACGGTTGCTTCCCTTC GGAGAGGAGGGACTCGAGATT	This work	55
HvATG1_3	AK252590	Fwd Rev	GCCGGCCTCTAGAAAAAGAA GTTGGGTTGGGAGGTCTGTT	This work	51
HvATG3	AK252967	Fwd Rev	GAAACAGACCTCCCAACCCA ATCAAAGCAGAAAGTGGGGC	This work	
HvATG5	AK362511	Fwd Rev	GCCGATCCTGAACCTGCGGC GGGCTCGCTGGAGGTGGTTT	This work	101
HvATG6	AK362923, AM075824	Fwd Rev	GAATGCAGCGTTGTTTGCAT ATTAAGGAGGGTGGAGCCAG	This work	
HvATG7	AK367931	Fwd Rev	GACTGGCCTCCATAGCATCT CTGTATTCACGCACTACCGC	This work	212
HvATG8_1	AK251678	Fwd	CGCGTCGCAAACCCTCGTCC	This work	123
		Rev	CGGTTAGCCTCCGCCTGCCT		
HvATG8_2	AK248733	Fwd Rev	ACCGAGCACCCCCTGGAGAG CGAAGCAGTCGGTGGCAAGGT	This work	249
HvATG8_3	AK250515	Fwd Rev	CTGTCTCCAGGAACGGCGCT ACGCCCATGCTTCCCAGAGG	This work	357
HvATG13	AK365609	Fwd Rev	CGCGATTCAAAACCACGAAC GAAGGAGGAGTTCGTTCGGA	This work	86
HvATG16	AK361491	Fwd Rev	AGCTTAATGAGGCCAATGCG GCTTCAGACCGACGAATGAC	This work	
HvATG18_1	AK364793	Fwd Rev	ATCAGGGTCGAGCACTATGG CTCAGCGGCATTGAAGATCC	This work	
HvATG18_2	AK371787	Fwd	TTTCCTGCTGTGAGGACTGT	This work	
		Rev	TGAAGGAACGTGGTCGGTAA		
HvATG18_3	AK364502	Fwd	GATCCGACAAGCAGCATCAG	This work	
		Rev	CGATCAGATTGATGAGCTTCAGA		
HvATG18_5	AK362065, AK371649	Fwd	GGAGGGGTTTTTGCCTTCAG	This work	
		Rev	CGCGGCATGACTTTATTCCA		
HvGS2	AK360336	Fwd	AAGCTGGCGCTGAAGGTATGAAGG	Goodal *et al.,* 2013	124
		Rev	GACGGAACCACAGGATCAACAAGAATG		
HvNAC13	AK376297	Fwd Rev	ATGCCGCCGCACATGATGTAC ACAGGTCGCCGGAATTAGCG	Christiansen *et al.,* 2011	
HvActin	AY145451	Fwd Rev	CGACAATGGAACCGGAATG CCCTTGGCGCATCATCTC	Rapacz *et al.,* 2012	
HvGAPDH	AAA32956	Fwd Rev	GCTCAAGGGTATCATGGGTTACG GCAATTCCACCCTTAGCATCAAAG	Hebelstrup *et al.,* 2010	98

PAPER 3

Physiological and metabolic consequences of autophagy deficiency for the management of nitrogen and protein resources in Arabidopsis leaves depending on nitrate availability

The aim of this work was to show the role of autophagy in the nitrogen management and proteolysis during ageing in *Arabidopsis thaliana*. This work was mainly part of Anne Guiboileau thesis, who was a PhD student that worked in my laboratory from 2008 to 2011. I contributed to the second paper of Anne Guiboileau by performing protease activity analyses (endopeptidases, carboxypeptidases and aminopeptidases) thanks to the training of Pr. Andreas Fischer who came to our laboratory in INRA-Versailles as an invited researcher by the CropLife ITN.

In this report, total soluble protein abundance, metabolite contents, C/N ratio and enzymatic activities were evaluated in wild type plants and Autophagy (*atg*) defective mutants grown under two different nitrate conditions: high (10 mM) and low (2 mM).

Results showed that *atg* mutants trend to accumulate large amount of nitrogen related compounds during senescence that includes proteins, ammonium and free amino acids. Western blot assays using specific antibodies showed an accumulation of catalase, glutamate dehydrogenase and ribosomal S6 and L13 subunits as well as degradation products of Rubisco LSU and GS2 proteins. This accumulation occurred in spite of a high endopeptidase and carboxypeptidase activities.

In contrast to nitrogen related compound accumulation, there was a decrease in carbohydrate contents including sugars (glucose, fructose and sucrose) and starch, which was reflected in the disruption of the C: N status in the *atg* mutants.

BLANK PAGE

Physiological and metabolic consequences of autophagy deficiency for the management of nitrogen and protein resources in Arabidopsis leaves depending on nitrate availability. Guiboileau et al, 2013. New Phytologist, Vol. 199, pp. 683–694.

CONCLUSION PERSPECTIVES

CONCLUSION and PROSPECTS

Scientific issues:

In this study we performed biochemical, physiological and molecular analyses of barley leaf senescence. I monitored natural and stress induced leaf senescence in two different models, vegetative stage (leaf rank in plantlets) and reproductive stage (flag leaves) grown under optimal and stress conditions including nitrate limitation and dark. We focused mainly on the measurements of senescence traits such as chlorophyll contents, photosynthesis and senescence-associated genes as well as the enzymatic activities related with nitrogen recycling and remobilisation such as proteases and glutamine synthetases.

It was found that in both models, leaf ranks and flag leaf, the same picture of leaf senescence was observed, including the decrease of all nitrogen containing compounds, an increase of nitrogen remobilisation markers such as GS1 proteins, high proteolytic activities and a decrease of Rubisco and GS2 proteins.

It was also observed that, in addition to ageing, during low nitrate conditions plants showed an increment of glutamine synthetase GS activity and GS1 protein contents indicating that nitrogen limiting conditions promote a high GS activity associated mainly with the nitrogen remobilisation function of GS1.Subsequently, the expression of the genes related to nitrogen remobilisation in barley *HvGS1* (glutamine synthetase 1) and *HvASN* (asparagine synthetase) was evaluated. In order to do this, the sequences of three barley *HvGS1* isoforms (*HvGS1_1, HvGS1_2* and *HvGS1_3*) previously described by Goodall *et al* (2013) and two *HvASN* isoforms (*HvASN1* and *HvASN2*) described by Moller *et al* (2003) were used to design specific primers and to measure their levels in our samples using RT-qPCR. Through sequence alignment analyses using the recently published barley genome sequence (IBSC, 2012) and *GS* and *ASN* sequences from other species as queries, two additional *HvGS1* genes, the prokaryote-like *HvGS1_4* and *HvGS1_5* and three *HvASN* genes, *HvASN3*, *HvASN4* and *HvASN5* were identified.

All five *HvGS1* genes were highly expressed in senescing leaves from both plantlets and reproductive stage compared to young ones, and in response to dark stress, only *HvGS1_3* was highly expressed while *HvGS1_4* and *HvGS1_5* were repressed. In the case of *HvASN* genes, their expression was highly induced during senescence in samples grown in high nitrate (HN) conditions but repressed under low nitrate (LN) conditions. The opposite

expression of *HvASN* genes during senescence in plants grown under different nitrate conditions, HN and LN, suggests that AS protein is needed for nitrogen remobilisation specifically under high nitrate. This also showed that natural and stress-induced senescence might have different gene expression patterns at least in the case of *HvASN*.

In flag leaves, *ASN* gene expression during senescence showed opposite patterns, as *HvASN3* increased with age while *HvASN4* decreased. Such differences might be attributed to the sugar:amino acid ratio in leaves, since asparagine synthetase expression can be regulated by the sugar content (Oliveira et al., 2002; Gaufichon *et al.*, 2010).

From phylogenetic analyses, it was found that *HvASN1* and *HvASN2* clustered with Arabidopsis *AtASN1*, while *HvASN3* and *HvASN4* were grouped with *AtASN2*. These similarities were also confirmed by the high expression of *HvASN1* under dark stress (in the same way as *AtASN1*, also called *Dark Inducible 6*) (Moller *et al.*, 2003; Oliveira *et al.*, 2002) and the repression of *HvASN3* gene expression during prolonged dark (similar to *AtASN2*, which is known to be repressed by dark and induced by sugars) (Gaufichon *et al.*, 2010).

Using similar methods, nineteen homologous genes of the autophagy pathway, and other senescence-related processes, were found in barley using *ATG* gene sequences from yeast, Arabidopsis and rice as queries. Specific primers were designed to measure transcript levels by RT-qPCR. Eight single genes (*HvATG3*, *HvATG5*, *HvATG6*, *HvATG7*, *HvATG9*, *HvATG12*, *HvATG13* and *HvATG16*) and three family genes (*HvATG1*, *HvATG8* and *HvATG18*) were found, the proteins of which showed sequence similarities with their homologous in yeast, Arabidopsis and rice as well as amino acid residues essentials for their function.

Transcript levels of these genes were in general highly increased in senescing leaves of plantlets (with exception of *HvATG5* and *HvATG18_3*, *HvATG13* and *HvATG6* in LN conditions). All *ATG* genes also were more highly expressed under LN conditions and dark stress due to carbon starvation. The least responsive gene to dark stress was *HvATG5*. Interestingly, in the reproductive stage, *HvATG5* levels were highly expressed in senescing flag leaves compared to younger leaves. Since the flag leaf is the major intermediary for nutrient remobilisation to the developing grain, such results agree with the role of *ATG5* in nitrogen remobilisation to the seeds reported by Guiboileau *et al* (2012). This is also consistent with the late expression of *AtATG5* during leaf senescence in Arabidopsis described by Avila-Ospina *et al* (2014).

My work also provides a metabolome analysis of plantlets and flag leaf senescence. Four significant senescence-related traits were observed (i) an increase of carbohydrates (sugar, lipids and fatty acids) probably products derived from the degradation of membranes and cell wall (ii) a decrease of hexoses and trioses from the glycolysis pathway (iii) an increase of organic acids from the TCA cycle and (iv) a decrease in most of the amino acids, with the exception of cysteine and lysine, related to the glutathione and the anaplerotic respiratory pathways respectively.

These data allow us to compare senescence-related metabolisms in barley and Arabidopsis. The accumulation of hexoses and minor amino acids in Arabidopsis senescing leaves occurs very differently in with barley. Such differences generate questions about the mechanisms of catabolism and remobilisation of nitrogen-containing compounds in these two species, and require further analyses to explore the specificities and the variability of the molecular and metabolic changes occurring during leaf senescence in both species.

In brief, we believe that the results of this work give rise to the possibility of further exploration of senescence-related processes including autophagy and nutrient remobilisation metabolism in barley and other crops such as wheat for example.

Short term prospects

Response of genetic and metabolic components to additional stress conditions such as drought and low temperatures

Due to the differential responses of plants to different types of stress that may cause senescence, it is important to identify the key processes that make plants either overcome poor conditions or guarantee the survival of their progeny. In the case of crops, good tolerance to difficult environmental conditions represents a characteristic highly desired by breeders with high agronomical and economical value. The measurement of expression levels of genes related to senescence or nitrate remobilisation such as *ATG, GS1* and *ASN* genes in barley grown under drought and cold stress could give an idea of the regulation of senescence and stress responses as well as the understanding of general or specific mechanisms used by monocot crops to face these situations. For example, the differential response of *AtASN* isoforms to light and sugar contents (Lam *et al.*, 2003; Moller *et al.*, 2003), the differential expression of the three *HvGS1* isoforms in distinct organs and according to the nitrogen source (Goodall *et al.*, 2013) and the increase in expression of *HvATG5* observed in old flag

leaves but not in old leaves of plantlets (this work) suggest that the regulation of senescence and nutrient remobilisation is influenced by specific environmental and developmental factors in each case.

Establishment of marker genes for senescence and nutrient remobilisation

The identification of genes related to senescence and nutrient remobilisation is also an important clue for understanding their regulation. The discovery of *SAG12* in Arabidopsis allowed monitoring of senescence in plants and to the unraveling of the importance of cysteine proteases for nutrient remobilisation (Grbic, 2003). In wheat, the *NAC* gene *TaNAM-B1* was shown not only to regulate senescence but also protein, Zn and Fe contents in the grain (Uauy *et al.,* 2006). In maize, two isoforms of glutamine synthetase, *ZmGS1-3* and *ZmGS1-4*, were shown to be involved with kernel yield and their relationship with the transport of asparagine from leaves to seeds was also suggested (Martin *et al.,* 2006). In barley, many genes have been associated with senescence under optimal and stress conditions (Parrott *et al.,* 2007; Hollmann *et al.,* 2014) but their specific function is still unknown. In this study it was seen, that some *ATG* genes, for instance *HvATG6*, *HvATG7*, *HvATG16* or *HvATG18* are highly expressed during senescence in both plantlets and flag leaf while *HvATG5* was over-expressed mainly in senescing flag leaves indicating that these genes could have distinct roles at different times of the senescence process possibly with *HvATG6, HvATG7, HvATG16* and *HvATG18* being regulators in the early stages of senescence, while *HvATG5* could be involved in later steps and the remobilisation of nutrients to developing grains as Arabidopsis (Guiboileau *et al.,* 2012; Avila-Ospina *et al.,* 2014). Other strategies such as identification of the proteases involved in the high proteolytic activity found in barley senescing leaves could lead to the identification of new senescence-related genes in barley.

Responses of homologous senescence and nutrient remobilisation-associated genes

In this work, barley homologues of yeast, Arabidopsis and rice *ATG, GS1* and *ASN* genes were identified and their transcript levels were measured during senescence and nutrient limitation. Previous studies have demonstrated the relationship of these genes with senescence, stress response and yield in Arabidopsis, maize and barley (Martin *at el,* 2006; Gaufichon *et al.,* 2010; Guiboileau *et al.,* 2012; Christiansen *et al.,* 2014; Hollmann *et al.,* 2014) as well as their conserved functionality through several plant species. The study of

homologous functions in crop plants could be a good strategy for finding new candidate genes with a potential agronomical importance. For instance, yeast *ATG8* homologous in Arabidopsis and soybean showed the role of this gene in plant senescence, nutrient stress resistance, nitrogen use efficiency and yield (Slavikova *et al.,* 2005; Xia *et al.,* 2012). The study of homologeus of maize *GS1-3* and *GS1-4*, sweet potato cysteine protease *SPCP3* or tobacco cysteine proteases *CP1* and *CP2* (Martin *et al.,* 2006; Chen *et al.,* 2006; Bayene *et al.,* 2006) in barley and other important crops such as rapeseed or wheat could give clues about the regulation of the senescence-related nutrient remobilisation that could be used for the improvement of yield or grain nutrient content.

Genome association studies

In order to make an association between the genes found in this work (*HvATG*, *HvGS* and *HvASN*) and senescence and nutrient remobilisation-associated traits, the analysis of their gene sequences in different barley varieties with known altered senescence timing and improved or impaired yield and GPC could be performed. With this, we could establish if single-nucleotide polymorphisms (SNPs) in our gene sequences are related to gene function, and therefore, if they are associated with our traits of interest (yield, GPC or delayed senescence) in these plant varieties. Similar studies were performed with barley *HvNAM-1* and *HvNAM-2*, the orthologues of wheat *TaNAM-B1* (Uauy *et al.,* 2006). Wheat varieties "Karl" (with low GPC) and "Lewis" (with high GPC) showed differences in two SNPs of *HvNAM-1* that translated two amino acid changes (Distelfeld *et al.,* 2008), which suggest a similar role of *HvNAM-1* in the regulation of GPC in barley as that observed in wheat.

Selection of candidates for functional analyses

Most of the genes described and further analyzed in this work proved to have a senescence related pattern and also to respond to nutrient stress. However, a selection of potential candidates for further functional analyses needs to be carried out in order to take a more specific approach. At the moment, our results have shown a differential expression of *HvATG5* in senescing leaves according to the developmental stage (highly expressed in senescing flag leaf and not in senescing plantlet leaves). This feature, together with previous reports of the important role of Arabidopsis *AtATG5* in nitrogen remobilisation (Guiboileau *et al.,* 2012), suggests the role of this gene in the regulation of nutrient remobilisation to the

grain and make it a good candidate for subsequent functional analysis using transgenic plants with increased or decreased expression of this gene.

Long Term Prospects

Functional analysis of barley senescence associated barley genes

The transformation of barley plants to manipulate the expression of genes related with lifespan and nutrient remobilisation for functional analysis is one of biggest interests of the CropLife consortium and the SATURNE (Senescence, AuTophagy, nUtrient Remobilisation and Nitrogen use Efficiency) group.

In this work, based on the results observed, a possible role of *HvATG5* in the remobilisation of nutrients to the grain during senescence has been suggested. This putative role is supported by previous studies where the association of *ATG5* with lifespan, stress response, metabolism and remobilisation of nutrients in other plants and animals is shown. For instance, Guiboileau *et al* (2012) showed that Arabidopsis *atg5* knockout plants are impaired in the remobilisation of nitrogen from leaves to seeds during senescence compared with wild-type plants. On the other hand, the over-expression of *ATG5* in mice leads to lifespan extension, leanness, increased insulin sensitivity and improve motor function, which is considered an *anti-ageing phenotype* (Pyo *et al.,* 2013).

All ATG functions are encoded by single genes in yeast. In other species, these ATG functions can be encoded by gene families. Depending on the species, one or more isoforms could encode an ATG function. Two examples of this are *ATG8* (9 genes in Arabidopsis; 3 genes in barley) and *ATG6* (1 single gene in Arabidopsis; 3 genes in rice). In the case of ATG5 function, only a single copy has been found in all species where this gene has been described. A very convenient result as the number of target genes for transgenics is reduced to one.

Our results, the fact that the function is regulated by just one gene and the strong evidence that supports the important role of *ATG5* in the regulation of lifespan and nutrient management in other species, make *HvATG5* a good candidate for subsequent functional analysis.

Another point that needs to be fully taken into account is the use of proper gene promoters in order to assure either the efficient over-expression or the suppression of our gene of interest. The promoter of the cauliflower mosaic virus (CaMV) 35S gene is the most commonly used

in dicots to drive transgene expression in a constitutive manner (Benfey and Chua, 1990). However, its activity in monocots is substantially lower (Christensen and Quail, 1996), which indicates the need of specific promoters for each dicots and monocots.

Currently, several monocot-derived promoters are used to engineer cereal crops, the maize *ZmUbi1* and the rice *OsAct1* (Actin-1), *OsTubA1* (Tubulin-A), *OsCc1* (Cytochrome c) and *OsRUB1* and *2* (Ubiquitin) are some examples (Park *et al.,* 2010). These promoters are highly active in monocot crops but each one can induce different patterns of expression depending on the cell type and developmental stage. For instance, *ZmUbi1* drives a high expression mostly in young leaves and roots, but when these organs mature, these expression levels decrease (Cornejo *et al.,* 1993). In contrast, the *OsCc1* promoter is very active in both vegetative and reproductive tissues of transgenic rice plants (Jang *et al.,* 2002).

The use of an inaccurate promoter could lead to poor correlations between the gene expression levels and the phenotype observed in transgenic plants.

Protein degradation during senescence

The nitrogen that is remobilized to the developing grains during barley senescence comes mainly from the proteolysis of proteins contained in senescing leaves. It has been previously described that this massive degradation is mediated not only by autophagy but also by other vesicular systems including, Rubisco Containing Bodies (RCB) and Senescence Associated Vacuoles (SAVs). Although the identity of the proteases involved in this degradation is not entirely known, the high expression of genes encoding cysteine protease activities has been observed in barley and other species during senescence suggesting that senescence-associated protein degradation is mainly vacuolar.

The regulation of plastidial protein degradation remains to be elucidated, though it has been hypothesized that non-vacuolar proteases could be involved in the degradation of proteins inside the chloroplast or within the autophagosomes, RCB and SAVs. In addition, it has been proposed that a high rate of ubiquitination and oxidation of proteins during senescence could make them targets of degradation by the proteasome.

The study of these degradation processes and the identification of the proteases related to both vacuolar and plastidial proteolysis could provide new target genes that can be used for the improvement of traits like yield, GPC and nutrient remobilization.

REFERENCES

Adam, Z., & Clarke, A. K. (2002). Cutting edge of chloroplast proteolysis. Trends in Plant Science, 7(10), 451–6. Retrieved from http://www.ncbi.nlm.nih.gov/pubmed/12399180

Akar, T., Avci, M., & Dusunceli, F. (2004). Barley: Post-harvest Operations (p. 64). Turkey.

Anderson, P. M., Oelke, E. A., & Simmons, S. R. (2013). Growth and development guide for spring barley. University of Minnesota. Retrieved from http://www.extension.umn.edu/agriculture/small-grains/growth-and-development/spring-barley/

Ashford, T., & Porter, K. (1962). Cytopkasmic components in hepatic cell lysosomes. Journal of Cell Biology, 12, 198–202.

Avila-Ospina, L., Moison, M., Yoshimoto, K., & Masclaux-Daubresse, C. (2014). Autophagy, plant senescence, and nutrient recycling. Journal of Experimental Botany, 65(14), 3799–3811. doi:10.1093/jxb/eru039

Avin-Wittenberg, T., Honig, A., & Galili, G. (2012). Variations on a theme: plant autophagy in comparison to yeast and mammals. Protoplasma, 249(2), 285–99. doi:10.1007/s00709-011-0296-z

Badr, A, Müller, K., Schäfer-Pregl, R., El Rabey, H., Effgen, S., Ibrahim, H. H., … Salamini, F. (2000a). On the origin and domestication history of Barley (Hordeum vulgare). Molecular Biology and Evolution, 17(4), 499–510. Retrieved from http://www.ncbi.nlm.nih.gov/pubmed/10742042

Baima, S, Haegi, A, Stroman, P, Casadoro, G. (1989). CHARACTERIZATION OF A CDNA CLONE FOR BARLEY LEAF GLUTAMINE-SYNTHETASE. Carlsberg Research Communications 54, 1-9.

Balazadeh, S., Kwasniewski, M., Caldana, C., Mehrnia, M., Zanor, M. I., Xue, G.-P., & Mueller-Roeber, B. (2011). ORS1, an H_2O_2-responsive NAC transcription factor, controls senescence in Arabidopsis thaliana. Molecular Plant, 4(2), 346–60. doi:10.1093/mp/ssq080

Balibrea Lara, E., Gonzalez Garcia, M., Tahira, F., Enheb, R., Lee, T., Proels, R., … Roitsch, T. (2004). Extracellular Invertase Is an Essential Component of Cytokinin-Mediated Delay of Senescence. The Plant Cell, 16(May), 1276–1287. doi:10.1105/tpc.018929.a

Bamforth, C. W. (2003). Barley and Malt Starch in Brewing : A General Review, 40(2), 89–97.

Barry, C. S. (2009). The stay-green revolution: Recent progress in deciphering the mechanisms of chlorophyll degradation in higher plants. Plant Science, 176(3), 325–333. doi:10.1016/j.plantsci.2008.12.013

Bassham, D. C. (2009). Function and regulation of macroautophagy in plants. Biochimica et Biophysica Acta, 1793(9), 1397–403. doi:10.1016/j.bbamcr.2009.01.001

Bellucci, E., Bitocchi, E., Rau, D., Nanni, L., Ferradini, N., Giardini, A., … Papa, R. (2013). Population structure of barley landrace populations and gene-flow with modern varieties. PloS One, 8(12), e83891. doi:10.1371/journal.pone.0083891

Benfey, P. N., & Chua, N. H. (1990). The Cauliflower Mosaic Virus 35S Promoter: Combinatorial Regulation of Transcription in Plants. Science (New York, N.Y.), 250(4983), 959–66. doi:10.1126/science.250.4983.959

Beyene, G., Foyer, C. H., & Kunert, K. J. (2006). Two new cysteine proteinases with specific expression patterns in mature and senescent tobacco (Nicotiana tabacum L.) leaves. Journal of Experimental Botany, 57(6), 1431–43. doi:10.1093/jxb/erj123

Bingham, I. J., Blake, J., Foulkes, M. J., & Spink, J. (2007). Is barley yield in the UK sink limited? Field Crops Research, 101(2), 212–220. doi:10.1016/j.fcr.2006.11.004

Borrell, A. K., van Oosterom, E. J., Mullet, J. E., George-Jaeggli, B., Jordan, D. R., Klein, P. E., & Hammer, G. L. (2014). Stay-green alleles individually enhance grain yield in sorghum under drought by modifying canopy development and water uptake patterns. The New Phytologist, 203(3), 817–30. doi:10.1111/nph.12869

Box, A. (2008). The Biology of Hordeum vulgare L . (barley) (p. 41).

Breeze, E., Harrison, E., McHattie, S., Hughes, L., Hickman, R., Hill, C., … Buchanan-Wollaston, V. (2011). High-resolution temporal profiling of transcripts during Arabidopsis leaf senescence reveals a distinct chronology of processes and regulation. The Plant Cell, 23(3), 873–94. doi:10.1105/tpc.111.083345

Briggs, D. E. (1978). Barley. Chapman & Hall. Retrieved from http://books.google.fr/books?id=uo0_AAAAYAAJ

Buchanan-Wollaston, V., Page, T., Harrison, E., Breeze, E., Lim, P. O., Nam, H. G., … Leaver, C. J. (2005). Comparative transcriptome analysis reveals significant differences in gene expression and signalling pathways between developmental and dark/starvation-induced senescence in Arabidopsis. The Plant Journal : For Cell and Molecular Biology, 42(4), 567–85. doi:10.1111/j.1365-313X.2005.02399.x

Caputo, C., Fatta, N., & Barneix, a J. (2001). The export of amino acid in the phloem is altered in wheat plants lacking the short arm of chromosome 7B. Journal of Experimental Botany, 52(362), 1761–8. Retrieved from http://www.ncbi.nlm.nih.gov/pubmed/11520864

Cerasoli, S., Maillard, P., Scartazza, A., Brugnoli, E., Chaves, M. M., & Pereira, J. (2004). Carbon and nitrogen winter storage and remobilisation during seasonal flush growth in two-year-old cork oak (Quercus suber L .) saplings, 61, 721–729. doi:10.1051/forest

Chen, L., Ortiz-Lopez, a, Jung, a, & Bush, D. R. (2001). ANT1, an aromatic and neutral amino acid transporter in Arabidopsis. Plant Physiology, 125(4), 1813–20. Retrieved from http://www.pubmedcentral.nih.gov/articlerender.fcgi?artid=88837&tool=pmcentrez&rendertype=abstract

Chi, Y., Yang, Y., Zhou, Y., Zhou, J., Fan, B., Yu, J.-Q., & Chen, Z. (2013). Protein-protein interactions in the regulation of WRKY transcription factors. Molecular Plant, 6(2), 287–300. doi:10.1093/mp/sst026

Chiba, A., Ishida, H., Nishizawa, N. K., Makino, A., & Mae, T. (2003). Exclusion of ribulose-1,5-bisphosphate carboxylase/oxygenase from chloroplasts by specific bodies in naturally senescing leaves of wheat. Plant & Cell Physiology, 44(9), 914–21. Retrieved from http://www.ncbi.nlm.nih.gov/pubmed/14519773

Chory, J., Nagpal, P., & Peto, C. a. (1991). Phenotypic and Genetic Analysis of det2, a New Mutant That Affects Light-Regulated Seedling Development in Arabidopsis. The Plant Cell, 3(5), 445–459. doi:10.1105/tpc.3.5.445

Christiansen, M. W., & Gregersen, P. L. (2014). Members of the barley NAC transcription factor gene family show differential co-regulation with senescence-associated genes during senescence of flag leaves. Journal of Experimental Botany, 1–14. doi:10.1093/jxb/eru046

Christiansen, M. W., Holm, P. B., & Gregersen, P. L. (2011). Characterization of barley (Hordeum vulgare L .) NAC transcription factors suggests conserved functions compared to both monocots and dicots. BMC Research Notes, 4(1), 302. doi:10.1186/1756-0500-4-302

Chung, T., Phillips, A. R., & Vierstra, R. D. (2010). ATG8 lipidation and ATG8-mediated autophagy in Arabidopsis require ATG12 expressed from the differentially controlled ATG12A AND ATG12B loci. The Plant Journal : For Cell and Molecular Biology, 62(3), 483–93. doi:10.1111/j.1365-313X.2010.04166.x

Chung, T., Suttangkakul, A., & Vierstra, R. D. (2009). The ATG autophagic conjugation system in maize: ATG transcripts and abundance of the ATG8-lipid adduct are regulated by development and nutrient availability. Plant Physiology, 149(1), 220–34. doi:10.1104/pp.108.126714

Cliquet, J. B., Deléens, E., Bousser, a, Martin, M., Lescure, J. C., Prioul, J. L., … Morot-Gaudry, J. F. (1990). Estimation of Carbon and Nitrogen Allocation during Stalk Elongation by C and N Tracing in Zea mays L. Plant Physiology, 92(1), 79–87. Retrieved from http://www.pubmedcentral.nih.gov/articlerender.fcgi?artid=1062251&tool=pmcentrez&rendertype=abstract

Consortium, T. I. B. G. S. (2012). A physical, genetic and functional sequence assembly of the barley genome. Nature, 491(7426), 711–716. Retrieved from http://dx.doi.org/10.1038/nature11543

Cornejo, M. J., Luth, D., Blankenship, K. M., Anderson, O. D., & Blechl, a E. (1993). Activity of a maize ubiquitin promoter in transgenic rice. Plant Molecular Biology, 23(3), 567–81. Retrieved from http://www.ncbi.nlm.nih.gov/pubmed/8219091

Dai, N., Schaffer, a, Petreikov, M., Shahak, Y., Giller, Y., Ratner, K., … Granot, D. (1999). Overexpression of Arabidopsis hexokinase in tomato plants inhibits growth, reduces photosynthesis, and induces rapid senescence. The Plant Cell, 11(7), 1253–66. Retrieved from http://www.pubmedcentral.nih.gov/articlerender.fcgi?artid=144264&tool=pmcentrez&rendertype=abstract

Davies, P. J., & Gan, S. (2012). Towards an integrated view of monocarpic plant senescence. Russian Journal of Plant Physiology, 59(4), 467–478. doi:10.1134/S102144371204005X

Deselm, C. J., Miller, B. C., Zou, W., Beatty, W. L., Meel, H. Van, Takahata, Y., … Virgin, H. W. (2011). Autophagy proteins regulate the secretory component of osteoclastic bone resorption. Developmental Cell, 21(5), 966–974. doi:10.1016/j.devcel.2011.08.016.Autophagy

Diaz, C., Purdy, S., Christ, A., Morot-Gaudry, J. F., Wingler, A., & Masclaux-Daubresse, C. (2005). Characterization of Markers to Determine the Extent and Variability of Leaf Senescence in Arabidopsis . A Metabolic Profiling Approach 1. Plant Physiology, 138(June), 898–908. doi:10.1104/pp.105.060764.898

Distelfeld, A., Avni, R., & Fischer, A. M. (2014a). Senescence, nutrient remobilisation, and yield in wheat and barley. Journal of Experimental Botany. doi:10.1093/jxb/ert477

Distelfeld, A., Avni, R., & Fischer, A. M. (2014b). Senescence, nutrient remobilisation, and yield in wheat and barley. Journal of Experimental Botany. doi:10.1093/jxb/ert477

Doelling, J. H., Walker, J. M., Friedman, E. M., Thompson, A. R., & Vierstra, R. D. (2002). The APG8/12-activating enzyme APG7 is required for proper nutrient recycling and senescence in Arabidopsis thaliana. The Journal of Biological Chemistry, 277(36), 33105–14. doi:10.1074/jbc.M204630200

Eckardt, N. a. (2008). Grass Genome Evolution. The Plant Cell Online, 20(1), 3–4. doi:10.1105/tpc.108.058586

Ensminger, A., Enminsger, M., Konlande, J., & Robson, J. (1994). Food and Nutrition Encyclopedia (2nd ed., p. 527). CRC Press.

Fan, S.-C., Lin, C.-S., Hsu, P.-K., Lin, S.-H., & Tsay, Y.-F. (2009). The Arabidopsis nitrate transporter NRT1.7, expressed in phloem, is responsible for source-to-sink remobilisation of nitrate. The Plant Cell, 21(9), 2750–61. doi:10.1105/tpc.109.067603

FAO. (2009). agribusiness handbook Barley Malt Beer (p. 67). Rome.

FAOSTAT. (2013). Barley culture statistics 2012. Retrieved July 25, 2014, from http://unstats.un.org/unsd/pocketbook/references.pdf

Feller, U., Anders, I., & Mae, T. (2008a). Rubiscolytics: fate of Rubisco after its enzymatic function in a cell is terminated. Journal of Experimental Botany, 59(7), 1615–24. doi:10.1093/jxb/erm242

Feller, U., Anders, I., & Mae, T. (2008b). Rubiscolytics: fate of Rubisco after its enzymatic function in a cell is terminated. Journal of Experimental Botany, 59(7), 1615–24. doi:10.1093/jxb/erm242

Fischer, A., & Feller, U. (1994). Senescence and protein degradation in leaf segments of young winter wheat : influence of leaf age, 45(270), 103–109.

Fischer, A. M. (2012). The Complex Regulation of Senescence. Critical Reviews in Plant Sciences, 31(2), 124–147. doi:10.1080/07352689.2011.616065

Floyd, B. E., Morriss, S. C., Macintosh, G. C., & Bassham, D. C. (2012). What to eat: evidence for selective autophagy in plants. Journal of Integrative Plant Biology, 54(11), 907–20. doi:10.1111/j.1744-7909.2012.01178.x

Forde, B. G., & Lea, P. J. (2007). Glutamate in plants: metabolism, regulation, and signalling. Journal of Experimental Botany, 58(9), 2339–58. doi:10.1093/jxb/erm121

Foyer, C. H., & Noctor, G. (2005). Redox homeostasis and antioxidant signaling: a metabolic interface between stress perception and physiological responses. The Plant Cell, 17(7), 1866–75. doi:10.1105/tpc.105.033589

Frančáková, H., Líšková, M., Bojňanská, T., & Mareček, J. (2012). Germination Index as an Indicator of Malting Potential, 30(4), 377–384.

Freundt, E. C., Czapiga, M., & Lenardo, M. J. (2007). Photoconversion of Lysotracker Red to a green fluorescent molecule. Cell Research, 17(11), 956–8. doi:10.1038/cr.2007.80

Fujiki, Y., Yoshimoto, K., & Ohsumi, Y. (2007). An Arabidopsis homolog of yeast ATG6/VPS30 is essential for pollen germination. Plant Physiology, 143(3), 1132–9. doi:10.1104/pp.106.093864

Gan, S., & Amasino, R. (1995). Inhibition of Leaf Senescence by Autoregulated Production of Cytokinin. Science, 270(14), 1–3.

Gatford, K. T., Basri, Z., Edlington, J., Lloyd, J., Qureshi, J. a., Brettell, R., & Fincher, G. B. (2006). Gene flow from transgenic wheat and barley under field conditions. Euphytica, 151(3), 383–391. doi:10.1007/s10681-006-9160-1

Geng, J., & Klionsky, D. J. (2008). The Atg8 and Atg12 ubiquitin-like conjugation systems in macroautophagy. “Protein modifications: beyond the usual suspects” review series. EMBO Reports, 9(9), 859–64. doi:10.1038/embor.2008.163

Goodall, A. J., Kumar, P., & Tobin, A. K. (2013). Identification and Expression Analyses of Cytosolic Glutamine Synthetase Genes in Barley (Hordeum vulgare L.). Plant and Cell Physiology, 54 (4), 492–505. doi:10.1093/pcp/pct006

Grbic, V. (2003). SAG2 and SAG12 protein expression in senescing Arabidopsis plants, (McGrath 1999), 263–269.

Gregersen, P. L. (2011). Senescence and Nutrient Remobilisation in Crop Plants. In The Molecular and Physiological Basis of Nutrient Use Efficiency in Crops (pp. 83–102). Wiley-Blackwell. doi:10.1002/9780470960707.ch5

Gregersen, P. L., Culetic, A., Boschian, L., & Krupinska, K. (2013). Plant senescence and crop productivity. Plant Molecular Biology, 82(6), 603–22. doi:10.1007/s11103-013-0013-8

Gregersen, P. L., & Holm, P. B. (2007). Transcriptome analysis of senescence in the flag leaf of wheat (Triticum aestivum L.). Plant Biotechnology Journal, 5(1), 192–206. doi:10.1111/j.1467-7652.2006.00232.x

Gregersen, P. L., Holm, P. B., & Krupinska, K. (2008). Leaf senescence and nutrient remobilisation in barley and wheat. Plant Biology (Stuttgart, Germany), 10 Suppl 1, 37–49. doi:10.1111/j.1438-8677.2008.00114.x

Guiboileau, A., Sormani, R., Meyer, C., & Masclaux-Daubresse, C. (2010a). Senescence and death of plant organs: nutrient recycling and developmental regulation. Comptes Rendus Biologies, 333(4), 382–91. doi:10.1016/j.crvi.2010.01.016

Guiboileau, A., Sormani, R., Meyer, C., & Masclaux-Daubresse, C. (2010b). Senescence and death of plant organs: nutrient recycling and developmental regulation. Comptes Rendus Biologies, 333(4), 382–91. doi:10.1016/j.crvi.2010.01.016

Guiboileau, A., Yoshimoto, K., Soulay, F., Bataillé, M.-P., Avice, J.-C., & Masclaux-Daubresse, C. (2012). Autophagy machinery controls nitrogen remobilisation at the whole-plant level under both limiting and ample nitrate conditions in Arabidopsis. The New Phytologist, 194(3), 732–40. doi:10.1111/j.1469-8137.2012.04084.x

Guiboileau, A, Avila-Ospina, L, Yoshimoto, K, Soulay, F, Azzopardi, M, Marmagne, A, Lothier, J, Masclaux-Daubresse, C. (2013). Physiological and metabolic consequences of autophagy defisciency for the management of nitrogen and protein resources in Arabidopsis leaves depending on nitrate availability. New Phytologist 199, 683-694

Guo, Y., & Gan, S. (2006). AtNAP, a NAC family transcription factor, has an important role in leaf senescence. The Plant Journal : For Cell and Molecular Biology, 46(4), 601–12. doi:10.1111/j.1365-313X.2006.02723.x

Guo, Y., & Gan, S.-S. (2014). Translational researches on leaf senescence for enhancing plant productivity and quality. Journal of Experimental Botany, 65(14), 3901–3913. doi:10.1093/jxb/eru248

Habash, D. Z., Bernard, S., Schondelmaier, J., Weyen, J., & Quarrie, S. a. (2007). The genetics of nitrogen use in hexaploid wheat: N utilisation, development and yield. TAG. Theoretical and Applied Genetics. Theoretische Und Angewandte Genetik, 114(3), 403–19. doi:10.1007/s00122-006-0429-5

Hanaoka, H., Noda, T., Shirano, Y., Kato, T., Hayashi, H., Shibata, D., … Ohsumi, Y. (2002). Leaf Senescence and Starvation-Induced Chlorosis Are Accelerated by the Disruption of an Arabidopsis Autophagy Gene 1, 129(July), 1181–1193. doi:10.1104/pp.011024.tein

Harris, K., Subudhi, P. K., Borrell, A., Jordan, D., Rosenow, D., Nguyen, H., … Mullet, J. (2007). Sorghum stay-green QTL individually reduce post-flowering drought-induced leaf senescence. Journal of Experimental Botany, 58(2), 327–38. doi:10.1093/jxb/erl225

Hayward, A. P., & Dinesh-Kumar, S. P. (2011). What can plant autophagy do for an innate immune response? Annual Review of Phytopathology, 49, 557–76. doi:10.1146/annurev-phyto-072910-095333

He, C., & Klionsky, D. J. (2009). Regulation mechanisms and signaling pathways of autophagy. Annual Review of Genetics, 43, 67–93. doi:10.1146/annurev-genet-102808-114910

He, Y., Fukushige, H., Hildebrand, D. F., & Gan, S. (2002). Evidence Supporting a Role of Jasmonic Acid in Arabidopsis Leaf Senescence 1. Plant Physiology, 128(March), 876–884. doi:10.1104/pp.010843.)

Heneen, W. K. (2010). Cytogenetics and Molecular Cytogenetics of Barley: A Model Cereal Crop with a Large Genome. In Barley (pp. 112–121). Wiley-Blackwell. doi:10.1002/9780470958636.ch5

Herrmann, B., & Feller, U. (1998). CO2, light and temperature influence senescence and protein degradation in wheat leaf segments. Physiologia Plantarum, 320–326.

Hickman, R., Hill, C., Penfold, C. a, Breeze, E., Bowden, L., Moore, J. D., … Buchanan-Wollaston, V. (2013). A local regulatory network around three NAC transcription factors in stress responses and senescence in Arabidopsis leaves. The Plant Journal : For Cell and Molecular Biology, 75(1), 26–39. doi:10.1111/tpj.12194

Hoffmann, A., Maurer, A., & Pillen, K. (2012). Detection of nitrogen deficiency QTL in juvenile wild barley introgression lines growing in a hydroponic system. BMC Genetics, 13, 88. doi:10.1186/1471-2156-13-88

Hofius, D., Munch, D., Bressendorff, S., Mundy, J., & Petersen, M. (2011). Role of autophagy in disease resistance and hypersensitive response-associated cell death. Cell Death and Differentiation, 18(8), 1257–62. doi:10.1038/cdd.2011.43

Hofius, D., Schultz-Larsen, T., Joensen, J., Tsitsigiannis, D. I., Petersen, N. H. T., Mattsson, O., … Petersen, M. (2009). Autophagic components contribute to hypersensitive cell death in Arabidopsis. Cell, 137(4), 773–83. doi:10.1016/j.cell.2009.02.036

Hollmann, J., Gregersen, P. L., & Krupinska, K. (2014). Identification of predominant genes involved in regulation and execution of senescence-associated nitrogen remobilisation in flag leaves of field grown barley. Journal of Experimental Botany, 1–11. doi:10.1093/jxb/eru094

Hörtensteiner, S. (2009). Stay-green regulates chlorophyll and chlorophyll-binding protein degradation during senescence. Trends in Plant Science, 14(3), 155–62. doi:10.1016/j.tplants.2009.01.002

Hsu, P.-K., & Tsay, Y.-F. (2013). Two phloem nitrate transporters, NRT1.11 and NRT1.12, are important for redistributing xylem-borne nitrate to enhance plant growth. Plant Physiology, 163(2), 844–56. doi:10.1104/pp.113.226563

Hunt, E., Gattolin, S., Newbury, H. J., Bale, J. S., Tseng, H.-M., Barrett, D. a, & Pritchard, J. (2010). A mutation in amino acid permease AAP6 reduces the amino acid content of the Arabidopsis sieve elements but leaves aphid herbivores unaffected. Journal of Experimental Botany, 61(1), 55–64. doi:10.1093/jxb/erp274

Hussien, A., Tavakol, E., Horner, D. S., Muñoz-Amatriaín, M., Muehlbauer, G. J., & Rossini, L. (2014). Genetics of Tillering in Rice and Barley. The Plant Genome, 7(1), 1–20. doi:10.3835/plantgenome2013.10.0032

Inoue, Y., Suzuki, T., Hattori, M., Yoshimoto, K., Ohsumi, Y., & Moriyasu, Y. (2006). AtATG genes, homologs of yeast autophagy genes, are involved in constitutive autophagy in Arabidopsis root tip cells. Plant & Cell Physiology, 47(12), 1641–52. doi:10.1093/pcp/pcl031

Izumi, M., Wada, S., Makino, A., & Ishida, H. (2010). The autophagic degradation of chloroplasts via rubisco-containing bodies is specifically linked to leaf carbon status but not nitrogen status in Arabidopsis. Plant Physiology, 154(3), 1196–209. doi:10.1104/pp.110.158519

Jakob, S. S., Rödder, D., Engler, J. O., Shaaf, S., Ozkan, H., Blattner, F. R., & Kilian, B. (2014). Evolutionary history of wild barley (Hordeum vulgare subsp. spontaneum)

analyzed using multilocus sequence data and paleodistribution modeling. Genome Biology and Evolution, 6(3), 685–702. doi:10.1093/gbe/evu047

Jang, I., Choi, W., Lee, K., Song, S. I., Nahm, B. H., & Kim, J. (2002). High-Level and Ubiquitous Expression of the Rice Cytochrome c Gene OsCc1 and Its Promoter Activity in Transgenic Plants Provides a Useful Promoter for Transgenesis of Monocots 1, 129(August), 1473–1481. doi:10.1104/pp.002261.1

Jing, H.-C., Schippers, J. H. M., Hille, J., & Dijkwel, P. P. (2005). Ethylene-induced leaf senescence depends on age-related changes and OLD genes in Arabidopsis. Journal of Experimental Botany, 56(421), 2915–23. doi:10.1093/jxb/eri287

Johansen, T., & Lamark, T. (2011). Selective autophagy mediated by autophagic adapter proteins. Autophagy, 7(3), 279–296. doi:10.4161/auto.7.3.14487

Jounai, N., Takeshita, F., Kobiyama, K., Sawano, A., Miyawaki, A., Xin, K.-Q., … Okuda, K. (2007). The Atg5 Atg12 conjugate associates with innate antiviral immune responses. Proceedings of the National Academy of Sciences of the United States of America, 104(35), 14050–5. doi:10.1073/pnas.0704014104

Jukanti, A. K., & Fischer, A. M. (2008). A high-grain protein content locus on barley (Hordeum vulgare) chromosome 6 is associated with increased flag leaf proteolysis and nitrogen remobilisation. Physiologia Plantarum, 132(4), 426–39. doi:10.1111/j.1399-3054.2007.01044.x

Jukanti, A. K., Heidlebaugh, N. M., Parrott, D. L., Fischer, I. a, McInnerney, K., & Fischer, A. M. (2008). Comparative transcriptome profiling of near-isogenic barley (Hordeum vulgare) lines differing in the allelic state of a major grain protein content locus identifies genes with possible roles in leaf senescence and nitrogen reallocation. The New Phytologist, 177(2), 333–49. doi:10.1111/j.1469-8137.2007.02270.x

Kassahun, B., Bidinger, F. R., Hash, C. T., & Kuruvinashetti, M. S. (2009). Stay-green expression in early generation sorghum [Sorghum bicolor (L.) Moench] QTL introgression lines. Euphytica, 172(3), 351–362. doi:10.1007/s10681-009-0108-0

Kichey, T., Hirel, B., Heumez, E., Dubois, F., & Le Gouis, J. (2007). In winter wheat (Triticum aestivum L.), post-anthesis nitrogen uptake and remobilisation to the grain correlates with agronomic traits and nitrogen physiological markers. Field Crops Research, 102(1), 22–32. doi:10.1016/j.fcr.2007.01.002

Kim, S.-H., Kwon, C., Lee, J.-H., & Chung, T. (2012a). Genes for plant autophagy: functions and interactions. Molecules and Cells, 34(5), 413–23. doi:10.1007/s10059-012-0098-y

Kim, S.-H., Kwon, C., Lee, J.-H., & Chung, T. (2012b). Genes for plant autophagy: functions and interactions. Molecules and Cells, 34(5), 413–23. doi:10.1007/s10059-012-0098-y

Koch, K. E. (1996). Carbohydrate-Modulated Gene Expression in Plants. Annual Review of Plant Physiology and Plant Molecular Biology, 47, 509–540. doi:10.1146/annurev.arplant.47.1.509

Komatsuda, T., Pourkheirandish, M., He, C., Azhaguvel, P., Kanamori, H., Perovic, D., … Yano, M. (2007). Six-rowed barley originated from a mutation in a

homeodomain-leucine zipper I-class homeobox gene. Proceedings of the National Academy of Sciences of the United States of America, 104(4), 1424–9. doi:10.1073/pnas.0608580104

Koppolu, R., Anwar, N., Sakuma, S., Tagiri, A., Lundqvist, U., Pourkheirandish, M., … Schnurbusch, T. (2013). Six-rowed spike4 (Vrs4) controls spikelet determinacy and row-type in barley. Proceedings of the National Academy of Sciences of the United States of America, 110(32), 13198–203. doi:10.1073/pnas.1221950110

Kraft, C., Deplazes, A., Sohrmann, M., & Peter, M. (2008). Mature ribosomes are selectively degraded upon starvation by an autophagy pathway requiring the Ubp3p/Bre5p ubiquitin protease. Nature Cell Biology, 10(5), 602–10. doi:10.1038/ncb1723

Kuzuoglu-Ozturk, D., Cebeci Yalcinkaya, O., Akpinar, B. A., Mitou, G., Korkmaz, G., Gozuacik, D., & Budak, H. (2012). Autophagy-related gene, TdAtg8, in wild emmer wheat plays a role in drought and osmotic stress response. Planta, 236(4), 1081–92. doi:10.1007/s00425-012-1657-3

Kwon, S. Il, Cho, H. J., Jung, J. H., Yoshimoto, K., Shirasu, K., & Park, O. K. (2010). The Rab GTPase RabG3b functions in autophagy and contributes to tracheary element differentiation in Arabidopsis. The Plant Journal : For Cell and Molecular Biology, 64(1), 151–64. doi:10.1111/j.1365-313X.2010.04315.x

Ladwig, F., Stahl, M., Ludewig, U., Hirner, A. a, Hammes, U. Z., Stadler, R., … Koch, W. (2012). Siliques are Red1 from Arabidopsis acts as a bidirectional amino acid transporter that is crucial for the amino acid homeostasis of siliques. Plant Physiology, 158(4), 1643–55. doi:10.1104/pp.111.192583

Lam, HM, Hsieh, MH, Coruzzi, G (1998) Reciprocal regulation of distinct asparagine synthetase genes by light and metabolites in Arabidopsis thaliana. Plant Journal 16: 345-353

Lam, HM, Wong, P, Chan, HK, Yam, KM, Chen, L, Chow, CM, Coruzzi, GM (2003) Overexpression of the ASN1 gene enhances nitrogen status in seeds of Arabidopsis. Plant Physiol 132: 926-935

Lee, Y., Kim, E.-S., Choi, Y., Hwang, I., Staiger, C. J., Chung, Y.-Y., & Lee, Y. (2008). The Arabidopsis phosphatidylinositol 3-kinase is important for pollen development. Plant Physiology, 147(4), 1886–97. doi:10.1104/pp.108.121590

Lenz, H. D., Haller, E., Melzer, E., Kober, K., Wurster, K., Stahl, M., … Nürnberger, T. (2011). Autophagy differentially controls plant basal immunity to biotrophic and necrotrophic pathogens. The Plant Journal : For Cell and Molecular Biology, 66(5), 818–30. doi:10.1111/j.1365-313X.2011.04546.x

Li, F., & Vierstra, R. D. (2012). Autophagy: a multifaceted intracellular system for bulk and selective recycling. Trends in Plant Science, 17(9), 526–37. doi:10.1016/j.tplants.2012.05.006

Lim, P. O., Kim, H. J., & Nam, H. G. (2007). Leaf senescence. Annual Review of Plant Biology, 58, 115–36. doi:10.1146/annurev.arplant.57.032905.105316

Lim, P. O., Lee, I. C., Kim, J., Kim, H. J., Ryu, J. S., Woo, H. R., & Nam, H. G. (2010). Auxin response factor 2 (ARF2) plays a major role in regulating auxin-mediated leaf

longevity. Journal of Experimental Botany, 61(5), 1419–30. doi:10.1093/jxb/erq010

Liu, L., Zhou, Y., Szczerba, M. W., Li, X., & Lin, Y. (2010). Identification and application of a rice senescence-associated promoter. Plant Physiology, 153(3), 1239–49. doi:10.1104/pp.110.157123

Liu, Y., & Bassham, D. C. (2012a). Autophagy: pathways for self-eating in plant cells. Annual Review of Plant Biology, 63, 215–37. doi:10.1146/annurev-arplant-042811-105441

Liu, Y., & Bassham, D. C. (2012b). Autophagy: pathways for self-eating in plant cells. Annual Review of Plant Biology, 63, 215–37. doi:10.1146/annurev-arplant-042811-105441

Liu, Y., Schiff, M., Czymmek, K., Tallóczy, Z., Levine, B., & Dinesh-Kumar, S. P. (2005). Autophagy regulates programmed cell death during the plant innate immune response. Cell, 121(4), 567–77. doi:10.1016/j.cell.2005.03.007

Lundgren Rose, T., Bonneau, L., Der, C., Marty-Mazars, D., & Marty, F. (2006). Starvation-induced expression of autophagy-related genes in Arabidopsis. Biology of the Cell / under the Auspices of the European Cell Biology Organization, 98(1), 53–67. doi:10.1042/BC20040516

Maiuri, M. C., Zalckvar, E., Kimchi, A., & Kroemer, G. (2007). Self-eating and self-killing: crosstalk between autophagy and apoptosis. Nature Reviews. Molecular Cell Biology, 8(9), 741–52. doi:10.1038/nrm2239

Martin, A., Lee, J., Kichey, T., Gerentes, D., Zivy, M., Tatout, C., … Hirel, B. (2006). Two cytosolic glutamine synthetase isoforms of maize are specifically involved in the control of grain production. The Plant Cell, 18(11), 3252–74. doi:10.1105/tpc.106.042689

Martínez, D. E., Bartoli, C. G., Grbic, V., & Guiamet, J. J. (2007). Vacuolar cysteine proteases of wheat (Triticum aestivum L.) are common to leaf senescence induced by different factors. Journal of Experimental Botany, 58(5), 1099–107. doi:10.1093/jxb/erl270

Martínez, D. E., Costa, M. L., & Guiamet, J. J. (2008). Senescence-associated degradation of chloroplast proteins inside and outside the organelle. Plant Biology (Stuttgart, Germany), 10 Suppl 1, 15–22. doi:10.1111/j.1438-8677.2008.00089.x

Masclaux, C., Valadier, M. H., Brugière, N., Morot-Gaudry, J. F., & Hirel, B. (2000). Characterization of the sink/source transition in tobacco (Nicotiana tabacum L.) shoots in relation to nitrogen management and leaf senescence. Planta, 211(4), 510–8. Retrieved from http://www.ncbi.nlm.nih.gov/pubmed/11030550

Masclaux-Daubresse, C., Carrayol, E., & Valadier, M.-H. (2005). The two nitrogen mobilisation- and senescence-associated GS1 and GDH genes are controlled by C and N metabolites. Planta, 221(4), 580–8. doi:10.1007/s00425-004-1468-2

Masclaux-Daubresse, C., Daniel-Vedele, F., Dechorgnat, J., Chardon, F., Gaufichon, L., & Suzuki, A. (2010). Nitrogen uptake, assimilation and remobilisation in plants: challenges for sustainable and productive agriculture. Annals of Botany, 105(7), 1141–57. doi:10.1093/aob/mcq028

Masclaux-Daubresse, C., Reisdorf-Cren, M., & Orsel, M. (2008). Leaf nitrogen remobilisation for plant development and grain filling. Plant Biology (Stuttgart, Germany), 10 Suppl 1(February 2007), 23–36. doi:10.1111/j.1438-8677.2008.00097.x

Matallana-Ramirez, L. P., Rauf, M., Farage-Barhom, S., Dortay, H., Xue, G.-P., Dröge-Laser, W., … Mueller-Roeber, B. (2013). NAC transcription factor ORE1 and senescence-induced BIFUNCTIONAL NUCLEASE1 (BFN1) constitute a regulatory cascade in Arabidopsis. Molecular Plant, 6(5), 1432–52. doi:10.1093/mp/sst012

Matile, P., Ginsburg, S., Schellenberg, M., & Thomas, H. (1988). Catabolites of chlorophyll in senescing barley leaves are localized in the vacuoles of mesophyll cells. Proceedings of the National Academy of Sciences of the United States of America, 85(24), 9529–32. Retrieved from http://www.pubmedcentral.nih.gov/articlerender.fcgi?artid=282787&tool=pmcentrez&rendertype=abstract

Matile, P., Stefan, H., & Thomas, H. (1999). Chloroplast to Gerontoplast Transition, 67–95.

McGregor, S. (1976). Insect Pollination Of Cultivated Crop Plants (p. 849). Tucson: United States Department of Agriculture.

Merkulova, E. a, Guiboileau, A., Naya, L., Masclaux-Daubresse, C., & Yoshimoto, K. (2014). Assessment and optimization of autophagy monitoring methods in Arabidopsis roots indicate direct fusion of autophagosomes with vacuoles. Plant & Cell Physiology, 55(4), 715–26. doi:10.1093/pcp/pcu041

Miao, Y., Jiang, J., Ren, Y., & Zhao, Z. (2013). The single-stranded DNA-binding protein WHIRLY1 represses WRKY53 expression and delays leaf senescence in a developmental stage-dependent manner in Arabidopsis. Plant Physiology, 163(2), 746–56. doi:10.1104/pp.113.223412

Miao, Y., Laun, T., Zimmermann, P., & Zentgraf, U. (2004). Targets of the WRKY53 transcription factor and its role during leaf senescence in Arabidopsis. Plant Molecular Biology, 55(6), 853–67. doi:10.1007/s11103-004-2142-6

Mickelson, S. (2003). Mapping of QTL associated with nitrogen storage and remobilisation in barley (Hordeum vulgare L.) leaves. Journal of Experimental Botany, 54(383), 801–812. doi:10.1093/jxb/erg084

Mitou, G., Budak, H., & Gozuacik, D. (2009). Techniques to study autophagy in plants. International Journal of Plant Genomics, 2009, 451357. doi:10.1155/2009/451357

Mitsuhashi, W., & Feller, U. (1992). Effects of light and external solutes on the catabolism of nuclear-encoded stromal proteins in intact chloroplasts isolated from pea leaves. Plant Physiology, 100(4), 2100–5. Retrieved from http://www.pubmedcentral.nih.gov/articlerender.fcgi?artid=1075913&tool=pmcentrez&rendertype=abstract

Møller, M. G., Taylor, C., Rasmussen, S. K., & Holm, P. B. (2003). Molecular cloning and characterisation of two genes encoding asparagine synthetase in barley (Hordeum vulgare L.). Biochimica et Biophysica Acta (BBA) - Gene Structure and Expression, 1628(2), 123–132. doi:10.1016/S0167-4781(03)00137-4

Moore, B., Zhou, L., Rolland, F., Hall, Q., Cheng, W.-H., Liu, Y.-X., … Sheen, J. (2003). Role of the Arabidopsis glucose sensor HXK1 in nutrient, light, and hormonal signaling. Science (New York, N.Y.), 300(5617), 332–6. doi:10.1126/science.1080585

Morris, K., MacKerness, S. a, Page, T., John, C. F., Murphy, a M., Carr, J. P., & Buchanan-Wollaston, V. (2000). Salicylic acid has a role in regulating gene expression during leaf senescence. The Plant Journal : For Cell and Molecular Biology, 23(5), 677–85. Retrieved from http://www.ncbi.nlm.nih.gov/pubmed/10972893

Munafó, D. B., & Colombo, M. I. (2001). A novel assay to study autophagy: regulation of autophagosome vacuole size by amino acid deprivation. Journal of Cell Science, 114(Pt 20), 3619–29. Retrieved from http://www.ncbi.nlm.nih.gov/pubmed/11707514

Nair, S. K., Wang, N., Turuspekov, Y., Pourkheirandish, M., Sinsuwongwat, S., Chen, G., … Komatsuda, T. (2010). Cleistogamous flowering in barley arises from the suppression of microRNA-guided HvAP2 mRNA cleavage. Proceedings of the National Academy of Sciences of the United States of America, 107(1), 490–5. doi:10.1073/pnas.0909097107

Nakatogawa, H., Ichimura, Y., & Ohsumi, Y. (2007). Atg8, a ubiquitin-like protein required for autophagosome formation, mediates membrane tethering and hemifusion. Cell, 130(1), 165–78. doi:10.1016/j.cell.2007.05.021

Noda, N. N., Ohsumi, Y., & Inagaki, F. (2010). Atg8-family interacting motif crucial for selective autophagy. FEBS Letters, 584(7), 1379–85. doi:10.1016/j.febslet.2010.01.018

Ohsumi, Y. (2001). Molecular dissection of autophagy: two ubiquitin-like systems. Nature Reviews. Molecular Cell Biology, 2(3), 211–6. doi:10.1038/35056522

Orsel, M., Moison, M., Clouet, V., Thomas, J., Leprince, F., Canoy, A.-S., … Masclaux-Daubresse, C. (2014). Sixteen cytosolic glutamine synthetase genes identified in the Brassica napus L. genome are differentially regulated depending on nitrogen regimes and leaf senescence. Journal of Experimental Botany. doi:10.1093/jxb/eru041

Ostersetzer, O., Kato, Y., Adam, Z., & Sakamoto, W. (2007). Multiple intracellular locations of Lon protease in Arabidopsis: evidence for the localization of AtLon4 to chloroplasts. Plant & Cell Physiology, 48(6), 881–5. doi:10.1093/pcp/pcm052

Park, S.-H., Yi, N., Kim, Y. S., Jeong, M.-H., Bang, S.-W., Choi, Y. Do, & Kim, J.-K. (2010). Analysis of five novel putative constitutive gene promoters in transgenic rice plants. Journal of Experimental Botany, 61(9), 2459–67. doi:10.1093/jxb/erq076

Parrott, D. L., Martin, J. M., & Fischer, A. M. (2010). Analysis of barley (Hordeum vulgare) leaf senescence and protease gene expression: a family C1A cysteine protease is specifically induced under conditions characterized by high carbohydrate, but low to moderate nitrogen levels. The New Phytologist, 187(2), 313–31. doi:10.1111/j.1469-8137.2010.03278.x

Parrott, D. L., McInnerney, K., Feller, U., & Fischer, A. M. (2007). Steam-girdling of barley (Hordeum vulgare) leaves leads to carbohydrate accumulation and accelerated

leaf senescence, facilitating transcriptomic analysis of senescence-associated genes. The New Phytologist, 176(1), 56–69. doi:10.1111/j.1469-8137.2007.02158.x

Parrott, D., Yang, L., Shama, L., & Fischer, A. (2005). Senescence is accelerated, and several proteases are induced by carbon "feast" conditions in barley (Hordeum vulgare L.) leaves. Planta, 989–1000. doi:10.1007/s00425-005-0042-x

Parzies, H. K., Schnaithmann, F., & Geiger, H. H. (2005). Pollen viability of Hordeum spp genotypes with different flowering characteristics. Euphytica, 145(3), 229–235. doi:10.1007/s10681-005-1167-5

Pate, S., & Dinesh-Kumar, S. (2008). Arabidopsis ATG6 is required to limit the pathogen-associated cell death response. Autophagy, 4(1), 20–27.

Paul, S., Kashyap, A., Jia, W., He, W., & Schaefer, B. (2012). Selective autophagy of the adaptator protein Bcl10 modulates T cell receptor activation of NF-kB. Immunity, 36(6), 947–958. doi:10.1016/j.immuni.2012.04.008.Selective

Phillips, A. R., Suttangkakul, A., & Vierstra, R. D. (2008). The ATG12-conjugating enzyme ATG10 Is essential for autophagic vesicle formation in Arabidopsis thaliana. Genetics, 178(3), 1339–53. doi:10.1534/genetics.107.086199

Pourkheirandish, M., & Komatsuda, T. (2007). The importance of barley genetics and domestication in a global perspective. Annals of Botany, 100(5), 999–1008. doi:10.1093/aob/mcm139

Pourtau, N., Jennings, R., Pelzer, E., Pallas, J., & Wingler, A. (2006). Effect of sugar-induced senescence on gene expression and implications for the regulation of senescence in Arabidopsis. Planta, 224(3), 556–68. doi:10.1007/s00425-006-0243-y

Prins, A., van Heerden, P. D. R., Olmos, E., Kunert, K. J., & Foyer, C. H. (2008). Cysteine proteinases regulate chloroplast protein content and composition in tobacco leaves: a model for dynamic interactions with ribulose-1,5-bisphosphate carboxylase/oxygenase (Rubisco) vesicular bodies. Journal of Experimental Botany, 59(7), 1935–50. doi:10.1093/jxb/ern086

Pyo, J.-O., Yoo, S.-M., Ahn, H.-H., Nah, J., Hong, S.-H., Kam, T.-I., … Jung, Y.-K. (2013). Overexpression of Atg5 in mice activates autophagy and extends lifespan. Nature Communications, 4, 2300. doi:10.1038/ncomms3300

Qin, G., Ma, Z., Zhang, L., Xing, S., Hou, X., Deng, J., … Gu, H. (2007). Arabidopsis AtBECLIN 1/AtAtg6/AtVps30 is essential for pollen germination and plant development. Cell Research, 17(3), 249–63. doi:10.1038/cr.2007.7

Radchuk, V. V, Borisjuk, L., Sreenivasulu, N., Merx, K., Mock, H.-P., Rolletschek, H., … Weschke, W. (2009). Spatiotemporal profiling of starch biosynthesis and degradation in the developing barley grain. Plant Physiology, 150(1), 190–204. doi:10.1104/pp.108.133520

Reggiori, F., Komatsu, M., Finley, K., & Simonsen, A. (2012). Selective types of autophagy. International Journal of Cell Biology, 2012, 156272. doi:10.1155/2012/156272

Reggiori, F., Tucker, K. a, Stromhaug, P. E., & Klionsky, D. J. (2004). The Atg1-Atg13 complex regulates Atg9 and Atg23 retrieval transport from the pre-

autophagosomal structure. Developmental Cell, 6(1), 79–90. Retrieved from http://www.ncbi.nlm.nih.gov/pubmed/14723849

Reid, D. (1985). Morphology and anatomy of the barley plant. In D. Rasmusson (Ed.), Barley (pp. 76–101). American Society of Agronomy, Crop Science Society of America, Soil Science Society of America. doi:doi:10.2134/agronmonogr26.c4

Reidel, E. J., Rennie, E. a, Amiard, V., Cheng, L., & Turgeon, R. (2009). Phloem loading strategies in three plant species that transport sugar alcohols. Plant Physiology, 149(3), 1601–8. doi:10.1104/pp.108.134791

Riddle, O., & Suneson, C. (1944). Crossing Studies With Male-Sterile Barley. Agronomy Journal, 62–65. Retrieved from https://dl.sciencesocieties.org/publications/aj/abstracts/36/1/AJ0360010062

Ritala, a., Nuutila, a. M., Aikasalo, R., Kauppinen, V., & Tammisola, J. (2002). Measuring Gene Flow in the Cultivation of Transgenic Barley. Crop Science, 42(1), 278–285. Retrieved from http://www.ncbi.nlm.nih.gov/pubmed/11756286

Robertson, L., & Stark, J. (1993). Idaho spring barley production guide. … -Idaho Agricultural Experiment Station. Retrieved from http://agris.fao.org/agris-search/search/display.do?f=1995/US/US95287.xml;US9505735

Rodriguez, V., Marginedo, M., J, G.-M., Isausti, P., & Benech-Arnold, P. (2001). Predicting Preharvest Sprouting Susceptibility in Barley : A Model Based on Temperature during Grain Filling. Agronomy Journal, 93, 1071–1079.

Sabelli, P. a, & Larkins, B. a. (2009). The development of endosperm in grasses. Plant Physiology, 149(1), 14–26. doi:10.1104/pp.108.129437

Saisho, D., & Takeda, K. (2011). Barley: emergence as a new research material of crop science. Plant & Cell Physiology, 52(5), 724–7. doi:10.1093/pcp/pcr049

Schippers, J. H. M., Jing, H., Hille, J., & Dijkwel, P. P. (2007). Developmental and hormonal control of leaf senescence, 9–44.

Schmalenbach, I., & Pillen, K. (2009). Detection and verification of malting quality QTLs using wild barley introgression lines. TAG. Theoretical and Applied Genetics. Theoretische Und Angewandte Genetik, 118(8), 1411–27. doi:10.1007/s00122-009-0991-8

Schmid, M., Davison, T. S., Henz, S. R., Pape, U. J., Demar, M., Vingron, M., … Lohmann, J. U. (2005). A gene expression map of Arabidopsis thaliana development. Nature Genetics, 37(5), 501–6. doi:10.1038/ng1543

Schuhmann, H., & Adamska, I. (2012). Deg proteases and their role in protein quality control and processing in different subcellular compartments of the plant cell. Physiologia Plantarum, 145(1), 224–34. doi:10.1111/j.1399-3054.2011.01533.x

Shaid, S., Brandts, C. H., Serve, H., & Dikic, I. (2013). Ubiquitination and selective autophagy. Cell Death and Differentiation, 20(1), 21–30. doi:10.1038/cdd.2012.72

Shibata, M., Oikawa, K., Yoshimoto, K., Kondo, M., Mano, S., Yamada, K., … Nishimura, M. (2013). Highly oxidized peroxisomes are selectively degraded via autophagy in Arabidopsis. The Plant Cell, 25(12), 4967–83. doi:10.1105/tpc.113.116947

Simons, M., Saha, R., Guillard, L., Clément, G., Armengaud, P., Cañas, R., … Hirel, B. (2014). Nitrogen-use efficiency in maize (Zea mays L.): from “omics” studies to metabolic modelling. Journal of Experimental Botany, 1–15. doi:10.1093/jxb/eru227

Simpson, R. J., & Dalling, M. J. (1981). Planta Nitrogen Redistribution During Grain Growth in Wheat (Triticum aestivum L .), 447–456.

Sinvany-villalobo, G., Davydov, O., Ben-ari, G., Zaltsman, A., Raskind, A., & Adam, Z. (2004). Expression in Multigene Families . Analysis of Chloroplast and Mitochondrial Proteases 1, 135(July), 1336–1345. doi:10.1104/pp.104.043299.review

Sláviková, S., Shy, G., Yao, Y., Glozman, R., Levanony, H., Pietrokovski, S., … Galili, G. (2005). The autophagy-associated Atg8 gene family operates both under favourable growth conditions and under starvation stresses in Arabidopsis plants. Journal of Experimental Botany, 56(421), 2839–49. doi:10.1093/jxb/eri276

Slavikova, S., Ufaz, S., Avin-Wittenberg, T., Levanony, H., & Galili, G. (2008). An autophagy-associated Atg8 protein is involved in the responses of Arabidopsis seedlings to hormonal controls and abiotic stresses. Journal of Experimental Botany, 59(14), 4029–43. doi:10.1093/jxb/ern244

Sreenivasulu, N., & Schnurbusch, T. (2012). A genetic playground for enhancing grain number in cereals. Trends in Plant Science, 17(2), 91–101. doi:10.1016/j.tplants.2011.11.003

Srivalli, S., & Khanna-Chopra, R. (2009). Delayed wheat flag leaf senescence due to removal of spikelets is associated with increased activities of leaf antioxidant enzymes, reduced glutathione/oxidized glutathione ratio and oxidative damage to mitochondrial proteins. Plant Physiology and Biochemistry : PPB / Société Française de Physiologie Végétale, 47(8), 663–70. doi:10.1016/j.plaphy.2009.03.015

Suttangkakul, A., Li, F., Chung, T., & Vierstra, R. D. (2011). The ATG1/ATG13 protein kinase complex is both a regulator and a target of autophagic recycling in Arabidopsis. The Plant Cell, 23(10), 3761–79. doi:10.1105/tpc.111.090993

Svenning, S., Lamark, T., Krause, K., & Johansen, T. (2011). Plant NBR1 is a selective autophagy substrate and a functional hybrid of the mammalian autophagic adapters NBR1 and p62/SQSTM1. Autophagy, 7(9), 993–1010. Retrieved from http://www.pubmedcentral.nih.gov/articlerender.fcgi?artid=3210314&tool=pmcentrez&rendertype=abstract

Sykorová, B., Kuresová, G., Daskalova, S., Trcková, M., Hoyerová, K., Raimanová, I., … Kamínek, M. (2008). Senescence-induced ectopic expression of the A. tumefaciens ipt gene in wheat delays leaf senescence, increases cytokinin content, nitrate influx, and nitrate reductase activity, but does not affect grain yield. Journal of Experimental Botany, 59(2), 377–87. doi:10.1093/jxb/erm319

Tamura, N., Oku, M., & Sakai, Y. (2010). Atg8 regulates vacuolar membrane dynamics in a lipidation-independent manner in Pichia pastoris. Journal of Cell Science, 123(Pt 23), 4107–16. doi:10.1242/jcs.070045

Tegeder, M. (2014). Transporters involved in source to sink partitioning of amino acids and ureides: opportunities for crop improvement. Journal of Experimental Botany, 65(7), 1865–78. doi:10.1093/jxb/eru012

Tegeder, M., & Rentsch, D. (2010). Uptake and partitioning of amino acids and peptides. Molecular Plant, 3(6), 997–1011. doi:10.1093/mp/ssq047

Thoenen, M., Herrmann, B., & Feller, U. (2007). Senescence in wheat leaves: is a cysteine endopeptidase involved in the degradation of the large subunit of Rubisco? Acta Physiologiae Plantarum, 29(4), 339–350. doi:10.1007/s11738-007-0043-4

Thomas, H. (2012). Tansley review Senescence, ageing and death of the whole plant, (October 2011).

Thomas, H., Morgan, W. G., Thomas, a. M., & Ougham, H. J. (1999). Expression of the stay-green character introgressed into Lolium temulentum Ceres from a senescence mutant of Festuca pratensis. TAG Theoretical and Applied Genetics, 99(1-2), 92–99. doi:10.1007/s001220051212

Thomas, H., & Ougham, H. (2014). The stay-green trait. Journal of Experimental Botany, 65(14), 3889–3900. doi:10.1093/jxb/eru037

Thomas, H., Ougham, H., Canter, P., & Donnison, I. (2002). What stay-green mutants tell us about nitrogen remobilisation in leaf senescence. Journal of Experimental Botany, 53(370), 801–8. Retrieved from http://www.ncbi.nlm.nih.gov/pubmed/11912223

Thomas, H., & Stoddart, J. L. (1980). LEAF SENESCENCEl +7685, 83–111.

Thompson, A. R., Doelling, J. H., Suttangkakul, A., & Vierstra, R. D. (2005). Autophagic Nutrient Recycling in Arabidopsis Directed by the ATG8 and ATG12 Conjugation Pathways 1. Plant Physiology, 138(August), 2097–2110. doi:10.1104/pp.105.060673.contents

Thompson, A. R., & Vierstra, R. D. (2005). Autophagic recycling: lessons from yeast help define the process in plants. Current Opinion in Plant Biology, 8(2), 165–73. doi:10.1016/j.pbi.2005.01.013

Tian, F. X., Gong, J. F., Wang, G. P., Wang, G. K., Fan, Z. Y., & Wang, W. (2012). Improved drought resistance in a wheat stay-green mutant tasg1 under field conditions, 56(30671259), 509–515.

Turgeon, R., & Wolf, S. (2009). Phloem transport: cellular pathways and molecular trafficking. Annual Review of Plant Biology, 60, 207–21. doi:10.1146/annurev.arplant.043008.092045

Uauy, C., Distelfeld, A., Fahima, T., Blechl, A., & Dubcovsky, J. (2006). A NAC Gene regulating senescence improves grain protein, zinc, and iron content in wheat. Science (New York, N.Y.), 314(5803), 1298–301. doi:10.1126/science.1133649

Ulker, B., Shahid Mukhtar, M., & Somssich, I. E. (2007). The WRKY70 transcription factor of Arabidopsis influences both the plant senescence and defense signaling pathways. Planta, 226(1), 125–37. doi:10.1007/s00425-006-0474-y

Ullrich, S. (2011). Barley Production, Improvement and Uses (p. 603). West Sussex, UK: A John Wiley & Sons, Inc. doi:10.1007/SpringerReference_4662

Van Doorn, W. G. (2008). Is the onset of senescence in leaf cells of intact plants due to low or high sugar levels? Journal of Experimental Botany, 59(8), 1963–72. doi:10.1093/jxb/ern076

Vanhee, C., Guillon, S., Masquelier, D., Degand, H., Deleu, M., Morsomme, P., & Batoko, H. (2011). A TSPO-related protein localizes to the early secretory pathway in Arabidopsis, but is targeted to mitochondria when expressed in yeast. Journal of Experimental Botany, 62(2), 497–508. doi:10.1093/jxb/erq283

Von Bothmer, R., Seberg, O., & Jacobsen, N. (1992). Genetic resources in the Triticeae. Hereditas, 116(1-2), 141–150. doi:10.1111/j.1601-5223.1992.tb00219.x

Wang, W.-Y., Zhang, L., Xing, S., Ma, Z., Liu, J., Gu, H., … Qu, L.-J. (2012). Arabidopsis AtVPS15 plays essential roles in pollen germination possibly by interacting with AtVPS34. Journal of Genetics and Genomics = Yi Chuan Xue Bao, 39(2), 81–92. doi:10.1016/j.jgg.2012.01.002

Watanabe, M., Balazadeh, S., Tohge, T., Erban, A., Giavalisco, P., Kopka, J., … Hoefgen, R. (2013). Comprehensive dissection of spatiotemporal metabolic shifts in primary, secondary, and lipid metabolism during developmental senescence in Arabidopsis. Plant Physiology, 162(3), 1290–310. doi:10.1104/pp.113.217380

Weaver, L. M., & Amasino, R. M. (2001). Senescence Is Induced in Individually Darkened Arabidopsis Leaves, but Inhibited in Whole Darkened Plants 1, 127(November), 876–886. doi:10.1104/pp.010312.876

Weaver, L. M., Gan, S., Quirino, B., & Amasino, R. M. (1998). A comparison of the expression patterns of several senescence-associated genes in response to stress and hormone treatment. Plant Molecular Biology, 37(3), 455–69. Retrieved from http://www.ncbi.nlm.nih.gov/pubmed/9617813

Wiebe, G., & Reid, D. (1961). Classification of barley varieties grown in the United States and Canada in 1958. Washington: U.S.D.A.

Wingler, A., Marès, M., & Pourtau, N. (2004). Spatial patterns and metabolic regulation of photosynthetic parameters during leaf senescence, 781–789. doi:10.1111/j.1469-8137.2003.00996.x

Wingler, A., Masclaux-Daubresse, C., & Fischer, A. M. (2009). Sugars, senescence, and ageing in plants and heterotrophic organisms. Journal of Experimental Botany, 60(4), 1063–6. doi:10.1093/jxb/erp067

Winter, H., Lohaus, G., & Heldt, H. W. (1992). Phloem Transport of Amino Acids in Relation to their Cytosolic Levels in Barley Leaves. Plant Physiology, 99(3), 996–1004. Retrieved from http://www.pubmedcentral.nih.gov/articlerender.fcgi?artid=1080575&tool=pmcentrez&rendertype=abstract

Wu, A., Allu, A. D., Garapati, P., Siddiqui, H., Dortay, H., Zanor, M.-I., … Balazadeh, S. (2012). JUNGBRUNNEN1, a reactive oxygen species-responsive NAC transcription factor, regulates longevity in Arabidopsis. The Plant Cell, 24(2), 482–506. doi:10.1105/tpc.111.090894

Xia, T., Xiao, D., Liu, D., Chai, W., Gong, Q., & Wang, N. N. (2012). Heterologous expression of ATG8c from soybean confers tolerance to nitrogen deficiency and increases

yield in Arabidopsis. PloS One, 7(5), e37217. doi:10.1371/journal.pone.0037217

Xie, Z., & Klionsky, D. J. (2007). Autophagosome formation: core machinery and adaptations. Nature Cell Biology, 9(10), 1102–9. doi:10.1038/ncb1007-1102

Xiong, Y., Contento, A. L., & Bassham, D. C. (2005). AtATG18a is required for the formation of autophagosomes during nutrient stress and senescence in Arabidopsis thaliana. The Plant Journal : For Cell and Molecular Biology, 42(4), 535–46. doi:10.1111/j.1365-313X.2005.02397.x

Xu, N., Gao, X.-Q., Zhao, X. Y., Zhu, D. Z., Zhou, L. Z., & Zhang, X. S. (2011). Arabidopsis AtVPS15 is essential for pollen development and germination through modulating phosphatidylinositol 3-phosphate formation. Plant Molecular Biology, 77(3), 251–60. doi:10.1007/s11103-011-9806-9

Yang, J. C., Zhang, J. H., Wang, Z. Q., Zhu, Q. S., & Liu, L. J. (2003). Involvement of abscisic acid and cytokinins in the senescence and remobilisation of carbon reserves in wheat, 1621–1631.

Yang, S.-D., Seo, P. J., Yoon, H.-K., & Park, C.-M. (2011). The Arabidopsis NAC transcription factor VNI2 integrates abscisic acid signals into leaf senescence via the COR/RD genes. The Plant Cell, 23(6), 2155–68. doi:10.1105/tpc.111.084913

Yang, Z., & Klionsky, D. (2009). An overview of the molecular mechanisms of autophagy. Curr Top Microbiol Immunol, 335, 1–32. doi:10.1007/978-3-642-00302-8

Yang, Z., & Klionsky, D. (2010). Eaten alive : a history of macroautophagy. Nat Cell Biol, 12(9), 814–822. doi:10.1038/ncb0910-814.Eaten

Yen, W., Legakis, J. E., Nair, U., & Klionsky, D. J. (2007). Atg27 Is Required for Autophagy-dependent Cycling of Atg9, 18(February), 581–593. doi:10.1091/mbc.E06

Yoshimoto, K., Hanaoka, H., Sato, S., Kato, T., Tabata, S., & Noda, T. (2004). Processing of ATG8s, Ubiquitin-Like Proteins, and Their Deconjugation by ATG4s Are Essential for Plant Autophagy. The Plant Cell, 16(November), 2967–2983. doi:10.1105/tpc.104.025395.et

Yoshimoto, K., Jikumaru, Y., Kamiya, Y., Kusano, M., Consonni, C., Panstruga, R., … Shirasu, K. (2009). Autophagy negatively regulates cell death by controlling NPR1-dependent salicylic acid signaling during senescence and the innate immune response in Arabidopsis. The Plant Cell, 21(9), 2914–27. doi:10.1105/tpc.109.068635

Young, A. R. J., Chan, E. Y. W., Hu, X. W., Köchl, R., Crawshaw, S. G., High, S., … Tooze, S. a. (2006). Starvation and ULK1-dependent cycling of mammalian Atg9 between the TGN and endosomes. Journal of Cell Science, 119(Pt 18), 3888–900. doi:10.1242/jcs.03172

Young, T. E., Giesler-Lee, J., & Gallie, D. R. (2004). Senescence-induced expression of cytokinin reverses pistil abortion during maize flower development. The Plant Journal : For Cell and Molecular Biology, 38(6), 910–22. doi:10.1111/j.1365-313X.2004.02093.x

Zavaleta-Mancera, H. a., Thomas, B. J., Thomas, H., & Scott, I. M. (1999). Regreening of senescent Nicotiana leaves: II. Redifferentiation of plastids. Journal of Experimental Botany, 50(340), 1683–1689. doi:10.1093/jxb/50.340.1683

Zelisko, A., García-Lorenzo, M., Jackowski, G., Jansson, S., & Funk, C. (2005). AtFtsH6 is involved in the degradation of the light-harvesting complex II during high-light acclimation and senescence. Proceedings of the National Academy of Sciences of the United States of America, 102(38), 13699–704. doi:10.1073/pnas.0503472102

Zentgraf, U., Laun, T., & Miao, Y. (2010). The complex regulation of WRKY53 during leaf senescence of Arabidopsis thaliana. European Journal of Cell Biology, 89(2-3), 133–7. doi:10.1016/j.ejcb.2009.10.014

Zhang, L., Tan, Q., Lee, R., Trethewy, A., Lee, Y.-H., & Tegeder, M. (2010). Altered xylem-phloem transfer of amino acids affects metabolism and leads to increased seed yield and oil content in Arabidopsis. The Plant Cell, 22(11), 3603–20. doi:10.1105/tpc.110.073833

Zientara-Rytter, K., Lukomska, J., Moniuszko, G., Gwozdecki, R., Surowiecki, P., Lewandowska, M., … Sirko, A. (2011). Identification and functional analysis of Joka2, a tobacco member of the family of selective autophagy cargo receptors. Autophagy, 7(10), 1145–58. doi:10.4161/auto.7.10.16617

Zohary, D. (1989). Pulse domestication and cereal domestication: How different are they? Economic Botany, 43(1), 31–34. doi:10.1007/BF02859322

Summary

Barley (*Hordeum vulgare* L.) is one of the most important cereals in the world. It was one of the first domesticated crops and was used for centuries for human food. As all plants, barley has a fundamental dependence of inorganic nitrogen and nitrogen remobilization efficiency is very important for grain filling and grain protein content. The aim of this work was then to give a picture of the leaf-senescence metabolism in barley leaves when plants are grown under low or high nitrate conditions. Biochemical, physiological and molecular analyses of barley leaf senescence were performed. Nitrogen management during leaf senescence was monitored measuring changes in the different nitrogen pools during leaf ageing. In addition a large metabolite profiling study was performed in order to determine the metabolic hallmarks of leaf senescence in barley. In parallel enzymes involved in nitrogen remobilization were studied measuring their activity and the transcript levels of their coding genes. There was a special focus on glutamine synthetase and asparagine synthetase enzymes and for autophagy machinery that are known to play a role in nitrogen remobilisation during leaf senescence. From all the sequences data available, cDNA, EST and genomic sequences, we could identified five genes coding for cytosolic glutamine synthetase (GS1), five genes coding for asparagine synthetase (AS) and 19 genes coding for autophagy machinery proteins. Transcript levels of all the genes identified were monitored during leaf senescence and depending on nitrate nutrition. Most of these genes were over-expressed in senescing leaves and differentially expressed depending on nitrate conditions. In addition to the characterization of autophagy, *GS1* and *ASN* genes, phylogenic and gene structures were analysed. All the sequences data provided by this work will be helpful to further translational and genetic association studies.

Résumé

L'orge (Hordeum vulgare L.) est l'une des céréales les plus importantes du monde et l'une des premières cultures domestiquées. Elle a été utilisée pendant des siècles pour l'alimentation humaine. Comme toutes les autres plantes, l'orge est dépendante de l'azote inorganique. L'efficacité de remobilisation de l'azote est donc très importante pour le remplissage des grains et pour la teneur en protéines du grain. L'objectif de ce travail est de donner une image du métabolisme des feuilles sénescence chez l'orge lorsque les plantes sont cultivées dans des conditions limitantes ou non en nitrates. Les analyses biochimiques, physiologiques et moléculaires de la sénescence des feuilles d'orge ont été réalisées. La gestion de l'azote pendant la sénescence des feuilles a été suivie par l'évolution des différents composés azotés au cours du vieillissement de la feuille. Une étude de profilage métabolique a été effectuée afin de déterminer les caractéristiques métaboliques de la sénescence des feuilles dans l'orge. En parallèle, les enzymes impliquées dans la remobilisation de l'azote ont été étudiées. Leurs activités et les niveaux de leurs transcripts ont été mesurés. Une attention particulière a été portée aux glutamine synthétases et asparagine synthétases et aux protéines de la machinerie de l'autophagie, processus connus pour jouer un rôle dans la remobilisation de l'azote pendant la sénescence des feuilles. A partir de toutes les données de séquences disponibles, ADNc, EST et séquences génomiques, cinq gènes codant pour les isoformes de glutamine synthétase cytosoliques (GS1), cinq gènes codant pour les isoformes d'asparagine synthétase (AS) isoformes et 19 gènes codant pour des protéines de la machinerie de l'autophagie ont été identifiés. Les expressions de tous les gènes identifiés ont été suivies au cours de la sénescence des feuilles et en fonction de l'alimentation en nitrates. La plupart de ces gènes sont sur-exprimés dans les feuilles sénescentes et de façon différentielle en fonction des conditions de nutrition. Toutes les données de séquences fournies par ce travail seront utiles à d'autres études translationelles et d'association génétique.